THE UNIVERSITY OF
SYDNEY

THE ROLE OF THE CORTICOMOTORNEURONS IN PATHOGENESIS OF AMYOTROPHIC LATERAL SCLEROSIS

PARVATHI MENON

A THESIS SUBMITTED IN FULFILMENT OF THE REQUIREMENTS FOR THE DEGREE OF DOCTOR OF PHILOSOPHY

FACULTY OF MEDICINE, WESTERN CLINICAL SCHOOL, WESTMEAD HOSPITAL.

UNIVERSITY OF SYDNEY

MARCH 2014

ACKNOWLEDGEMENTS

The completion of the research studies undertaken as part of my PhD degree and culminating in the submission of this thesis has involved significant contributions from a number of individuals and institutions to whom I am extremely grateful and whose efforts I would like to acknowledge. My supervisor, Associate Professor Steve Vucic, had conviction in my abilities and encouraged me to undertake this career path. He has generously provided constant support, guidance and encouragement to achieve my goals and most importantly to acquire the skills to pursue the path of ongoing clinical research work. My co-supervisor Professor Matthew Kiernan has constantly provided encouragement, valuable advice and high standards to aspire towards. I owe them sincere gratitude for providing me with a career opportunity which provides immense daily work satisfaction. Scholarship funding by the University of Sydney, Lake-Bonnamy post graduate scholar ship and the Motor Neuron Disease Research Institute of Australia/National Health and Medical Research Council co-funded postgraduate scholarship is gratefully acknowledged. My colleagues in the department of Neurology, Westmead Hospital, have, at all levels, been extremely generous and supportive of my research efforts and I would like to acknowledge their constant support and encouragement. I am also grateful to all patients and subjects who participated in the research studies. To the ever hopeful and generous patients, in particular, I am grateful for a perspective on life and for the inspiration to continue ongoing research work. Lastly, but most importantly, I would like to acknowledge my teachers through the years and my family for their immeasurable contribution to my present achievement, their belief in my ability and constant encouragement to achieve my best.

ABSTRACT

Amyotrophic lateral sclerosis (ALS) is a progressive, degenerative disease of the motor system clinically defined by the presence of upper and lower motor neuron (LMN) signs. The site of onset of pathophysiology within the motor system in ALS remains unresolved and this thesis examines the role of the corticomotor neuron in the pathogenesis of ALS.

The diagnostic utility of the split-hand sign in ALS involving preferential wasting of the 'thenar' group of intrinsic hand muscles namely the abductor pollicis brevis (APB) and first dorsal interosseous (FDI) was established by recording the split-hand index (SI) which was noted to reliably differentiate ALS from mimic neuromuscular disorders. The cortical and axonal excitability characteristics of the 'thenar' muscles namely the APB and FDI was compared with the hypothenar abductor digiti minimi (ADM) with threshold tracking transcranial magnetic stimulation (TMS) studies revealing cortical hyperexcitability to be a feature of ALS pronounced over the 'thenar' muscles while axonal hyperexcitability while a feature of ALS, did not selectively affect the prominently wasted 'thenar' muscles. Cortical hyperexcitability was also noted to precede the development of lower motor neuron dysfunction in a clinically and neurophysiologically normal APB muscle. The selective vulnerability of muscles in ALS was further defined by the split hand plus sign with a greater degree of cortical hyperexcitability over the preferentially wasted APB muscle in ALS patients when compared with a similarly innervated and relatively preserved flexor pollicis longus (FPL) muscle.

In summary, corticomotorneuronal hyperexcitability as a marker of corticomotorneuronal dysfunction predominates over the muscles which are preferentially wasted in ALS and precedes evidence of lower motor neuron loss. The findings presented in this thesis support the primacy of

the corticomotor neuron in the pathogenesis of the split hand phenomenon and suggest a mechanism for the pathogenesis of ALS.

Keywords: ALS, split-hand sign, cortical hyperexcitability

CONTENTS

PREFACE

The term amyotrophic lateral sclerosis was introduced by the French neurologist Jean-Martin Charcot (1825-1893) in 1874 in his two lectures gathered in Volume 2 of his Oeuvres Completes. Using the technique known as the "anatomo-clinical method", a two-part method to determine the correlation between clinical signs detected during life and anatomical lesions seen at death, Charcot synthesized prior studies and enumerated the steps that led to the unified concept presented in 1874 of a condition resulting in weakness involving both muscle atrophy as well as spasticity and contractures and associated with spinal gray matter involvement (amyotrophy) and white matter damage (lateral sclerosis). The wording of the term reflects Charcot's belief that the amyotrophy was, in fact, due to spread of the disease from the lateral columns to the spinal and bulbar gray matter. However, mechanisms underlying the pathogenesis of amyotrophic lateral sclerosis (ALS) remain unresolved specifically the sequence of progress of pathology. Selective vulnerability of the 'thenar' intrinsic hand muscles to wasting, a phenomenon termed the split hand sign has been noted to be a specific feature of ALS and provides a unique opportunity to understand the pathogenesis of ALS. The present thesis attempts to assess the role of the corticomotor neuron in the pathogenesis of ALS utilising threshold tracking cortical and axonal excitability studies along with clinical assessment, routine neurophysiology studies and motor unit potential analysis.

PUBLICATIONS

Literature Review

Menon, P., Kiernan, M. C. & Vucic, S. Appearance, phenomenology and diagnostic utility of the split hand in amyotrophic lateral sclerosis. (Review) Neurodeg Dis Management 2011; 1**,** 457-462.

Menon, P., Vucic, S. Utility of Dissociated Intrinsic Hand Muscle Atrophy in the Diagnosis of Amyotrophic Lateral Sclerosis. *J. Vis. Exp.* (85), e51056, doi:10.3791/51056 (2014).

Chapter 1

Menon, P., Kiernan, M. C., Yiannikas, C., Stroud, J. & Vucic, S. Split-hand index for the diagnosis of amyotrophic lateral sclerosis. Clin Neurophysiol 2013; 124**,** 410-416.

Chapter 2

Menon, P., Kiernan, M. C. & Vucic, S. Cortical excitability differences in hand muscles follow a split-hand pattern in healthy controls. Muscle & Nerve 2013.

Chapter 3

Menon, P., Kiernan, M. C. & Vucic, S. ALS pathophysiology: Insights from the split-hand phenomenon. Clinical Neurophysiology 2014; 125**,** 186-193.

Chapter 4

Menon, P., Kiernan, M. C. & Vucic, S. Cortical Dysfunction Underlies the Development of the Split-Hand in Amyotrophic Lateral Sclerosis. PloS one 2014; 9**,** e87124.

Chapter 5

Cortical hyperexcitability precedes lower motor neuron dysfunction in ALS
Clinical Neurophysiology Ms. No. CLINPH-D-14-7441. Submitted following revision Mar 2014

Chapter 6

Menon, P., Bae, J. S., Mioshi, E., Kiernan, M. C. & Vucic, S. Split-hand plus sign in ALS: Differential involvement of the flexor pollicis longus and intrinsic hand muscles. Amyotrophic Lateral Sclerosis and Frontotemporal Degeneration 2013; 14**,** 315-318.

Chapter 7

Bae, J. S., Menon, P., Mioshi, E., Kiernan, M. C. & Vucic, S. Cortical excitability differences between flexor pollicis longus and APB. Neuroscience Letters 2013; 541**,** 150-154.

Chapter 8

Bae, J. S., Menon, P., Mioshi, E., Kiernan, M. C. & Vucic, S. Cortical hyperexcitability and the split-hand plus phenomenon: Pathophysiological insights in ALS. Amyotrophic Lateral Sclerosis and Frontotemporal Degeneration 2014**,** 1-7.

AWARDS

1. Best presentation award for poster titled '**Cortical Hyperexcitability of the Thenar Group of Intrinsic Hand Muscles may contribute to the Split-Hand Sign in ALS'** (Chapter 4) at the ANZAN 15th Biennial Clinical Neurophysiology Workshop Oct 2013.

2. The 'ANZAN James Lance young investigator award' at the Asia Oceania Congress of Neurology, Melbourne 2012 for the presentation titled **'Cortical Hyperexcitability Precedes Lower Motor Neuron Dysfunction in Sporadic ALS'** (Chapter 5).

3. MND Victoria 'Nina Buscombe Travel Award 2012' with presentation at the Australian National MND Symposium, Adelaide 2012, of research findings titled **'Cortical Hyperexcitability precedes Lower Motor Neuron Dysfunction in Sporadic ALS'** (Chapter 5).

LITERATURE REVIEW

Introduction

Amyotrophic Lateral Sclerosis (ALS), also known as motor neuron disease (MND), is a rapidly progressive and universally fatal neurodegenerative disorder of the human motor system, first described in the mid-19th century by the French neurologist Jean Martin Charcot (1). Although ALS is clinically characterised by progressive neurological deterioration and co-existence of upper and lower motor neuron signs, recent discoveries have indicated a heterogeneous nature of ALS (2). In addition to the ALS phenotype, the varied clinical presentations of ALS/MND include (i) progressive muscle atrophy (PMA), a clinically pure LMN phenotype, (ii) primary lateral sclerosis (PLS), a clinically pure UMN phenotype and (iii) progressive bulbar palsy (PBP), an isolated bulbar phenotype with relative preservation of spinal motor neurons. More recently, an association between ALS and frontotemporal degeneration (FTD) has been established, suggesting that ALS forms a continuum with primary neurodegenerative disorders, a notion underscored by the identification of the c9orf72 hexanucleotide expansion (3-5). Despite the clinical heterogeneity, median survival of ALS/MND remains 3 years, with 10% of patients surviving over 8 years (6, 7).

Amyotrophic lateral sclerosis

In European-based population studies the incidence of ALS appears uniform at 2.16 per 100,000 person-years with a prevalence of 4-6 per 100,000 (8). The overall lifetime risk of developing ALS is 1 in 400, with incidence slightly higher in males [1.2-1.5:1] (8). Sporadic ALS peaks between the ages of 50 to 75 years and declines after the age of 80 (6), with the age-specific incidence remaining stable over the past decade (9). The frequency of ALS is significantly lower in non-Caucasian populations (10, 11), suggesting a role for genetic factors in ALS

susceptibility. Other ALS/MND phenotypes are less frequent, including PMA (10% of cases), PLS (1-3%) and progressive bulbar palsy (1-2%) of all cases. A genetic etiology has been identified in up to 20% of apparently "sporadic" and 60% of familial ALS cases, in which two or more family members are clinically affected, with at least 16 genes and genetic loci implicated in ALS pathogenesis (12). For the purposes of this thesis, MND is synonymous with ALS.

Clinical Features

Amyotrophic lateral sclerosis exhibits a diverse and complex clinical phenotype, critical for understanding of disease pathophysiology and diagnosis. Clinically, ALS is characterised by co-existence of upper and lower motor neuron signs encompassing multiple body regions, with evidence of progressive deterioration (2, 13, 14). Lower motor neuron signs are clinically characterized by fasciculations, muscle wasting and weakness, while UMN signs include slowness of movement, increased tone, hyper-reflexia and extensor plantar responses. The majority of ALS patients present with limb-onset disease (65-75%) (15-17), typically spreading along the neuraxis to affect contiguous motor neurons (18, 19). Preferential wasting and weakness of thenar muscles, termed the ***split-hand phenomenon*** (*see below*) is a specific feature of ALS (20, 21). While fasciculations are a cardinal feature of ALS, they are infrequently the presenting symptom (22, 23). Patients presenting solely with fasciculations and muscle cramping should be monitored as these patients may infrequently progress to develop ALS (24). Extra-ocular and sphincter muscles are preserved until advanced stages of the disease (25), and sensory nerves are not typically affected (6).

Bulbar-onset disease, evident in 20% of cases, is characterized by flaccid or spastic dysarthria, dysphagia, hoarseness, tongue wasting, weakness and fasciculations as well as emotional lability and pathologically brisk jaw reflexes (2). Dysphasia may potentially result in aspiration pneumonia, malnutrition and weight loss, all adverse prognostic features (26). Respiratory dysfunction develops in advanced stages of ALS, ultimately resulting in terminal respiratory failure (27), although rarely may be the presenting symptom (28-30).

Of further relevance, atypical ALS phenotypes include progressive muscular atrophy, the "pure" LMN phenotype, encompassing the flail-arm and flail leg variants of ALS. The flail-limb variants are characterised by neurogenic weakness confined to the shoulder girdle (flail-arm > 24 months) or lower limbs (flail-leg) for a prolonged period with absence of UMN signs (31-36). One-third of PMA cases develop UMN dysfunction (37, 38), while PLS patients may develop LMN signs within four years of disease-onset (39). The PBP phenotype remains localized within the bulbar region for a prolonged period (>6 months) and is characterized by female predominance and UMN bulbar dysfunction, although clinical features of ALS typically develop in the upper and lower limbs (40). Although survival is typically prolonged in these unusual phenotypes, the mortality rates for the generalized forms of PMA appear similar to ALS (37).

In addition to pure motor symptoms, subtle cognitive abnormalities may be evident in up to 50% of ALS patients (41, 42), characterized by executive dysfunction, language and memory impairment along with behavioural abnormalities, which may precede the onset of motor symptoms (6, 41, 42). Recognition of cognitive dysfunction has implication for vital management of ALS, as these symptoms may adversely impact on patient compliance and

decision-making abilities. At the extreme end of the spectrum, frontotemporal dementia may develop in up to 15% of ALS patients (8, 41), and is clinically characterized by executive and language dysfunction, irrational behavioural, personality changes, apathy, poor insight, loss of empathy, irritability and disinhibition (43). The presence of psychiatric features in the setting of FTD-ALS may be indicative of the c9orf72 expansion (43).

Split-hand sign

The "***split hand***" sign refers to preferential wasting of the thenar group of muscles, including the abductor pollicis brevis (APB) and first dorsal interosseous (FDI), when compared to the abductor digit minimi (ADM) (Fig. 1) (21, 44). This pattern of dissociated muscle atrophy is frequently observed in ALS, and may differentiate ALS from potential mimic disorders (20, 44). The ability to quantify the split hand sign, through the development of a split-hand index (SI), was recently demonstrated to be of diagnostic significance in ALS (Chapter 1).

The mechanisms underlying the development of the split hand in ALS remains to be fully elucidated, and resolution of this issue could be of pathophysiological significance in ALS. Dysfunction of local spinal segments are unlikely to account for the split hand phenomena given that all involved muscles are innervated by the same myotomes (C8, T1). Currently, three potential mechanisms have been suggested as possible pathophysiological processes underlying the development of the split hand, including cortical hyperexcitability, increased peripheral nerve excitability and increased metabolic demands of the motor neurons innervating the APB and FDI muscles (20, 44).

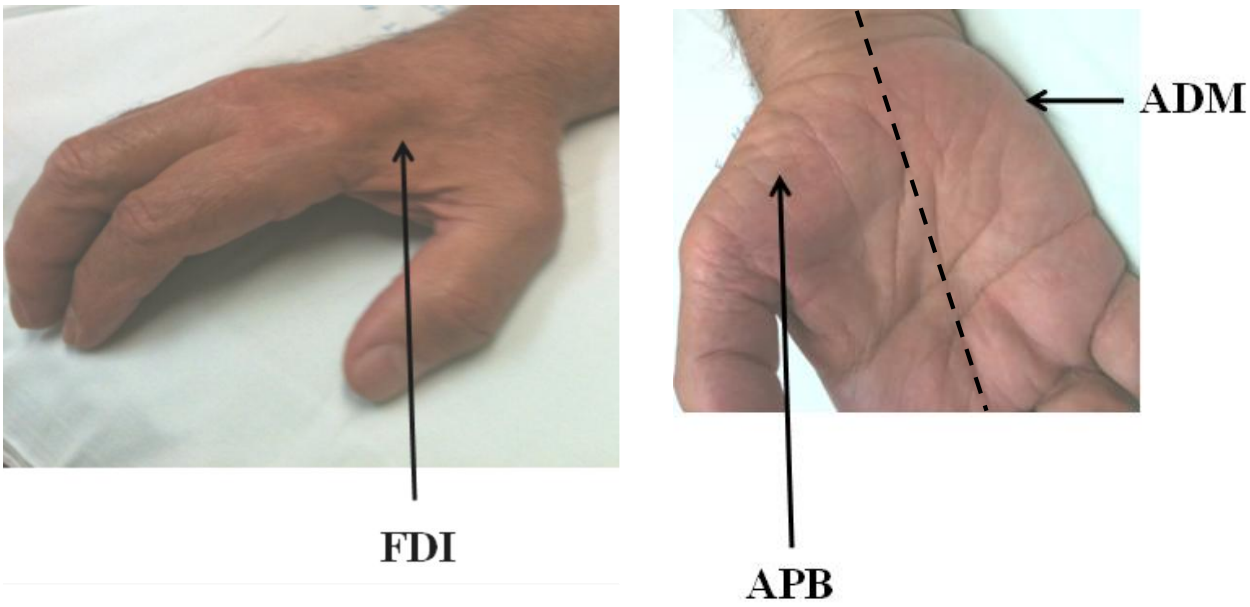

Figure 1: The split hand sign refers to preferential atrophy of the abductor pollicis brevis (APB) and first dorsal interosseous (FDI) muscles when compared to abductor digit minimi (ADM). The split hand phenomenon sign appears to be a specific feature of ALS.

A cortical mechanism was suggested by the notion of corticomotoneuronal primacy in ALS pathogenesis, a view first considered by Charcot (1). Subsequently, the ***dying forward" hypothesis*** was proposed, which suggested that corticomotoneuronal hyperexcitability induced motor neuron degeneration via an anterograde glutamate-mediated excitotoxic process (25). Support for a dying forward hypothesis was based on a number of important clinical and neurophysiological observations, including: (i) a relative preservation of extraocular and sphincter muscles in ALS, postulated to be due to a paucity of corticomotoneuronal projections onto the motor nuclei innervating the extraocular muscles; (ii) absence of an animal model of ALS, ascribed to a lack of direct corticomotoneuronal-anterior horn cell connections (45); (iii) rarity of pure lower motor neuron forms of ALS, with subclinical upper motor neuron dysfunction invariably detected with TMS studies (46); (iv) that asymmetric and variable motor deficits evident in ALS may be a explained by the complex anatomical association of the

corticomotoneuron-anterior horn cell synaptic relationship (45, 47, 48); and (v) that transcranial magnetic stimulation (TMS) studies have reported that cortical hyperexcitability is an early feature of sporadic ALS (49), preceding the development of familial ALS (50). Further, this increase in cortical excitability appeared to be a process specific for ALS in the context of neuromuscular disorders, clearly differentiating ALS from mimic disorders (51-53), thereby arguing against the notion that the increase in cortical excitability representing cortical plasticity. The association between the split hand sign and cortical hyperexcitability may be explained by a greater cortical representation of the thenar complex group of muscles (APB and FDI). This greater cortical representation is required in humans since the thenar complex group of muscles (both APB and FDI) are vital for fine fractionated hand movements (45). As a result, a greater corticomotoneuronal input onto the anterior horn cells innervating the APB and FDI muscles may result in greater anterior horn cell degeneration, via a glutamate excitotoxic process leading to the split hand sign. Support for such a mechanism was provided by TMS studies that revealed larger motor evoked potential (MEP) amplitudes over the thenar muscles when compared to the ADM in healthy controls, thereby suggesting a stronger corticomotoneuronal input to the thenar muscle complex (54). In addition, the MEP amplitudes were significantly reduced when recording over the thenar muscles in ALS patients, but not when recording over the ADM muscle, thereby suggesting that corticomotoneuronal dysfunction contributed to the split hand pattern of muscle atrophy in ALS.

Alternatively, it has also been suggested that the split hand sign may be explained by differences in membrane properties of motor axons innervating the various intrinsic hand muscles. Specifically, an increase of strength-duration time constant (SDTC) and latent addition (LA) was

reported in motor axons innervating the APB and FDI when compared to ADM in a group of healthy controls (55). Given that both SDTC and LA are biomarkers for persistent nodal sodium conductances, these findings suggest that upregulation of nodal persistent sodium conductances may contribute to the development of the split hand sign in ALS. Interestingly, upregulation of persistent nodal sodium conductances is a well-documented pathophysiological feature of ALS (56-58), linked to the process of neurodegeneration (59). Recently, axonal excitability studies have reported hyperexcitability of motor axons innervating the APB muscle when compared to axons innervating the ADM, suggesting a potential role of altered axonal properties in development of the split hand in ALS. The finding of upregulated nodal persistent sodium conductances in spinobulbar muscular atrophy (or Kennedy's disease) (60), a mimic disorder in which the split hand sign does not appear to be a feature, may potentially argue against such a mechanism.

In addition to central and peripheral nerve hyperexcitability, increased metabolic demands on the anterior horn cells (AHCs) innervating the APB and FDI muscles has also been suggested as a potential mechanism underlying the development of the split hand. Humans are distinct from animals in that fine fractionated movement are well developed and frequently used for daily activities (45). Give that the thenar complex groups of muscles (APB and FDI) are vital for the proper execution of these complex fine fractionated movements, it is apparent that the FDI and APB are used more frequently than the hypothenar muscles in daily activities. As a result, the metabolic demand on the spinal motor neurons innervating the APB or FDI muscles might be increased which in turn would result in greater oxidative stress and ultimately degeneration. A potential weakness of the metabolic demand hypothesis is that over a lifetime the whole of the

hand is used very actively, thereby making it difficult to see how the median aspect of the hand, namely the APB/FDI muscles, would be selectively involved. Consequently, while the mechanisms underlying the development of the split hand sign remain to be fully elucidated in ALS, a cortical basis seems to be supported.

Neurophysiological features

Nerve conduction studies (NCS) and electromyography (EMG) are essential investigations in ALS that may assist in the exclusion of ALS-mimic disorders (2), such as demyelinating neuropathies (61), and aid with the diagnosis. In ALS, motor NCS are normal in early stages of the disease, but with disease progression there is decline in the compound muscle action potential (CMAP) amplitude, reflecting axonal loss (62). Importantly, the CMAP amplitude correlates with outcome and functional disability (63) and has been utilised as a prognostic biomarker in clinical trials (63, 64). The changes in CMAP amplitude may be accompanied by a mild reduction in motor conduction velocity (> 70% of the lower limit of normal) and mild prolongation of distal motor and F-wave latencies (more than 30% of upper limit of normal) due to loss of large diameter fast-conducting fibres (62, 65, 66). The neurophysiological index, derived by multiplying the CMAP amplitude with the F-wave frequency and dividing the product by the distal motor latency, has been as a sensitive biomarker of disease progression in ALS (67, 68). Sensory NCSs are normal and overt abnormalities of sensory NCSs should raise suspicion of an alternative diagnosis (62, 65, 66).

Electromyography (EMG) is essential in identifying LMN loss in ALS and the most frequently recognized abnormalities include fasciculations, ongoing changes [fibrillation potentials and

positive sharp waves (PSWs)], along with chronic neurogenic changes (large-amplitude, long-duration, polyphasic motor unit potentials [Figure 2) (62, 66). Importantly, ongoing changes may be evident in clinically normal muscles and hence EMG may aid in an early diagnosis of ALS (24, 39).

Surviving motor units may fire spontaneously, resulting in fasciculations which are a classical feature of ALS and usually become generalised although they are rarely the presenting feature (22, 24). Importantly widespread fasciculations exhibiting a higher firing rate and increased frequency of double fasciculations in ALS (69), and when detected in the tongue are highly specific for ALS . Fasciculations are generated at the nerve terminals, though some arise at more proximal regions including at the level of the motor neuron (70-72). With disease progression, fasciculations may develop a complex morphology reflecting remodelling of the underlying motor unit (73). At a molecular level, upregulation of persistent sodium conductances combined with reduced potassium currents, appears to underlie the development of fasciculations in ALS (56).

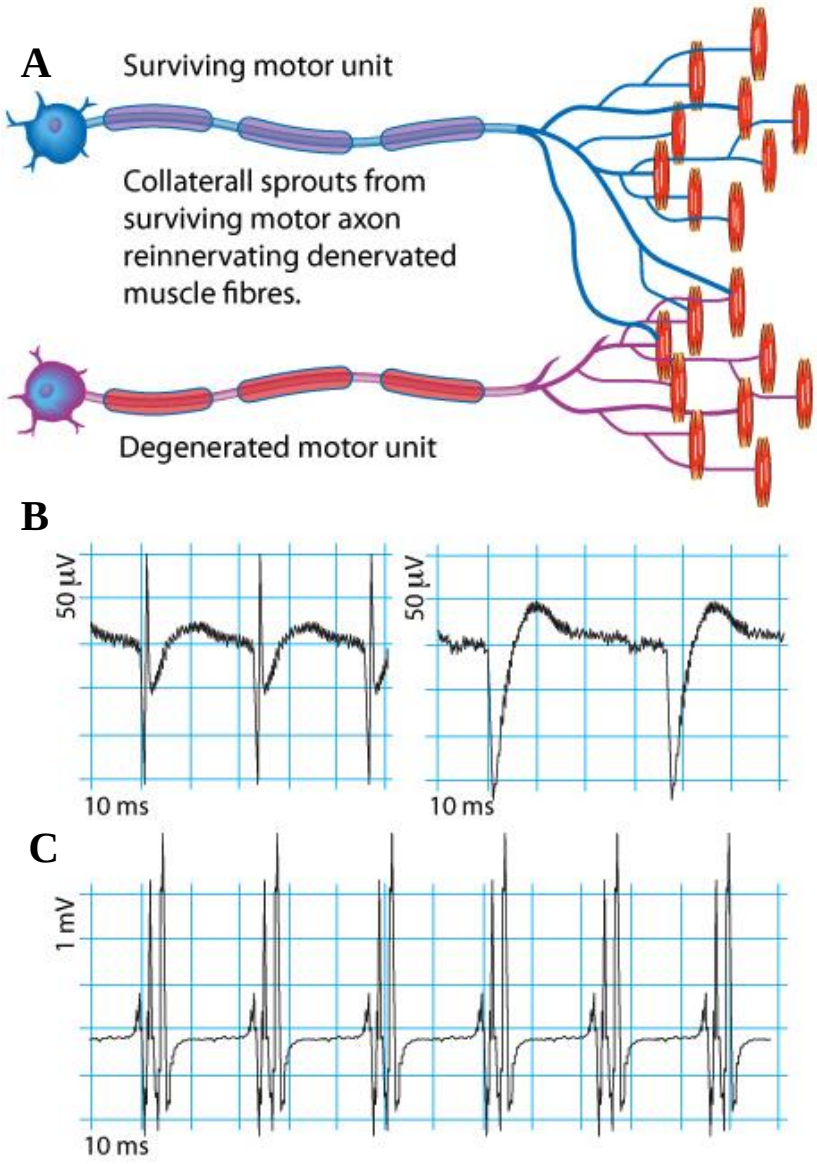

Figure 2: (A) Ongoing degeneration of motor neurons along with collateral sprouting of surviving motor neurons results in classical electromyography findings including **(B)** ongoing denervation (fibrillation potentials and positive sharp waves) along with **(C)** chronic neurogenic changes (large amplitude, long-duration, polyphasic motor units action potentials with reduced voluntary recruitment).

While the EMG changes may not be specific for ALS when found in isolation, the sensitivity and specificity of the EMG findings, as they conform to the Awaji criteria, has been recently established (74-81). Specifically, the Awaji criteria were developed in order to facilitate an earlier diagnosis of ALS, primarily in a research setting (82). These consensus criteria proposed that neurophysiological findings of ongoing and chronic neurogenic changes could be equated with the clinical features of LMN dysfunction. In addition, the presence of fasciculation potentials was deemed to be a biomarker of denervation, equivalent to the finding of ongoing changes. Quantitative dysfunction of UMNs was not captured with the Awaji criteria, thereby potentially precluding the diagnosis of ALS prior to development of widespread neurogenic changes or in the setting of atypical phenotypes such as such as the flail-arm variant (31).

Less conventional neurophysiological techniques for establishing LMN dysfunction in ALS include motor unit number estimation (83), electrode impedance myography (84), and axonal excitability [***see below***] (85, 86), although these techniques are not routinely applicable. Separately, TMS techniques (*see below*) may be utilised to assess UMN dysfunction, and features of cortical hyperexcitability, prolonged central motor conduction time and cortical inexcitability have been documented in ALS (87). Recently, beta-band intramuscular coherence was developed to assess UMN dysfunction in ALS (88), although at present it is utilized as a research tool.

Pathophysiology of ALS

Although the mechanisms underlying ALS pathogenesis remain to be fully elucidated, emerging evidence suggests the importance of genetic factors and dysfunction of vital molecular pathways

including oxidative stress, glutamate excitotoxicity, mitochondrial dysfunction, axonal transport systems, and dysfunction of glial cells, with resultant damage of critical target proteins and organelles within the motor neuron, thereby underlying neurodegeneration (89-94) (Fig. 3). A genetic etiology has been identified in up to 20% of apparently sporadic and 60% of familial ALS cases, with at least 16 genes and genetic loci implicated in ALS pathogenesis (12).

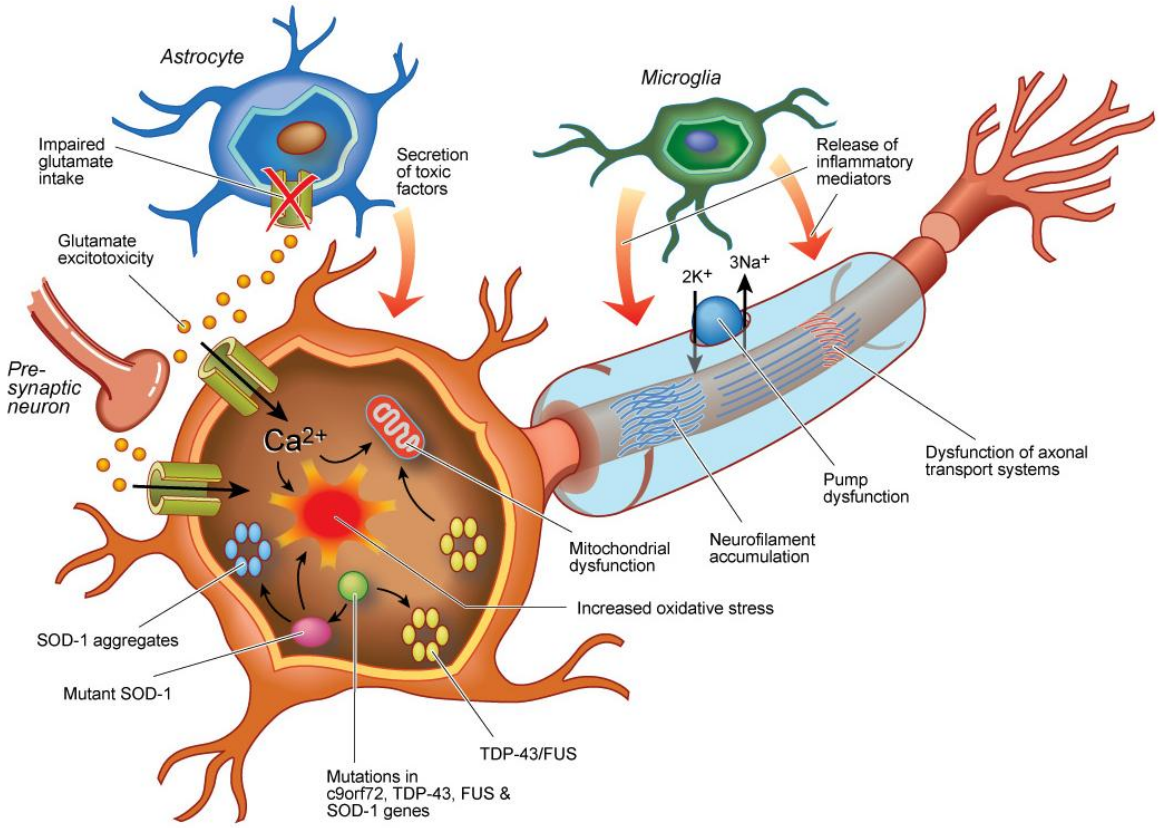

Figure 3: The pathophysiological mechanisms underlying neurodegeneration in amyotrophic lateral sclerosis (ALS) appear to be multifactorial with evidence of a complex interplay between molecular and genetic pathways. Dysfunction of the astrocytic excitatory amino acid transporter 2 (EAAT2) results in reduced uptake of glutamate from the synaptic cleft and thereby glutamate excitotoxicity. Glutamate-induced excitotoxicity results in increased influx of Na^{+} and Ca^{2+} ions and ultimately neurodegeneration through activation of Ca^{2+}-dependent enzymatic pathways. In addition, glutamate excitotoxicity results in generation of free radicals which in turn contributes to neurodegeneration. Mutations in the c9orf72, TDP-43 and FUS result in dyregulated RNA metabolism that ultimately leads to formation of intracellular aggregates which are harmful to neurons. Of further relevance, mutant SOD-1 enzyme increases oxidative stress, induces mitochondrial dysfunction, forms intracellular aggregates and adversely affect neurofilament and axonal transport processes. Activation of microglia results in secretion of proinflammatory cytokines, producing further toxicity.

Glutamate-mediated excitotoxicity appears to be an important mechanism in ALS pathogenesis (2, 95). Glutamate is the major excitatory neurotransmitter in the central nervous system (96, 97), synthesized from reductive deamination of alpha-ketoglutarate or from the action of amino acids aminotransferases (97). Approximately 20% of the total glutamate pool is stored in presynaptic nerve terminals and during impulse transmission; glutamate is released from presynaptic neurons through the effects of depolarization, diffusing across the synaptic cleft to activate postsynaptic receptors. Their excitatory signal is terminated upon removal of glutamate from the synaptic cleft by specific glutamate re-uptake transporters located on both neurons and astrocytes (98, 99). Within astrocytes, glutamate is converted into glutamine by the enzyme glutamine synthetase, and then returned to the neuron for resynthesis of glutamate (100).

Glutamate excitotoxicity is mediated by excessive activation of the postsynaptic glutamate receptors (97). Glutamate receptors are broadly classified into ionotropic or metabotropic receptors (97). Binding of glutamate to ionotropic receptors results in a conformational change within the receptor thereby enabling the passage of Na^+ and Ca^{2+} ions through a central pore. Metabotropic glutamate receptors are linked via G-proteins to second-messenger enzymes, which in turn can regulate a host of cellular activities (101). Based on pharmacological studies, glutamate ionotropic receptors are further classified as: (i) ***N-methyl-D-aspartate (NMDA)***, (ii) ***α-amino-3-hydroxy-5-methyl-4-isoxazolepropionic acid (AMPA)***, and (iii) ***kainite*** receptors. This pharmacological classification is supported by cloning studies that have identified six different families of glutamate ionotropic receptors that conform to the original agonist studies (101). ***N-methyl-D-aspartate*** receptors are permeable to influx of Na^+ and Ca^{2+} and efflux of K^+ (101). An essential feature of NMDA receptors is their voltage-dependent blockade by Mg^{2+}

binding within the channel pore, which can be alleviated by depolarization (102). NMDA receptors are involved in excitatory neurotransmission, which is characterized by a slow rise time and decay. As such, the NMDA receptors are involved in complex physiological processes, such as generation of rhythmic motor activity (103), regulation of neuronal migration during embryogenesis (104) and in memory (105).

The NMDA receptor complex is composed of different subunits derived from 6 genes; NMDAR1 (eight splice variants described), NMDAR2 (A-D) and NMDAR3 (A,B) (97, 101). While the NMDAR1 subunit forms the basic structure of the receptor (97), the NMDAR2 subunit determines ion channel properties and forms ligand-binding sites (106-108). Functional and pharmacological properties of NMDA receptors are determined through specific combination of NMDAR1 and NMDAR2 subunits (106, 109). In addition, there are regional variations in the expression of NMDA receptor subtypes (106, 109-115), with the NMDAR3B subunit heavily expressed in somatic motoneurons (116, 117).

AMPA receptors mediate a rapid influx of monovalent ions, such as Na^+, K^+ and chloride (Cl^-), but unlike NMDA receptors are impermeable to Ca^{2+} (97). Four AMPA receptor subtypes have been cloned (*Glu*R1-4) and are composed of three transmembrane domains (M1, M3, M4) and a fourth cytoplasmic hairpin loop (M2), which contributes to the pore-lining region (101, 118). The AMPA receptor exists as a pentameric structure in vivo, which is formed by the arrangement of subunits to create receptor diversity (97). The GluR2 subunit influences the Ca^{2+} permeability of AMPA receptors, whereby those receptors expressing an immature GluR2 subunit are more

permeable to Ca^{2+} ions. Following activation of these AMPA receptors, excessive influx of Ca^{2+} results in neurodegeneration through activation of Ca^{2+}-dependent pathways (97, 101).

Functional ***kainate receptors*** are likely to be heteromeric pentamers of the various kainate subunits. It is recognized that the receptor complexes are present in both presynaptic and postsynaptic neuronal membranes. It may be that they have inhibitory effects when presynaptic receptor complexes are stimulated(119). Studies suggest that the specific kainate receptor subunit composition influences function(120). The kainite receptors are thought to modulate slow, albeit small, synaptic responses. Their longer duration and the concomitantly longer integration time provide synapses with specific integrative capabilities. Kainate receptors are involved in short-term synaptic plasticity, particularly at the mossy fiber synapses and also seem to be involved in long-term plastic phenomena. However, their signal transduction pathways, which are probably dual, need to be clarified and despite their wide distribution their exact role in excitability needs to be elucidated(121).

The role of glutamate in ALS pathogenesis

In ALS, glutamate excitotoxicity has been postulated to induce anterior horn cell degeneration via a transsynaptic anterograde process mediated by corticomotoneurons (25). Support for such a mechanism has been provided by transcranial magnetic stimulation studies (TMS) which have demonstrated that cortical hyperexcitability, a biomarker of glutamate excitotoxicity, is an early feature in sporadic and familial ALS, linked to motor neuron degeneration (49, 50, 94, 122-127). In addition, longitudinal studies in asymptomatic SOD-1 mutation carriers revealed that cortical hyperexcitability developed prior to the clinical onset of ALS (50), a feature also evident in the

G93A SOD-1 mouse model (128). Of relevance, loss of γ-amino butyric acid (GABA) secreting parvalbumin-positive inhibitory interneurons in the motor cortex of ALS patients may further contribute to the development of cortical hyperexcitability (129), a finding underscored by recent neuroradiological studies reporting a significant reduction of GABA within the motor cortex of ALS patients (130).

Molecular-based studies have provided further evidence for glutamate-mediated excitotoxicity in ALS. Specifically, molecular studies established significant reduction in the expression and function of the astrocytic glutamate transporter (EAAT2), which mediates glutamate reuptake at synapses thereby inducing glutamate excitotoxicity, in the superoxide dismutase-1 (SOD-1) mouse model and the motor cortex and spinal cord of ALS patients (95, 131-134). Of further relevance, dysfunction of the EAAT2 transporter appears to be a pre-clinical feature in the SOD-1 mouse model (135, 136), and an increase in the expression and transporter activity of EAAT2 increases the lifespan of mutant SOD-1 mice (137). In addition, activation of caspase-1, which normally inhibits the EAAT2 transporter, was reported in the SOD-1 mouse model prior to onset of motor neuron degeneration and clinical features of ALS (135, 136). However, the presence of EAAT2 appears to delay motor neuron degeneration rather than being a primary process and other mechanisms, such as SOD-1 aggregation and caspase-3 activation, appeared to be important (138).

At a postsynaptic level, increased expression of AMPA receptors with the unedited GluR2 subunit has been reported in ALS (139-143). This editing defect appears to be specific for ALS, thereby rendering the motor neurons more permeable to Ca^{2+}, potentially explaining the

increased sensitivity of motor neurons to excitotoxicity (97, 144). Further support for glutamate excitotoxicity has been provided by the clinical benefit of riluzole in ALS patients (145-149). Specifically, riluzole is a glutamate antagonist that exerts effects in the central nervous system by reducing the release of glutamate from pre-synaptic nerve terminals and enhancing the reuptake of glutamate (150-153).

For the glutamate hypothesis to be a plausible mechanism of motor neuron degeneration in ALS, it must explain how motor neurons became selectively damaged through overactivity of the glutamatergic system and provide a mechanism by which degeneration occurs. A number of cell-specific molecular features possessed by the motor neurons render them vulnerable to glutamate toxicity in ALS. Motor neurons affected in ALS preferentially express AMPA receptors lacking the functional GluR2 subunit, thereby rendering the motor neurons more permeable to Ca^2 (139, 140, 142, 143). In addition, motor neurons vulnerable to degeneration lack the intracellular expression of proteins parvalbumin and calbindin D28k which are required to buffer intracellular Ca^{2+} (154). Of further relevance, increased expression of the inositol 1,4,5-triphosphate receptor 2 (ITPR2) gene was reported in ALS (155). The ITPR2 is involved in glutamate-mediated neurotransmission, whereby stimulation of glutamate receptors results in binding of inositol 1, 4, 5-triphosphate to ITPR2, which subsequently increases intracellular calcium (155, 156). Aberrant activity of ITPR2 results in higher intracellular concentration of Ca^{2+} leading ultimately to neurodegeneration (157). Of further relevance, motor neurons in ALS, at least in animal models, appear to be larger, with an increase in distal dendritic branching (158). Consequently, the input conductance of the motor neurons is increased rendering the

motor neuron more vulnerable to electrical and metabolic stresses, in particular those imparted by glutamate excitotoxicity (150).

Although details of the molecular mechanisms by which glutamate exerts neurotoxicity are still to be fully elucidated, several pathways have been defined. Initially, an influx of Na^+ and Cl^- ions occurs along with water molecules, resulting in acute neuronal swelling that is reversible with removal of agonist (159-161). Subsequently, an influx of Ca^{2+} ions occurs via activation of ionotropic receptors such as the NMDA and Ca^{2+}-permeable AMPA receptors, as well activation of voltage-gated Ca^{2+} channels (159, 162). Ultimately, activation of these ionic pathways results in increased intracellular Ca^{2+} concentration and activation of Ca^{2+}-dependent enzymatic pathways leading to neuronal death (144, 160, 163, 164). Further, glutamate excitotoxicity results in production of free radicals that can further damage the intracellular organelles thereby causing cell death (165-167).

Glutamate excitotoxicity and site of disease onset in ALS

In his original manuscript, Charcot concluded that in ALS the amyotrophy was, in fact, due to spread of the disease from the lateral columns to the spinal and bulbar gray matter as a downstream effects (1, 168). This view was not universal and Charcot's contemporary, Gower's, argued that the degeneration was a uniform and single event. Over the past two decades the site of ALS onset has been revisited (11), to a large extent precipitated by the advent of modern non-invasive technology such as TMS. Three schools of thought have developed pertaining to the role of the UMN, and related pathophysiological processes in ALS:

(i) "the *dying forward*" hypothesis; (ii) "the *dying back*" hypothesis and (iii) "the *independent degeneration*" hypothesis (Fig. 2).

The ***dying forward hypothesis*** proposed that ALS was primarily a disorder of the corticomotoneurons, which connect monosynaptically with anterior horn cells (25). Corticomotoneuronal hyperexcitability was postulated to induce anterior horn cell degeneration transsynaptically via an anterograde glutamate-mediated excitotoxic process (25, 94). This dying forward hypothesis was based on a number of poignant clinical observations including: (i) relative preservation of extraocular and sphincter muscles in ALS, postulated to be due to a paucity of corticomotoneuronal projections onto the motor nuclei innervating these muscles; (ii) absence of an animal model of ALS, ascribed to a lack of direct corticomotoneuronal-anterior horn cell connections (45, 169); (iii) rarity of pure lower motor neuron forms of ALS, with subclinical upper motor neuron dysfunction invariably detected with TMS studies (46); and (iv) the specificity of dissociated muscle atrophy (20, 21, 44), termed the split hand phenomenon in ALS remains best explained by a dying forward mechanism (44) (Chapter 1).

Utilising TMS technology, it is becoming increasingly apparent that cortical hyperexcitability develops as an early feature in sporadic and familial ALS, linked to the process of motor neuron degeneration (49, 50, 94, 122-126). Furthermore, longitudinal studies in asymptomatic SOD-1 mutation carriers established that cortical hyperexcitability developed prior to the clinical onset of ALS (50), a feature also reported in the G93A SOD-1 mouse model (128). In keeping with a cortical origin of ALS is the now accepted view that ALS and frontotemporal dementia (FTD) represent an overlapping continuum of the same disorder (170, 171), an observation further

underscored by recent genetic discoveries that increased hexanucleotide repeat expansions in the first intron of C9ORF72 gene (9p21) [*see below*] was associated with both ALS and FTD (172, 173).

Some have argued that the development of cortical hyperexcitability in ALS, is not a primary event, but rather a compensatory down-regulation of inhibitory control in order to compensate for spinal motor neuron loss (174). This possibility was investigated by undertaking cortical excitability studies in Kennedy's disease (KD), a slowly progressive, X-linked recessive inherited neurodegenerative disorder of motor and sensory neurons (175), resulting from increased expansion of the CAG repeat sequence (coding glutamine) in the androgen receptor (AR) gene (Xq11-12) (176). Threshold tracking transcranial magnetic stimulation (TMS) studies in KD patients revealed normal cortical excitability when compared to typical ALS patients. Furthermore, comparison of KD to a pure lower motor neuron variant of ALS (177, 178), termed flail arm variant ALS, established the presence of cortical hyperexcitability in the latter cohort of patients (178). Together, these findings suggest that the development of cortical hyperexcitability does not represent a simple down-regulation of intracortical inhibitory processes in ALS.

The ***dying back hypothesis*** proposed that ALS was primarily a disorder of the lower motor neurons, with pathogens retrogradely transported from the neuromuscular junction to the cell body where they exert their deleterious effects (179). Although some pathological studies have indirectly supported a dying back process (180-182), no pathogens of any type have been identified in relation to ALS. The presence of widespread dysfunction within the frontal cortex,

including the primary, supplementary and pre-frontal motor cortices in ALS remains difficult to reconcile with any dying back process (183-185). In addition, the absence of central pathology in other lower motor neuron disorders such as Kennedy's disease or poliomyelitis provides a further argument against a dying back process (51, 186).

The ***independent degeneration hypothesis*** suggests that the upper and lower motor neurons degenerate independently and concurrently (187). Limited neuropathological studies provide indirect support for independent degeneration whereby the degeneration of upper and lower motor neurons appeared to be independent (188, 189). These correlative morphological techniques, however, were significantly confounded by the anatomical and functional complexity of the corticomotoneuronal system (190). In particular, there remains considerable variability in the corticomotoneuronal to anterior horn cell ratio, due to synaptic changes, and as such, attempts to correlate upper and lower motor neurons as a "one-off" on autopsy studies are divorced from clinical and in-vivo reality (186).

Oxidative stress and SOD-1 gene

In concert with glutamate excitotoxicity, oxidative stress appears to be important pathophysiological mechanisms in ALS, in part as a result of mutations in the SOD-1 gene (94). Mutations in the SOD-1 gene, the first ALS gene reported and mapped to the long arm of chromosome 21 [21 q22.1] (191), was postulated to exert pathogenic effects by acquisition of aberrant cytotoxic enzyme activity (192-194). The SOD-1 gene spans 11 kilobases of genomic DNA, comprising five exons and four introns (195), and encodes a highly conserved 153-amino acid protein, which together with a catalytic copper (Cu) ion and a stabilizing zinc (Zn) ion form

a subunit (192, 195). A disulfide bridge stabilizes each subunit, and the two identical subunits combine through non-covalent bonds to form the Cu-Zn SOD-1 enzyme. The main function of the SOD-1 enzyme involves free radical scavenging whereby the enzyme catalyses the conversion of the superoxide anion to molecular oxygen and hydrogen peroxide, which in turn is reduced to water by glutathione peroxidase and catalase (160, 192, 196). The Cu-Zn SOD enzyme constitutes 0.5-1% of soluble protein in the brain and spinal cord, and is located within the cytosol, nucleus and between mitochondrial membranes (192, 197, 198).

To date, 166 SOD-1 mutations have been reported, underlying 14-23% of familial and 1-7 % of sporadic ALS cases (192, 199-202). The majority are missense mutations resulting in a single amino acid substitution and preserving the SOD-1 protein length, while nonsense or deletion mutations have also been reported that either introduce novel nucleotides or remove existing nucleotides resulting in alteration of the polypeptide length (192, 193, 203). Globally, the most frequent mutation is the substitution of aspartate for alanine (D90A), followed by alanine to valine (A4V) and isoleucine for threonine (I113T) (192, 193). An autosomal dominant pattern of inheritance is evident with most mutations, except for the D90A mutation, which may be transmitted in an autosomal recessive manner. Intra- and interfamilial variation in penetrance, age and site of disease onset, rate of disease progression and survival has been reported for most SOD-1 mutations(192), with approximately 50% of patients expressing the disease by age 43 and more than 90% by 70 years (192, 194, 199, 204-206). Some mutations, such as the I113T may be transmitted asymptomatically from grandparents to grandchildren (207, 208).

The pathophysiological mechanisms by which SOD-1 gene mutation leads to neurodegeneration remains enigmatic (90). Aberrant biochemical activity of the SOD-1 enzyme (toxic gain of function) has been suggested as a potential pathogenic mechanism in ALS (209-213). Specifically, SOD-1 mutations may induce structural changes regulating increased production of hydroxyl and free radicals (214, 215), as well as nitration of tyrosine residues on proteins (212, 216, 217). Evidence for oxidative damage has been inferred from biomarker and pathological studies in ALS patients (218-223) as well as studies in the transgenic SOD-1 mouse models (213). While oxidative damage seems an attractive pathogenic mechanism, findings of normal SOD-1 activity in some mutants (224), absence of correlation between dismutase activity and disease severity (225), and lack of beneficial effects of antioxidants in ALS patients (226), suggests that mechanisms other than oxidative stress may contribute to pathogenesis in ALS.

Alternatively, mutations in the SOD-1 gene may lead to conformational instability and misfolding of the SOD-1 peptide, resulting in formation of toxic intracellular aggregates. In the transgenic SOD-1 mouse model and human ALS cases, immunoreactive SOD-1 aggregates were reported in motor neurons and glial cells (210, 227, 228). Whether the intracellular aggregates were neurotoxic to motor neurons remains unknown, although a number of possible cytotoxic mechanisms have been proposed, including; (i) co-aggregation with vital cellular constitutes, (ii) inhibition of normal proteosomic function, and (iii) exerting mechanical or biochemical effects on the cell, such as disruption of axonal transport systems (90, 209, 210, 229).

Mitochondrial dysfunction

In conjunction with glutamate excitotoxicity and oxidative stress, there is mounting evidence that mitochondrial dysfunction exerts an important role in the pathophysiology of ALS (90, 230-235). Mitochondria are intracellular organelles whose main function is to generate energy for the cell in the form of ATP. Under conditions of excessive Ca^{2+} load, as may be evident with glutamate excitotoxicity (236), mitochondrial production of free radicals induces injury of critical neuronal cellular proteins and DNA. In addition, mitochondria remain sensitive to free radical damage at both the protein and DNA level, resulting in further mitochondrial dysfunction (237). Mitochondrial damage may in turn enhance glutamate excitotoxicity by disrupting the normal resting membrane potential, thereby resulting in a loss of the normal voltage-dependent Mg^{2+} mediated block of NMDA receptor channels (97, 160).

Mitochondrial degeneration and dysfunction has been reported in ALS patients and in the transgenic SOD-1 mouse model (232, 235, 238). Ultrastructural abnormalities of muscle mitochondria, paracrystalline inclusions, and abnormal cristae have been reported in ALS (231, 234, 239). Dysfunction of mitochondrial enzymes involved in energy generation, such as Cytochrome C Oxidase and respiratory chain complexes I and IV, as well as down-regulation of nuclear genes encoding mitochondrial components within the motor cortex have been reported in ALS (233, 234, 239-241). Of further relevance, mitochondrial dysfunction including reduction in protein import, impairment in Ca^{2+} sequestering ability and an exaggerated depolarizing response of the inner mitochondrial membrane to Ca^{2+} stimulation may occur in the pre-symptomatic stages of ALS (242-246). Ultimately, severe damage to the mitochondrial

membrane potential, respiration, and electron transfer chain ensues, resulting in reduced ATP synthesis and neurodegeneration (150).

The transportation and distribution of mitochondria within the neurons appears to be impaired in ALS (150). Mitochondria are normally highly mobile organelles, evident in both the axons and dendrites (247). The movement of mitochondria is regulated through Ca^{2+} signalling and synaptic activity (247). An increase in intracellular Ca^{2+} concentration, as occurs with glutamate excitotoxicity, interrupts the movement of mitochondria within the cell, in particular at the level of the synapse (248). Abnormalities of mitochondrial distribution and transport have been reported in ALS, with evidence of reduced distribution in the axons and more frequent pauses in mitochondrial movements (249). Importantly, the slow and fast axonal transport systems, vital for mitochondrial transport, seem to be impaired in ALS and have been linked to glutamate excitotoxicity (150, 249, 250). Ultimately, this interruption in mitochondrial mobility may result in depletion of energy supply in critical neuronal segments, essential for the maintenance of the resting membrane potential and generation of action potentials, with resultant neuronal degeneration.

From a therapeutic perspective, a recent phase II trial of dexpramipexole, a pharmacological agent that enhances mitochondrial function (251), was shown to be effective in slowing ALS disease progression and reducing mortality over a 24 week period potentially offering hope in ALS (252). Unfortunately, a phase III, multicenter international trial, undertaken to assess the clinical efficacy of dexpramipexole as add on therapy to riluzole in ALS, was shown to be ineffective (253).

Other molecular mechanisms

Other mechanisms like impairment of axonal transport systems (229, 254, 255), dysfunction of endosomal trafficking (229, 256-258) along with neuroinflammation (259-261) and endoplasmic reticulum stress response (262, 263) have all been implicated in ALS pathogenesis. While these mechanisms contribute to neurodegeneration, they appear to be secondary events in ALS.

Non-cell autonomous processes

An emerging concept in ALS pathogenesis pertains to non-cell autonomous processes, whereby neighbouring glial cells mediate motor neuron cell death (92, 95, 264). Studies in transgenic mouse models reported that modulation of mutant SOD-1 expressed in microglia, slowed disease progression (264). In addition, astrocytes expressing the mutant SOD-1 gene exerted toxic effects in cultured primary motor neurons(265, 266), and silencing of mutant SOD-1 genes in astrocytes significantly slowed disease progression (267). Importantly, non-neuronal cells appear to be important in regulating disease progression rather than initiating motor neuron disease (259, 264), and an interaction between motor neurons and non-neuronal cells seems to be critical in ALS pathogenesis (268-270). The mechanisms by which non-neuronal cells exert toxicity remain unclear, although multiple interacting mechanisms appear to be responsible (271). Specifically, impairment of passive properties of astrocytes, such as uptake or recycling of neurotransmitters and regulation of extracellular ion homeostasis, along with activation of microglia cells with consequently increased secretion of neurotoxic agents, such as glutamate and pro-inflammatory cytokines, appear to be important mechanisms (92).

Insights into pathogenesis from recent advances in ALS genetics

C9orf72 hexanucleotide expansion

A major advance in the genetic understanding of ALS pathogenesis occurred with the discovery of the dominantly inherited c9orf72 gene [increased hexanucleotide repeat expansion (GGGGCC)], which appeared to underlie over 40% of familial and 20% of sporadic ALS cases in the original series (172, 173), although subsequent studies have established a frequency of 4.1-8.3% of c9orf72 mutations in apparently "sporadic" ALS cases (272). This monumental discovery has radically altered the understanding of ALS pathogenesis, implying that ALS is a multisystem neurodegenerative disorder, rather than a pure neuromuscular disease (12), with potentially central origins. Underscoring this notion are findings that the c9orf72 hexanucleotide expansions are causative in both ALS and frontotemporal dementia (172, 173). Importantly, accumulation of TDP-43 along with p62 positive TDP-43 negative inclusions in hippocampus and cerebellar neurons appears to be the neuropathological hallmark of c9orf72 associated ALS and FTD (273), suggesting the existence of a common pathophysiological pathway.

The mechanisms by which c9orf72 gene expansion leads to neurodegeneration in ALS remains to be fully elucidated (172, 173), although three potential pathogenic mechanisms have been proposed, including (i) haploinsufficiency, (ii) repeat RNA-mediated toxicity and (iii) dipeptide protein toxicity related to repeat associated non-ATG (start codon) translation (RAN) of the expanded c9orf72 gene (274). Evidence for haploinsufficiency is suggested by studies reporting a reduction in the c9orf72 short and long isoforms in ALS patients (172, 173, 275), although a reduction in the corresponding c9orf72 protein is yet to be established. In addition, reduced expression of the c9orf72 transcript in the zebra fish model of ALS resulted in motor axonal

degeneration with locomotion deficit, providing additional support for the notion that haploinsufficiency may be a contributing factor in ALS pathogenesis (276).

Of further relevance, RNA-mediated toxicity, via sequestration of RNA-binding proteins, has also been proposed as a potential pathophysiological mechanism. Such a mechanism was inferred from observations of intranuclear RNA foci containing c9orf72 hexanucleotide repeats (173), and supported by findings that specific RNA-binding proteins (hnRNP A3 and ADARB2) associate with the c9orf72 expansion resulting in formation of intranuclear and cytoplasmic inclusions (277). More recently, studies utilizing induced pluripotent stem cell differentiated neurons from C9orf72 patients provided additional support for RNA toxicity, questioned the haploinsufficiency theory, and importantly established that the pathophysiological and pathological changes were mitigated by antisense oligonucleotide therapeutic approaches (278).

In addition, non-ATG related translation of the c9orf72 expansion, referred to as RAN translation(279), has also been proposed as a potential pathogenic mechanism (280, 281). Specifically, RAN translation results in generation of insoluble di-peptides (anti-C9RANT), which form intraneuronal (nuclear and cytoplasmic) inclusions within the CNS and appear to be specific for c9orf72 associated ALS/FTD (281). Given that neuronal degeneration and dysfunction may result from accumulation of insoluble proteins, and that C9RANT-positive pathology appears specific for c9orf72 related ALS/FTD, novel therapeutic strategies aimed at modulating such a process, including the aforementioned antisense strategies, may prove useful.

Transactive-region DNA-binding protein (TARDBP) and fused in sarcoma (FUS) Mutations in DNA/RNA-processing genes, transactive-region DNA-binding protein gene (TARDBP) (282) and fused in sarcoma (FUS) gene (283) have also been linked with development of ALS, representing 4-6% of familial and 0.7-2% of sporadic ALS (202, 284). TDP-43 and FUS are ubiquitously expressed proteins involved in DNA repair, regulation of RNA translation, splicing, transport, micro RNA biogenesis and formation of stress granules(274, 285-288). To date, approximately 50 mutations have been identified in each gene, and most mutations are dominantly inherited (282, 289). The mutations are localized to a highly conserve C-terminal glycerine-rich domain of the protein (282), while FUS mutations are located in the C-terminal nuclear localization signal domain that appears important in translocation of the FUS protein into the nucleus (289). The mutant proteins (TDP-43 and FUS) are redistributed from the nucleus to the cytoplasm, resulting in toxicity. Although most TARDBP and FUS mutation cases exhibit an ALS phenotype; association with FTD and Parkinsonism has been reported (290-297).

While the pathophysiological mechanisms by which mutations in these RNA-processing genes result in motor neuron degeneration remains to be fully defined, emerging evidence suggests the existence of multiple mechanisms including gain of toxicity, loss of nuclear function, or formation of large stress granules(274). Support for a toxic gain of function has been provided by studies in the transgenic mouse models, whereby increased expression of the mutated TDP-43 protein levels leads to neurodegeneration through dysfunction of cellular organelles and proteins(298-305). The severity of cortical and spinal motor neuron degeneration appears proportional to the TDP-43 protein levels (299), suggesting a potential role for TDP-43 in

regulating disease severity. Alternatively, loss of nuclear TDP-43 accompanied by accumulation of TDP-43 aggregates in the cytoplasm has been well established in ALS patients(306), implying a potential role for a TDP-43 loss of nuclear function mechanism in ALS pathogenesis. Emerging evidence from transgenic mouse models provides support for such a notion, whereby inactivation of the TARDBP gene leads to development of the ALS phenotype (307, 308). As with TDP-43, the finding of cytoplasmic FUS positive inclusions in ALS patients (283, 289) implies a loss of nuclear function of FUS as a potential mechanism in ALS pathogenesis. Support for such a notion was provided by studies demonstrating that expression of a FUS variant in transgenic mice, at lower levels than endogenous FUS, leads to selective motor neuron degeneration (309). Conversely, a toxic-gain of function of mutated FUS has also been inferred from studies demonstrating that expression of mutated FUS in *Caenorhabditis elegans* leads to progressive motor dysfunction in that could not be rescued by over expression of wild-type FUS (310).

Of further relevance, TDP-43 and FUS associate with cytoplasmic stress granules, that under physiological conditions function to temporarily suppress translation of mRNA and store pre-RNA complexes during periods of cellular stress, thereby safe-guarding the coded RNA information from deleterious chemicals (285, 311, 312). Pathological TDP-43 and FUS mutants appear to exhibit a greater propensity to associate with cytoplasmic stress granules and to form larger stress granules with altered dynamics (283, 285, 313-315). While the mechanisms by which altered stress granule dynamics induce neuronal degeneration in ALS remains to be fully elucidated, sequestration of RNA-binding proteins and repression of RNA translation along with formation of pathological inclusions have been proposed as potential mechanisms(285, 316-318).

Interestingly, a two-hit hypothesis has been proposed for FUS related ALS, whereby mislocalization of the mutated FUS protein may occur as the first step followed by cellular stress which induces formation of cytoplasmic inclusions and ultimately neurodegeneration (283, 317). Therapeutic interventions involving FUS or TDP43 are far more challenging and require a better understanding of the mechanisms of toxicity.

Other genes in ALS

Mutations in genes regulating ubiquitination (ubiquilin-2, UNC13A)(319, 320), endosomal trafficking [vesicle-associated membrane protein/synatobrevin-associated protein, charged multivesicular body protein] (256, 257, 321), autophagy and protein homeostasis (valosin-containing protein, optineurin, p62/SQSTM1) (322-324), have all been associated with ALS. These genetic mutations are dominantly inherited and appear to exert a pathogenic effect by disrupting the function of vital cellular processes ultimately leading to neurodegeneration (274).

Axonal Excitability Testing

Indirect information regarding resting membrane potential and axonal ion channel function may be gained through axonal excitability studies by using a technique called ***threshold tracking*** (85, 86). Threshold in this context refers to the stimulus current required to produce a specific potential. With threshold tracking, changes in the test stimulus current intensity required to generate a preset amplitude can be adjusted on-line to keep the target amplitude constant (*see Methodology*). Assessment of axonal excitability, and thereby axonal ion channel function, may provide unique insights into mechanisms underlying the generation of symptoms in ALS, such as fasciculations and cramps, as well as processes responsible for motor neuron degeneration in

ALS (56, 57, 325-327). Using a recently developed protocol, the following parameters of axonal excitability are measured: threshold; strength-duration time constant; rheobase; threshold electrotonus; current/threshold relationship; and recovery cycle.

(i) Threshold

Threshold is defined as the stimulus current required to activate an axon or to produce a compound muscle action potential of fixed size and can be used as a surrogate marker of membrane potential (85). Threshold may be utilised as a surrogate biomarker of membrane potential, whereby membrane hyperpolarization increases and depolarization decreases the membrane threshold. It should be stressed that threshold may not accurately reflect membrane potential, in conditions such as hyperventilation or nerve ischemia, and in such circumstances the ambiguity may be resolved by measuring other indices of axonal excitability (328-332).

(ii) Strength duration time constant and rheobase

The strength-duration time constant (τ_{SD}), also known as chronaxie, is a measure of the rate at which the threshold current for a target potential declines as the stimulus duration is increased (333-335). In human peripheral nerves, τ_{SD} can be calculated by using the ratio between stimulus-response curves for two different stimulus durations according to Weiss' formula (336). Rheobase is the threshold current (mA) for stimulus of infinitely long duration (85). Both the τ_{SD} and rheobase are properties of the nodal membrane, being dependent on passive membrane properties and persistent Na^+ channel conductances [I_{NaP}] (337).

Persistent Na^+ currents, which constitute 1-2% of the total Na^+ current (337-339), are conducted through voltage-gated Na^+ channels composed of one alpha (α) and four beta (β1-4) subunits (340, 341). The α subunits are organized in four homologous domains (I-IV), each consisting of six transmembrane α helices (S1-S6) and a pore loop located between the S5 and S6 segments that acts as a selectivity filter. The S4 segments of each domain functions as a voltage sensor. Inactivation of Na^+ channels is mediated by a short intracellular loop connecting homologous domains III and IV, which fold into the channel structure and blocks the pore from the inside during sustained membrane depolarization. Inactivation of I_{NaP} is either very slow or incomplete (342). To date, ten distinct Na^+ channel isoforms have been identified, Na_v 1.1 to Na_v 1.9 and Na_x (340, 341, 343), with I_{NaP} conducted by the Na_v1.6 isoform which is expressed at the nodes of Ranvier (340, 341, 343, 344).

Although the exact mechanisms underlying I_{NaP} are yet to be determined, it has been suggested that a uniform population of Na^+ channels may generate both transient and persistent Na^+ currents by switching between different gating modes (345). Phosphorylation of amino-acid residues within the alpha subunit of voltage-gated Na^+ channels may underlie these gating changes (346, 347).

The strength duration-time constant and rheobase may be influenced by the resting membrane potential, such that depolarization reduced the rheobase and prolonging the τ_{SD} , while hyperpolarization exerts the opposite effects. In addition, changes in nerve architecture, as may occur with axonal loss or demyelination, may also influence the τ_{SD}, as may discrete changes in nodal Na^+ conductances (348-351). In ALS, the τ_{SD} is prolonged, thereby suggesting that

upregulation of I_{NaP} may underlie the generation of fasciculations and cramping, as well as neurodegeneration (49, 56, 58, 59, 126, 351, 352).

(iii) Threshold Electrotonus

Threshold electrotonus describes the changes in threshold produced by long-lasting subthreshold currents and provides insight into into both nodal and internodal membrane conductances (86). Conditioning currents are subthreshold and do not trigger an action potential, but rather result in local changes in the membrane potential (85, 86). TE is usually measured with 1 ms current pulses, a duration which is long compared to the time constant of the nodes of Ranvier but short compared with the time constants of the internodal membrane and slowly activating ion channels (353). Changes in threshold current are measured at varying conditioning-time intervals in response to a subthreshold conditioning current (354, 355). Conventionally, TE is plotted such that an increase in excitability (threshold reduction) produces an upwards deflection and a decrease in excitability a downward deflection. This convention was adopted so that changes in threshold electrotonus would resemble the underlying changes in membrane potential. The threshold tracking protocol of axonal excitability testing utilizes test stimuli of 1-ms duration to produce the target CMAP response (40% of maximal) and changes in threshold induced by subthreshold polarizing currents of 100 ms in duration, set to + 40% (depolarizing) and − 40% (hyperpolarizing) of the control threshold current (354).

The initial fast response ("F" phase, Fig. 4) reflects rapid changes in threshold at the node of Ranvier, resulting from the application of either a depolarizing or hyperpolarizing subthreshold current. Subsequently, an "S1" phase develops, as indicated by slower changes in threshold over

tens of milliseconds in depolarizing and hyperpolarizing directions, and reflects the spread of current to the internodal membrane (Fig. 4). During depolarization, the S1 phase peaks at 20 ms after the onset of the current pulse, after which threshold begins to return to baseline, the S2 phase. This S2 phase occurs due to activation of nodal and internodal slow K^+ channels (86, 356).

In hyperpolarization, the S1 phase peaks at 100-150 ms after the onset of the subthreshold conditioning current and proceeds to return to baseline thereafter, termed the S3 phase (Fig. 4). The S3 phase probably reflects activation of inward rectifying currents (I_H) (85, 86, 357, 358). On termination of the subthreshold conditioning currents there is an overshoot of threshold with both depolarization and hyperpolarization. With depolarization, slow K^+ channels mediate the overshoot, while in hyperpolarization the overshoot is mediate by I_H.

Voltage-gated K^+ channels are members of the voltage-gated ion channel protein superfamily (359), and are composed of four alpha pore-forming subunits and accessory β subunits (360). Voltage-gated K^+ currents are activated by depolarization, and three types of currents have been identified, including two fast (I_{Kf1} and I_{Kf2}) and one slow current (I_{Ks}). The slow (S) channels underlie the S2 phase of TE, exhibit slower deactivating kinetics and are located at both the node and internode (357, 361-365). The main function of S channels is to limit inappropriate repetitive firing of axons after an action potential and to maintain the internodal resting membrane potential (361, 366).

Threshold electrotonus is influenced by changes in the membrane potential such that depolarization leads to a reduction in the S1 and S2 phases, termed "fanning in" appearance, and is due to activation of paranodal and internodal K^+ channels (85, 86, 367). Conversely,

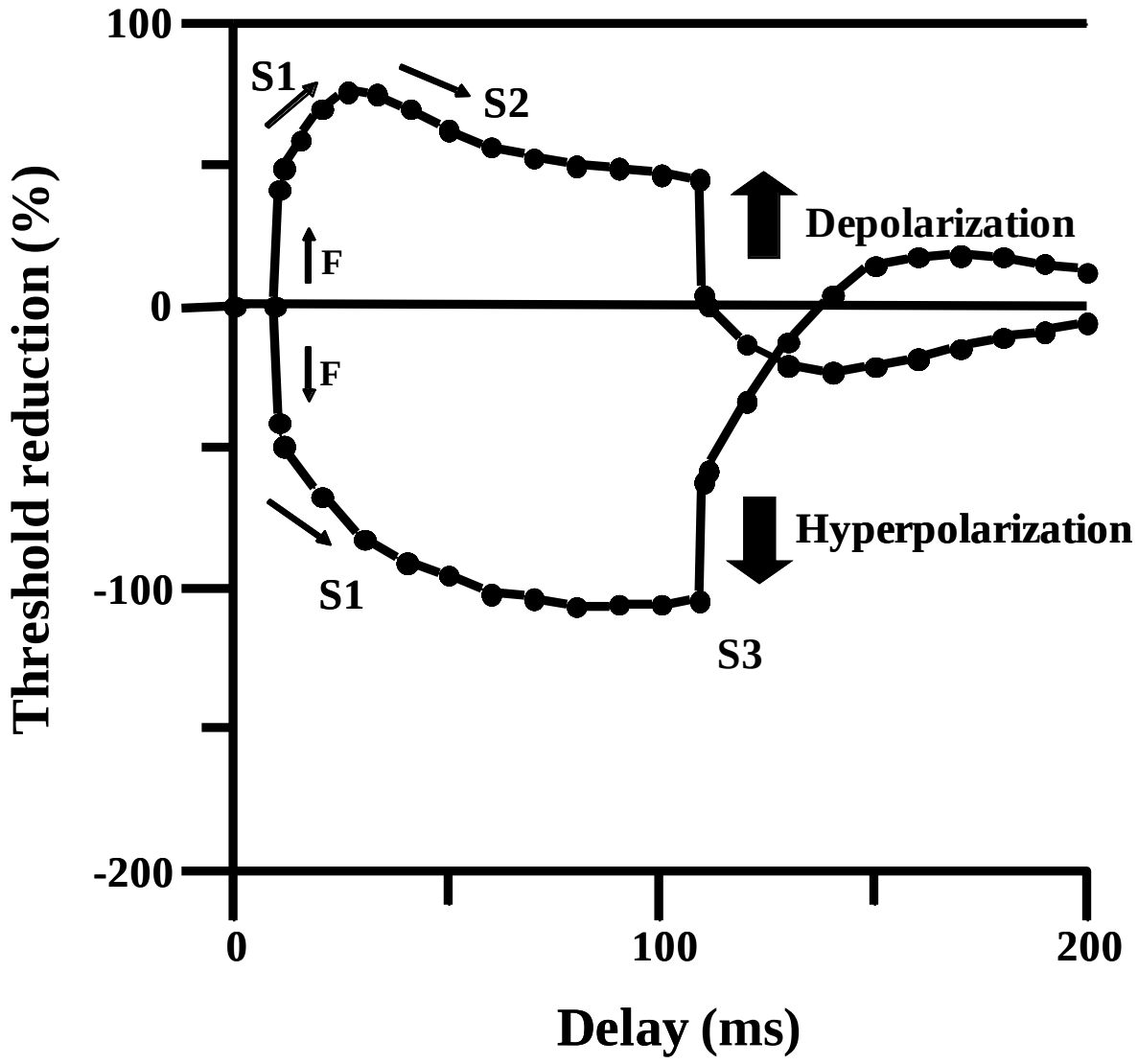

Figure 4: Threshold changes to polarising currents of 100 ms duration set to ± 40% of resting threshold. Changes are plotted with threshold reductions, with depolarisation represented as an upward deflection and hyperpolarization in a downward direction.

hyperpolarization closes the paranodal and internodal K^+ channels, thereby increasing the S1 and S2 phases producing a fanning out appearance (85, 86, 367).

Changes in TE were described in ALS, with two distinct responses previously reported, including (i) the *type I response*, whereby greater threshold reductions in TE were evident during depolarization and (ii) *type II response*, describing an unexpected rapid increase in threshold during depolarisation (56, 368). Reduction in internodal slow K^+ channel conduction was reported as the underlying mechanism. Importantly, abnormalities of TE have also been reported in autoimmune neuropathies, such as multifocal motor neuropathy (369), in metabolic and chemotherapeutic related neuropathies (357, 370-376).

(iv) Current threshold relationship (I/V)

The current-threshold relationship (I/V, Fig. 5) refers to changes in threshold occurring in response to long duration subthreshold currents (200ms duration) that are applied in a ramp like fashion from +50% (depolarizing) to −100% (hyperpolarizing) of the control threshold in 10% steps (354, 355). Conventionally, threshold increases are plotted to the left and threshold decreases to the right (Fig. 5). The I/V relationship estimates rectifying properties of both nodal and internodal axonal segments (86). The I/V gradient induced by depolarizing sub-threshold currents reflects conduction through outward rectifying K^+ channels, while the I/V gradient during hyperpolarizing sub-threshold currents reflects inwardly rectifying conductances [I_H] (86).

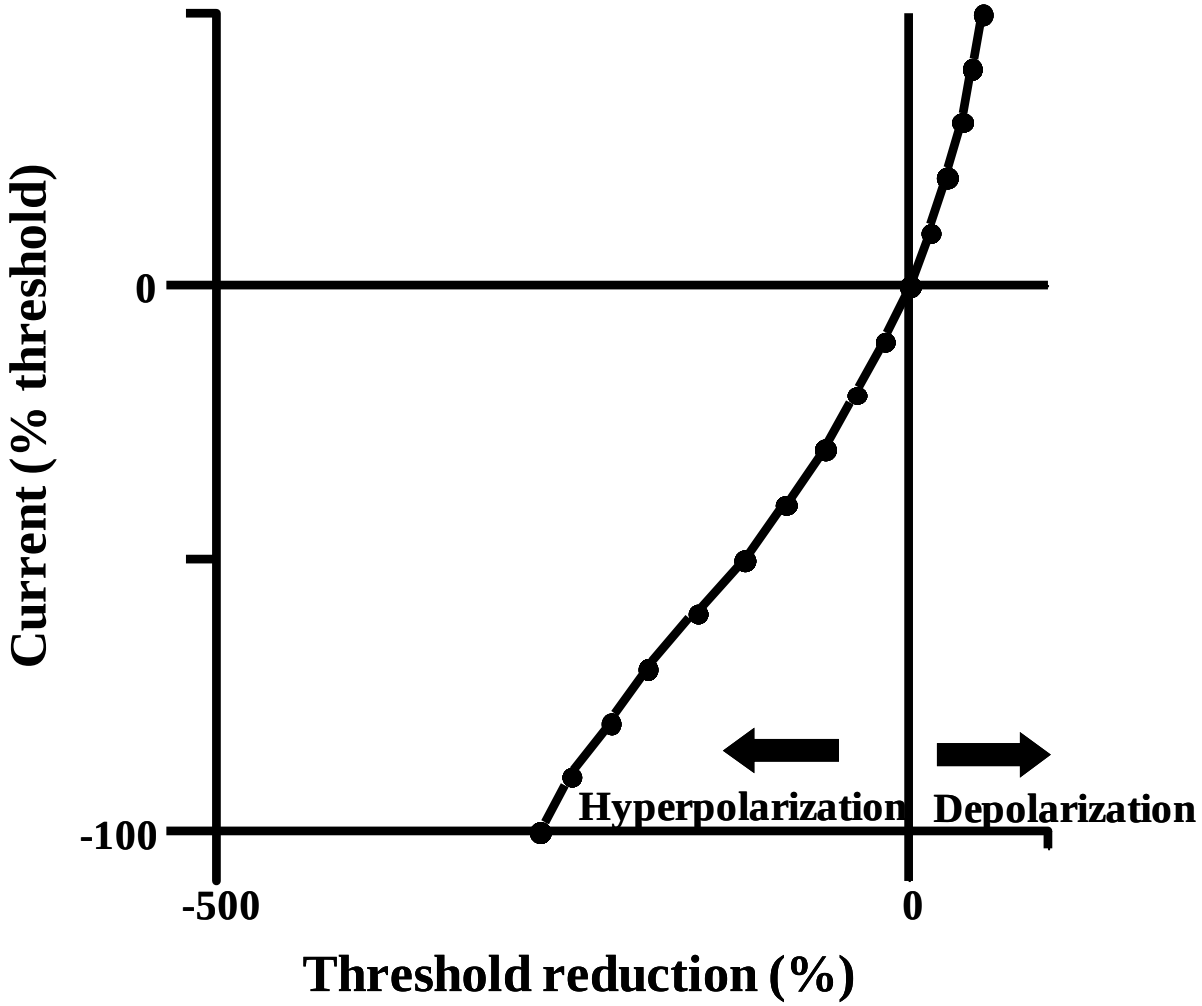

Figure 5: Current-threshold relationship: normalised threshold changes at the end of 200 ms duration currents are plotted, with depolarization represented to the right and hyperpolarization to the left. The conditioning current is varied from +50 % to –100 % of control threshold.

Two types of current underlie inward rectification (377). The first type, the classic inward rectifier, is a pure K^+ conducting channel, which is activated at membrane potentials negative to the K^+ equilibrium potential (378, 379). The second type of inward rectification is mediated by a channel that exhibits conductance for both Na^+ and K^+ (380, 381). This current begins to activate at between -45 mV and -60 mV and peaks at -110 mV(378, 382). The second I_H current activates and deactivates slowly, and the magnitude of the I_H current is also dependent on extracellular K^+ concentration (381).

A major function of internodal I_H is to limit axonal excitability in response to high-frequency activity (380). The I_H current may be critical in preventing conduction failure resulting from high-frequency activity which can induce failure of impulse conduction in axons with a reduced safety factor of transmission (383). Motor nerves may have a predilection to develop activity-dependent conduction failure when affected by disease, particularly primary demyelinating neuropathies (384, 385), in contrast to sensory nerves, due to the reduced expression of I_H in motor nerves (386, 387).

(v) The recovery cycle of axonal excitability

Following conduction of an action potential, axons undergo a series of stereotyped excitability changes known as the recovery cycle (Fig. 6). Initially, a period of total axonal inexcitability develops lasting for 0.5-1 ms during which the axon cannot generate an action potential, termed **absolute refractory period**. Subsequently, the axon enters a **relative refractory period (RRP)**, which may last for up to 4 ms, during which an action potential may be generated by a stronger than normal stimulus current. The RRP may be measured as either the point at which the

recovery cycle curve crosses the x-axis (ms) or as an increase in current required to generate a potential [termed refractoriness] (Fig 6).

The absolute refractory period results from inactivation of nodal voltage-gated transient Na^+ channels, while the RRP results from gradual recovery of these channels from inactivation (388). These transient Na^+ channels are of the $Na_v1.6$ isoform, and consist of alpha and beta (β) subunits (341), and exhibit "fast" activation and inactivation kinetics, namely the channels open rapidly with depolarization and inactivate rapidly (341, 389). Transient Na^+ currents appear to underlie the rapid phase of depolarization of the action potential (85).

Changes in membrane potential influence Na^+ channel kinetics, and thereby affect refractoriness (85). At resting membrane potential, ~ 30% of Na^+ channels are inactivated and with hyperpolarization there is a shift to reduce the degree of "inactivated" Na^+ channels leading to a decrease in refractoriness. Conversely, depolarizing increases the extent of Na^+ channel inactivation and thereby increases refractoriness (85). In addition, refractoriness is extremely temperature sensitive, with refractoriness being increased by reduction in limb temperature (390, 391).

Refractoriness is followed by a period of increased axonal excitability, termed **superexcitability**, which may last for ~ 15 ms and is mediated by re-excitation of the nodal membrane by the current spreading from the internodal membrane following an action potential, the depolarizing long-lasting after depolarization [DAP] (392). The amplitude and time course of DAP is limited

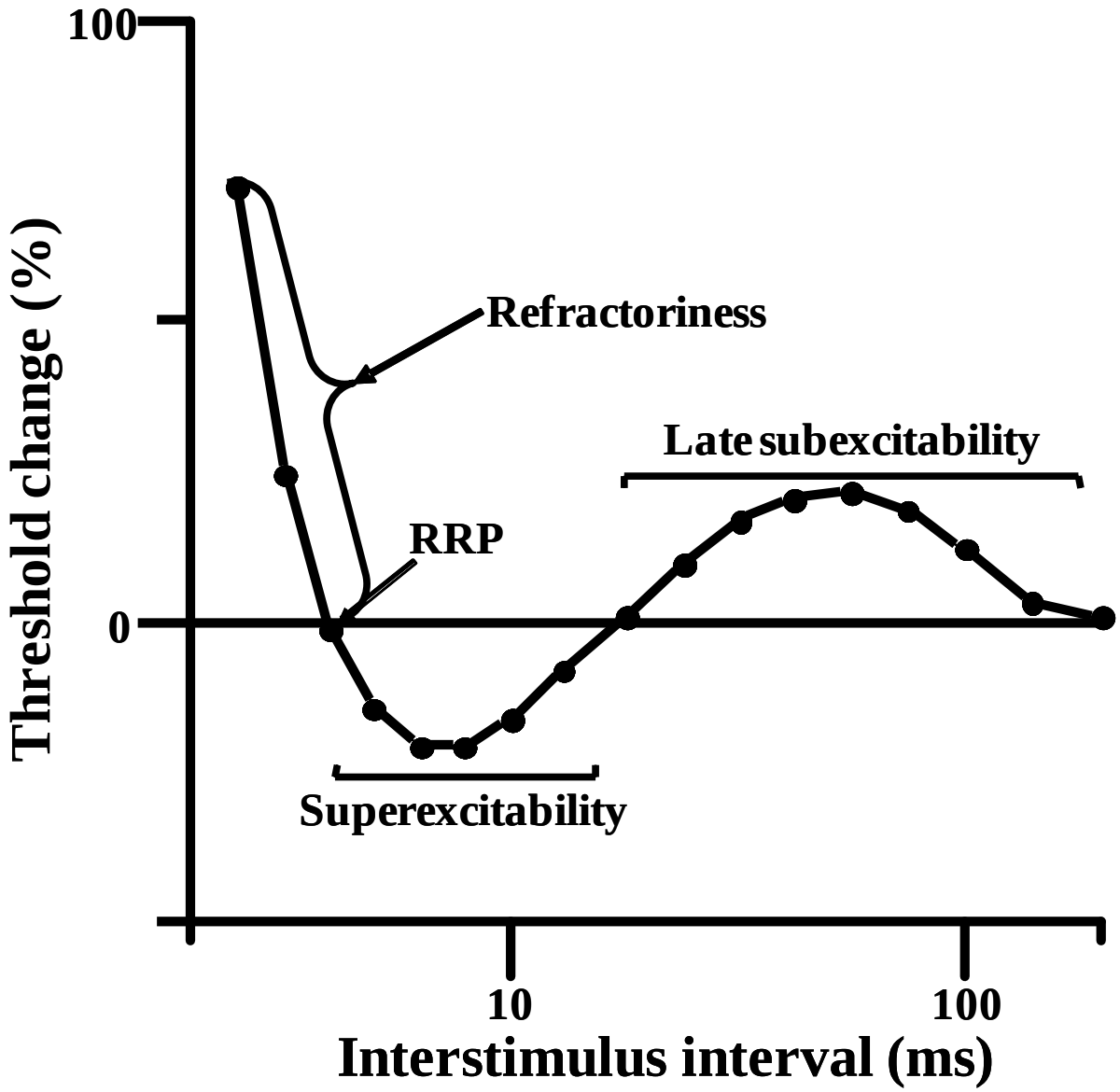

Figure 6: Recovery cycle of excitability is assessed by tracking the changes in threshold that occur following a supramaximal conditioning stimulus of 1-ms duration. RRP refers to the relative refractory period.

by activation of paranodal and juxtaparanodal K^+ channels, which serve to reduce the degree of DAP, and thereby superexcitability, by shunting the internodal current (393). Paranodal K^+ channels are classified into fast (F) channels and intermediate (I) channels (363, 364, 394). F channels are activated at potentials between -40 and +40 mV and deactivate very rapidly at potentials between -120 mV and -65 mV (365, 395, 396). In contrast, I channels are first activated by depolarization to around -70 mV, become fully activated at around -40 mV and deactivate slowly (396).

Superexcitability is influenced by changes in membrane potential, such that membrane depolarization reduces superexcitability by limiting Na^+ influx and increasing K^+ efflux through paranodal and juxtaparanodal fast K^+ channels (397). Conversely, membrane hyperpolarization increases DAP and therefore superexcitability. As such, superexcitability may be used as an indicator of membrane potential (354).

The last phase of the recovery cycle, referred to as **late sub excitability**, denotes a reduction in axonal excitability and lasts for ~ 100ms. Late sub excitability is mediated by activation of nodal slow K^+ channels (380) and is influenced by both the membrane potential and the K^+ equilibrium potential. Consequently, current induced membrane depolarization would serve to increase late sub excitability, while membrane depolarization secondary to increases in extracellular K^+ concentration, as may occur with ischemia or renal failure, will lead to reduction of late subexcitability (367, 370, 373, 398).

Assessment of cortical excitability

In order to assess the function of the central nervous system, and thereby shed further light on ALS pathophysiology, ***transcranial magnetic stimulation (TMS)*** was utilised. TMS is a relatively painless neurophysiological technique which non-invasively stimulates the human motor cortex, and was first described by Barker and colleagues (399).

Principles of magnetic stimulation

Magnetic stimulators consist of a capacitor, a device for storing charge, which when discharged, initiates a flow of current through a coil and generates a magnetic field. The magnetic field induces an electric field in a nearby conductor (cortical neurons), thereby resulting in current flow and neural stimulation (400, 401). The position at which the nerve is excited by magnetic stimulation depends on the voltage gradient parallel to the nerve fibre. Given that neural anatomy in the brain is complex, the point of excitation occurs at bends, branch points or at the transition from cell body to axon (402). As such, the orientation of neurons, relative to the induced electric field, is critical in determining which neurons are activated.

Importantly, the physical properties of the coil also influence neural excitation, such that circular coils induce maximum current at the coil circumference. Consequently, coils placed at the vertex, with the edge overlying the hand area, will preferentially stimulate the primary motor area. Of further relevance, the more focal "figure-of-eight coil", formed by two smaller adjacent circular coils, requires specific positioning and orientation over the motor cortex to ensure adequate activation (400, 401, 403). The direction of current flow will dictate which hemisphere is stimulated, with current flowing from a posterior-anterior direction (i.e. inion to nasion) most

effective at stimulating the motor cortex. For a circular coil positioned at the vertex, clockwise current in the coil (viewed from above) stimulates the right hemisphere (400, 401, 403).

From animal experiments it has been demonstrated that cortical stimulation results in generation of complex corticomotoneuronal volleys composed of direct [**D]-waves** (due to direct stimulation of the corticospinal axon) and multiple indirect [**I]-waves** arising from transsynaptic excitation of pyramidal cells via excitatory cortical interneurons (404). In humans, TMS activates the motor cortex at a depth of approximately 1.5 to 2.1 cm (405) and cervical epidural recordings have confirmed the presence of D and I-waves, at intervals of 1.5-2.5 ms (406, 407). The I-waves are numerically labelled such that the first I-wave is called I1, the second I2, the third I3 and so on (407). I-waves are best elicited by cortical currents directed in a posterior-anterior direction, whereas D-waves are produced preferentially if the current runs in a lateral to medial direction (408-412). The production of I-waves may not be sequential, such that I3 waves may be recruited initially, prior to prior to other I-waves, if the stimulating conditions are optimal (413). Although numerous models have been proposed to attempt to explain how I-waves are produced within the motor cortex, the mechanisms continue to remain elusive (414).

In the clinical setting, and for the purpose of this thesis, the assessment of cortical excitability and the integrity of corticospinal pathways are best assessed by measuring the following parameters: (i) threshold; (ii) motor evoked potential (MEP) amplitude; (iii) central conduction time; (iv) cortical silent period; and (v) short interval intracortical inhibition and facilitation.

(i) Motor threshold

Motor threshold (MT) reflects the ease with which corticomotoneurons are excited and is proposed to be assessed by the International Federation of Clinical Neurophysiology as the minimum stimulus intensity required to elicit a small (usually >50 μV) motor evoked potential (MEP) in the target muscle in 50% of trials (415). With recent adaptation of threshold tracking techniques, MT can also be measured as the stimulus intensity required to elicit and maintain a target MEP response of 0.2 mV (416-418). Motor threshold reflects the density of corticomotoneuronal projections onto spinal motor neurons, with intrinsic hand muscles exhibiting the lowest MTs due to the highest density of projections (419-421). MTs are lower in the dominant hand (421) and correlate with the ability to perform fine fractionated finger movements (422) as well as reflecting the density of corticomotoneuronal projections, MTs may also be a biomarker of cortical neuronal membrane excitability (405, 423, 424). Motor thresholds are influenced by the glutamatergic neurotransmitter system, through AMPA receptors, whereby excessive glutamate activity reduces MTs (425). In contrast pharmacological blockade of voltage-gated sodium channels raises MT (426). Of further relevance, MTs are influenced by the state of wakefulness and by the extent of target muscle activation (400, 427).

In ALS, abnormalities in MT have been inconsistent. While some TMS studies reported an increased MT or even an inexcitable motor cortex (428-435), others have documented either normal or reduced MT (49, 50, 122, 174, 436, 437). Importantly, longitudinal studies have established a reduction of MTs early in the disease course, increasing to the point of cortical inexcitability with disease progression (437). The early reduction in MTs appears most pronounced in ALS patients with profuse fasciculations, preserved muscle bulk and hyper-

reflexia (186). Fasciculations may precede other features of ALS by many months and taken in association with reduced MT may in some cases suggest a cortical origin of fasciculations (438). Glutamate excitotoxity along with reduced GABA inhibition may underlie the development of reduced motor thresholds in ALS. As such, a reduction of MT early in the disease process may supports an anterograde transsynaptic process, whereby cortical hyperexcitability underlies the development of progressive neurodegeneration.

(ii) Motor evoked potential (MEP Amplitude)

The MEP amplitude reflects a summation of complex corticospinal volleys consisting of D and I waves onto the spinal motor neuron (423, 439). At threshold, TMS elicits I-waves at intervals of 1.5 ms, that increase in amplitude with increasing stimulus intensity (439). The increase in MEP amplitude with increasing stimulus intensity may be utilised to generate a ***stimulus-response curve*** which follows a sigmoid function (440). The MEP amplitude reflects the density of corticomotoneuronal projections onto spinal and bulbar motor neurons (441), but probably assesses the function of cortical neurons that are less excitable or are positioned further away from the centre of the TMS field (401). In order to account for LMN dysfunction, the MEP amplitude should be expressed as a percentage of the maximum peripheral CMAP response (415). It should be stressed that the sensitivity, and thereby diagnostic utility of the MEP/CMAP ratio in detecting UMN dysfunction, is limited by a large inter-subject variability (401, 442).

The MEP responses may also be modulated by a variety of neurotransmitter systems within the central nervous system (441, 443). Specifically, GABAergic neurotransmission via $GABA_A$ receptors suppresses while glutamatergic and noradrenergic neurotransmission enhances the

MEP amplitude (444). Of interest, these changes in MEP amplitude occur independently of MT changes, suggesting that physiological mechanisms underlying the generation of the MEP amplitude and MT are varied.

In ALS, abnormalities of MEPs have been extensively documented (87, 401). Specifically, the MEP amplitude is reportedly increased in both the sporadic and familial forms of ALS, being most prominent in early stages of the disease process (31, 49, 50). In addition, the MEP amplitude correlates with surrogate biomarkers of axonal degeneration, thereby providing an association between cortical hyperexcitability and motor neuron degeneration (49, 126). The increase in MEP amplitude in ALS is not evident in mimic disorders, despite a comparable degree of LMN dysfunction, arguing against the notion that such increases represent simple cortical plasticity (51-53, 445).

(iii) Central motor conduction time (CMCT)

Central motor conduction time refers to the time from stimulation of the motor cortex to the arrival of corticospinal volley at the spinal motor neuron (415). Multiple factors contribute to the CMCT including, time to activate the corticospinal cells, conduction time of the descending volley down the corticospinal tract, synaptic transmission and activation of spinal motor neurons (446). The CMCT may be calculated by using either the F-wave method (see Methodology) or cervical (or lumbar) nerve root stimulation methods (447, 448). Given that both methods estimate the CMCT (400, 446), and that a variety of technical, physiological and pathological factors influence CMCT (446), a range of normative CMCT data exists.

In ALS, CMCT is may be prolonged in approximately 20% of cases (430, 437, 449), probably reflecting degeneration of the fastest conducting corticomotoneuronal axons and/or increased desynchronization of corticomotoneuronal volleys secondary to the axonal loss (436, 450, 451). Assessment of CMCT may be especially useful when UMN signs are equivocal (430, 437). The sensitivity of detecting a prolonged CMCT may be improved by recording from both upper and lower limb muscles, or from cranial muscles in ALS patients with bulbar-onset disease (87, 403, 435).

(iv) Cortical silent period (CSP)

The cortical silent period (CSP) refers to the interruption of voluntary electromyography (EMG) activity in a target muscle induced by a magnetic stimulation over the contralateral motor cortex (452). The CSP duration is measured from the onset of the MEP response to resumption of voluntary EMG activity (441, 452). Increases in magnetic stimulus intensity lead to more prolonged CSP duration (452-454).

The mechanisms underlying the development of CSP appear complex. The early segment of the CSP is mediated by spinal processes (453, 455), while the late segment of is mediated by long-lasting inhibitory post-synaptic potential (IPSP), generated via gamma-aminobutyric acid type B ($GABA_B$) receptors (401, 453, 455, 456), a notion supported by pharmacological studies (457, 458). $GABA_B$ receptors are metabotropic receptors that couple to Ca^{2+} and K^+ channels via G proteins and second messenger systems and are located at both the pre-and postsynaptic nerve terminals (459). Post-synaptic $GABA_B$ receptors mediate CSP by inducing an increase in K^+ efflux upon activation of a specific G-protein, thereby resulting in hyperpolarization of the

postsynaptic membrane (459). In contrast, presynaptic $GABA_B$ receptors mediate inhibition of voltage-gated Ca^{2+} channels resulting in inhibition of neurotransmitter release (460-462). In addition to being modulated by $GABA_B$ receptors, CSP is also influenced by density of the corticomotoneuronal projections onto motor neurons, motor attention, the extent of voluntary drive and other neuromodulators, such as dopamine (401, 426, 463, 464).

In ALS, abnormalities of CSP duration are well documented (441). Specifically, an unchanged or reduced CSP duration both have been reported in ALS, with CSP duration reduction being most prominent early in the disease process (49-51, 125, 174, 445, 449, 465-467). The reduction of CSP duration appears to be specific for ALS among neuromuscular disorders, being normal in Kennedy's disease, acquired neuromyotonia and distal hereditary motor neuronopathy with pyramidal features (51-53, 445). Although the mechanisms underlying CSP duration reduction in ALS remain to be fully established, decreased motor drive and reduced GABAergic inhibition, either due to degeneration of inhibitory interneurons or dysfunction of $GABA_B$ receptors, may underlie the reduction of CSP duration in ALS.

(v) Paired-pulse techniques

Transcranial magnetic stimulation may assess cortical excitability via a paired-pulse technique in which a conditioning stimulus modulates the effects of a second test stimulus. Several different paired-pulse paradigms have been developed (87, 401, 441), but use of *short interval intracortical inhibition (SICI)*, *intracortical facilitation (ICF)* and *long interval intracortical inhibition (LICI)* have been most frequently utilised in ALS clinical research as methods to

determine cortical excitability. For the purposes of the current thesis, the following discussion will focus on paradigms measuring SICI and ICF.

Short interval intracortical inhibition is measured via a paired-pulse paradigm, in which a subthreshold conditioning stimulus (set to 70 of RMT) is delivered at a pre-determined time intervals before a suprathreshold test stimulus (417, 468-470). In the original paradigm, the conditioning and test stimuli remained constant and the effects of the conditioning stimulus was measured by recording changes in the MEP amplitude. When the interstimulus interval (ISI) was set between 1-5 ms, the test response was inhibited ***(SICI)***. Increasing the interstimulus interval to between 7 and 30 ms resulted in the facilitation of the test response ***(ICF)*** (401).

There is compelling evidence that SICI and ICF originate at the level of the motor cortex (439, 470). Specifically, epidural recordings of descending corticospinal volleys with a reduction in the number and amplitude of late I-waves, namely I2 and I3, with I-wave suppression remaining up to an ISI of 20 ms, which is the typical duration of the inhibitory postsynaptic potential mediated through $GABA_A$ receptors (469, 471). Conversely ICF was associated with an increase in the I-wave amplitude, being reduced by $GABA_A$ receptor agonists (426). The inhibitory properties of the ionotropic $GABA_A$ receptors is related to selective gating of Cl^- ions resulting in hyperpolarization (472, 473). The $GABA_A$ receptors consist of five protein subunits arranged around a central pore, whereby each subunit consists of an extracellular N-terminal domain, followed by three membrane spanning domains (M 1-3), of which the M2 domain forms the pore channel, an intracellular loop and a fourth membrane spanning domain (M4) (474). Sixteen different subunits could potentially comprise the $GABA_A$ receptor, including $\alpha 1–6$, $\beta 1–3$, $\gamma 1–3$,

δ, ε, π and θ, with the α1β2/3γ2, α2β3γ2, and α3β3γ2 subunit combinations being the most frequent (474-476). Importantly, SICI appears to be mediated by $GABA_A$ receptors comprised of the alpha 1 subtype (477). Of further relevance, SICI and ICF are also modulated by other cortical neurotransmitter systems including glutamate (87, 478-480), dopamine (426, 481) and norepinephrine (426), and selective serotonin re-uptake inhibitors (482). Importantly, SICI and ICF appear to be physiologically distinct processes as evident by lower thresholds for activation of SICI and that SICI remains independent of the direction of subthreshold conditioning current flow within the motor cortex, while ICF appears to be preferentially generated by current flowing in a posterior-anterior direction (483).

A potential limitation of the original "constant stimulus" technique related to marked variability in the MEP amplitude with consecutive stimuli (469, 484). The variability of the MEP responses may in part relate to spontaneous fluctuations in the resting threshold of cortical neurons. To overcome this limitation, a ***threshold tracking technique*** was developed, whereby a constant target MEP response (0.2 mV) was tracked by a test stimulus (416, 417). Utilizing threshold tracking, two phases of SICI were identified (416, 417, 485, 486), a smaller phase at ISI ≤1 ms and larger phase at ISI 3 ms. Synaptic neurotransmission through the $GABA_A$ receptor has been shown to mediate the second phase of SICI (471, 487-489), however, the precise mechanisms underlying the first phase of SICI remains a matter of debate. It was initially suggested that the first phase of SICI reflected local excitability properties, particularly relative refractoriness of cortical axons, with resultant resynchronization of cortico-cortical and corticomotoneuronal volleys (416, 490). Subsequently, it was argued that synaptic processes may best explain the

development of the initial phase of SICI, possibly driven by activation of cortical inhibitory circuits that were distinct from circuits mediating the later SICI phase (485, 486, 491).
A reduction or absence of SICI, together with an increase in ICF, all indicative of cortical hyperexcitability, have been documented in sporadic and familial ALS patients (49-51, 53, 174, 290, 478, 492-495). Of relevance, cortical hyperexcitability appears to be an early feature in ALS, correlating with measures of peripheral neurodegeneration and preceding the clinical development of familial ALS (49, 50).

Abnormalities of SICI in ALS, are mediated by degeneration of inhibitory cortical interneurons (496) along with glutamate-mediated excitotoxicity (478, 480). Underscoring this notion that a complex pathophysiological process may underlie SICI abnormalities in ALS are findings of SICI reduction at low (40% of resting motor threshold (RMT), medium (70% of RMT) and high (90% of RMT) conditioning stimulus intensities (497). As such, preserving the integrity of intracortical inhibitory circuits, and counteracting excitatory cortical circuits, may serve as potential therapeutic options in ALS. Consequently, the current thesis will utilize novel cortical and axonal excitability techniques in sporadic ALS patients, in order to determine the pathophysiological processes underlying neurodegeneration in ALS, particularly whether cortical dysfunction precedes the development of LMN dysfunction and underlies the development of the split-hand sign.

METHODOLOGY

Subjects

The healthy subjects used as controls had no clinical evidence of a peripheral nerve disorder or any history of medical conditions known to affect peripheral nerve function. Further, they were confirmed to not be on medication which could alter the parameters of cortical excitability testing (426, 498-500). Patients with ALS with a history of other illnesses like diabetes mellitus, known to cause neuropathy were excluded from all axonal excitability studies. All patients were diagnosed with clinically possible, probable or definite ALS as defined by the Awaji criteria(82). All patients were followed up over the three year period to confirm the progression of disease and confirmation of the diagnosis. All patients and subjects gave written informed consent to the procedures, which had been approved by the Sydney West Area Health Service Human Research Ethics Committees and the University of Sydney Human Research Ethics committee.

Equipment

The following equipment was used to carry out the studies in this thesis:

Hardware requirements:

1) Personal computer fitted with a 16-bit data acquisition card (National Instruments PCI-MIO-16E-4) that sampled signals at 10 kHz.

2) Isolated linear bipolar constant stimulator (maximal output ± 50 mA) (DS5, Di
gitimer, Welwyn Garden City, UK)

3) Conventional non-polarisable 5-mm Ag-AgCl surface EMG electrodes (3M Healthcare, MN, USA) for stimulation and recording.

4) Preamplifier and filter (3 Hz-3 kHz) for recording sensory and motor potentials Nikolet-Biomedical EA-2 amplifier (Cardinal Health Viking Select version 11.1.0, Viasys Healthcare Neurocare Group, Madison, USA).

5) Electronic noise was further filtered by using a Hum Bug (Hum Bug 50/60 Hz Noise Eliminator, Quest Scientific Instruments, North Vancouver, Canada)

6) Two high-power magnetic stimulators which were connected via a BiStim device (Magstim Co., Whitland, South West Wales, UK).

7) Circular stimulation coil for transcranial magnetic stimulation (Magstim Company: High Power 90mm Coil -P/N9784-00)

8) Purpose built thermometer for measuring skin temperature.

9) Synergy EMG machine, Neurocare Group, Madison, USA.

10) 26 G concentric EMG needle (Dantec DCN™ Disposable Concentric Needle Electrodes)

Software requirements:

1) Data acquisition and stimulation delivery (both electrical and magnetic) were controlled by a computerised threshold tracking programme, QTRACS software version 16/02/2009 (© Professor Hugh Bostock, Institute of Neurology, Queen Square, London, UK).

2) Quantitative EMG was performed using the Multi-MUP software (Synergy EMG machine, Neurocare Group, Madison, USA)

Stimulating and Recording Paradigms

Peripheral nerve studies described in Chapters 1-5 were undertaken on motor axons of the median nerve (Fig. 7a) and or the ulnar nerve (Fig 7b,7c) using conventional non-polarisable 5-mm Ag-AgCl surface EMG electrodes (3M Healthcare, MN, USA). The median nerve was

stimulated electrically at the wrist, with the cathode placed at the wrist crease and the anode located in the mid-forearm. The resultant compound muscle action potentials (CMAPs) were recorded via surface electrodes with the active recording electrode positioned over the motor point of the abductor pollicis brevis (APB) and the reference electrode placed 4 cm distally(354) over the proximal phalanx of the thumb (Fig 7A). The ulnar nerve was stimulated electrically at the wrist with the cathode repositioned to the medial wrist crease lateral to the flexor carpi ulnaris tendon. CMAP amplitude was recorded over the first dorsal interosseous (FDI) muscle with the active electrode positioned over the motor point of the FDI while the reference electrode remained positioned approximately 4 cm distal at the base of the thumb (Fig 7B). Abductor digiti minimi (ADM) muscle CMAP recording was performed with the recording electrode positioned over the belly of the muscle and the reference electrode positioned approximately 4 cm distal on the little finger (Fig 7C). Peripheral nerve studies described in Chapter 7 and 8 with recording of CMAP over the flexor pollicis longus (FPL) muscle was performed with the active electrode positioned over the motor point of the FPL in the lateral forearm and reference electrode placed over the radial styloid and stimulation of the median nerve at the elbow. The baseline-to-negative peak amplitude and onset latency for the CMAP were determined.

Figure 7A

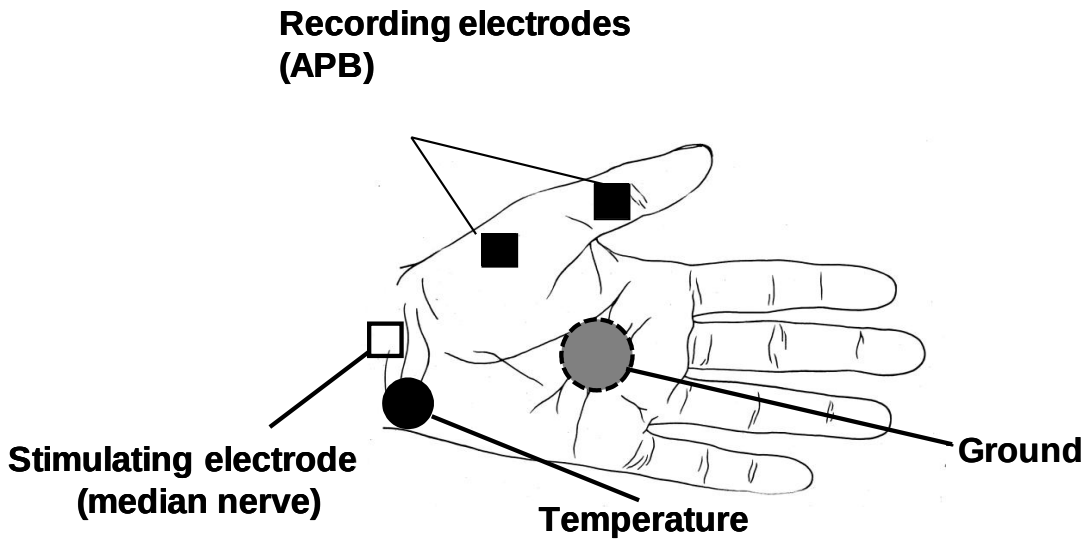

Figure 7B

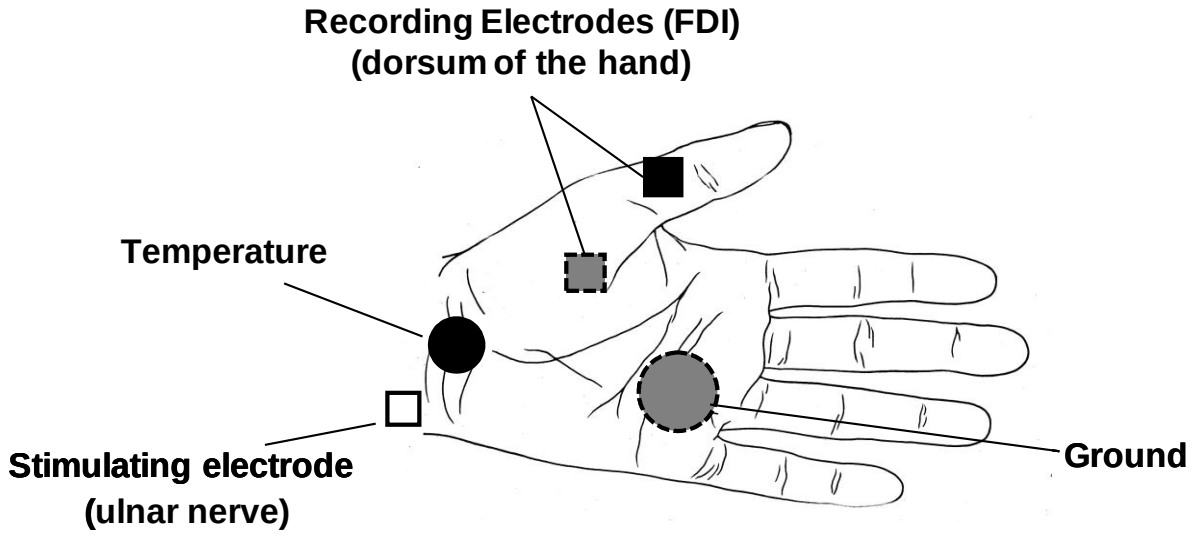

Figure 7C

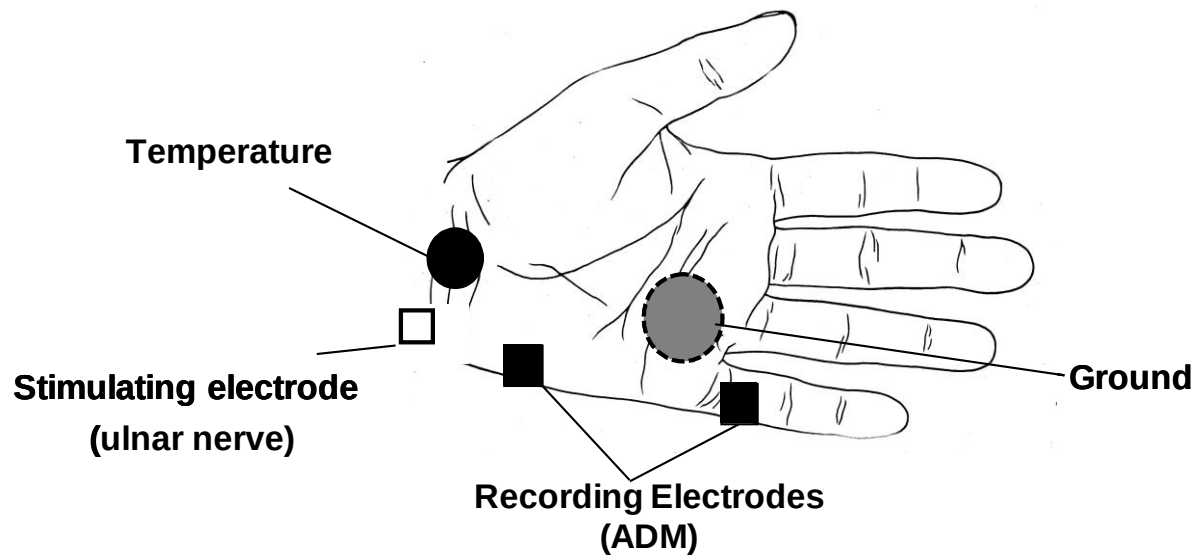

Figure 7:(A) Configuration of stimulating and recording electrodes for peripheral nerve stimulation. The median motor is stimulated at the wrist with recording over the abductor pollicis brevis muscle (APB) **(B)** Stimulating electrode is moved medially to be positioned over the ulnar nerve at the wrist with recording over the first dorsal interosseous (FDI) and **(C)** abductor digiti minimi (ADM) muscle. The motor evoked potentials are recorded over the three intrinsic hand muscles using the same recording electrode configuration.

Cortical excitability studies, described in Chapters 2,3,5,7,8 were performed by transcranial magnetic stimulation (TMS), whereby the motor cortex was stimulated by means of a 90 mm circular coil oriented to induce a current flow in a posterior-anterior direction in order to activate the motor cortex. The coil, initially centered over the vertex, was moved in the antero-posterior and medial-lateral directions in order to find the optimal position for evoking responses of maximal amplitude from the target muscle namely the abductor pollicis brevis (APB), first dorsal interosseous (FDI), abductor digiti minimi (ADM) and the flexor pollicis longus (FPL) muscle. The currents were generated by two high-power magnetic stimulators which were connected via

a BiStim device (Magstim Co., Whitland, South West Wales, UK) so that conditioning and test stimuli could be independently set and delivered through one coil. The magnetic evoked potentials (MEPs) were recorded using surface electrodes and the peak-to-peak amplitude and onset latency were determined for MEPs.

Threshold tracking and excitability protocols

Axonal excitability can be investigated using threshold tracking, where 'threshold' refers to the stimulus current required to produce a target potential (85, 86). Axonal excitability studies incorporating threshold tracking provide information about the membrane properties of axons at the site of stimulation. With threshold tracking, resting threshold is measured and nerve excitability is altered by changing the nerve environment, by applying a conditioning polarizing current(85). This technique provides information about membrane potential and axonal ion channel function.

The threshold tracking software used in this thesis was an automated tracking system whereby the test stimulus intensity was automatically increased or decreased in percentage steps after each response, depending on the difference between the recorded and target responses (Fig. 8). For measurement of multiple excitability parameters, an automated multiple excitability protocol, TRONDF version 16/02/2009 (© Professor Hugh Bostock, Institute of Neurology, Queen Square, London, UK) was used that contained a proportional tracking system, in which the change in test stimulus current intensity was proportional to the difference (or error) between the recorded response and target response. Proportional tracking can be more efficient, especially when excitability changes abruptly.

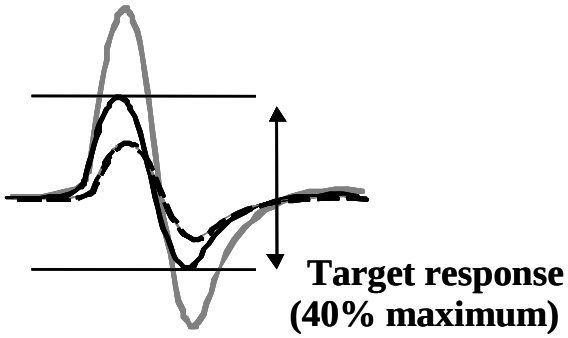

Figure 8: In threshold tracking, the target response is set to 40% of the supramaximal compound muscle action potential (CMAP) amplitude. When the CMAP amplitude is smaller than the target response (dashed black line), the subsequent test stimulus current intensity is increased. When the CMAP amplitude is larger than the target response (grey line), the subsequent test stimulus current intensity is reduced. If the CMAP amplitude is equal to the target response, the subsequent test stimulus intensity remains unchanged.

Multiple excitability measures: sequence of recordings

To commence the protocol, stimulus-response (SR) curves were generated using test current impulses of 0.2- and 1-ms (Fig. 9A, B). The peak amplitude, measured from baseline to negative peak, generated by the current intensity of 1 ms duration was used to set the target response (40% of supramaximal CMAP response). Stimuli were increased in 4% steps, with two responses averaged at each step until three averages were considered maximal. The ratio between the SR curves for two different stimulus durations that produced the same CMAP response were used to calculate the rheobase, defined as the threshold current for a target response when the stimulus is of infinitely long duration (85, 86), and strength-duration time constant (τ_{SD}; Fig. 9D) of motor axons of different thresholds using Weiss' formula (85, 86, 334).

The threshold changes that occur in response to subthreshold depolarizing and hyperpolarizing pulses, referred to as threshold electrotonus, were measured by altering nerve excitability using

prolonged sub-threshold polarizing currents of 100 ms duration, set to + 40% (depolarizing) and - 40% (hyperpolarising) of controlled threshold current(85, 86). Three stimulus combinations were tested sequentially: test stimulus alone (measured control threshold current); test stimulus + depolarizing current; test stimulus + hyperpolarizing current. Threshold was tested at 26 time points before, during and after the 100 ms polarizing pulse. The stimulus combinations were repeated until three valid estimates were recorded within 15% of target response(354).

A current-threshold relationship (I/V) was obtained by tracking the changes in threshold of 1 ms test pulses that occurred following sub-threshold polarizing currents of 200-ms duration which were altered in ramp fashion from +50% (depolarizing) to -100% (hyperpolarizing) of controlled threshold in 10% steps. Stimuli with conditioning currents were alternated with test stimuli until three valid threshold estimates were recorded. The I/V relationship estimates rectifying properties of both nodal and internodal segments of the axon(380, 501). The I/V gradient during depolarizing sub-threshold currents reflects conduction through outward rectifying K^+ channels, while the I/V gradient during hyperpolarizing sub-threshold currents reflects inwardly rectifying conductances activated by hyperpolarization(354, 378).

Finally, the recovery of axonal membrane excitability, referred to as the recovery cycle, was assessed by tracking the changes in threshold that occurred following a supramaximal conditioning stimulus of 1 ms duration. Eighteen conditioning-test stimulus intervals were studied, decreasing from 200 to 2 ms. Three stimulus combinations were recorded: (i) unconditioned test stimulus (1 ms duration); (ii) supramaximal conditioning stimulus alone; (iii) conditioning and test stimuli in combination. The response in (ii) was subtracted on-line from

response in (iii) so as to eliminate contamination of the measured CMAP response by the supramaximal conditioning response at short interstimulus intervals. Each stimulus combination was repeated until 4 valid estimates were obtained(354).

Following completion of the recovery cycle, a profile of nerve excitability was generated using a customized plotting program (QTRACP version 16/02/2009), consisting of six different plots (Fig. 9A-F). The 95% confidence limits were calculated as mean ± $t_{0.05}$ SD (where $t_{0.05}$ is the value of Student's t-test which the probability of a larger value is 0.05) such that 95% of individual observations would fall within the limits if the variables were distributed normally. For data plotted on logarithmic axes (Fig 9A, 9F), the logarithm of the variable was assumed to be normally distributed, and the mean plotted is the geometric mean. Differences in excitability parameters were analysed using Student's t-test. A probability (P) value of < 0.05 was considered statistically significant. All results are expressed as mean ± standard error of the mean.

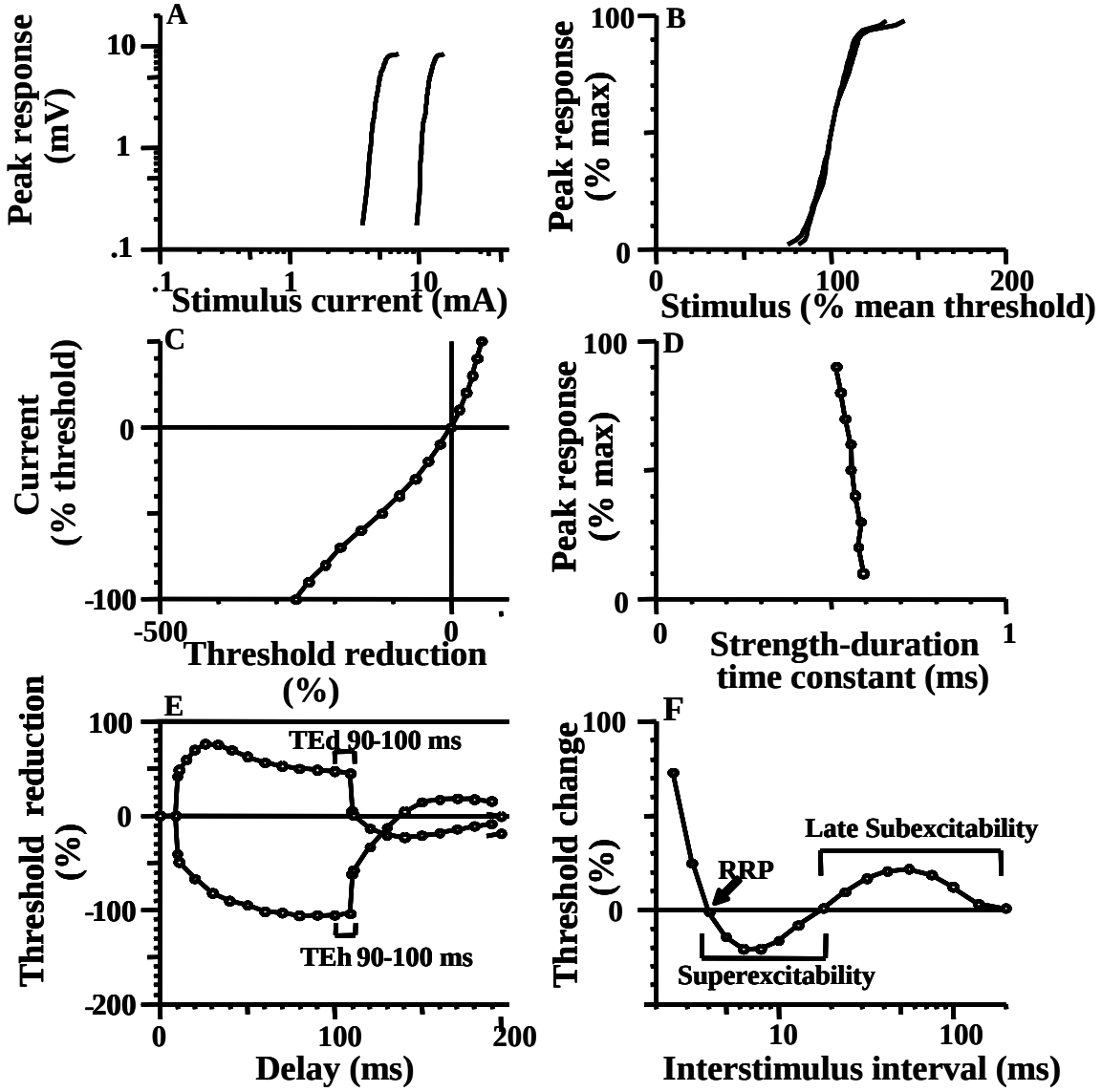

Figures 9: Six plots of excitability parameters recorded from abductor pollicis brevis muscle for a single subject. **(A)** Absolute stimulus-response relationship. **(B)** Normalised stimulus-response relationship. **(C)** Current-threshold relationship. **(D)** Strength-duration time constant. **(E)** Threshold electrotonus. The conditioning-test interval corresponding to hyperpolarising threshold electrotonus at 90-100 ms (The 90-100 ms) and depolarising threshold electrotonus at the same time interval (Ted 90-100 ms) are depicted. **(F)** Recovery cycle, demonstrating the time point at which the relative refractory period (RRP) is measured, as well as superexcitability and late subexcitability.

Upon completion of the excitability protocol, values for multiple excitability measures were automatically generated. The stimulus intensity (mA) was measured as the current required to elicit a target response set to 40% of maximal CMAP for a stimulus of 1 ms duration. Strength-duration time constant (ms), which reflects nodal persistent Na^+ conductances(502), was calculated for nine motor axonal populations, starting from axons contributing to CMAP responses between 5-15% up to the maximum of 85-95%, increasing in 10% batches(354) Rheobase (mA), defined as the threshold current for a target response when the stimulus is of infinitely long duration, was also calculated. Stimulus-response slope was calculated from the normalized SR curves by subtracting the stimulus that evoked a 25% maximal CMAP response from that which evoked a 75% response and dividing the result by the stimulus evoking a 50% response.

Threshold electrotonus parameters were calculated from data in Fig. 9E. TEd (peak) refers to the peak threshold reduction produced by a subthreshold depolarizing current. The reduction in threshold was measured at three time points relative to onset of the subthreshold depolarizing current, i.e. at 10-20 ms, TEd (10-20 ms), 40-60 ms TEd (40-60 ms), and at 90-100 ms TEd (90-100 ms). Threshold changes were also measures at similar latencies following a subthreshold hyperpolarizing current and are referred to as TEh (10-20 ms) and TEh (90-100 ms). S2 accommodation was calculated as the difference between the peak threshold reduction in the depolarizing direction and the plateau value, i.e. TEd (peak) – TEd (90-100 ms). The peak threshold increase at the end of depolarizing current and peak threshold reduction at the end of hyperpolarizing current were averaged over 20 ms and are referred to as TEd (undershoot) and TEh (overshoot).

From the I/V graph, the following parameters were recorded; (i) resting I/V slope, calculated from polarizing currents between +10% to -10%, minimal I/V slope, calculated by fitting a straight line to each three adjacent points in turn, and (iii) hyperpolarizing I/V slope, calculated from polarizing current between 0-100%.

For the recovery cycle of axonal excitability the following parameters were measured; (i) relative refractory period (RRP, ms), defined as the first intercept at which the recovery curve crosses the x-axis; (ii) superexcitability, expressed as a percentage reduction in threshold current, was calculated as the minimum mean of three adjacent point at conditioning-test intervals of 5-15 ms and (iii) late subexcitability (%), as the maximum mean of three adjacent points at interstimulus intervals > 15 ms.

Normative values for these parameters have been established for the median nerve motor axons(56, 354); while normative values for the ulnar motor axons to the FDI and ADM muscles were established as part of the current project(503).

Cortical excitability studies

For studies assessing cortical excitability described in Chapters 2, 4, 5, 7 and 8; TMS was applied to the motor cortex by means of a 90 mm circular coil oriented to induce a current flow in a posterior-anterior direction in order to activate the motor cortex. The coil, initially centered over the vertex, was moved in the antero-posterior and medial-lateral directions in order to find the optimal position for evoking responses of maximal amplitude from the target muscle. The currents were generated by two high-power magnetic stimulators which were connected via a

BiStim (Magstim Co., Whitland, South West Wales, UK) so that conditioning and test stimuli could be independently set and delivered through one coil.

TMS threshold tracking (Fig. 10)**:** Paired pulse cortical stimulation was performed using the threshold tracking TMS protocol(417). Briefly, the output (MEP response) was fixed and changes in the test stimulus intensity required to generate a target response, when preceded by either sub- or suprathreshold conditioning stimuli, were measured. This technique is analogous to that used in the assessment of peripheral nerve excitability.

Fisher and colleagues (2002) established that the relationship between the logarithm of the MEP amplitude and the stimulus was close to linear over a hundred-fold range of responses, from about 0.02 to 2 mV(504). Based on these observations a small target response of 0.2 mV (±20%), in the middle of this linear range, was selected for the present study and subsequently tracked. Resting motor threshold (RMT) was defined as the stimulus intensity required to produce and maintain the target MEP response (0.2 mV peak-to-peak)(417).

Initially, the SR curve for cortical stimulation was determined by increasing the intensity of the magnetic stimulus to the following levels: 60, 80, 90, 100, 110, 120, 130, 140 and 150% RMT. Three stimuli were delivered at each level of stimulus intensity. The maximum MEP amplitude (mV) and MEP onset latency (ms) were recorded. Central motor conduction time (CMCT, ms) was calculated according to the F-wave method(505, 506).

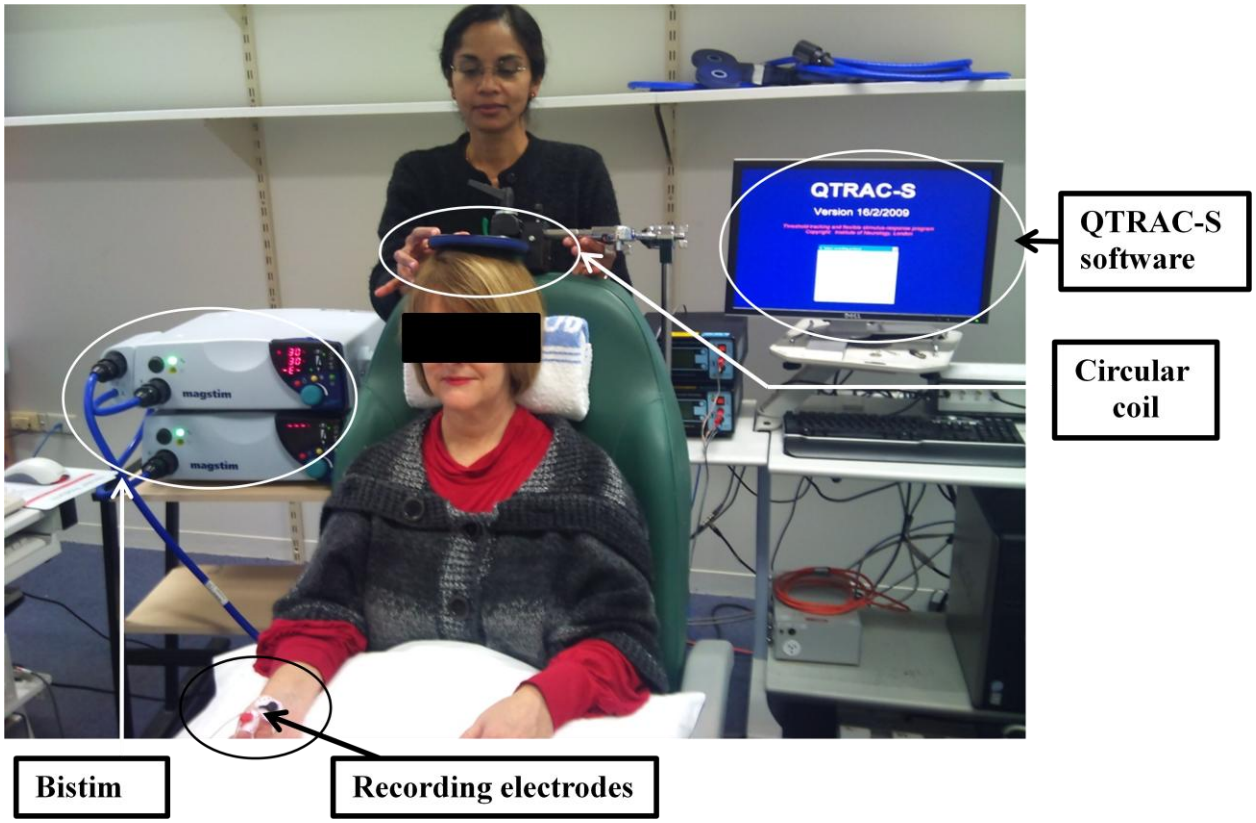

Figure 10: Threshold tracking transcranial magnetic stimulation: equipment and recording configuration.

The cortical silent period (CSP) induced by single-pulse TMS was recorded while performing a weak voluntary contraction, estimated by the investigators as representing 10-30 % of maximum voluntary contraction. Audio feedback was provided to the subject to sustain the contraction at the required force while the magnetic stimulus intensity was varied as for the SR curve. The duration of the silent period was measured from the beginning of MEP to the return of EMG activity(507).

A paired-pulse paradigm was developed(417) whereby a subthreshold conditioning stimulus preceded a suprathreshold test stimulus at increasing interstimulus intervals (ISIs) as follows: 1, 1.5, 2, 2.5, 3, 3.5, 4, 5, 7, 10, 15, 20, and 30 ms. The subthreshold conditioning stimulus (70% RMT) was such that it did not evoke a response. Stimuli were delivered sequentially as a series of three channels (Fig. 11): channel 1 tracked the stimulus intensity required to produce the unconditioned test response (i.e., RMT; shown in Fig. 12A,B); channel 2 monitored the subthreshold conditioning stimulus so as to ensure that an MEP response was not produced and that the subject remained relaxed; and channel 3 tracked the stimulus required to produce the target MEP when conditioned by a subthreshold stimulus equal in intensity to that on channel 2. Tracking was deemed acceptable when the test stimulus produced two consecutive MEP responses that were within 20% of the target response (0.2 mV) or consistently oscillated about the target. The three channels were applied sequentially. Stimuli were delivered every 5-10 seconds (stimulus delivery was limited by the charging capability of the BiStim system) and the computer advanced to the next ISI only when tracking met the target criteria. Precision of the tracking method was limited by the fact that the intensity of the magnetic stimulus was restricted to integral values from 1% to 100% of maximum stimulator output.

Intracortical inhibition induced by a conditioning stimulus was measured as the increase in the test stimulus intensity required to evoke the target MEP. Inhibition was calculated off-line using the following formula(504):

Inhibition = (Conditioned test stimulus intensity – RMT)/RMT * 100
Facilitation was measured as the decrease in the conditioned test stimulus intensity required to evoke the target MEP.

Each data point was weighted (QTRACS software version 16/02/2009) such that any measures recorded outside the threshold target window (0.2mV, peak-to-peak) contributed least to the data analysis. All results are expressed as mean ± standard error of the mean. Student t-test was used for assessing differences between two groups. Analysis of variance (ANOVA) was used for multiple comparisons to assess the difference between the conditioned test and unconditioned test stimuli at different ISIs. A probability (P) value of < 0.05 was considered statistically significant.

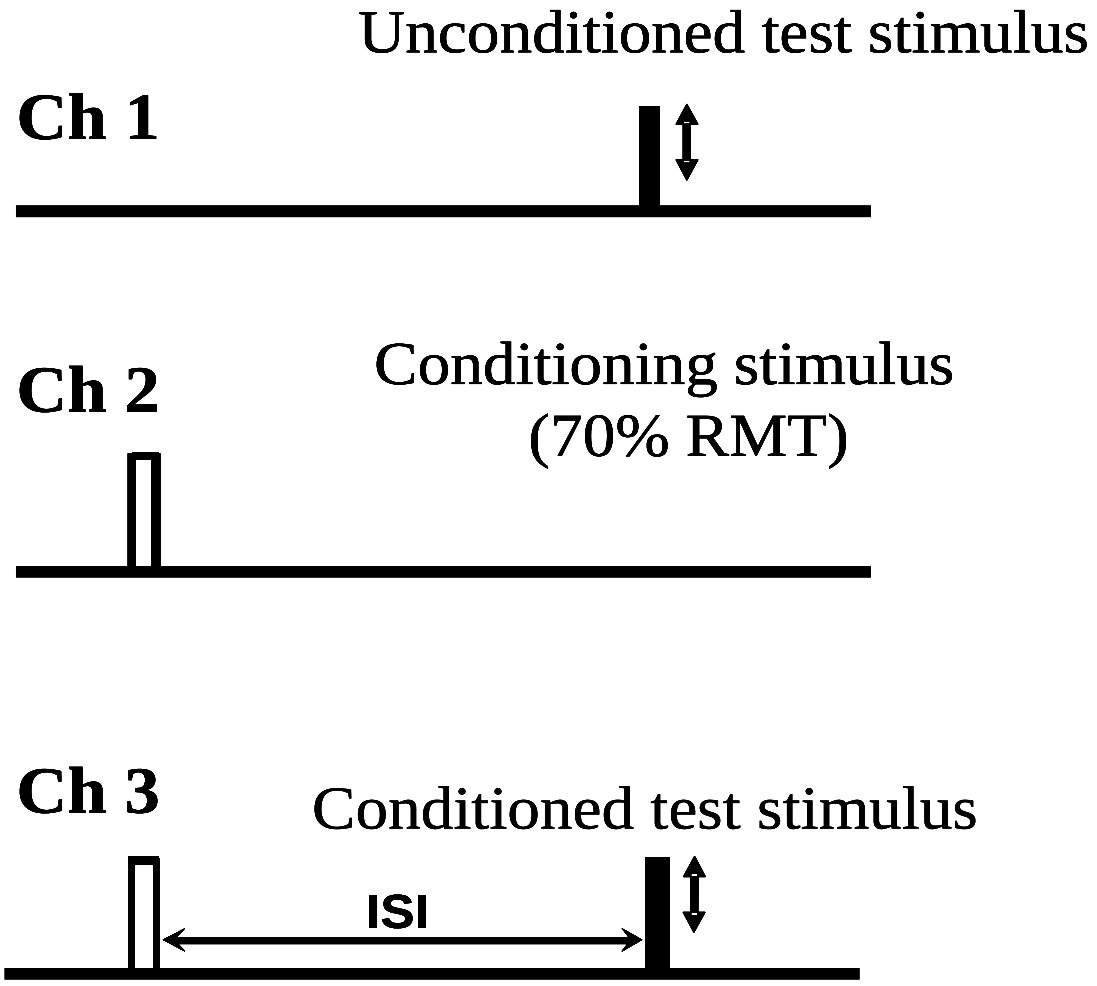

Figure 11: Experimental paradigm and configuration of stimulus patterns used in Chapters 4-8. Cortical excitability was assessed by measuring changes in stimulus intensity required to generate a target magnetic evoked potential response of 0.2 mV, recording over the abductor pollicis brevis. Channel 1 = unconditioned test stimulus, measuring resting motor threshold (RMT); Channel 2 = conditioning stimulus, which was set to subthreshold (70% RMT) when assessing short interval intracortical inhibition; Channel 3 = conditioned test stimulus at different interstimulus intervals (ISIs). SICI was measured by increasing ISI from 1-30 ms. *Reproduced with permission S.Vucic 2007*

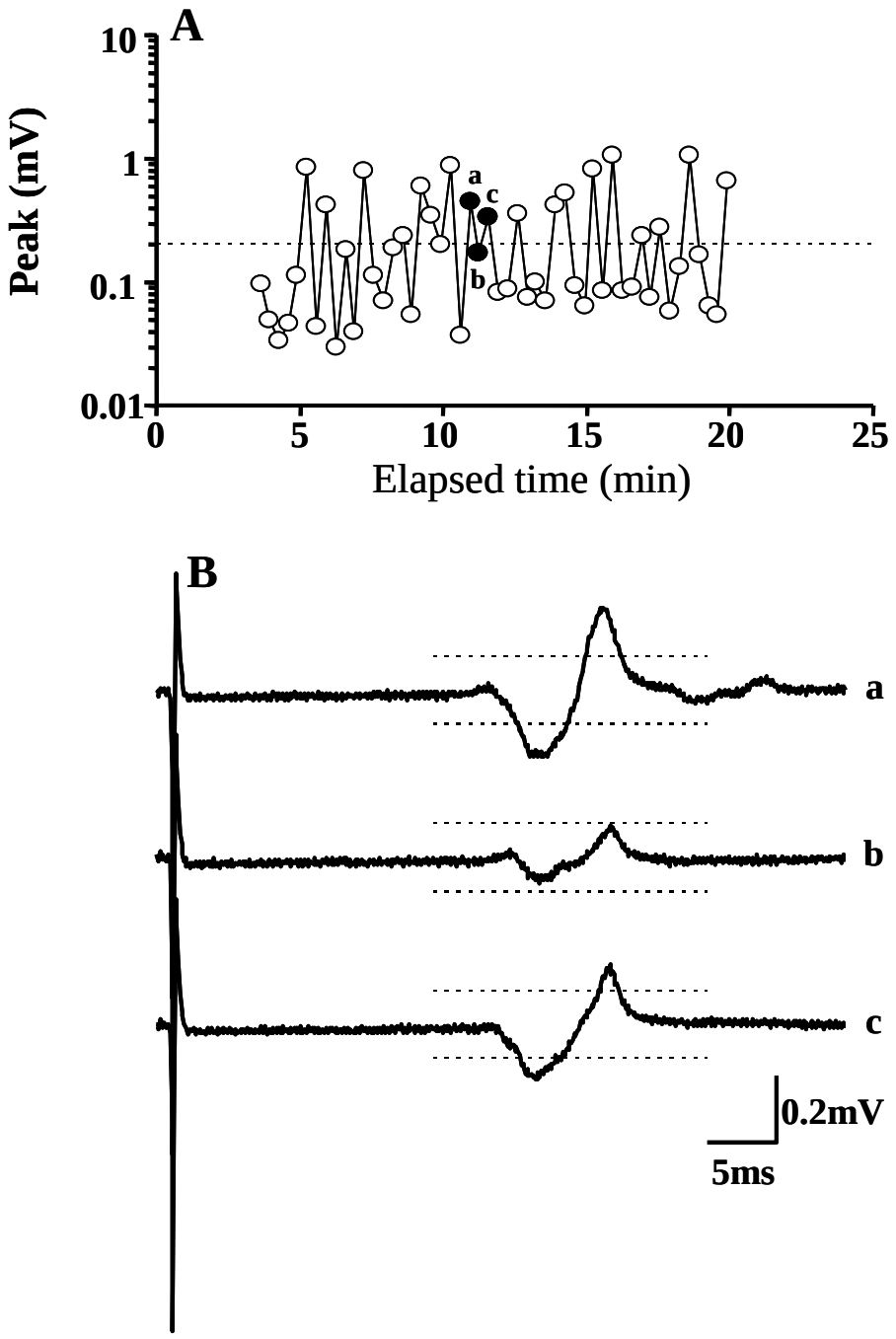

Figure 12: **(A)** Illustration of threshold tracking. The dashed horizontal line represents the target output of 0.2 mV which was "tracked". The circles (clear and filled) represent the magnitude of the motor evoked potential (MEP) amplitude with each stimulus. **(B)** Illustration of three MEP responses of different amplitude. The MEP response is initially larger **(a)**, then smaller **(b)**, and again larger **(c)** then the target output of 0.2 mV in three consecutive stimuli. These are depicted as filled circles in Figure A. The dashed horizontal lines represent the tracking windows, which were set to 0.2 mV (peak-to-peak). *Reproduced with permission S.Vucic 2007*

Multi MUP technique of Quantitiative EMG

Motor unit potential (MUP) analysis for compensatory renervation, which may be an early feature of LMN involvement in ALS (73), was performed in the experiment detailed in Chapter 5.The Multi MUP technique was utilised which is an automated decomposition technique of EMG analysis based on a multiple template matching technique, which makes it possible to identify several clearly definable MUPs from each recording site. It is not used primarily to study their firing pattern; hence it is considered quite acceptable that some MU discharges are not identified in the epoch. The method is called multi-MUP analysis since many different MUPs are usually obtained from each recordings site (508-510).

Multi MUP acquisition involved EMG recording from an electrode position with crisp EMG signal with filter settings of 5 Hz for high pass and 10 kHz for low pass with a free running sweep. Muscle contraction was maintained at 5-30% of maximum force and several MUPs were seen which were separated from each other by a discernible baseline. The recording was continued without needle movement during the analysis epoch (5-10 s). One to two skin insertions were required and a few different sites were sampled with each insertion. Roughly more than 20 MUPs are collected, with the aim of having at least 20 MUPs after editing. Duration of recording averaged about 3-5 min (508, 510).

Multi MUP analysis Signals with amplitude exceeding 50μV and a short rise time (Fig 13) were identified and each identified MUP was checked against previous templates for classification. The new MUP was considered to match a template when the difference in shape was less than a

predefined value.

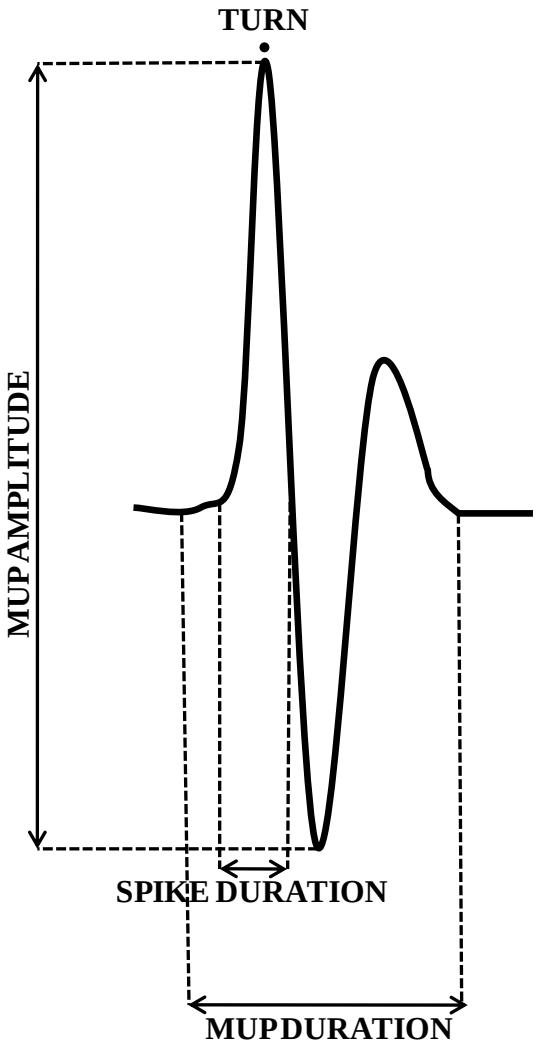

Figure 13: representation of a motor unit with the parameters of significance to distinguish pathological states from normal controls

Identical MUPs formed a class while unmatched MUP's were taken as the template for a new class. At each recording site, the classes were sorted in descending order of the number of matches and six classes with the highest number of matches were averaged. Classes must contain more than a predetermined number of data to be accepted and the

individual MUPs and the averaged MUP were displayed superimposed. Each detected discharge of the averaged MUP was displayed on the time axis.

MultiMUP editing MUPs that were duplicates and those with a noisy baseline or other obvious artifacts were first deleted. Among the remaining MUPs, the automatic duration cursor setting was manually corrected if necessary.

Clinical Scores in Amyotrophic Lateral Sclerosis

A neurological history and physical examination were undertaken in all ALS patients. All ALS patients were clinically staged using the amyotrophic lateral sclerosis functional rating scale-revised (ALSFRS-R)(511) . The ALSFRS-R is a questionnaire-based, 12-item functional rating scale administered to the patient or, if the patient cannot communicate effectively, to an informant such as the carer. The ALSFRS-R incorporates assessment of bulbar function, fine motor function, gross motor function and respiratory function. Functional scores in each domain are graded from 0 (complete dependence for that function) to 4 (normal function), resulting in a total ALSFRS-R score ranging from 0 to 48 (normal).

Muscle strength in all patients was assessed using the Medical Research Council (MRC) rating scale (512) with the following group of muscles tested bilaterally yielding a total MRC score of 90: shoulder abduction; elbow flexion; elbow extension; wrist dorsiflexion; finger abduction; thumb abduction; hip flexion; knee extension; ankle dorsiflexion. The MRC scale is a five point scale ranging from 0 (no movement) to 5 (normal strength).

The Triggs hand score (513) was utilised to evaluate hand function in chapter 8 with function graded as follows: 0 = normal; 1 = mild to moderate hand weakness without impairment of dexterity; 2 = weak with significant impairment of dexterity (i.e., difficulty with handwriting and buttoning clothes); and 3 = marked weakness-major disability and loss of fine motor control. Patients were also graded in terms of upper motor neuron (UMN) "burden", by totalling the number of pathological UMN signs on examination. These were taken as pathologically brisk biceps, supinator, triceps, finger, knee and ankle reflexes, and extensor plantar responses assessed bilaterally and brisk facial and jaw jerks. Tendon reflexes were graded as 0 = normal, 1 = brisk without spread or present in a wasted muscle, 2 = brisk with reflex spread (maximum possible score 16)(514).

Chapter 1

Diagnostic Utility of the Split-Hand Sign in ALS

Summary

Preferential wasting of the 'thenar' group of muscles including the first dorsal interosseous; the split hand sign, appears to be a specific feature of ALS. The present study developed a novel split hand index (SI) and assessed its diagnostic utility in ALS. 170 consecutive patients with neuromuscular symptoms (44 ALS, 126 patients with other neuromuscular disorders) were prospectively recruited according to standards for reporting of diagnostic accuracy (STARD) criteria. The SI was derived by dividing the product of the compound muscle action potential (CMAP) amplitude recorded over the first dorsal interosseous and abductor pollicis brevis by the CMAP amplitude recorded over the abductor digiti minimi. The SI was significantly reduced in ALS patients (ALS 3.5±0.6; compared with patients with other neuromuscular disorders 9.1±0.3, $P<0.0001$), particularly in limb-onset ALS (2.3±0.5, $P<0.0001$). Receiver operating characteristic curve analysis indicated that SI reliably differentiated ALS from patients with other neuromuscular disorders (area under curve ALS 0.83, $P<0.0001$) with an optimal SI cut-off value of 5.2 exhibiting a sensitivity of 74% and specificity 80. The split hand index robustly differentiates ALS from mimic disorders. The split hand index is a simple measure that could be utilized in a standard neurophysiology setting. A reduction in SI distinguishes ALS from mimic disorders, potentially facilitating an earlier diagnosis of ALS.

Introduction

The diagnosis of amyotrophic lateral sclerosis (ALS) relies on the identification of combined upper and lower motor neuron signs in the same body region, with evidence of disease progression (2). The absence of a diagnostic test and the heterogeneity of the ALS clinical phenotypes has tended to result in diagnostic delay, estimated to be 14 months (515). As a consequence, institution of neuroprotective therapies such as riluzole is often delayed (184), and recruitment into clinical trials may be reduced (516).

The clinically based *El Escorial criteria* developed in order to aid the diagnosis of ALS (14) were too stringent and insensitive at diagnosing ALS in the early stages of the disease (17, 184, 515, 517). A recent modification, termed the *Awaji-Shima criteria*, were developed whereby the presence of neurophysiological parameters of lower motor neuron (LMN) dysfunction such as fasciculation's, fibrillation potentials, positive sharp waves and chronic neurogenic changes were regarded as equivalent to the clinical findings of LMN dysfunction (82). The Awaji-Shima criteria have been established to be sensitive (74-77, 518), although, the increase in diagnostic sensitivity appeared to be restricted to ALS patients with bulbar onset disease (518).

Dissociated atrophy of intrinsic hand muscles, including the abductor pollicis brevis (APB) and first dorsal interosseous (FDI), with relative preservation of the hypothenar muscles, the split hand sign (Figure 1.1), appears to be an early clinical feature of ALS (20, 21, 54). A recent study has addressed the specificity of the sign and suggested a potential role in facilitating the clinical diagnosis of ALS (20).

The clinical observation of dissociated hand muscle atrophy may provide an opportunity to develop a simple neurophysiological biomarker for the diagnosis of ALS. The split hand index (SI) was derived by multiplying the compound muscle action potential (CMAP) amplitude recorded over the APB muscle by the CMAP amplitude recorded over the FDI muscle and dividing this product by the CMAP amplitude recorded over the abductor digiti minimi (ADM) (519). The aim of the present study was to assess the diagnostic utility of the split hand index in ALS, and in particular to determine whether SI may reliably differentiate ALS from mimic disorders.

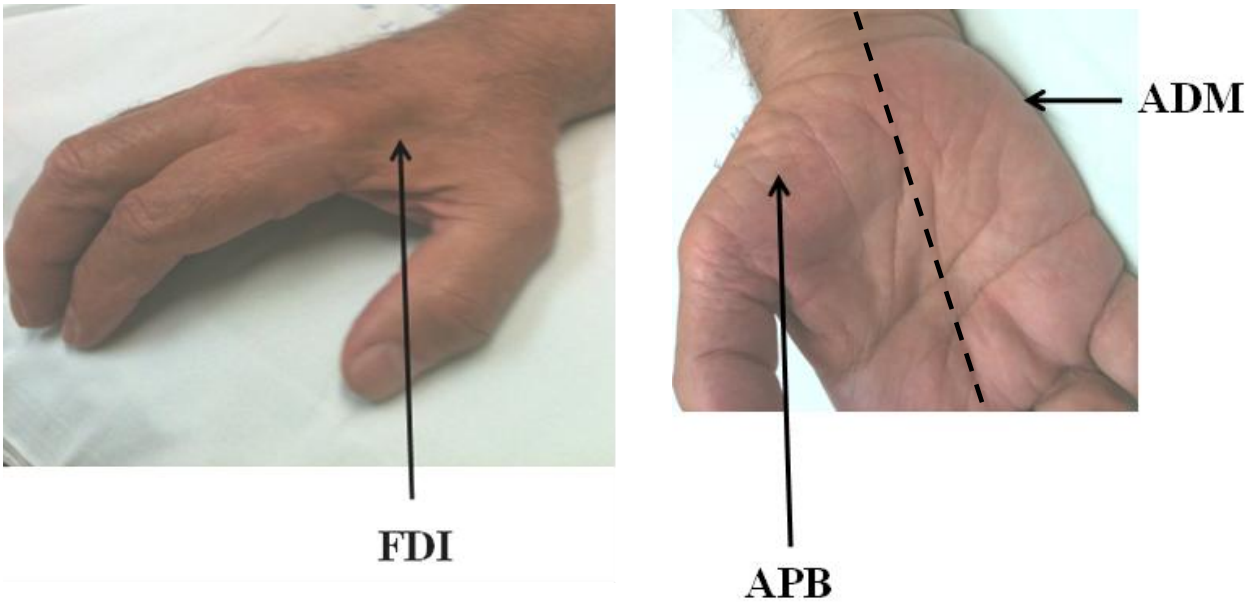

$$\textit{Split hand index (SI)} = \frac{CMAP_{APB} * CMAP_{FDI}}{CMAP_{ADM}}$$

Figure 1.1: An illustration of the split-hand sign in a patient with amyotrophic lateral sclerosis. Specifically, the split hand sign refers to preferential wasting of the abductor pollicis brevis (APB) and first dorsal interosseous (FDI) muscles in comparison to the abductor digit minimi (ADM). The novel split hand index is calculated by multiplying the compound muscle action potential (CMAP) amplitude recorded over the APB by that recorded over the FDI and dividing the product by the CMAP amplitude recorded over the ADM

Materials and Methods

In total, 170 patients were prospectively and consecutively recruited into the study according to the standards for reporting of diagnostic accuracy (STARD) criteria. The inclusion criteria included all patients with clinical neuromuscular features affecting the upper limbs, referred to the neurophysiology laboratories at Westmead and Prince of Wales Hospitals from June 2010 to December 2011 (Figure 1.2). Patients deemed not to be suffering with a neuromuscular disorders were excluded from the study. After extensive investigations and clinical follow-up 26% patients (26 males, 18 females, mean age 59.6 years: age range 29-81 years) were eventually diagnosed with ALS according to the Awaji-Shima criteria (82) of whom 76% were in the definite or probable diagnostic category. All ALS patients were consecutively recruited and no preference was given to ALS patients followed for a longer period of time. The remaining 74% patients were confirmed to have patients with other neuromuscular disorders (64 males, 62 females; mean age 54 years; age range 20-89 years, Figure 1.2) following extensive investigations and follow-up.

All ALS patients were clinically staged using the Amyotrophic Lateral Sclerosis Functional Rating Scale-Revised (ALSFRS-R) (511) and ALSFRS-R progression rate, a marker of survival, was estimated according to the previously reported formula; (48-ALSFRS-R)/duration of symptoms (520). Muscle strength was assessed using Medical Research Council (MRC) rating scale (521). Specifically, the following muscle groups were assessed bilaterally yielding a total MRC score of 90: shoulder abduction; elbow flexion; elbow extension; wrist dorsiflexion; finger abduction; thumb abduction; hip flexion; knee extension; ankle dorsiflexion. ALS patients were classified according to the site of disease onset as either limb or bulbar-onset. All ALS patients

gave informed consent to the procedures, which were approved by the South East Sydney and Sydney West Area Health Service Human Research Ethics Committees.

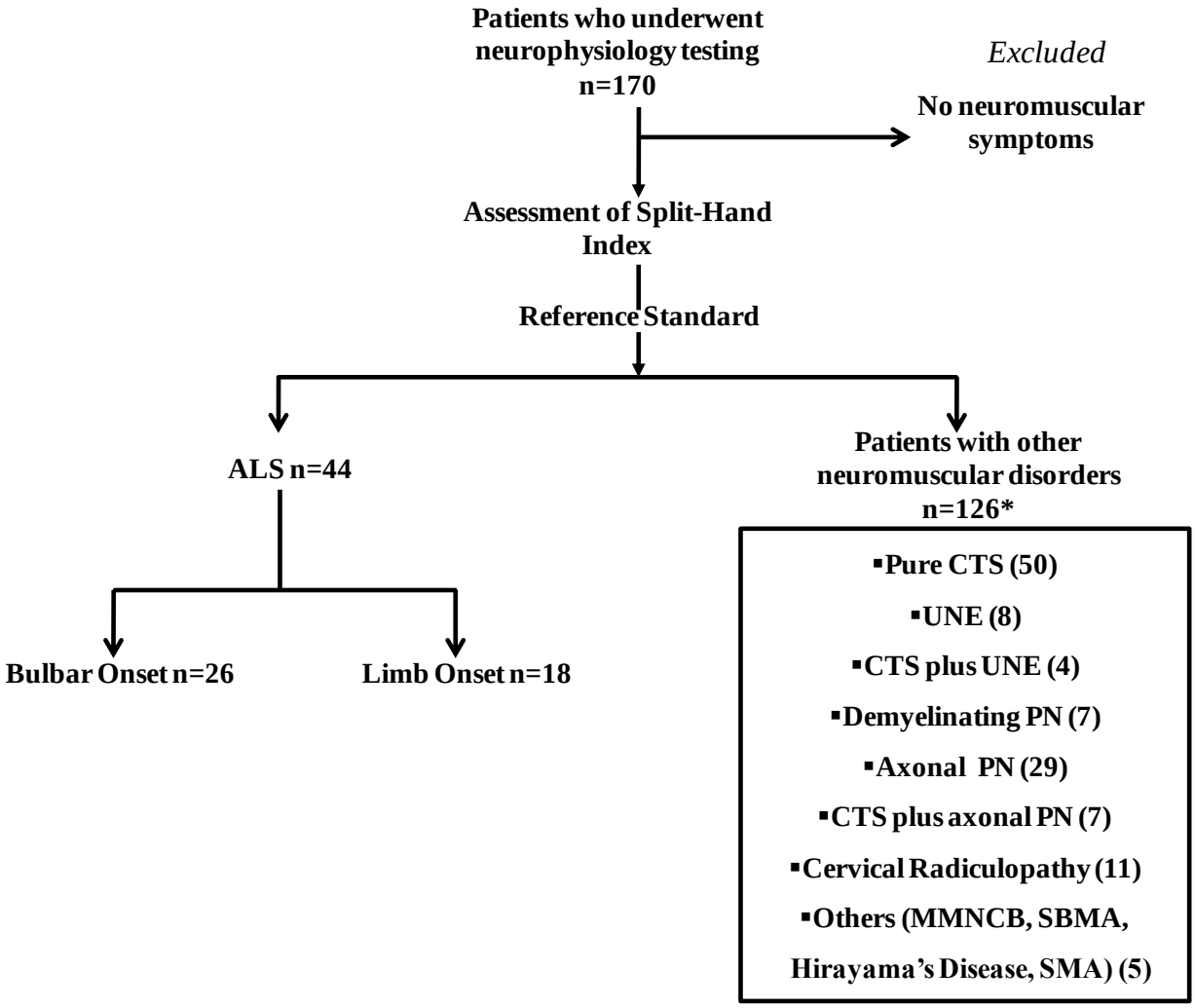

Figure 1.2: Flow diagram of patient recruitment according to the standards for reporting of diagnostic accuracy (STARD) criteria which subsequent differentiation into the amyotrophic lateral sclerosis (ALS), based on Awaji criteria, and patients with other neuromuscular disorders based on the reference standard. The ALS group was further subdivided into limb-onset and bulbar-onset. The group comprising patients with other neuromuscular disorders included entrapment neuropathies [carpal tunnel syndrome (CTS) and ulnar neuropathy at the elbow (UNE)], axonal sensorimotor polyneuropathy [PN] (axonal neuropathy of undetermined etiology (N=24), diabetic neuropathy (N=4), amyloid neuropathy (n=1)] demyelinating polyneuropathy [Guillain-Barre syndrome] (N=2), chronic inflammatory demyelinating polyradiculoneuropathy (N=3) and Charcot-Marie Tooth disease type 1A (N=2)], cervical radiculopathy (11), multifocal motor neuropathy with conduction block (MMNCB, N=2), spino-bulbar muscular atrophy (SBMA, N=1), Hirayama's disease (N=1), spinal muscular atrophy (SMA, N=1). *In 5 patients, the neurophysiological study was normal, despite the patients presenting with neuromuscular symptoms.

Neurophysiological studies

Prior to assessing the split hand index patients underwent routine nerve conduction studies and electromyography (EMG) using the Oxford Teca Synergy EMG machine (Oxford Instruments, Old Woking, Surrey, England). In all patients median, ulnar, common peroneal and tibial motor nerves, as well as the sural, median and ulnar sensory nerves were assessed. Needle EMG testing was performed in at least 3 regions on the ALS patients. Needle EMG testing was not routinely undertaken in patients with other neuromuscular disorders unless the diagnosis was not apparent on NCS, or if there was a suspicion of cervical radiculopathy, vasculitic neuropathy or ALS. Filter settings were set between 3 Hz and 10 KHz while the upper limb temperature was maintained at 32ºC. The median and ulnar nerves were stimulated electrically at the wrist, and the resultant baseline-to-peak CMAP amplitude (mV) was recorded over the APB, FDI and ADM muscles using 10-mm gold disc electrodes (Grass, USA) positioned in a belly tendon arrangement. Specifically, the G1 electrode (active) was positioned over the midpoint of the respective muscle ensuring a negative take-off of the CMAP response, while the G2 electrode (reference) was positioned over the base of thumb (APB and FDI) and base of digit 5 (ADM). The distance between the cathode and active (G1) recording electrodes for APB and ADM muscles was 5 cm, while the distance between the cathode and active (G1) electrode was not measured for the FDI muscle. The split-hand index (SI), which quantifies the extent of dissociated intrinsic hand muscle atrophy, was derived by multiplying the CMAP amplitude recorded over the APB and FDI muscles, and dividing this product by the CMAP amplitude recorded over the ADM muscle, as follows:

$$SI = \frac{APB_{CMAP} * FDI_{CMAP}}{ADM_{CMAP}}$$

In addition to the CMAP amplitude, the median nerve distal motor latency (ms), and F-wave frequency were recorded. Subsequently, the neurophysiological index (NI) for the median nerve was derived according to the following formula (522):

$$NI = \frac{\text{CMAP amplitude *F wave frequency (\%)}}{\text{Distal motor latency}}$$

Statistical Analysis

To assess for significant differences in the split hand index between ALS and patients with other neuromuscular disorders patients a Student's t-test was used. In addition, an analysis of variance (ANOVA) was utilized for multiple comparisons. Receiver operating characteristic (ROC) curves were undertaken to determine the diagnostic utility of the split hand index. From ROC curve analysis the ***sensitivity***, defined as the probability of having the disease when the test is positive, and ***specificity***, defined as the probability of not having the disease when the test is negative, were determined. From the sensitivity and specificity data, the positive and negative likelihood ratios (LR), were defined. Spearman's rho (non-parametric data) and Pearson's correlation coefficient (parametric data) were used to examine the relationship between the SI, clinical measures of ALS and the neurophysiological index. A probability (P) value of < 0.05

was considered statistically significant. Results are expressed as mean ± standard error of the mean for parametric data and median with interquartile range for non-parametric data.

Results

Clinical features

Of the 44 ALS patients 76% satisfied the Awaji-Shima criteria for inclusion in the "definite" or "probable" diagnostic category, while 24% were classified as "possible". The mean disease duration in ALS patients from symptom onset to testing was 18.9 ± 3.1 months. Limb-onset disease was evident in 59% of patients while bulbar-onset was noted in 41% of patients. The median ALSFRS-R score at time of testing was 41(32-45), while the median value for the MRC sum score was 75 (66-87), both indicating a moderate degree of disability in the ALS patient cohort. The diagnosis in patients with other neuromuscular disorders is outlined in figure 1.2, and none of the patient in this cohort developed ALS. In addition, there were no exclusions from the prospectively recruited cohort of 170 patients.

Neurophysiological studies disclosed a significant reduction of CMAP amplitude recorded over the APB (ALS, 3.9 ± 0.5 mV; patients with other neuromuscular disorders 8.1 ± 0.2 mV, $P < 0.001$), FDI (ALS, 4.8 ± 0.7 mV; patients with other neuromuscular disorders 10.7 ± 0.3 mV, $P < 0.001$) and ADM (ALS, 6.1 ± 0.5 mV; patients with other neuromuscular disorders 9.7 ± 0.2 mV, $P < 0.001$) in ALS patients when compared to the patients with other neuromuscular disorders. In addition, the neurophysiological index recorded from the median nerve was significantly reduced in ALS patients when compared to patients with other neuromuscular disorders (ALS 0.8±0.1; patients with other neuromuscular disorders 2.1±0.1 $P<0.001$).

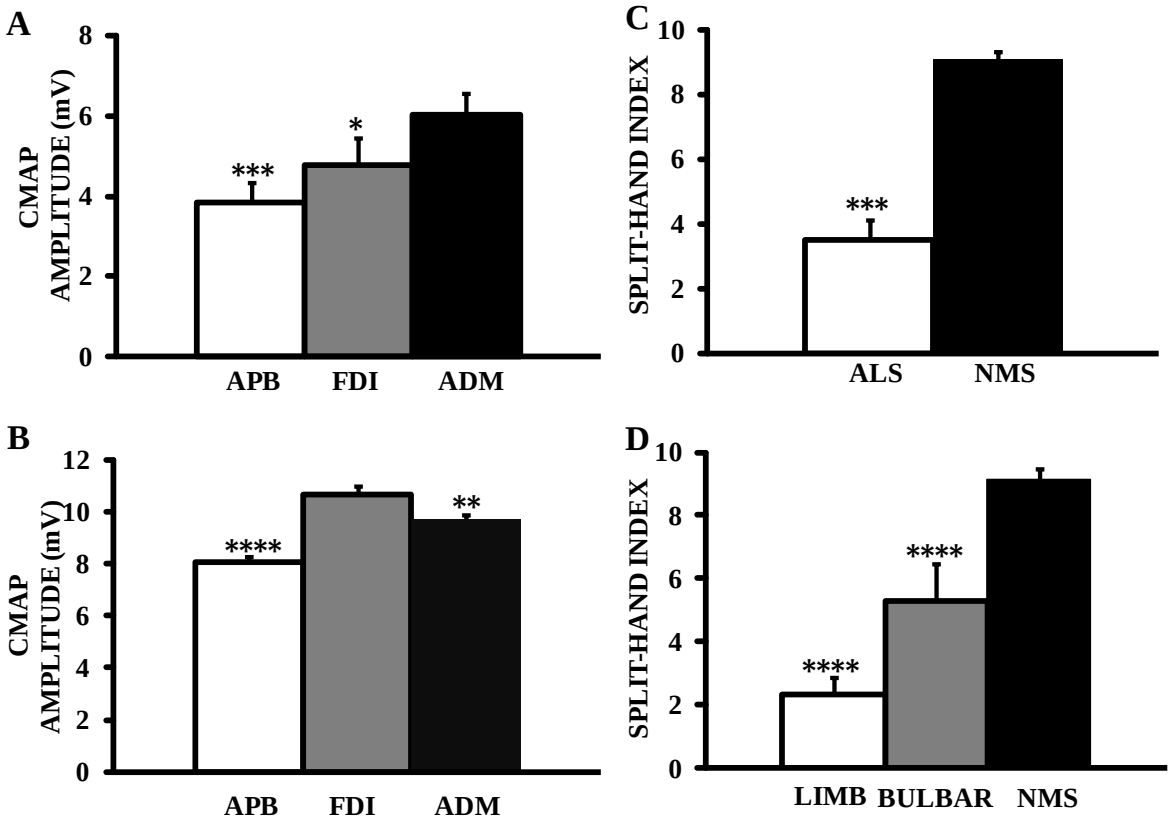

Figure 1.3: (A) The compound muscle action potential (CMAP) amplitude was significantly reduced when recorded over the abductor pollicis brevis (APB) ($P<0.0001$) and first dorsal interosseous (FDI) ($P<0.05$) muscles compared to abductor digiti minimi (ADM) muscle in amyotrophic lateral sclerosis (ALS). **(B)** Interestingly, the CMAP amplitudes recorded over the FDI was greater than that recorded over the ADM ($P<0.01$) muscles and APB ($P<0.0001$) muscles in patients with other neuromuscular disorders (NMS). **(C)** There was a significant reduction of the split-hand index (SI) in ALS patients when compared to patients with other neuromuscular disorders ($P<0.0001$). **(D)** Although the reduction in SI was a uniform finding in ALS, it was most pronounced in patients with limb-onset disease ($P<0.0001$).

Split hand index

Of relevance, the reduction in the CMAP amplitude was significantly greater when recorded over the abductor pollicis brevis (APB 3.9 ± 0.5mV; ADM 6.1 ± 0.5mV $P < 0.0001$, Fig. 1.3A) and first dorsal interosseous (FDI 4.8 ± 0.7mV; ADM 6.1 ± 0.5mV $P < 0.05$, Fig. 1.3A) muscles

compared to CMAP responses recorded over the abductor digit minimi muscle in ALS patients. In contrast, the FDI CMAP amplitudes (10.7±0.3mV) were significantly greater compared to CMAP amplitudes recorded over APB (8.1±0.2mV P <0.0001, Fig. 1.3B) and ADM (9.7±0.2mV P <0.01, Fig.1.3B) muscles in patients with other neuromuscular disorders.

Combining the CMAP amplitudes into the ***split hand index***, it was evident that the SI was significantly reduced in ALS patients when compared to patients with other neuromuscular disorders (ALS 3.5 ± 0.6, [0-8.3]; patients with other neuromuscular disorders 9.1 ± 0.3, 0-18.9, P < 0.0001, Fig. 1.3C). Sub-group analysis revealed that although the reduction in the split hand index was a uniform finding in ALS patients evident in both bulbar-onset (bulbar-onset ALS SI 5.3 ± 1.2 [0-15.0]; patients with other neuromuscular disorders 9.1 ± 0.3, P < 0.0001, Fig. 1.3D), and limb-onset ALS (2.3 ± 0.5 [0-9.9], P < 0.0001, Fig 1.3D), the reduction in SI was most prominent in patients with limb-onset disease (P < 0.0001). In addition, there was also a significant reduction of SI in ALS when compared to a control group where only focal compressive neuropathies, such as CTS, were excluded (ALS 3.5 ± 0.6, [0-8.3]; "non-compressive" neuromuscular disorder patients 8.1 ± 0.5, [0-17.2], P < 0.0001).

Diagnostic utility of the split hand index

To determine the diagnostic utility of the split hand index, analysis of ROC curves in the entire ALS cohort disclosed an area under the curve (AUC) of 0.83 (P < 0.0001), suggesting a good diagnostic accuracy of the split hand index. Of further relevance, a split hand index value of 5.2 was potentially useful in differentiating ALS from patients with other mimicking ALS disorders with a sensitivity of 74%, specificity of 80% (Fig. 1.4A). In addition, sub group analysis of ROC curves in ALS patients with limb-onset disease revealed an AUC of 0.90 (P < 0.0001),

suggesting that the SI is an excellent diagnostic test at differentiating limb-onset ALS from mimic disorders (Fig 1.4B). An SI value of 5.2 differentiated limb-onset ALS from controls with a sensitivity of 80% and specificity of 80% (Fig 1.4B). Taken together, these findings suggest that the SI may be a useful diagnostic test at differentiating ALS, in particular limb-onset ALS, from patients with other neuromuscular disorders in a clinical setting.

In order to assess the diagnostic potential of the split hand index, values were compared between ALS patients meeting the definite and probable category of the Awaji-Shima criteria at the time of testing to those patients classified as "possible" ALS. Although, as expected, the reduction in SI was most prominent in patients meeting the Awaji-Shima criteria ($ALS_{DEFINITE/PROBABLE}$ SI 3.0 ± 0.5; patients with other neuromuscular disorders 9.1 ± 0.3, $P < 0.001$, Fig. 1.5A), a significant reduction in SI was also evident in patients classified as "possible" ALS

when compared to patients with other neuromuscular disorders ($ALS_{POSSIBLE}$ SI 5.1 ± 0.8; patients with other neuromuscular disorders (9.1 ± 0.3, $P < 0.01$)(Fig 1.5B). Of relevance, 64% of patients classified as possible ALS by the Awaji criteria at the time of assessment, exhibited an SI of < 5.2. Taken together, these findings suggest that assessing split hand index in a clinical cohort may reliably distinguish ALS from patients with other neuromuscular disorders and support a diagnosis of ALS in up to 64% of patients not meeting the Awaji criteria.

Combining measures of disease severity, clinical assessment and the split hand index, it was evident that the SI significantly correlated with measures of peripheral disease burden, including the neurophysiological index ($R = 0.8$, $P < 0.001$), total MRC score (rho= 0.7, $P < 0.001$) and the

MRC score from the APB (rho=0.8, $P < 0.001$). In addition, the SI had a significant negative correlation with the rate of progression of ALSFRS-R (rho = - 0.4, $P < 0.05$) suggesting that patients with rapid clinical progression had lower values for SI.

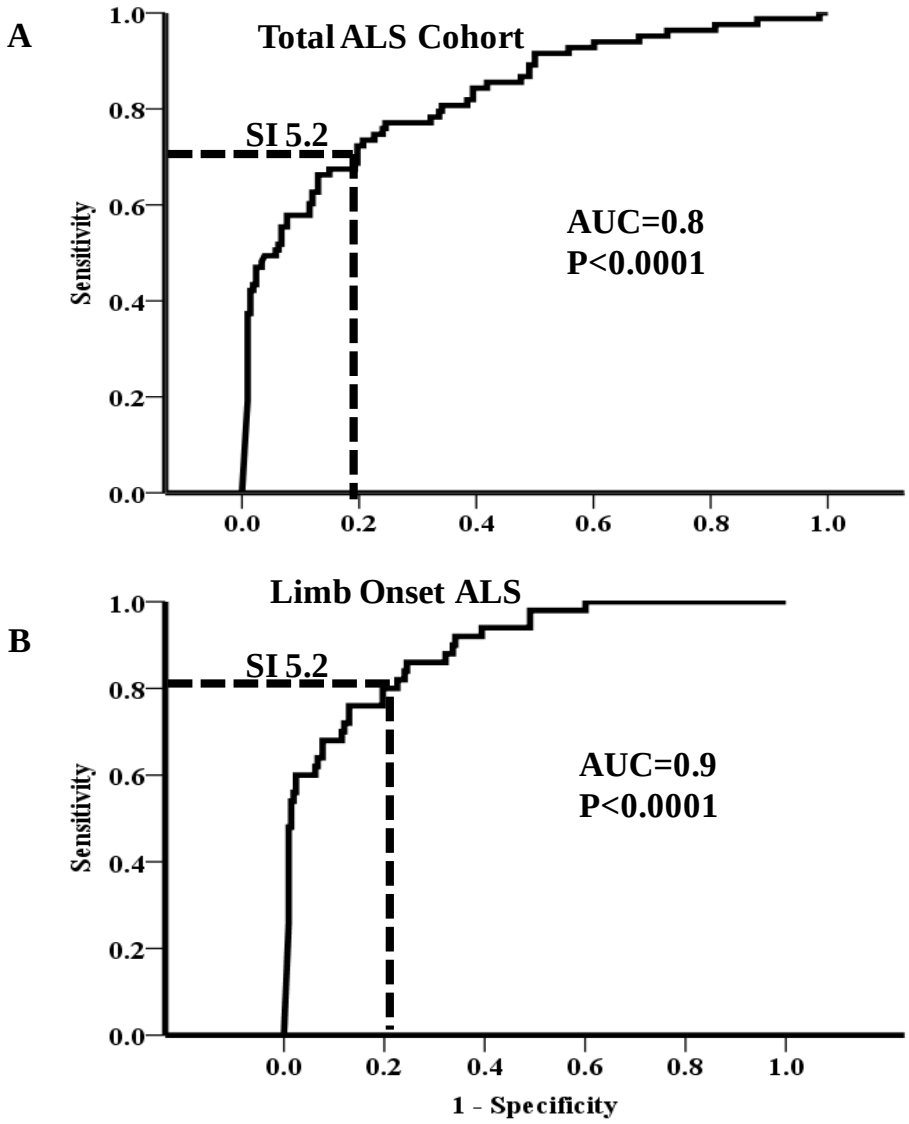

Figure 1.4: (A) Receiver operating characteristic (ROC) curve analysis revealed that the split hand index (SI) reliable differentiated amyotrophic lateral sclerosis (ALS) from patients with other neuromuscular disorders (NMS), with an area under the curve (AUC) of 0.83 (P<0.0001). In addition, a cut-off value of 5.2 differentiated ALS from NMS with a sensitivity of 74% and specificity of 80%. (**B)** Sub-group analysis of ROC curves in ALS patients with limb-onset disease suggested that the SI exhibited a greater diagnostic robustness, with an AUC of 0.9 (P<0.0001), sensitivity of 80% and specificity of 80%.

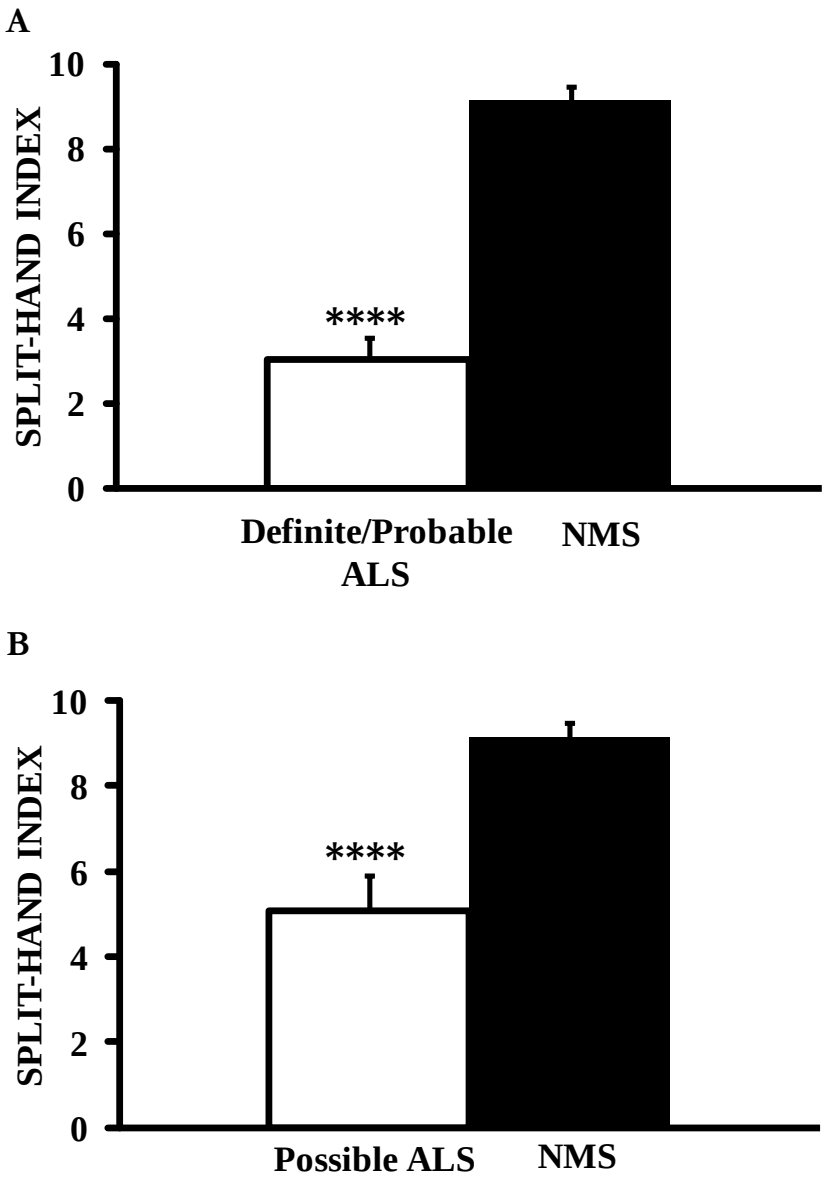

Figure 1.5: (A) The split hand index (SI) was significantly reduced in patients with amyotrophic lateral sclerosis (ALS) classified as 'definite/probable' according to the Awaji criteria ($P<0.0001$). (**B)** There was a significant reduction of SI in patients classified as 'possible' ALS when compared to patients with other neuromuscular disorders (NMS) ($P<0.0001$), thereby suggesting that the SI may aid in the earlier diagnosis of ALS.

Discussion

The present study has developed a novel neurophysiological biomarker, termed the split-hand index, based on the clinical observations obtained from ALS patients. In the current prospective study, the SI reliably distinguished ALS from patients with other neuromuscular disorders early in the disease process. Specifically, a split hand index value of 5.2 or less reliably differentiated ALS from other neuromuscular disorders. Although this reduction in the split hand index was a uniform finding across the different ALS phenotypes, it was most pronounced in limb-onset ALS patients. Of further relevance, a substantial proportion of ALS patients classified as "possible" on the Awaji-Shima criteria, exhibited an abnormal split-hand index, suggesting that the reduction in SI may be an early feature in ALS. Further, the split-hand index correlated with established biomarkers of ALS disease progression, namely the ALSFRS-R, neurophysiological index, muscle strength scores and rate of ALSFRS-R progression. Taken together, findings from the present series suggests a diagnostic utility of the split hand index in ALS, complementing other clinical techniques to potentially aid an earlier diagnosis of ALS.

Diagnosis of ALS

Currently, the diagnosis of ALS relies on identifying a combination of upper and lower neuron dysfunction, with evidence of disease progression (185). In the absence of a pathognomonic test, clinical criteria were developed to aid an early diagnosis of ALS, encompassing both upper and lower motor neuron signs (14). Such clinical criteria, however, were found to be insensitive, often resulting in a diagnostic delay (17, 184, 515, 517). Consequently, a modification of the clinical criteria was developed whereby the finding of fasciculations and other electromyography (EMG) features of lower motor neuron dysfunction, were equated with clinical features of lower

motor neuron dysfunction (82). Although the Awaji-Shima criteria increased the diagnostic sensitivity in some ALS phenotypes (74, 77, 518) extensive EMG sampling is typically required, potentially limiting its clinical applicability. In addition, the EMG findings of lower motor neuron dysfunction are not specific for ALS.

Less conventional neurophysiological techniques such as motor unit number estimation (MUNE) (523), axonal excitability (56, 57), neurophysiological index (NI) (522) and electrode impendence myography (84, 524), do not reliably differentiate ALS from mimic disorders. It should be acknowledged, however, that both MUNE and NI were developed primarily as tools for quantifying disease progression rather than being diagnostic biomarkers for ALS. Further, sophisticated magnetic resonance imaging techniques detecting abnormalities of the corticomotoneuronal system and molecular studies assessing aberrant expression of muscle proteins, such as Nogo-A and Nogo-B, have also been proposed as non-neurophysiological diagnostic biomarkers (2, 184, 525, 526). These techniques, however, may not be widely available and their sensitivity may be limited.

The split hand index is a simple neurophysiological measure that can be readily performed in a clinical setting without the need for sophisticated neurophysiological techniques. The finding that the split hand index reliably differentiates ALS from patients with other neuromuscular disorders, in particular limb-onset ALS, underscores the diagnostic utility of the split hand index. In addition, the finding that the reduction in the split hand index was an early feature in ALS, being evident in 64% of ALS patients classified in the “possible” diagnostic category according to the Awaji criteria, suggests a utility for the SI in establishing an earlier diagnosis of ALS.

The present study may also serve to re-affirm the underlying pathophysiology of ALS. Specifically, given that the thenar complex group of muscles (APB and FDI) exhibit a greater cortical representation (45), the clinical observation of the split hand sign may suggest a cortical onset of ALS (20, 44, 54). The findings that preferential atrophy of APB and FDI muscles was a specific feature of ALS, as illustrated by the split hand index, provides support for a cortical origin of ALS.

Utility of the split-hand index in ALS

The ability to recruit ALS patients into treatment trials at an earlier stage in the disease process, and to reliably monitor the effects of therapeutic agents, remains an important trial design strategy in assessing the effectiveness of future therapeutic agents at an early stage in drug development. At present, patient enrollment into therapeutic trials remains low (17, 516, 527), in part accounted for by reliance on stringent diagnostic criteria (14). In particular, ALS patients who are in the early stages of the disease process may not be enrolled into therapeutic trials, the very group that would probably derive most benefit from any neuroprotective therapies (516, 528). The findings in the present study suggests a utility for the split hand index in establishing an earlier diagnosis of ALS and thereby aiding patient recruitment into therapeutic trials. Of further interest, the finding that SI correlated with traditional measures of disease progression, such as the ALSFRS-R, muscle strength scores, neurophysiological index and ALSFRS-R progression rate, may suggest a role in complementing other neurophysiological biomarkers, such as MUNE and NI, in monitoring disease progression, although this has to be further confirmed in longitudinal studies.

Chapter 2

Cortical Excitability Differences in Hand Muscles follow a Split-Hand Pattern in Healthy Controls.

Summary

Subsequent to establishing the diagnostic utility of the split hand sign in ALS; differences in cortical and axonal excitability characteristics of intrinsic hand muscles was explored with the aim of determining whether differences in excitability differentiate muscles which undergo preferential atrophy in amyotrophic lateral sclerosis namely the abductor pollicis brevis (APB) and first dorsal interosseous (FDI). Excitability studies were undertaken using threshold tracking techniques in 26 healthy controls with responses recorded over APB, FDI and abductor digiti minimi. Short interval intracortical inhibition was significantly greater over the APB and FDI. In addition, motor evoked potential amplitude was greater, while cortical silent period duration was longer when recording over the APB and FDI. At a peripheral level, the strength-duration time constant was greater when recorded over the APB. This study establishes that differences in cortical excitability follows the split-hand pattern in healthy controls, a finding potentially explained by evolution of specialized activity of APB/FDI in complex hand tasks.

Introduction

Preferential atrophy of the abductor pollicis brevis (APB) and first dorsal interosseous (FDI) with relative preservation of abductor digit minimi (ADM), termed the split-hand sign, is a specific clinical feature of amyotrophic lateral sclerosis (ALS)(20, 21, 519, 529). The pathophysiological mechanisms underlying this unusual pattern of dissociated muscle atrophy remains to be fully elucidated, although both cortical and peripheral mechanisms have been proposed (54, 55, 519).

A cortical basis for the split-hand was inferred from the knowledge that the APB and FDI muscles are vital in the execution of skilled hand movements, such as precision grip (530-539). Consequently these muscles would be expected to exhibit a greater cortical representation in comparison to the hypothenar muscles (45). Importantly, significant differences in cortical excitability were reported previously between distal and proximal upper limb muscles(540). Specifically, the degree of intracortical inhibition and facilitation were significantly greater when recorded over the thenar muscles (APB) compared to biceps brachii, suggesting a more prominent cortical representation of the thenar muscles (540). Given that anterior horn cell degeneration in ALS may in part be mediated by corticomotoneuronal excitotoxicity(25, 44, 49, 50, 87), the development of the split-hand phenomenon could be explained by differences in cortical excitability between the muscles. Importantly, transcranial magnetic stimulation (TMS) studies have reported a preferential dysfunction of corticomotoneuronal input to the thenar muscles (APB), thereby suggesting a cortical basis for the split-hand phenomenon (54).

At the peripheral level, differences in excitability properties of motor axons innervating the thenar and hypothenar muscles were reported in healthy humans, with evidence of more prominent upregulation of persistent Na^+ conductances in motor axons innervating APB and FDI muscles compared to the ADM(55). While these findings established significant differences in axonal excitability properties across the range of intrinsic hand muscles, thereby implying a peripheral basis for the split-hand, differences in cortical excitability between the 3 muscles was not assessed. Consequently, this study combined threshold tracking TMS and axonal excitability techniques to dissect out the differences in cortical and axonal excitability between APB, FDI, and hypothenar muscles, with a specific aim of determining whether the excitability differences follow a split-hand pattern.

Methods and Materials

Participants

Studies were undertaken on 26 healthy volunteers (14 men, 12 women; mean age 48.9 years, age range 24-67 years). None of the subjects had symptoms or clinical signs of central or peripheral nervous system dysfunction, and were not receiving psychotropic medications at the time of testing. Subjects gave written informed consent to the procedures, and all procedures were approved by the Western Sydney Local Health District Human Research Ethics Committee.

Experimental tasks

Axonal excitability

Initially, axonal excitability studies were undertaken on the median and ulnar motor nerves according to a previously described protocol (354). The median and ulnar nerves were stimulated at the wrist using 5 mm non-polarizable Ag-AgCl electrodes (3M Healthcare, MN,

USA) with the anode positioned ~ 10 centimeters proximal to the cathode over the lateral forearm. Stimulation was computer controlled and converted to current using an isolated linear bipolar constant current simulator (maximal output ± 50 mA; DS5, Digitimer, Welwyn Garden City, UK). Compound muscle action potentials (CMAPs) were recorded from the abductor pollicis brevis (APB), first dorsal interosseous (FDI), and abductor digit minimi (ADM) muscles with the active (G1) electrode positioned over the motor point and reference (G2) electrode placed over the base of the proximal thumb (APB and FDI) and fifth digit (ADM), respectively. Such a belly-tendon arrangement of electrodes enabled minimal cross-talk between the three muscles. Test current pulses were applied at 0.5s intervals and combined with either sub-threshold polarizing currents or suprathreshold conditioning stimuli according to previously described protocol (354, 355). The motor evoked potential (MEP) amplitude was measured from baseline to negative peak, with the target set at 40% of maximum for all tracking studies. Proportional tracking was utilized to determine the changes in threshold current required to produce and maintain a target response (86).

The following axonal excitability parameters were measured: (i) strength-duration time constant (τ_{SD}) and rheobase, determined according to the Weiss formula (86, 336); (ii) threshold electrotonus (TE) recorded with sub-threshold depolarizing currents at 10-20 ms [TEd (10-20 ms)], 40-60 ms [TEd (40-60 ms)], and 90-100 ms [TEd (90-100 ms)], and with hyperpolarizing currents at 10-20 ms, TEh (10-20 ms) and at 90-100 ms, TEh (90-100 ms); (iii) hyperpolarizing current-threshold relationship (I/V) calculated from polarizing current between +50 and -100%; (iv) recovery cycle parameters including the relative refractory period (RRP, ms), refractoriness at 2ms (%), superexcitability (%), and late subexcitability (%).

Cortical excitability

Cortical excitability studies were undertaken using a 90 mm circular coil connected to 2 high-power magnetic stimulators connected via a BiStim device (Magstim Co., Whitlands, South West Wales, UK). The coil position was adjusted for each muscle such that an optimal stimulating site was determined as indicated by a point on the skull vertex at which maximal MEP amplitude was evoked by the smallest TMS current.

(i) Paired-pulse threshold tracking TMS was undertaken according to a previously reported technique (416, 417). Briefly, the MEP amplitude was fixed, and changes in the test stimulus intensity required to generate a target response of 0.2 mV (± 20%), when preceded by sub-threshold conditioning stimuli, were measured. The MEP was recorded over the APB, FDI, and ADM muscles. Resting motor threshold (RMT) was defined as the stimulus intensity required to maintain the target MEP of 0.2 mV (±20%). A value of 0.2 mV was selected as the tracking target, rather than the conventional value of 0.05 mV used in the constant stimulus TMS technique (401), given that the former target response (0.2 mV) lies in the middle of the linear logarithmic stimulus-response relationship over a hundred-fold range of responses from about 0.02 to 2 mV (416). As such, larger variations in MEP amplitude would translate to smaller variations in stimulus intensity (the outcome variable), potentially enabling more accurate recordings of TMS parameters.

Short-interval intracortical inhibition (SICI) was determined over the following interstimulus intervals (ISIs): 1, 1.5, 2, 2.5, 3, 3.5, 4, 5, and 7 ms, while intracortical facilitation (ICF) was measured at ISIs of 10, 15, 20, 25, and 30 ms. Stimuli were delivered sequentially as a series of

three channels: **Channel 1**: stimulus intensity, or threshold (% maximal stimulator output) required to produce the unconditioned test response (i.e., RMT); **Channel 2**: sub-threshold conditioning stimulus (70% RMT); and **Channel 3** tracks the stimulus (% maximal stimulator output) required to produce the target MEP when conditioned by a sub-threshold stimulus equal in intensity to 70% of RMT. A sub-threshold conditioning stimulus set to 70%RMT was shown previously to result in maximal SICI (485). Stimuli were delivered every 5–10 s (stimulus delivery was limited by the charging capability of the BiStim system), and the computer advanced to the next ISI only when tracking was stable.

(ii) Single pulse TMS technique was utilized to determine the MEP amplitude (mV) and cortical silent period duration (ms). The MEP amplitude was recorded with magnetic stimulus intensity set to 150% of RMT and normalized by being expressed as a percentage of the relevant muscles' CMAP response. Subsequently to recording the MEP, the cortical silent period (CSP) duration was assessed by instructing the subject to contract the target muscle at ~30% of maximal voluntary contraction with TMS intensity set to 150% of RMT. The CSP duration was measured from onset of MEP to return of EMG activity (455).

Recordings of the CMAPs and MEPs were amplified and filtered (3 Hz-3 kHz) using a Nikolet-Biomedical EA-2 amplifier (Cardinal Health Viking Select version 11.1.0, Viasys Healthcare Neurocare Group, Madison, Wisconsin, USA) and sampled at 10 kHz using a 16-bit data acquisition card (National Instruments PCI-MIO-16E-4). Responses were further filtered for electronic noise by using a Hum Bug (Hum Bug 50/60 Hz Noise Eliminator, Quest Scientific Instruments, North Vancouver, Canada). Data acquisition and stimulation delivery were

controlled by QTRACS software (TROND-F, version 16/02/2009, © Professor Hugh Bostock, Institute of Neurology, Queen Square, London, UK). Temperature was monitored with a purpose built thermometer at the stimulation site.

Statistical Analysis

SICI was measured as the increase in the test stimulus intensity required to evoke the target MEP. Inhibition was calculated off-line as follows (417):

Inhibition = (Conditioned test stimulus intensity – RMT)/RMT * 100

Facilitation was measured as the decrease in the conditioned test stimulus intensity required to evoke a target MEP. Each data point was weighted (by the QTRACS software) such that any measures recorded outside the threshold target window, defined as values within 20% of the tracking target of 0.2mV (peak-to-peak), contributed least to the data analysis. All results were expressed as mean ± standard error of the mean. Paired samples *t*-test was used for assessing differences between 2 groups, while analysis of variance (ANOVA) with *post-hoc* testing (Bonferroni correction) was used for multiple comparisons. The Pearson correlation coefficient was used to examine the relationship between parameters. A probability (*P*) value of <0.05 was considered statistically significant.

Parameter	APB [SEM]	FDI [SEM]	ADM [SEM]	*P*-value APB vs FDI	*P*-value APB vs ADM	*P*-value FDI vs ADM
CMAP amplitude (mV)	12.1 [0.7]	15.6 [1.1]	13.7 [0.6]	< **0.05**	0.50	0.09
RMT (%)	55.6 [1.7]	57.2 [2.1]	55.5 [1.9]	0.26	0.46	0.07
Peak SICI ISI 3ms (%)	22.7 [2.7]	23.5 [3.3]	16.2 [3.0]	0.44	< **0.05**	< **0.05**
MEP amplitude (%)	18.4 [2.6]	14.9 [1.3]	12.7 [1.1]	0.09	< **0.05**	< **0.05**
CSP duration (ms)	200.4 [8.1]	202.4 [6.8]	187.2 [6.0]	0.38	< **0.05**	< **0.001**
SDTC (ms)	0.49 [0.02]	0.43 [0.01]	0.43 [0.01]	< **0.05**	< **0.05**	1.0
Rheobase (mA)	1.49 [0.19]	2.16 [0.15]	2.05 [0.26]	< **0.001**	< **0.05**	0.35
TEd (10-20 ms) (%)	69.0 [1.0]	67.3 [0.9]	64.5 [1.0]	0.10	< **0.01**	< **0.05**
TEd (40-60 ms) (%)	52.9 [0.9]	50.0 [0.7]	50.5 [0.8]	0.10	0.14	1.0
TEd (90-100 ms) (%)	45.3 [0.8]	43.2 [0.8]	45.2 [0.7]	0.34	1.0	0.44
RRP (ms)	3.7 [0.3]	3.3 [0.1]	3.3 [0.2]	0.12	0.12	0.45
Superexcitability (%)	-21.7 [1.4]	-23.2 [1.1]	-22.8 [1.2]	0.19	0.22	0.36
Late subexcitability (%)	14.6 [1.0]	14.6 [1.4]	7.6 [1.28]	0.50	< **0.001**	< **0.001**

Table 2.1: Cortical and axonal excitability data. Peak SICI at ISI 3 ms and CSP duration were reduced significantly, while the MEP amplitude was increased when recording over the APB and FDI muscles compared to ADM. In addition, the CMAP amplitude was significantly larger when recording over FDI compared to APB. In contrast, resting motor threshold was comparable between groups. Of further relevance, the strength-duration time constant (SDTC) was increased significantly when recording over the APB. Interestingly, depolarizing threshold electrotonus at 10-20 ms (TEd 10-20 ms) was increased significantly when recording over APB and FDI, while there was no significant difference in depolarizing threshold electrotonus at 40-60 ms (TEd 40-60 ms) and threshold electrotonus at 90-100 ms (TEd 90-100 ms) across the range of intrinsic hand muscles. Of further relevance, the RRP was comparable across the 3 intrinsic hand muscles. All data are expressed as mean (standard error of the mean).

Results

Cortical Excitability

A complete sequence of recordings was obtained from all subjects. Peak-to-peak CMAP amplitude was significantly smaller when recorded from the APB compared to the FDI (F=3.4, $P<0.05$, Table 1). In contrast, CMAP amplitudes recorded over the ADM ($P= 0.50$) were comparable to those recorded from the APB but smaller when compared to FDI ($P = 0.09$), although this reduction was not significant.

Paired-pulse threshold tracking TMS was utilized to assess SICI and ICF from the APB, FDI and ADM. Initially, the resting motor threshold (RMT) was recorded from each muscle and defined as the stimulus intensity required to produce and maintain a target MEP of 0.2 mV. The RMT was comparable between the muscles (Table 2.1). Subsequently SICI, defined as the conditioned stimulus intensity required to produce and maintain the target MEP of 0.2 mV, was assessed. It was significantly greater when recording over the APB and FDI compared to ADM (F = 6.0, $P< 0.005$, Fig. 2.1A). In addition, peak SICI was significantly greater when recording over the APB and FDI muscles compared to ADM (Fig. 2.1B, Table 2.1). Following SICI, a period of intracortical facilitation may develop between ISI of 10-30ms. The mean ICF between ISIs 10-30 ms was not significantly different between the 3 muscles (Fig. 2.1A).

Single-pulse TMS disclosed that the MEP amplitude, expressed as a percentage of the CMAP, was significantly greater when recording over the APB and FDI compared to the ADM (Fig. 2.2A, Table 2.1). In contrast, there were no significant differences in MEP amplitude between

APB and FDI muscles. Of further relevance, the CSP duration was the significantly longer when recorded over the APB and FDI muscles compared to ADM (Fig. 2.2B, Table 2.1).

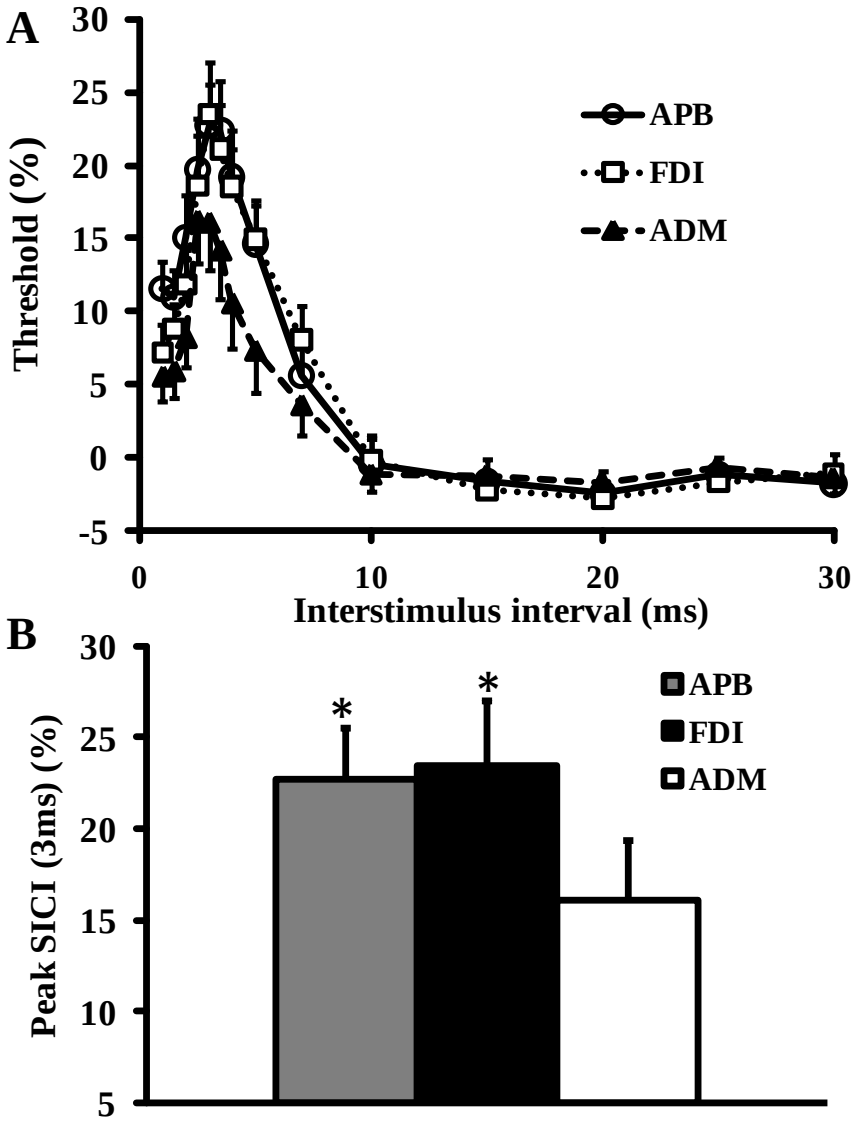

Figure 2.1: **(A)** SICI was significantly greater when recording over the APB and FDI muscles compared to ADM. **(B)** In addition, peak SICI was also significantly greater when recording over the APB and FDI muscles. *P< 0.05

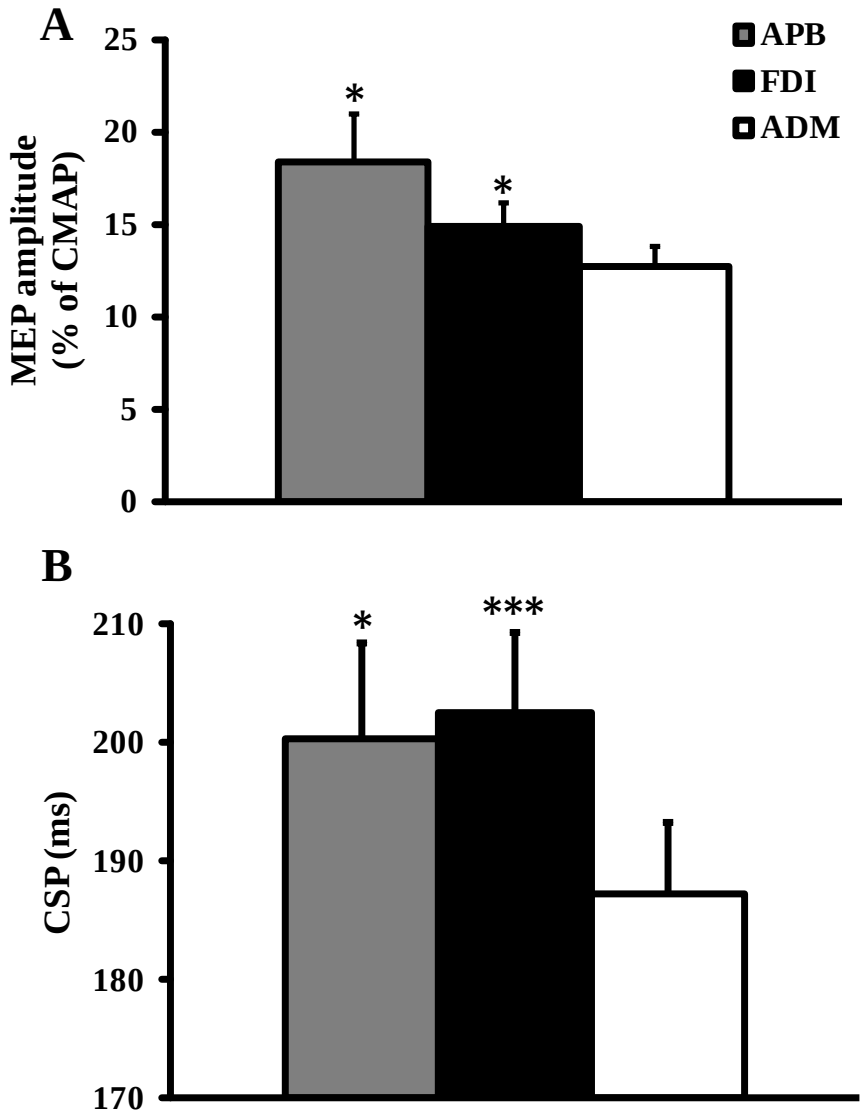

Figure 2.2: (A) The MEP amplitude, expressed as a percentage of the CMAP, was significantly greater when recording over the APB and FDI muscles compared to abductor ADM. **(B)** The CSP duration was significantly longer when recording from the APB and FDI muscles. **P*< 0.05; ****P*<0.001.

Axonal Excitability

Strength-duration time constant (τSD), a biomarker of nodal persistent Na^+ conductance, and rheobase, defined as the threshold current for a stimulus of infinitely long duration, were

assessed to define the strength-duration properties of the median and ulnar nerve motor axons (85, 86, 333, 337, 541). The strength duration time constant was significantly increased when recording over the APB muscle compared to the FDI and ADM (Fig. 2.3A, Table 2.1). In addition, the rheobase was significantly reduced when recording over the APB compared to FDI (Fig. 2.3B, Table 2.1) and ADM (Fig. 2.3B, Table 2.1) muscles. Of further relevance, the mean threshold to activate the median motor nerve was reduced when compared to the ulnar nerve (F=2.8, P = 0.06), although this reduction was not significant.

Measurement of threshold electrotonus, a biomarker of paranodal and internodal axonal conductances (85, 86), revealed further differences between the three intrinsic hand muscles. Specifically, depolarizing threshold electrotonus at 10-20 ms was significantly increased when recording over the APB and FDI compared to ADM (F=5.2, P<0.01, Fig.2.4, Table 2.1). In contrast, there were no significant differences in depolarizing TE at 40-60 ms (Fig. 2.4A) and 90-100 ms (Fig 2.4A, Table 2.1). In addition, there was no significant difference in hyperpolarizing TE between groups (F = 0.05, P = 0.96).

Subsequent to assessing TE, the recovery cycle of axonal excitability was recorded in response to a supramaximal conditioning stimulus. Late subexcitability was increased significantly when recording from the APB and FDI muscles (F = 11.4, P < 0.001, Fig. 2.5 A, B, Table 2.1). In contrast, there were no significant differences in the RRP (Fig. 2.5A, Table 2.1), refractoriness at 2 ms (F=0.5, P=0.61), and superexcitability (Fig. 2.5A, Table 2.1). Further, there were no significant differences in hyperpolarizing I/V gradient between the APB, FDI and ADM muscles (F = 2.5, P = 0.09).

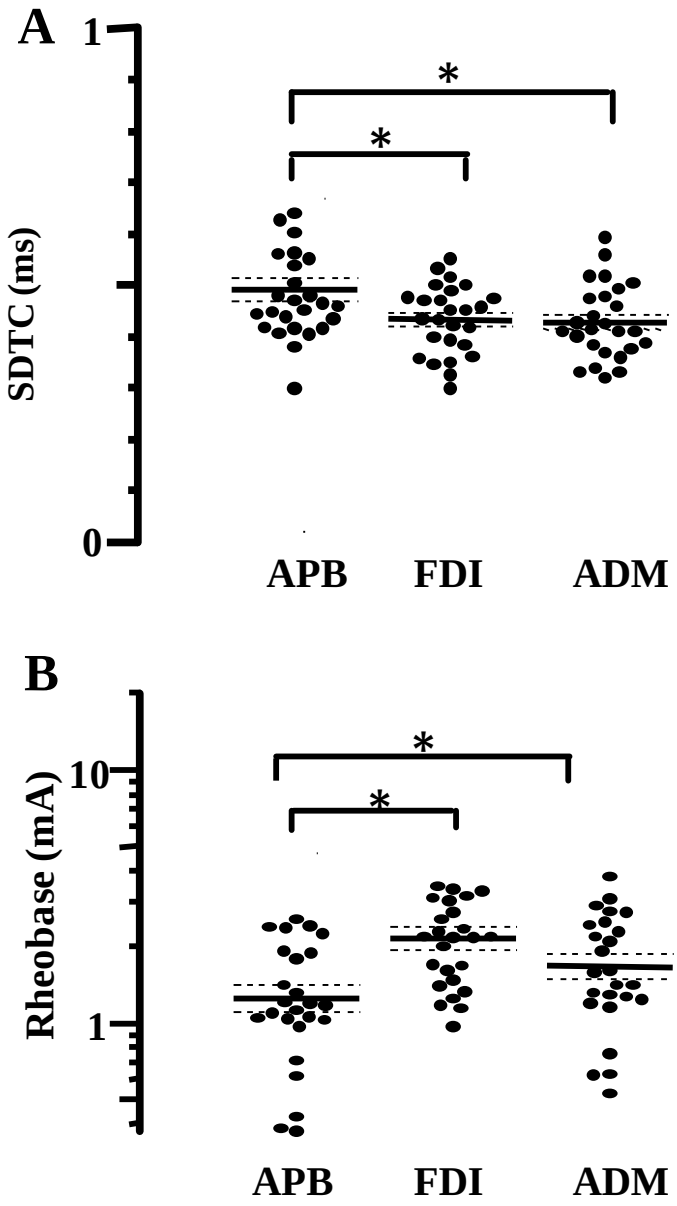

Figure 2.3: (A) The strength-duration time constant, a biomarker of persistent Na^+ conductances, was significantly longer when recording from the APB and FDI muscles compared to ADM. **(B)** The rheobase was significantly smaller when recording over the APB.

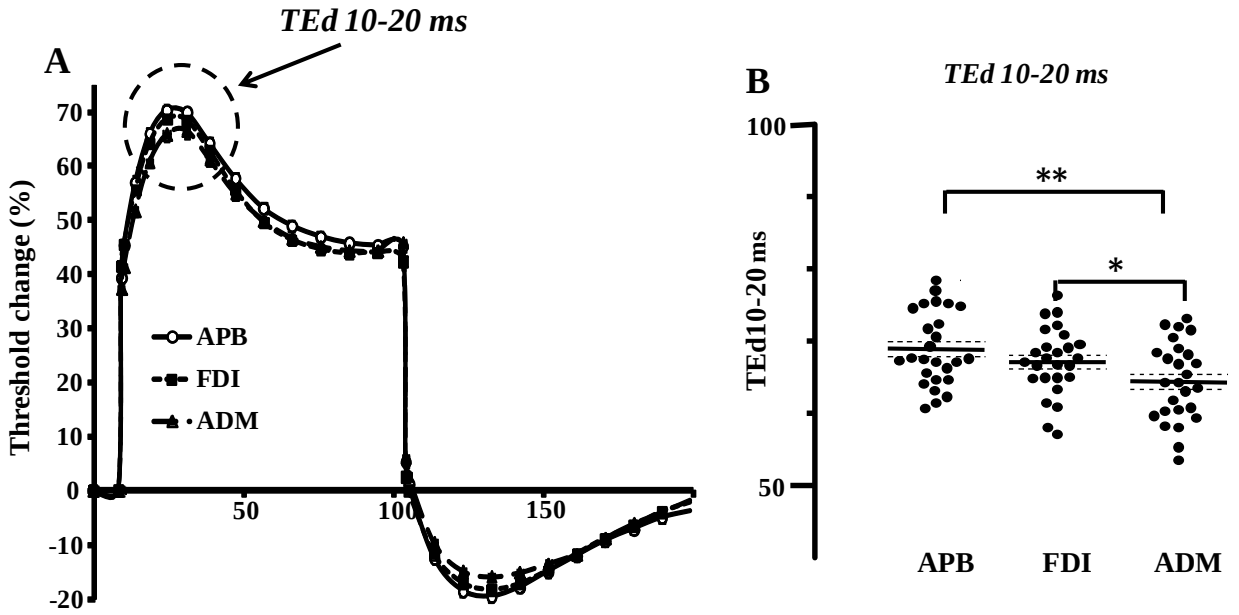

Figure 2.4: **(A)** Depolarizing threshold electrotonus at 10-20 ms (TEd 10-20 ms), a biomarker of paranodal fast K^+ currents, was significantly increased when recording over the APB and FDI compared to ADM. There were no significant differences in other depolarizing TE parameters. **(B)** Scatter plots illustrating that TEd 10-20 ms was significantly greater when recording over APB and FDI. **P*< 0.05; ***P*< 0.01.

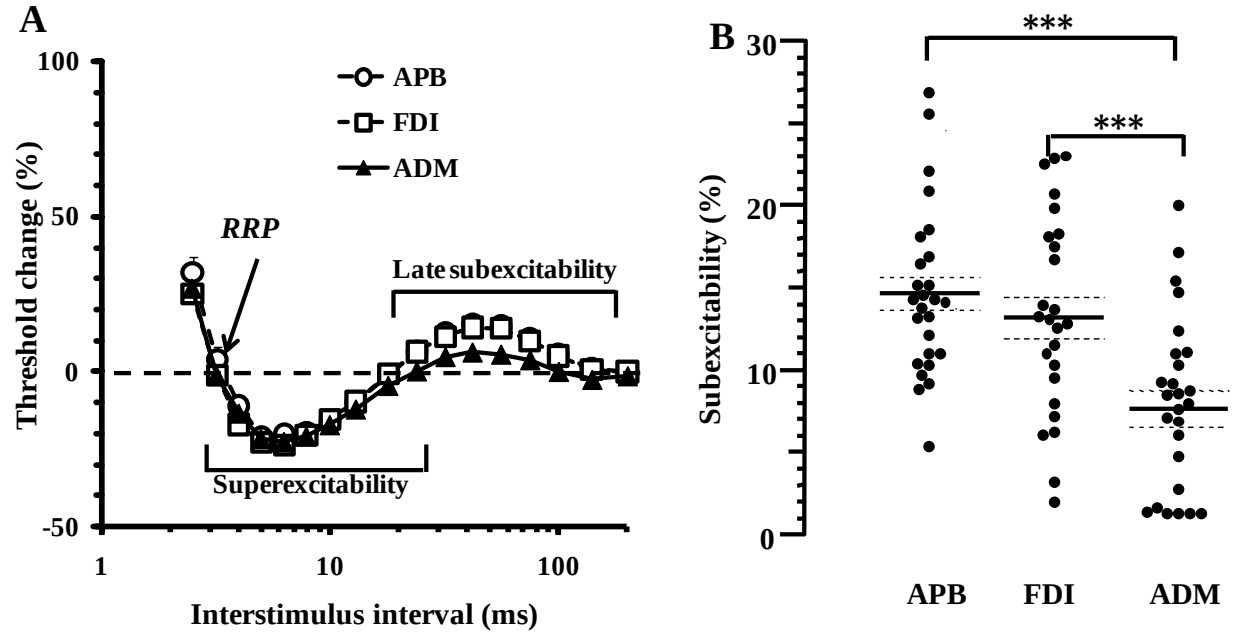

Figure 2.5: **(A)** Recovery cycle of excitability revealed that late sub-excitability was significantly larger when recording over APB and FDI compared to ADM. There were no significant differences in the RRP and superexcitability. **(B)** Scatter plots illustrating a significant increase in late subexcitability when recording over APB and FDI. ****P*<0.001.

Correlation studies

There were no significant correlations between SICI and strength duration time constant (R = -0.05, *P* =0.34), TEd 10-20 ms (R = 0.14, *P* =0.13), or MEP amplitude (R = -0.13, *P* = 0.19). In addition, MEP amplitude and CSP duration did not correlate with strength duration time constant or TEd (10-20 ms). Taken together, these findings suggest that the changes in central and peripheral nerve excitability were independent processes.

Discussion

The present study has established significant differences in cortical and axonal excitability between the APB, FDI, and ADM muscles. Specifically, SICI and MEP amplitude were significantly larger, while the CSP duration was significantly longer when recording from the APB and FDI. Taken together, these findings establish the presence of significant differences in cortical excitability between the 3 intrinsic hand muscles, with implications of a greater strength of intracortical inhibition and larger corticomotoneuronal output to the APB and FDI muscles. Separately, the strength-duration time constant was significantly longer and rheobase smaller, but only when recording over the APB. The differences in neurophysiological findings, particularly cortical excitability, could have potentially evolved from the differential use of these muscles in complex hand movements. Mechanisms underlying the changes in central and peripheral nerve excitability and their clinical implications will form the basis of the discussion.

Cortical mechanisms underlying differences in TMS parameters

It has been well established that cortical mechanisms underlie the generation of many features of the muscle activation that occurs in response to TMS, such as SICI (150, 401). Studies assessing

the effects of paired-pulse stimuli (conditioning-test paradigm) at short time intervals required to generate SICI have revealed a reduction in number and amplitude of indirect (I)-waves (waves I_2 and later) in corticospinal volleys (469, 470, 490, 542, 543), with implications that SICI originates at a cortical level, most likely the M1 cortex. Interestingly the time course of I-wave inhibition was similar to the typical duration of inhibitory postsynaptic potentials mediated through $GABA_A$ receptors (469, 471), thereby suggesting that SICI was mediated by inhibitory cortical interneurons acting via $GABA_A$ receptors (401, 441, 468, 544). Studies in non-human primates have provided additional evidence for a cortical origin of SICI, whereby direct

stimulation of the M1 cortex in macaque primates resulted in descending I-wave volleys, similar to that reported in humans (545). In the present study, SICI was larger when recording over the APB and FDI, suggesting a greater potency of the inhibitory circuits subserving the APB and FDI muscles. Given that the APB and FDI are involved in the execution of numerous hand movements, one of which is precision grip (531-533, 536, 537, 546, 547), such findings may have evolved from the differential actions of these muscles in complex hand movements.

In addition to SICI changes, the MEP amplitude was larger when recording over APB and FDI. The MEP amplitude is a biomarker of the density of corticomotoneuronal projections onto spinal motor neurons, in part reflecting the optimal conduction from M1 to spinal motor neurons (150, 401). Consequently, the findings of larger MEP amplitudes would seem to imply a greater corticomotoneuronal input to spinal motor neurons innervating the APB and FDI. Importantly, these findings are in keeping with previous studies that reported larger MEP amplitudes during performance of a complex task (190), further underscoring the notion that these changes in MEP

amplitude may have resulted from specific activity of APB and FDI muscles during the execution of complex hand tasks.

Of further relevance, there were significant changes in the CSP duration between the 3 muscles. Specifically, the CSP duration is in part mediated by cortical inhibitory circuits, acting via $GABA_B$ receptors(150, 452, 453, 457, 458, 548, 549). The CSP duration may also be influenced by the strength of corticomotoneuronal projections onto spinal motor neurons (401). Consequently, the findings in this study suggest further that intracortical inhibitory tone and corticomotoneuronal input were larger to the APB and FDI muscles. Alternatively, it could also be argued that the changes in CSP duration could be a function of the MEP amplitude (550). This seems an unlikely explanation given that there was no correlation between CSP duration and MEP amplitude.

In addition to a greater corticomotoneuronal output, a further explanation for these findings may relate to specific properties of corticomotoneurons innervating the APB and FDI muscles. Specifically, recent studies in macaque primates have established the existence of unique M1 output neurons, identified as pyramidal tract neurons (PTN), that discharge in response to the observation of precision grip by a human experimenter (551). Some of these PTNs with mirror properties were identified as exerting corticomotoneuronal effects on hand muscles, and while they discharged during action observation, were not associated with muscle contractions. Of further relevance, the PTN discharges were reduced greatly during action observation compared with trials in which the monkey itself executed the grasp, which may reflect a mechanism for controlling the motor system in a way that suppresses undesired movement. Given that these

PTNs with mirror properties appear to be important in execution of complex hand tasks, it could be argued that the corticomotoneuronal innervations of the APB and FDI motor neurons is more complex when compared to hypothenar motor neurons, thereby in-part accounting for the present findings.

Alternatively, it could also be argued that the differences in cortical excitability could be related to the use of a circular coil, which exerts effects over a wider cortical area, thereby resulting in non-specific activation of the motor cortex (552). This seems unlikely given that the coil position was altered such that an optimal MEP was elicited prior to assessment of each muscle. Importantly, previous TMS studies failed to establish any qualitative differences in the patterns of inhibition when using a circular or focal figure-of-eight coil (540). It is accepted that inadvertent stimulation of short interval facilitatory circuits may have contributed to differences in cortical excitability, in particular the differences in SICI. This is underscored by the fact that TMS studies utilizing the constant stimulus technique, with lower conditioning stimulus intensities, failed to document any significant differences in SICI between the different intrinsic hand muscles (552-555), while studies utilizing higher conditioning stimulus intensities reported findings similar to the present study (556). A significant contribution from inadvertent stimulation of facilitatory pathways seems an unlikely explanation, given that in previous threshold tracking TMS studies we have established that maximal SICI develops when sub-threshold conditioning stimuli were set to 70% of RMT (485).

In addition to changes in cortical excitability, there were also significant differences in axonal excitability, although they were most prominent when recording over the APB. Specifically, the

strength-duration time constant, a biomarker of nodal persistent Na^+ channel conductance (337), was increased significantly when recording over the APB. Moreover, early depolarizing threshold electrotonus (TEd 10-20 ms), a biomarker of fast paranodal K^+ conductances (85, 86), was increased when recording over the APB and FDI, but not the ADM. While some of the axonal excitability findings are in keeping with previous studies (55), suggesting a greater degree of hyperexcitability of motor axons innervating the APB and FDI muscles, there were important differences. Specifically, in the present study the τ_{SD} was only increased when recording from the APB, while Bae and colleagues reported comparable increases of τ_{SD} from the thenar and FDI muscles (55). In addition, the relative refractory period and refractoriness were comparable between the three muscles, contrasting with previous findings (55). A potential explanation for the discordant findings may relate to the variability of individuals to perform fractionated finger movements, a notion in part supported by a considerable overlap of axonal excitability values in this study. It could also be argued that the changes in axonal excitability account for differences in the cortical excitability findings between the three muscles. This seems unlikely, given that downstream axonal excitability changes are unlikely to influence corticomotoneuronal input to the motor neurons, a notion supported by an absence of correlation between measures of cortical and axonal excitability.

Clinical implications

Preferential atrophy of the APB and FDI muscles, with relative preservation of the ADM, termed the ***split hand***, is a specific feature of neurodegenerative disorders such as amyotrophic lateral sclerosis (ALS) (2, 20, 21, 130, 184, 519). While the precise pathophysiological processes underlying the development of the split hand remains to be elucidated, both central and

peripheral mechanisms have been proposed (44). A cortical basis for the split hand was based on observations that thenar muscles were responsible for fractionated finger movements and thereby receive a greater cortical representation and corticomotoneuronal input (44). Consequently, greater corticomotoneuronal input onto spinal motor neurons innervating the APB and FDI muscles may result in preferential degeneration of these spinal motor neurons via a transsynaptic anterograde excitotoxic mechanism.

The findings of greater SICI, MEP amplitude, and longer CSP duration to the APB and FDI would support a hypothesis of greater corticomotoneuronal input to these muscles and are concordant with previous TMS studies (54). In addition to cortical processes, differences in membrane properties of axons innervating the intrinsic hand muscles could contribute to development of the split-hand. Previously, upregulation of persistent Na^+ conductances, as measured by strength-duration time constant and latent addition, along with reduction in fast K^+ current were reported in APB and FDI axons (55). Although upregulation of persistent Na^+ conductances was only evident in the APB axons in the present study, reduction in fast K^+ currents was evident in both the APB and FDI axons. Ultimately, such changes in axonal excitability would render the APB and FDI axons hyperexcitable, thereby potentially predisposing them to neurodegeneration via Ca^{2+}-mediated mechanisms (557). Given that persistent Na^+ conductances were not upregulated in FDI axons; this may suggest a predominance of cortical processes in development of the split-hand phenomenon. If verified in future ALS cohorts, such findings could be of potential pathophysiological significance.

Chapter 3

ALS Pathophysiology: Insights from the Split-Hand Phenomenon

Summary

Subsequent to the study in normal subjects establishing differences in cortical excitability that follow the split-hand pattern, the present study was aimed at assessing whether peripheral mechanisms, mediated through axonal dysfunction, may contribute to development of the split-hand phenomenon in amyotrophic lateral sclerosis (ALS). Median and ulnar nerve motor axonal excitability studies were undertaken in 21 ALS patients with motor responses recorded over the abductor pollicis brevis (APB), abductor digit minimi (ADM) and first dorsal interosseous (FDI) muscles, and results compared to 24 controls. The split-hand index (SI), an objective biomarker of preferential atrophy of APB and FDI muscles, was significantly reduced in ALS (SI_{ALS} 7.8±1.7, $SI_{CONTROLS}$ 13.1±1.1, $P<0.0001$). Axonal excitability studies identified significant prolongation of strength-duration time constant in ALS patients when recording over the APB ($P<0.05$) and ADM axons ($P<0.05$) but not FDI axons ($P=0.22$). Greater changes in depolarising threshold electrotonus were also evident across the range of intrinsic hand muscles and were accompanied by increases of superexcitability in APB ($P<0.01$) and FDI ($P<0.05$) axons. The present study reinforces the significance of the split-hand phenomenon in ALS and argues against a significant peripheral contribution in the underlying development. Axonal dysfunction may appear as a downstream process that develops secondary to the intrinsic pathophysiological origins of ALS.

Introduction

Dissociated atrophy of intrinsic hand muscles, termed the ***split hand phenomenon***, refers to preferential wasting of abductor pollicis brevis (APB) and first dorsal interosseous (FDI) muscles with relative preservation of the abductor digit minimi (ADM) (21, 558). The split-hand sign appears to be an early and specific clinical feature of amyotrophic lateral sclerosis (ALS), not evident in other common clinical mimic neuromuscular disorders (20, 21, 54, 519, 529), although it has been reported with normal ageing and in some neurodegenerative disorders such as spinocerebellar ataxia type 3, juvenile muscular atrophy and autosomal dominant spinal muscular atrophy (559, 560).

The mechanisms underlying the development of the split-hand pattern of wasting in ALS remains to be elucidated, with resolution of this issue of potential pathophysiological importance in understanding ALS onset and patterns of disease spread. Given that wasted intrinsic hand muscles are innervated by an overlap of similar myotomes (C8-T1), dysfunction of local spinal segments are unlikely to account for the split-hand phenomena in ALS per se. Rather, three potential mechanisms have been proposed including a cortical-based process related to a larger central representation of the thenar complex group of muscles (APB/FDI), abnormalities at a peripheral level and increased metabolic demands of the motor neurons innervating the thenar and FDI muscles (20, 54, 519, 529).

Perhaps of relevance, upregulation of persistent Na^+ conductances, as reflected by an increase in strength-duration time constant, and reduction in K^+ currents, have been extensively documented in ALS (31, 56-58, 126, 561, 562). Importantly, changes in axonal excitability,

particularly upregulation of persistent Na^+ conductances, have been linked to the process of neurodegeneration and survival in ALS (57, 562). While these studies established that dysfunction of axonal ion channel conductances was part of the pathophysiological process in ALS, only single nerves were assessed, precluding any conclusions as to whether specific or more generalized abnormalities in axonal excitability contributed to the development of the split-hand phenomenon.

A study in healthy controls reported a relative increase in strength-duration time constant and greater abnormalities of threshold electrotonus in motor axons innervating the APB and FDI muscles compared to ADM (55). These findings implied that axons innervating the thenar muscles and FDI may seem physiologically prone to develop hyperexcitability and thereby susceptible to degeneration in ALS. Recently, a greater increase in strength-duration time constant and more prominent abnormalities of depolarising threshold electrotonus were reported in axons innervating the APB muscle compared to ADM in sporadic ALS (563). While these findings suggested that dysfunction at a peripheral axonal level may contribute to the development of the split hand, the excitability properties of FDI axons was not assessed. As a consequence, axonal excitability properties of motor axons innervating the APB, FDI and ADM muscles were assessed "en bloc", in order to determine whether dysfunction at a peripheral axonal level determined the pathophysiological basis of the split hand in ALS.

Methods

Studies were undertaken on 21 amyotrophic lateral sclerosis (ALS) patients with clinically probable or definite ALS (16 male, 5 female: mean age: 55 years, 32-73) as defined by the Awaji

criteria (82). All patients provided written informed consent to the procedures which were approved by the Western Sydney Local Health District Human Research Ethics Committee.

Clinical Phenotyping

ALS patients were clinically staged using the amyotrophic lateral sclerosis functional rating scale-revised (ALSFRS-R) score (511) and according to site of disease onset as limb or bulbar-onset. Muscle strength was assessed by utilising the Medical Research Council (MRC) score (512), with the following muscle groups assessed bilaterally yielding a total MRC score of 90: shoulder abduction; elbow flexion; elbow extension; wrist dorsiflexion; finger abduction; thumb abduction; hip flexion; knee extension; ankle dorsiflexion. In addition, ALS patients were classified according to the extent of lower motor neuron dysfunction as indicated by compound muscle action potential (CMAP) amplitudes, measured from baseline-to-peak, into "early stage" and "more advanced" patients as follows: (i) APB normal amplitude (CMAP≥4 mV); reduced amplitude (<4 mV); (ii) ADM normal amplitude (CMAP≥5.5 mV); reduced amplitude (<5.5 mV); (iii) FDI, normal amplitude (CMAP≥7.7 mV); reduced amplitude (<7.7 mV). All patients underwent extensive neurophysiological, radiological and biochemical investigations and patients with coexisting neurological disorders such as median and ulnar nerve entrapment neuropathies and peripheral neuropathy were excluded from the study. Patients suffering with diabetes mellitus or chronic renal failure were excluded and all patients and controls were confirmed to not be on medications that could affect the results.

Axonal excitability studies

All ALS patients underwent axonal excitability studies on the median and ulnar motor nerves according to a previously described protocol (354). Briefly the median and ulnar nerves were stimulated at the wrist using 5 mm non-polarizable Ag-AgCl electrodes (3M Healthcare, MN, USA) with the CMAP responses recorded over APB, FDI and ADM muscles. All studies were undertaken unilaterally, from the more clinically affected limb that exhibited a split-hand phenomenon. As such, the changes in axonal excitability are more likely to reflect the pathophysiology underlying the split-hand. The following axonal excitability parameters were measured: (i) strength-duration time constant (τ_{SD}) and rheobase; (ii) threshold electrotonus (TE) recorded with sub-threshold depolarizing currents at 10-20 ms (TEd [10-20 ms]), 40-60 ms (TEd [40-60 ms]), and 90-100 ms (TEd [90-100 ms]), and with hyperpolarizing currents at 10-20 ms, TEh [10-20 ms] and at 90-100 ms, TEh [90-100 ms]; (iii) hyperpolarizing current-threshold relationship (I/V) calculated from polarizing currents between +50 and -100%; (iv) recovery cycle parameters including relative refractory period (RRP, ms), superexcitability (%) and late subexcitability (%).

In addition, the CMAP onset latency and twenty F-wave responses were also recorded from each muscle from which the neurophysiological index (NI) was derived (65). The split-hand index (SI) was also calculated according to a previously reported formulae (529).

$$SI = \frac{CMAP_{APB} * CMAP_{FDI}}{CMAP_{ADM}}$$

Recordings of CMAP responses were amplified and filtered (3 Hz-3 kHz) using a Nikolet-Biomedical EA-2 amplifier (Cardinal Health Viking Select version 11.1.0, Viasys Healthcare

Neurocare Group, Madison, Wisconsin, USA) and sampled at 10 kHz using a 16-bit data acquisition card (National Instruments PCI-MIO-16E-4). Data acquisition and stimulation delivery were controlled by QTRACS software (TROND-F, version 16/02/2009, © Professor Hugh Bostock, Institute of Neurology, Queen Square, London, UK). Temperature was monitored with a purpose built thermometer at the stimulation site and maintained at or above 32°C.

Statistical analysis

Axonal excitability studies were compared to 24 age-matched controls (13 males; 11 females, mean age 51.1±2.2 years). Student t-test was utilised to assess differences between means in patients and controls. Pearson's correlation coefficients were used to examine the relationship between parameters. Shapiro-Wilk test disclosed that all neurophysiological data, namely axonal excitability and conventional neurophysiological data, was normality distributed. A probability (P) value of <0.05 was considered statistically significant, and the probability values were corrected for multiple comparisons. Results were expressed as mean ± standard error of the mean and median (interquartile range).

Results

Clinical features

The clinical features for the 21 ALS patients are summarised in Table 3.1. A split-hand pattern of atrophy was evident in 53% of patients. Bulbar-onset disease was evident in 40% and limb-onset disease in 60% of ALS patients. Although the split-hand sign was more frequently observed in limb-onset (62%) compared to bulbar-onset disease (37%), this difference was not

significant (P=0.33). At time of assessment, the median disease duration from symptom onset was 10 (5-17) months, while the median ALSFRS-R was 43 (41-46), suggesting a moderate degree of disability. In addition, the median total MRC score was 81 (74-87), upper limb MRC score 54 (50-58) and lower limb score 30 (28-30), reaffirming a mild to moderate degree of impairment. Given that ALS patients were in the early stages of the disease at time of recruitment, 40% were receiving riluzole while 60% were not taking riluzole at the time of axonal excitability studies.

Prior to conducting axonal excitability studies the degree of the lower motor neuron dysfunction was determined. The CMAP amplitude was significantly reduced from all three muscles in ALS patients compared to controls (APB $CMAP_{ALS}$ 5.6±0.8 mV, $CMAP_{CONTROLS}$ 8.4±0.5, P<0.001; FDI $CMAP_{ALS}$ 5.5±0.9mV, $CMAP_{CONTROLS}$ 10.3±0.9mV, P<0.001; ADM $CMAP_{ALS}$ 6.5±0.5mV, $CMAP_{CONTROLS}$ 10.1±0.5 mV, P<0.001). In addition, the NI was also significantly reduced (APB NI_{ALS} 1.3±0.2, $NI_{CONTROLS}$ 1.9±0.2, P<0.001; FDI NI_{ALS} 1.3±0.3, $NI_{CONTROLS}$ 2.9±0.2, P<0.0001; ADM NI_{ALS} 1.6±0.2, $NI_{CONTROLS}$ 2.8±0.1, P<0.0001).

Of further relevance, the spit-hand index was significantly reduced in ALS patients (SI_{ALS} 7.8±1.7, $SI_{CONTROLS}$ 13.1±1.1, P<0.0001). While the reduction in SI was a ubiquitous finding, it was most prominent in limb-onset patients ($SI_{LIMB\text{-}ONSET}$ 6.7±1.3; $SI_{BULBAR\text{-}ONSET}$ 7.4±1.6), although this difference was not significant (P=0.39). Taken together, these findings indicate a greater degree of lower motor neuron dysfunction in ALS patients, with split-hand pattern of atrophy being a feature in ALS.

PATIENTS	AGE/ SEX	SITE OF ONSET	DURATION (MONTHS)	ALSFRS-R	MRC UL	MRC LL	MRC TOTAL
1	51/M	LIMB	21	33	47	18	65
2	42/M	LIMB	17	41	44	30	74
3	73/M	LIMB	30	44	51	30	81
4	69/F	LIMB	14	47	51	30	81
5	62/M	LIMB	5	46	58	30	88
6	45/M	LIMB	3	46	56	30	86
7	48/M	LIMB	5	42	60	20	80
8	64/M	LIMB	7	47	57	30	87
9	41/M	LIMB	6	43	53	27	80
10	68/M	LIMB	9	48	58	30	88
11	66/M	LIMB	9	47	50	30	80
12	56/F	LIMB	14	34	52	22	74
13	68/M	LIMB	12	42	26	30	56
14	57/M	BULBAR	3	44	60	30	90
15	71/F	BULBAR	12	42	42	30	72
16	52/F	BULBAR	24	36	54	30	84
17	39/M	BULBAR	10	32	47	20	67
18	64/M	BULBAR	30	23	54	28	82
19	49/F	BULBAR	21	42	60	30	90
20	58/M	BULBAR	4	43	60	30	90
21	32/M	BULBAR	4	43	54	30	84
MEAN/MEDIAN	**55.9**		**10**	**43**	**54**	**30**	**81**
SEM (IQR)	**2.6**		**(5-17)**	**(41-46)**	**(51-58)**	**(28-30)**	**(74-87)**

Table 3.1: Axonal excitability studies were undertaken on 21 amyotrophic lateral sclerosis (ALS) patents, 16 males (M) and 5 females (F). All patients were clinically staged using the amyotrophic lateral sclerosis functional rating scale–revised (ALSFRS-R, range 0 to 48), as well as the Medical Research Council (MRC) score for muscle strength. Muscle strength was assessed from the upper limbs (UL, maximal MRC score 60) and the lower limbs (maximal MRC score 30, *see* Methods), resulting in a total MRC score of 90. All results were expressed as either mean ± standard error of the mean (SEM) or median with interquartile range (IQR).

The strength-duration time constant (τ_{SD}), a biomarker of nodal persistent Na^+ conductance (86), was significantly longer in ALS patients when recording from APB (ALS_{APB} 0.51±0.02 ms; controls 0.47±0.02 ms, P<0.05, Fig. 3.1A, B) and ADM (ALS_{ADM} 0.50±0.02 ms; controls 0.43 ±0.01 ms, P<0.01, Fig. 3.1C, D), but not FDI muscles (ALS_{FDI} 0.44±0.03 ms; controls 0.43±0.01 ms, P=0.22, Table 2). There were no significant differences in rheobase between ALS patients and controls (ALS_{APB} 1.40±0.1 mA; controls 1.55±0.2 mA, P=0.16; ALS_{FDI} 2.57± 0.38 mA; controls 2.55±0.43 mA, P=0.49; ALS_{ADM} 1.95±0.26 mA; controls 1.80±0.19 mA, P=0.33, Table 2). The increase in τ_{SD} was independent of therapeutic status, being evident in patients receiving riluzole and those who were yet to be commenced on riluzole when recording from APB ($APB\tau_{SD\ ON\ RILUZOLE}$ 0.52±0.02 ms, P<0.05; APB $\tau_{SD\ NO\ RILUZOLE}$ 0.53±0.02 ms, P<0.05) and ADM ($ADM\tau_{SD\ ON\ RILUZOLE}$ 0.50±0.03 ms, P<0.05; $ADM\tau_{SD\ NO\ RILUZOLE}$ 0.50±0.02 ms, P<0.05) muscles.

Threshold Electrotonus, a biomarker of internodal and paranodal K^+ currents (85), revealed greater changes in sub-threshold depolarizing TE when recording from all three muscles. Specifically, depolarizing TE at 90-100 ms was significantly greater when recording over the APB (ALS 50.3±1.5%; controls 44.7±0.8%, P<0.001, Fig. 3.2A, B), ADM (ALS 48.1±1.0%; controls 45.5±0.7%, P<0.05, Fig. 3.2C, D) and FDI (ALS 45.1±1.5%; controls 40.0±2.2%, P < 0.05, Fig. 3.2E, F) muscles in ALS. These changes were accompanied by a significant increase in TEd at 40-60 ms in APB (ALS 56.1±1.7%; controls 52.6±1.0%, P<0.05, Fig. 3.3A, B) and ADM (ALS 53.6±1.3%; controls 50.8±0.9%, P<0.05, Fig. 3.3C, D), but not FDI axons (P=0.11).

PARAMETER	APB	Control	P	FDI	Control	P	ADM	Control	P
SDTC (ms)	0.52	0.47	**0.03**	0.44	0.43	0.33	0.50	0.43	**0.01**
Rheobase (mA)	1.35	1.55	0.19	2.57	2.56	0.49	1.95	1.81	0.33
TEd 10-20ms (%)	70.67	69.38	0.22	66.14	67.34	0.22	65.77	64.98	0.30
TEd 40-60ms (%)	56.08	52.65	**0.04**	52.52	50.40	0.11	53.55	50.76	**0.04**
TEd 90-100ms (%)	50.26	44.67	**<0.005**	45.19	39.95	**0.03**	48.07	45.45	**0.02**
TEh 90-100ms (%)	-125.92	-119.12	0.17	-120.15	-116.89	0.25	-116.74	-119.37	0.33
Resting I/V gradient	0.56	0.64	**0.03**	0.60	0.59	0.46	0.59	0.60	0.35
Hyperpolarising I/V gradient	0.41	0.36	**0.04**	0.59	2.29	0.08	0.37	0.51	0.20
RRP (ms)	3.61	3.43	0.3	3.13	3.35	0.14	3.37	3.31	0.40
Superexcitability (%)	-26.53	-21.58	**0.007**	-27.60	-23.14	**0.01**	-24.75	-23.49	0.24
Late Subexcitability (%)	11.85	13.32	0.17	12.12	13.97	0.21	11.34	7.98	0.06

Table 3.2: Axonal excitability studies were undertaken on the median and ulnar motor nerves with responses recorded from the abductor pollicis brevis (APB), first dorsal interosseous (FDI) and abductor digit minimi (AMD) muscles. The strength-duration time constant (SDTC) was significantly prolonged in the APB and ADM motor axons. In addition, greater changes in depolarising threshold electrotonus (TEd) were evident at 90-100 ms (TEd 90-100 ms) in motor axons innervating all three muscles and at 40-60 ms (TEd 40-60 ms) in the APB and ADM motor axons. In contrast, there were no significant changes in the hyperpolarizing threshold electrotonus at 90-100 ms (TEh 90-100 ms) or relative refractory period (RRP) in the APB, ADM and FDI motor axons. Interestingly, the resting and hyperpolarising current/threshold relationship (I/V), was increased in the APB motor axons.

The type II abnormality, in which there is a sudden decrease in membrane excitability marked by an abrupt increase in threshold (86), was not evident in the ALS cohort from any of the muscles studied. In addition, there were no significant changes in depolarising TE at 10-20 ms and in hyperpolarising TE when recording over the APB, FDI or ADM muscles when compared to controls (Table 3.2).

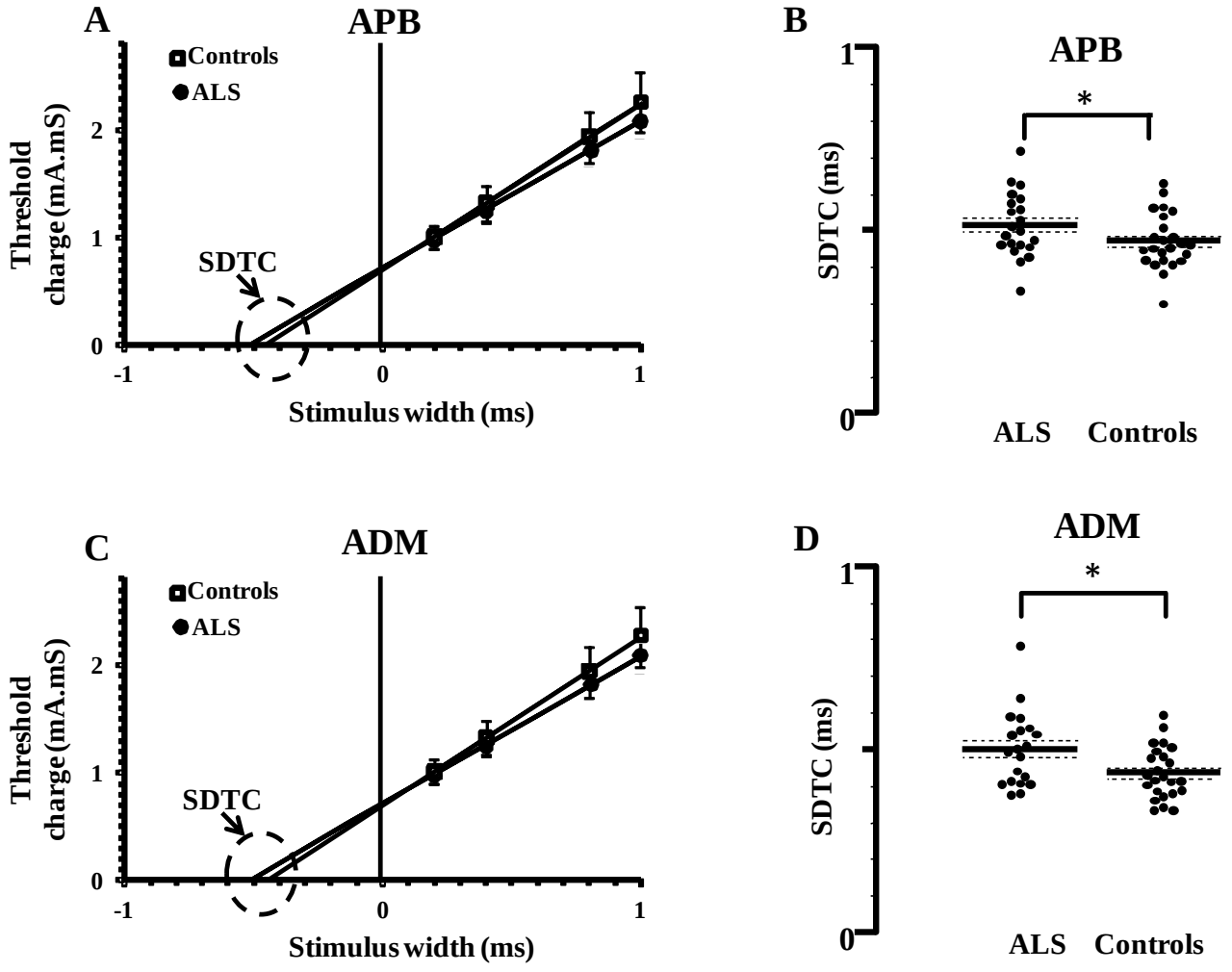

Figure 3.1: The strength-duration time constant, a biomarker of persistent Na^+ conductances, was significantly increased in the **(A, B)** abductor pollicis brevis (APB) and **(C, D)** abductor digit minimi (ADM) motor axons in amyotrophic lateral sclerosis (ALS) patients compared to controls. *P < 0.05.

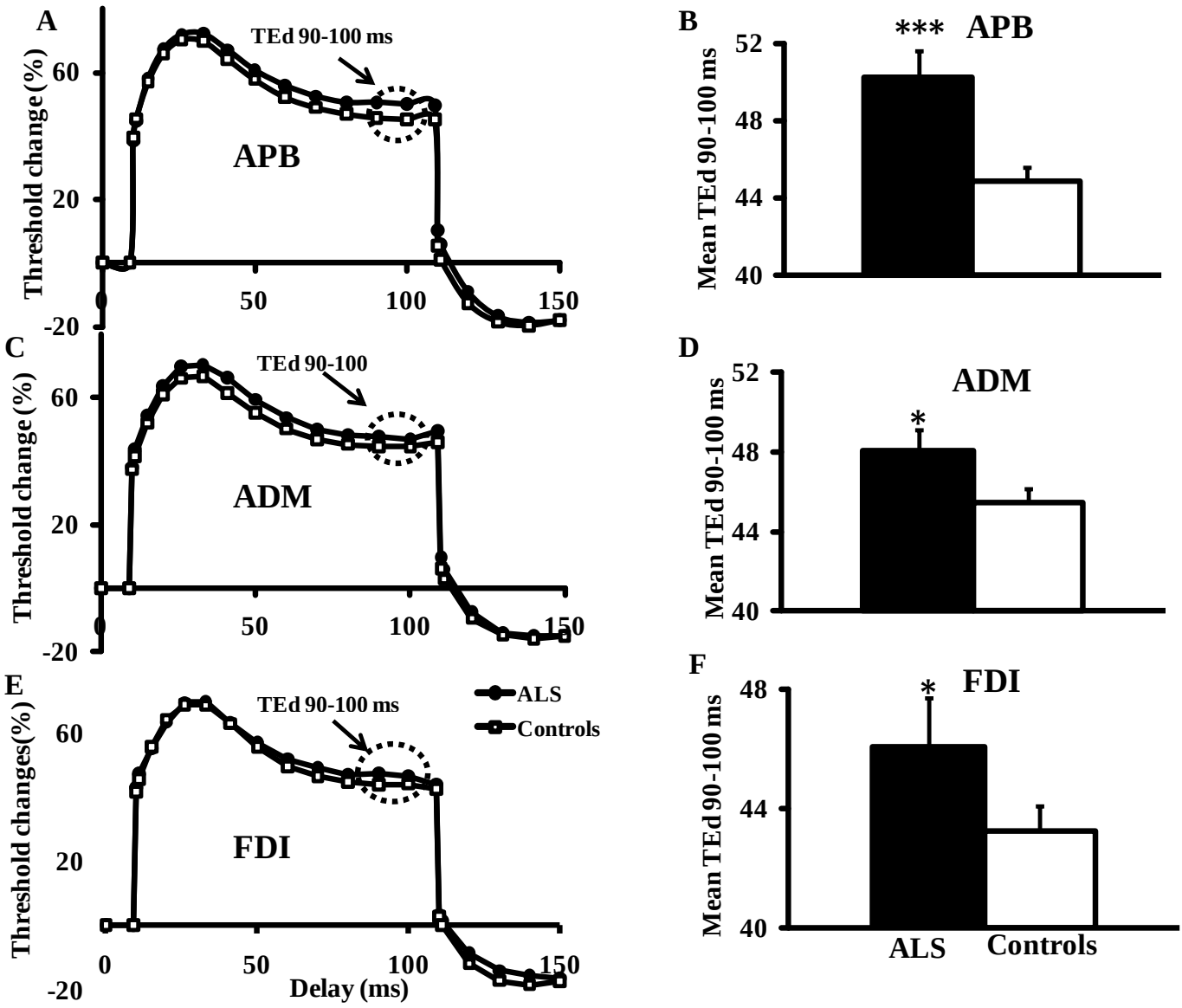

Figure 3.2: Depolarising threshold electrotonus (TEd) is a biomarker of internodal slow K^+ currents. There was a significant increase in TEd at 90-100 ms (TEd 90-100ms) when recording from the **(A, B)** abductor pollicis brevis (APB), **(C, D)** abductor digit minimi (ADM) and **(E, F)** first dorsal interosseous (FDI) muscles in amyotrophic lateral sclerosis (ALS) patients compared to controls. *P < 0.05; ***P < 0.001.

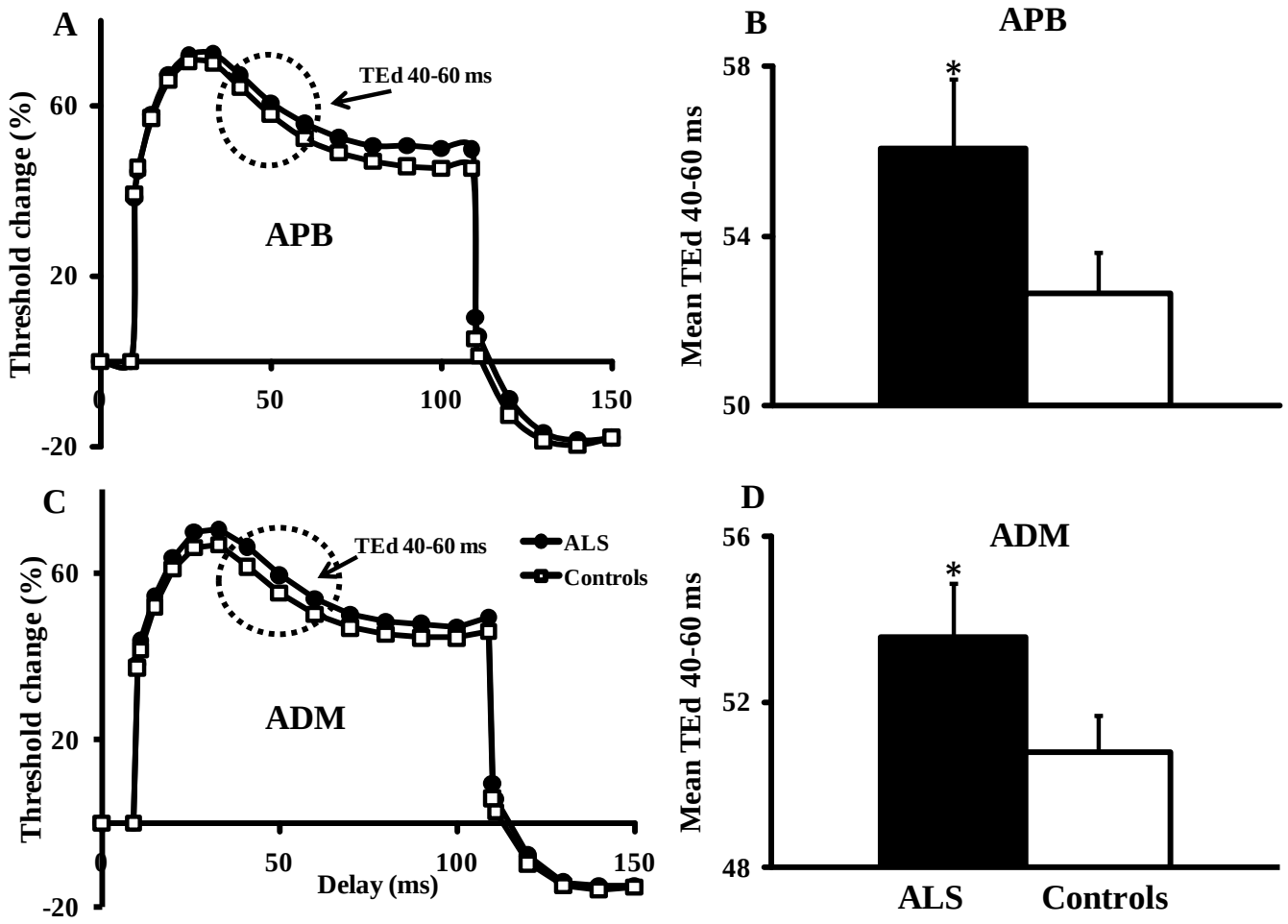

Figure 3.3: Depolarising threshold electrotonus AT 40-60 ms, also a biomarker of internodal slow K^+ currents, was increased when recording from the **(A, B)** abductor pollicis brevis (APB) and **(C, D)** abductor digit minimi (ADM) muscles in amyotrophic lateral sclerosis (ALS) patients compared to controls. *P < 0.05

In addition to changes in threshold electrotonus, there was a significant increase in superexcitability when recording from the APB (ALS -26.5±1.3%; controls -21.6±1.5%, P<0.01, Fig.3.4A, B) and FDI (ALS -27.6±1.4%; controls -23.1±1.2%, P<0.05, Fig. 3.4 C, D), but not ADM (ALS -24.8±1.2%; controls -23.5±1.3%, P=0.24). There was no significant difference in the relative refractory period or late sub-excitability in ALS patients compared to controls when recording over the three muscles (Table 3.2).

Finally, the ***current/threshold (I/V) relationship*** was significantly different between ALS patients and controls, but only when recording from APB axons. Specifically, the resting (ALS 0.55±0.02, controls 0.64±0.04, P<0.05) and hyperpolarising I/V (ALS 0.41±0.02, controls 0.36±0.01, P<0.05) gradients were significantly increased in ALS patients when recording over the APB. In contrast, there were no significant differences in the current threshold relationship when recording from the ADM and FDI (Table 3.2).

Correlations with clinical and neurophysiological parameters

In order to further clarify the contribution of peripheral axonal dysfunction to the development of the split-hand in ALS, axonal excitability parameters were correlated with clinical features and established neurophysiological biomarkers of LMN loss including the CMAP amplitude and neurophysiological index. Combining these parameters, it was evident that the τ_{sd} recorded from the APB and ADM was significantly correlated with CMAP amplitude (R_{APB} = -0.49, P<0.05; R_{ADM} = -0.53, P<0.01) and neurophysiological index (R_{APB} = -0.46, P < 0.05; R_{ADM} = -0.40, P<0.05).

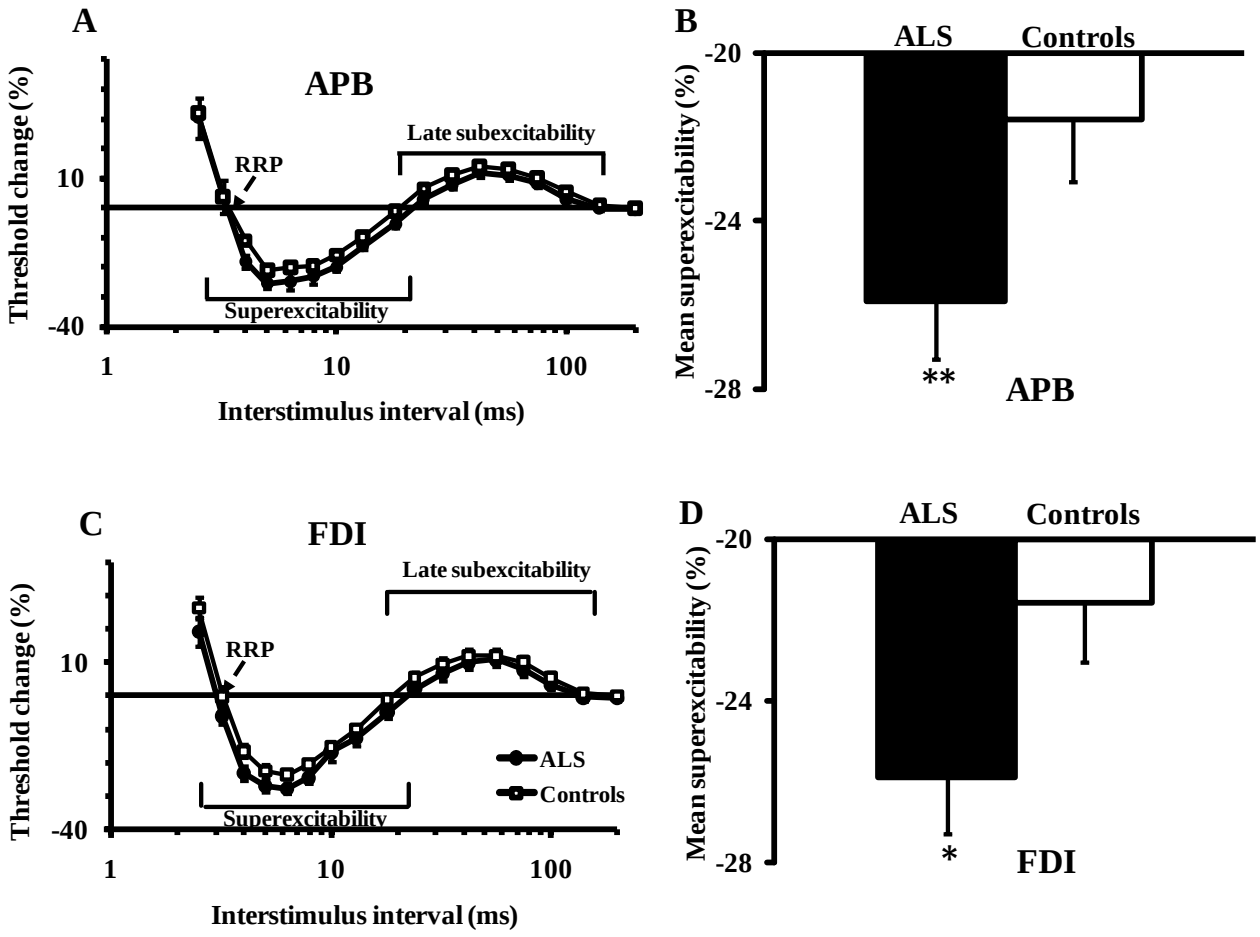

Figure 3.4: The recovery cycle of excitability revealed a significant increase in superexcitability when recording from the **(A, B)** abductor pollicis brevis (APB), **(C, D)** first dorsal interosseous (FDI) muscles in amyotrophic lateral sclerosis (ALS) patients compared to controls. There was no significant difference in the relative refractory period (RRP) and late subexcitability between ALS patients and controls. *P < 0.05; **P < 0.01.

In addition, the τ_{SD} was significantly greater in ALS patients with a greater lower motor neuron dysfunction when recording from APB ($\tau_{SD\ CMAP<4mV}$ 0.56±0.03 ms, P<0.05; $\tau_{SD\ CMAP>4mV}$ 0.48±0.01 ms, P<0.05) and ADM ($\tau_{SD\ CMAP<5.5mV}$ 0.65±0.05 ms, P<0.05; $\tau_{SD\ CMAP>5.5mV}$ 0.41±0.03 ms, P<0.05) muscles. In contrast, there was no significant correlation between the τ_{SD} recorded from FDI and the CMAP amplitude (R=0.15, P=0.26) and NI (R = -0.13, P=0.30).

Of further relevance, depolarising threshold electrotonus at 90-100 ms was significantly correlated with CMAP amplitude (R = -0.49, P<0.05), NI (R=-0.46, P<0.05) and disease duration (Rho = 0.40, P < 0.05), but only when recording from the APB. In contrast, there was no significant correlation of clinical scores with any of the axonal excitability parameters. These findings suggest that while peripheral axonal dysfunction correlates with lower motor neuron dysfunction and thereby axonal degeneration, such axonal dysfunction does not appear to follow a split-hand pattern distribution.

Discussion

The split-hand pattern of atrophy is a specific clinical feature of ALS, for which the underlying pathophysiological basis remains to be elucidated (20, 529, 558). Dysfunction at a peripheral axonal level has been proposed as a potential mechanism for the development of the split-hand phenomenon in ALS (563). The findings in the present study have established abnormalities across all motor axons innervating the APB, FDI and ADM muscles, although such changes did not follow a split-hand distribution. Specifically, the strength-duration time constant was prolonged in APB and ADM axons, but not FDI axons. Importantly, the prolonged τ_{SD} correlated with conventional biomarkers of lower motor neuron dysfunction, namely the CMAP

amplitude and neurophysiological index, suggesting that abnormalities of τ_{SD} were linked to the process of neurodegeneration. In addition, greater changes to depolarising threshold electrotonus were also evident in axons innervating all three muscles, accompanied by an increase in superexcitability. Taken together, these findings suggest widespread dysfunction of axonal membrane conductances, with evidence of reduced K^+ currents in all three motor axons accompanied by upregulation of persistent Na^+ conductances in APB and ADM axons. Importantly, the changes in axonal membrane conductance did not appear to follow a split-hand pattern, thereby arguing against a notion that axonal processes form the pathophysiological basis of the split-hand phenomenon in ALS.

Axonal dysfunction and split-hand

The strength-duration time constant is an established biomarker of persistent Na^+ conductances (337). In sporadic and familial ALS, prolongation of the τ_{SD} has been extensively documented and linked to the process of neurodegeneration (56-58, 126, 351, 561, 562). In addition, prolongation of τ_{SD} was reported to be a predictor of poorer survival in sporadic ALS (562). Importantly, a recent study documented significantly greater prolongation of the τ_{SD} in APB axons when compared to ADM axons (563). While these findings imply a role for axonal dysfunction, particularly upregulation of persistent Na^+ conductances, in the development of the split-hand sign in ALS, the function of FDI axons was not assessed. In the present study, a comparable increase in τ_{SD} was evident in APB and ADM axons, while there was no significant increase of τ_{SD} in FDI axons. As such, our findings could argue against a significant contribution of axonal dysfunction in development of the split-hand phenomenon in ALS. Alternatively, the

differences in τ_{SD} between APB/ADM and FDI motor axons could be potentially explained by existence of a "second split" in the ALS intrinsic hand muscles.

Of further relevance, a significant reduction in depolarising TE was evident in the current ALS cohort and did not appear to follow a split-hand pattern. Given that depolarising TE is a biomarker of internodal slow K^+ currents (85, 86, 357), the findings from the study suggests that reduction in K^+ currents was a feature in ALS, in keeping with the previously established modelled hypothesis (57). The reduction in K^+ currents, however, was comparable across the motor axons, further arguing against the notion that axonal dysfunction significantly contributed to development of the split-hand phenomenon in ALS.

The changes in depolarising TE were accompanied by an increase in superexcitability, a biomarker of paranodal fast K^+ channel conductances (85, 86, 357). Interestingly, the changes in superexcitability followed a split-hand distribution, being most prominent in APB and FDI axons. Consequently, it could be argued that a reduction in fast K^+ conductances in the APB and FDI axons may contribute to development of the split-hand. While such a notion could not be absolutely discounted, it seems unlikely that axonal dysfunction significantly contributed to the development of the split-hand in ALS given that other parameters of axonal ion channel function, namely τ_{SD} and depolarising TE, did not follow a split-hand pattern.

A potential explanation for discordant findings between the current ALS cohort and previous studies (563) may relate to differences in lower motor neuron dysfunction. Namely, degeneration of motor axons expressing an upregulation of persistent Na^+ conductances could

have accounted for differences in τ_{SD} findings in ADM axons. In addition, it could also be argued that such a neurodegenerative process may have also accounted for the $\Tau_{SD}$ findings in the FDI axons. This seems unlikely given that $\Tau_{SD}$ appears to increase with a greater degree of lower motor neuron dysfunction and has been previously linked to the process of neurodegeneration (351). Of further relevance, differences in the ability to perform fractionated finger movements by ALS patients could have also contributed to these discordant findings. This, again, seems unlikely given the absence of a significant correlation between axonal excitability parameters and ALSFRS-R fine motor scores in the present study.

Differences in treatment practices, as pertaining to riluzole usage, may have contributed to the discordant findings. Namely, none of the patients in the Japanese study were receiving riluzole at time of assessment, while 40% of ALS patients in the current cohort were receiving riluzole therapy. Given that riluzole exerts modulating effects on axonal ion channel function (153), it could be argued that differences in axonal membrane function may have been accounted for by treatment practices. This again seems unlikely given that previous studies have demonstrated that riluzole reduces superexcitability and refractoriness (480), findings not evident in the current cohort. In addition, there were no differences in axonal function, particularly τ_{SD} prolongation, in ALS patients "on" or "off" riluzole.

Upstream effects, at spinal motor neuron or supraspinal levels, may have accounted for the discordant axonal excitability findings. Specifically, dysfunction of central nervous systems pathways may influence the biophysical properties of motor axons via transsynaptic processes (564, 565). Given that cortical dysfunction may vary across the ALS phenotypes(40, 52), it

could be argued that the discordant findings simply reflect changes at a central nervous system level.

What underlies the split-hand phenomenon in ALS?

The pathophysiological mechanisms underlying the split-hand phenomenon in ALS remains to be fully elucidated. Peripheral axonal processes, as previously suggested (563), don't appear to significantly contribute to the development of the split-hand. However, a preferential degeneration of lower motor neurons innervating the APB and FDI muscles, without a parallel change in axonal excitability, could not be absolutely discounted. Rather, cortical mechanisms may be a more likely underlying mechanism for the split-hand phenomenon (54), especially in light of the knowledge that the thenar group of muscles (APB/FDI) are critical in execution of fractionated finger movements and thereby exhibit a larger cortical representation (44). Cortical hyperexcitability is an established pathophysiological process in ALS and linked to the process of peripheral neurodegeneration (49-52, 126). Given the larger cortical representation of the thenar muscles, it could be argued that preferential degeneration of APB/FDI motor neurons may be mediated by cortical processes via an anterograde transsynaptic excitotoxic mechanism, thereby resulting in the split-hand phenomenon. Studies assessing cortical function to thenar (APB/FDI) and hypothenar muscles may yet prove useful in resolving the pathophysiological basis of the split-hand phenomenon in ALS.

Chapter 4

Cortical Dysfunction may underlie the ALS Split-Hand

Summary

Subsequent to establishing the lack of a significant peripheral contribution to the mechanism underlying the development of the split-hand phenomenon in ALS; the present study dissected out the relative contribution of cortical and peripheral processes in the development of the split-hand phenomenon. Cortical and axonal excitability studies were undertaken on 26 ALS patients, with motor responses recorded over the APB, FDI and ADM muscles. Results were compared to 21 controls. Short interval intracortical inhibition (SICI), a biomarker of cortical excitability, was significantly reduced across the range of intrinsic hand muscles ($APB_{SICI\ ALS}$ 0.3±2.0 %, $APB_{SICI\ controls}$ 16.0±1.9%, P<0.0001; $FDI_{SICI\ ALS}$ 2.7±1.7%, $FDI_{SICI\ controls}$ 14.8±1.9%, P<0.0001; $ADM_{SICI\ ALS}$ 2.6±1.5%, $ADM_{SICI\ controls}$ 9.7±2.2%, P< 0.001), although the reduction was most prominent when recorded over APB/FDI. Changes in SICI were accompanied by a significant increase in motor evoked potential amplitude and reduction of cortical silent period duration, all indicative of cortical hyperexcitability, and these were most prominent from the APB/FDI. At a peripheral level, a significant increase in strength-duration time constant and reduction in depolarising threshold electrotonus were evident in ALS, although these changes did not follow a split-hand distribution**.** Cortical dysfunction contributes to development of the split-hand in ALS, thereby implying an importance of cortical hyperexcitability in ALS pathogenesis.

Introduction

Amyotrophic lateral sclerosis (ALS) is a rapidly progressive neurodegenerative disorder of the motor neurons(2). Weakness and wasting of the abductor pollicis brevis (APB) and first dorsal interosseous (FDI) muscles, with relative preservation of abductor digiti minimi (ADM), may be a clinical feature of ALS, termed the ***split-hand*** (20, 21). The pathophysiological mechanisms underlying the development of this split-hand phenomenon have not been established, although, central and peripheral processes have been implicated (44, 55, 529). Resolution of this issue could provide unique insights into ALS pathophysiology and potentially guide future neuroprotective strategies.

Debate continues regarding the mechanisms of motor neuron degeneration in ALS. It has been argued that corticomotoneuronal hyperexcitability may induce anterior horn cell degeneration via an anterograde glutamatergic mechanism (25). Support for such a mechanism has been indirectly provided by transcranial magnetic stimulation (TMS) studies establishing cortical hyperexcitability as an early feature of ALS and linked to neurodegeneration(49, 50, 52, 125, 126). Given that APB and FDI muscles are critical for execution of complex hand tasks, and thereby exhibit a larger cortical representation (45), it could follow that preferential dysfunction of corticomotoneuronal pathways innervating the APB/FDI motor neurons may underlie development of the split-hand (44).

Previous TMS studies have established significant differences in cortical excitability across a range of upper limb muscles in healthy subjects (540, 566). Specifically, the degree of intracortical inhibition and corticomotoneuronal output was greater to thenar muscles compared

to biceps brachii and hypothenar muscles, suggesting a greater cortical representation and corticomotoneuronal projections to thenar muscles (540, 566). Interestingly, preferential dysfunction of thenar corticomotoneuronal projections has been reported in ALS (54).

Peripheral processes have also been implicated in development of the split-hand phenomenon. Studies in healthy controls have reported more prominent persistent Na^+ conductances and less K^+ currents in the APB and FDI motor axons (55), thereby suggesting that motor axons innervating the APB/FDI were hyperexcitable and prone to degeneration. Underscoring this notion were findings of more prominent hyperexcitability of APB axons in a Japanese ALS cohort (352). In contrast, a more recent study established that axonal dysfunction was evident across the range of intrinsic hand muscles and was not consistent with a split-hand distribution (567). Rather, it was suggested that abnormalities of axonal excitability may reflect downstream effects of primary neurodegenerative processes (567). Consequently, the aim of the present study was to determine whether cortical hyperexcitability underlies the development of the split-hand sign in ALS.

Material and Methods

Cortical and axonal excitability studies were undertaken on 26 patients with clinically probable or definite ALS as defined by the Awaji criteria (82). The diagnosis of ALS was confirmed in patients initially classified as probable ALS by longitudinal follow-up. All patients provided written informed consent to the procedures which were approved by the Western Sydney Local Health District Human Research Ethics Committee.

Clinical phenotype

All ALS patients were clinically staged using the amyotrophic lateral sclerosis functional rating scale-revised (ALSFRS-R) score (511) and categorised according to site of disease onset. Muscle strength was assessed using the Medical Research Council (MRC) score (512), with the following muscle groups assessed bilaterally yielding a total MRC score of 90: shoulder abduction; elbow flexion; elbow extension; wrist dorsiflexion; finger abduction; thumb abduction; hip flexion; knee extension; ankle dorsiflexion.

Cortical excitability

Cortical excitability studies were undertaken by applying a 90 mm circular coil connected to two high-power magnetic stimulators connected via a BiStim device (Magstim Co., Whitlands, South West Wales, UK) with recording of motor evoked response over the APB, FDI and ADM muscles. The circular coil was chosen over a focal (figure-of-eight) coil as the former was easier to use with less frequent overheating of the coil itself. Importantly, previous studies reported no qualitative differences in the pattern of inhibition and facilitation when using either a circular coil or a focal (figure-of-eight) coil (540). In addition, a previous study incorporating the threshold tracking TMS technique utilised a focal coil (416) and established a similar pattern. This study reported two phases of short- interval intracortical inhibition at, ISI 1 ms and at ≤ 3 ms, an identical pattern of short-interval intracortical inhibition to that reported in our own normative study (417).

The circular coil was adjusted in both antero-posterior and medial-lateral direction until the optimal position for an MEP response was obtained from the relevant muscle according to a

previously reported technique (568). Specifically, the optimal scalp position was established by determining the site at which the smallest TMS stimulus intensity (threshold) evoked an MEP response. This point on the scalp was marked with a skin marking pencil and the coil was positioned over this site for the duration of the experiment by a purpose built coil stand.

Paired-pulse threshold tracking TMS was undertaken according to a previously reported technique (417). Briefly, the MEP amplitude was fixed and changes in the test stimulus intensity required to generate a target response of 0.2 mV (± 20%), when preceded by sub-threshold conditioning stimulus, was measured. Resting motor threshold (RMT) was defined as the stimulus intensity required to maintain the target MEP response of 0.2 mV (±20%). Short-interval intracortical inhibition (SICI) was determined over the following interstimulus intervals (ISIs): 1, 1.5, 2, 2.5, 3, 3.5, 4, 5, and 7 ms, while intracortical facilitation (ICF) was measured at ISIs of 10, 15, 20, 25 and 30 ms. Stimuli were delivered sequentially as a series of three channels: **channel 1**: stimulus intensity, or threshold (% maximum stimulator output) required to produce the unconditioned test response (RMT); **channel 2**: sub-threshold conditioning stimulus (70% RMT); and **channel 3** tracks the stimulus required to produce target MEP when conditioned by a sub-threshold stimulus (70% RMT). Stimuli were delivered every 5s and the computer advanced to next ISI only when tracking was stable.

SICI was measured as the increase in the test stimulus intensity required to evoke the target MEP. Inhibition was calculated off-line as follows (417):

Inhibition = (Conditioned test stimulus intensity – RMT)/RMT * 100

Facilitation was measured as the decrease in the conditioned test stimulus intensity required to

evoke a target MEP.

Single pulse TMS technique was utilized to determine the MEP amplitude (mV), MEP onset latency (ms) and cortical silent period (CSP) duration (ms). The MEP amplitude was recorded with magnetic stimulus intensity set to 150% of RMT. Three stimuli were delivered at this level of stimulus intensity. Central motor conduction time (CMCT, ms) was calculated according to the F-wave method (569). Cortical silent period duration was assessed by instructing the subject to contract the target muscle at ~30% of maximal voluntary contraction with TMS intensity set to 150% of RMT. The CSP duration was measured from onset of MEP to return of EMG activity.

Axonal Excitability

In the same sitting, axonal excitability studies were undertaken on the median and ulnar motor nerves according to a previously described protocol (354). Compound muscle action potential (CMAP) responses were recorded from APB, FDI and ADM muscles with the active electrode positioned over the motor point and reference electrode placed over the base of the proximal thumb (APB and FDI) and fifth digit (ADM) respectively. From the CMAP amplitude, the split-hand index (SI) was calculated according to the previously reported formula (529):

$$\textbf{Split hand index} = \frac{\textbf{CMAP}_{\textbf{APB}} * \textbf{CMAP}_{\textbf{FDI}}}{\textbf{CMAP}_{\textbf{ADM}}}$$

The following axonal excitability parameters were measured: (i) strength-duration time constant (τ_{SD}) and rheobase; (ii) threshold electrotonus (TE) recorded with sub-threshold depolarizing

currents at 10-20 ms (TEd [10-20 ms]), 40-60 ms (TEd [40-60 ms]), and 90-100 ms (TEd [90-100 ms]), and with hyperpolarizing currents at 10-20 ms, TEh [10-20 ms] and at 90-100 ms, TEh [90-100 ms]; (iii) hyperpolarizing current-threshold relationship (I/V) calculated from polarizing current between +50 and -100%; (iv) recovery cycle parameters including the relative refractory period (RRP, ms), superexcitability (%) and late subexcitability (%).

Recordings of the CMAP and MEP responses were amplified and filtered (3 Hz-3 kHz) using a Nikolet-Biomedical EA-2 amplifier (Cardinal Health Viking Select version 11.1.0, Viasys Healthcare Neurocare Group, Madison, Wisconsin, USA) and sampled at 10 kHz using a 16-bit data acquisition card (National Instruments PCI-MIO-16E-4). Responses were further filtered for electronic noise by using a Hum Bug (Hum Bug 50/60 Hz Noise Eliminator, Quest Scientific Instruments, North Vancouver, Canada). Data acquisition and stimulation delivery were controlled by QTRACS software (TROND-F, version 16/02/2009, © Professor Hugh Bostock, Institute of Neurology, Queen Square, London, UK). Temperature was monitored with a purpose built thermometer at the stimulation site.

Statistical Analysis

Cortical and axonal excitability studies in ALS patients were compared to control data obtained from 21 healthy controls (13 men, 8 women: mean age 50 years, 24-67 years). Student t-test was used for assessing differences between two groups. Pearson's and Spearman's correlation coefficients were used to examine the relationship between parameters. Shapiro-Wilk test was used to assess for normality of data. A probability (P) value of <0.05 was considered statistically

significant. Results were expressed as mean ± standard error of the mean and median (interquartile range).

Results

Clinical features

At time of testing, the median disease duration was 9.5 months (6-17 months), indicating that those studies were undertaken towards the earlier stages of the disease (Table 4.1). In addition, the median ALSFRS-R score was 43 (41-46) while the median MRC sum score was 83 (79-88), suggesting a mild to moderate level of functional impairment at time of assessment. Seventy-three percent of patients exhibited limb-onset disease while 27% reported bulbar-onset disease. The split-hand sign was evident in 62% of ALS patients at time of testing, but with follow-up 95% of patients developed a split-hand sign. The split-hand sign was more frequently observed in limb-onset ALS patients (73%) when compared to bulbar-onset disease (27%).

Cortical excitability

Prior to undertaking cortical and axonal excitability studies, the degree of peripheral disease burden was formally assessed. There was a significant reduction of CMAP amplitude recorded over the APB ($P<0.001$), FDI ($P<0.001$) and ADM ($P<0.001$) muscles compared to controls. The split-hand index was significantly reduced in ALS (SI_{ALS} 4.7±0.8; $SI_{CONTROL}$ 13.4±1.0, $P<0.0005$), confirming that the split-hand phenomenon was evident in the present ALS cohort.

PATIENT	AGE	SEX	ONSET SITE	DURATION (MONTHS)	ALSFRS-RR	MRC SUM	SI
1	32	M	BULBAR	4	43	84	2.1
2	57	M	BULBAR	3	44	90	10
3	52	F	BULBAR	48	36	84	8.5
4	64	F	BULBAR	10	44	90	4.9
5	58	M	BULBAR	5	43	90	7.4
6	58	M	BULBAR	15	44	90	9.5
7	48	F	BULBAR	21	42	90	13
8	64	M	LIMB	7	47	87	5
9	69	M	LIMB	8	42	56	0
10	57	F	LIMB	9	45	83	6.4
11	64	M	LIMB	12	41	79	3.3
12	60	M	LIMB	6	42	82	1.7
13	62	M	LIMB	5	46	88	3.9
14	51	M	LIMB	20	33	65	0.1
15	42	M	LIMB	17	41	74	0
16	48	M	LIMB	5	42	80	9.8
17	56	F	LIMB	16	34	74	0.2
18	44	M	LIMB	3	46	86	0.9
19	58	F	LIMB	30	31	37	11.8
20	68	M	LIMB	10	48	88	6.3
21	69	F	LIMB	8	43	86	1.1
22	66	M	LIMB	9	47	80	2.8
23	69	F	LIMB	14	47	81	0
24	69	F	LIMB	8	46	79	7.9
25	73	M	LIMB	24	44	81	0
26	65	M	LIMB	17	41	71	5.3
MEAN/ MEDIAN	**58.6**	**17M**	**19 LIMB**	**9.5**	**43**	**83**	**4.4**
SEM/(IQR)	**1.9**	**9F**	**7 BULBAR**	**(6-17)**	**(41-46)**	**(79-88)**	**0.8**

Table 4.1: Clinical features for the 26 amyotrophic lateral sclerosis patients. All patients were graded using the amyotrophic lateral sclerosis functional rating scale revised (ALSFRS-R). Muscle strength was assessed using the Medical Research Council (MRC) score. The split hand index (SI) was calculated in all patients.

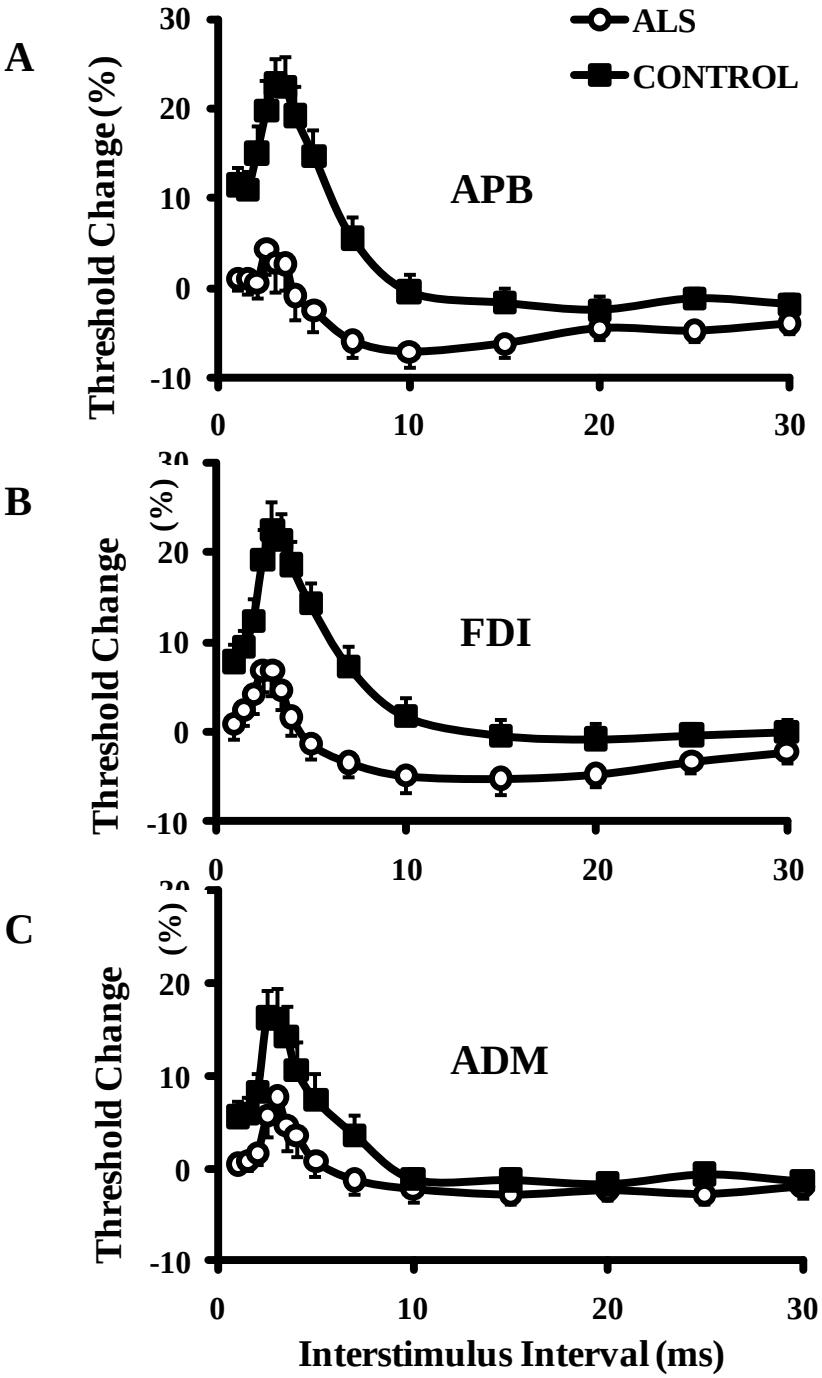

Figure 4.1: Short interval intracortical inhibition (SICI) was significantly reduced and intracortical facilitation (ICF) increased when recording over the **(A)** abductor pollicis brevis (APB) and **(B)** first dorsal interosseous (FDI) muscles. **(C)** There was a significant reduction of SICI when recording over the abductor digit minimi (ADM) muscle, while there was no significant difference (NS) in ICF. The degree of SICI reduction was more prominent when recording over the APB and FDI muscles. *****P < 0.05; *******P< 0.001; ********P< 0.0001

Paired-pulse threshold tracking TMS studies disclosed a marked reduction of SICI across the range of intrinsic hand muscles, although this reduction was most prominent when recorded over the APB and FDI (Fig. 4.1A-C). Averaged SICI, between ISIs 1 to 7 ms, was significantly reduced over the APB (ALS 0.3±2.0 %; controls 16.0±1.9%; P<0.0001), FDI (ALS 2.7±1.7%; controls 14.8±1.9%; P<0.0001) and ADM (ALS 2.6±1.5%; controls 9.7±2.2%; P< 0.001, Fig. 4.2 A-C) muscles, although the degree of reduction was more prominent over APB and FDI (SICI reduction $_{APB}$, 98%; SICI reduction $_{FDI}$ 81%; SICI reduction $_{ADM}$ 73%, F = 2.8, P < 0.05, Fig. 4.2D). Of further relevance, peak SICI at ISI 3 ms was also significantly reduced across the range of intrinsic hand muscles (ALS_{APB} 2.8±3.2 %, controls $_{APB}$ 22.7±2.8, P<0.001; ALS_{FDI} 6.8±2.8%, controls $_{FDI}$ 23.5±2.5%, P<0.001; ALS_{ADM} 7.7±2.9%, controls $_{ADM}$ 16.1±3.2%, P< 0.05, Fig. 4.3 A-C), although the reduction was again most prominent over the APB and FDI (SICI reduction $_{APB}$, 81%; SICI reduction $_{FDI}$ 70%; SICI reduction $_{ADM}$ 52%, F = 2.0, P < 0.05, Fig. 4.3D).

Following SICI, a period of **intracortical facilitation** develops between ISI 10-30ms. The mean ICF between ISIs 10-30 ms was significantly increased in ALS patients when recorded over the APB (ALS -5.3±1.2%, controls -1.4±1.3%, P< 0.05) and FDI muscles (ALS -4.1±1.4%, controls -0.53±1.4 %, P<0.05) but not ADM (P=0.18).

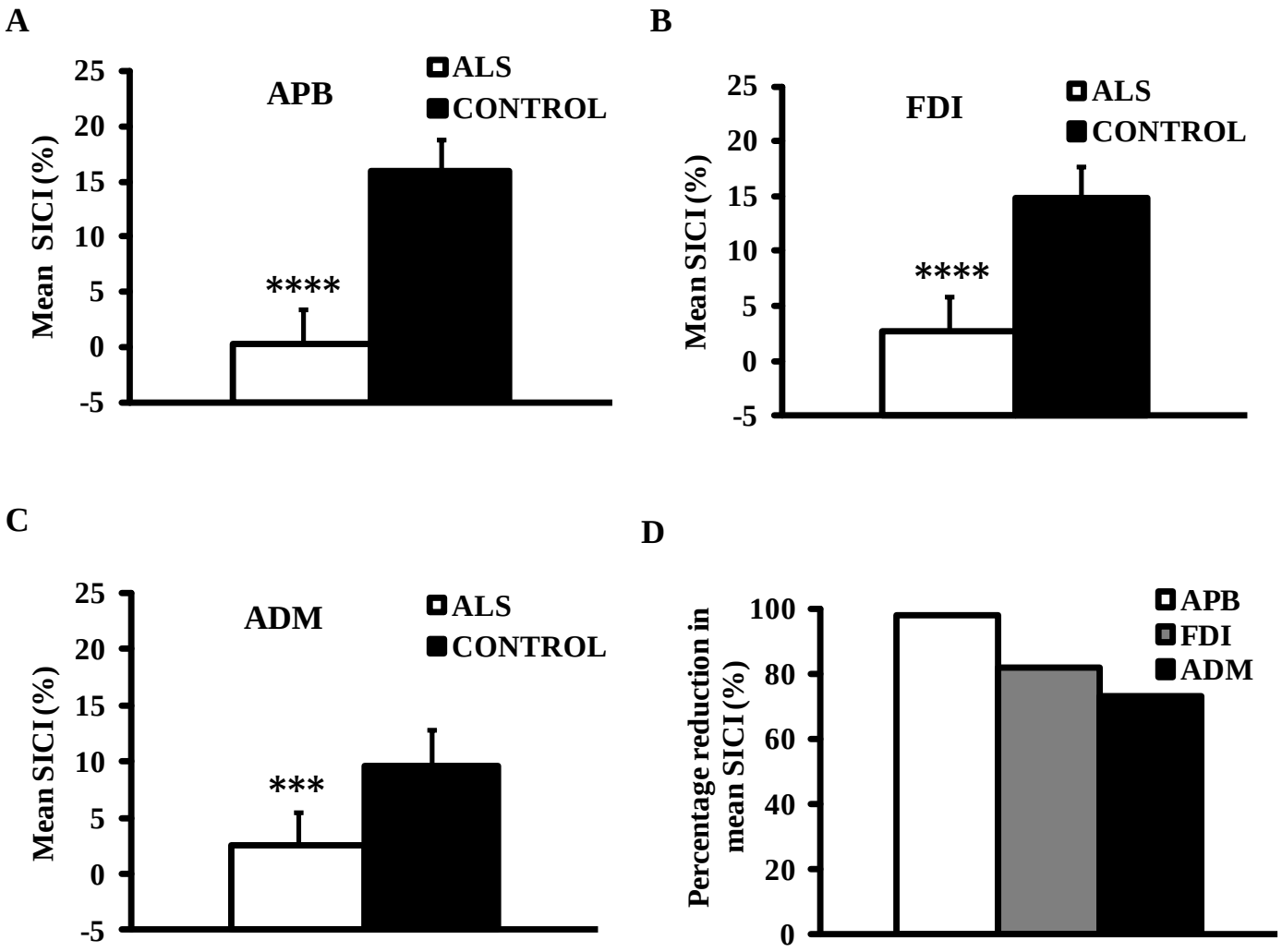

Figure 4.2: Mean short interval intracortical inhibition (SICI), over interstimulus intervals 1-7 ms, was significantly reduced when recording over the **(A)** abductor pollicis brevis (APB), **(B)** first dorsal interosseous (FDI), and **(C)** abductor digit minimi (ADM) muscles. **(D)** The reduction in mean SICI was most prominent when recording over the APB muscle.
*******P< 0.001; ********P< 0.0001

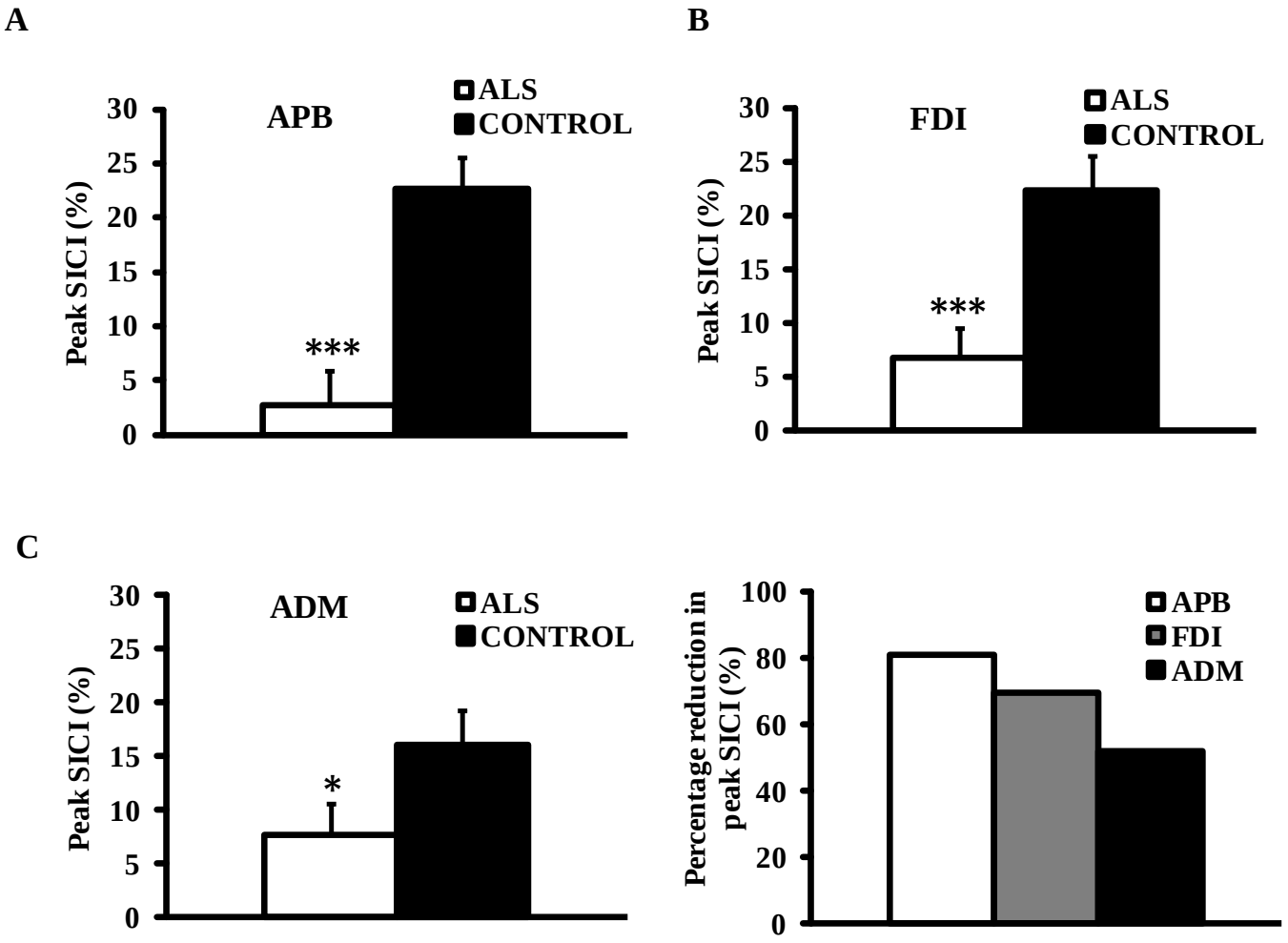

Figure 4.3: Peak short interval intracortical inhibition (SICI) at interstimulus interval 3 ms was significantly reduced when recording over the **(A)** abductor pollicis brevis (APB), **(B)** first dorsal interosseous (FDI), and **(C)** abductor digit minimi (ADM) muscles. **(D)** The reduction in peak SICI was most prominent when recording from the APB. ***P < 0.05; ****P < 0.001.

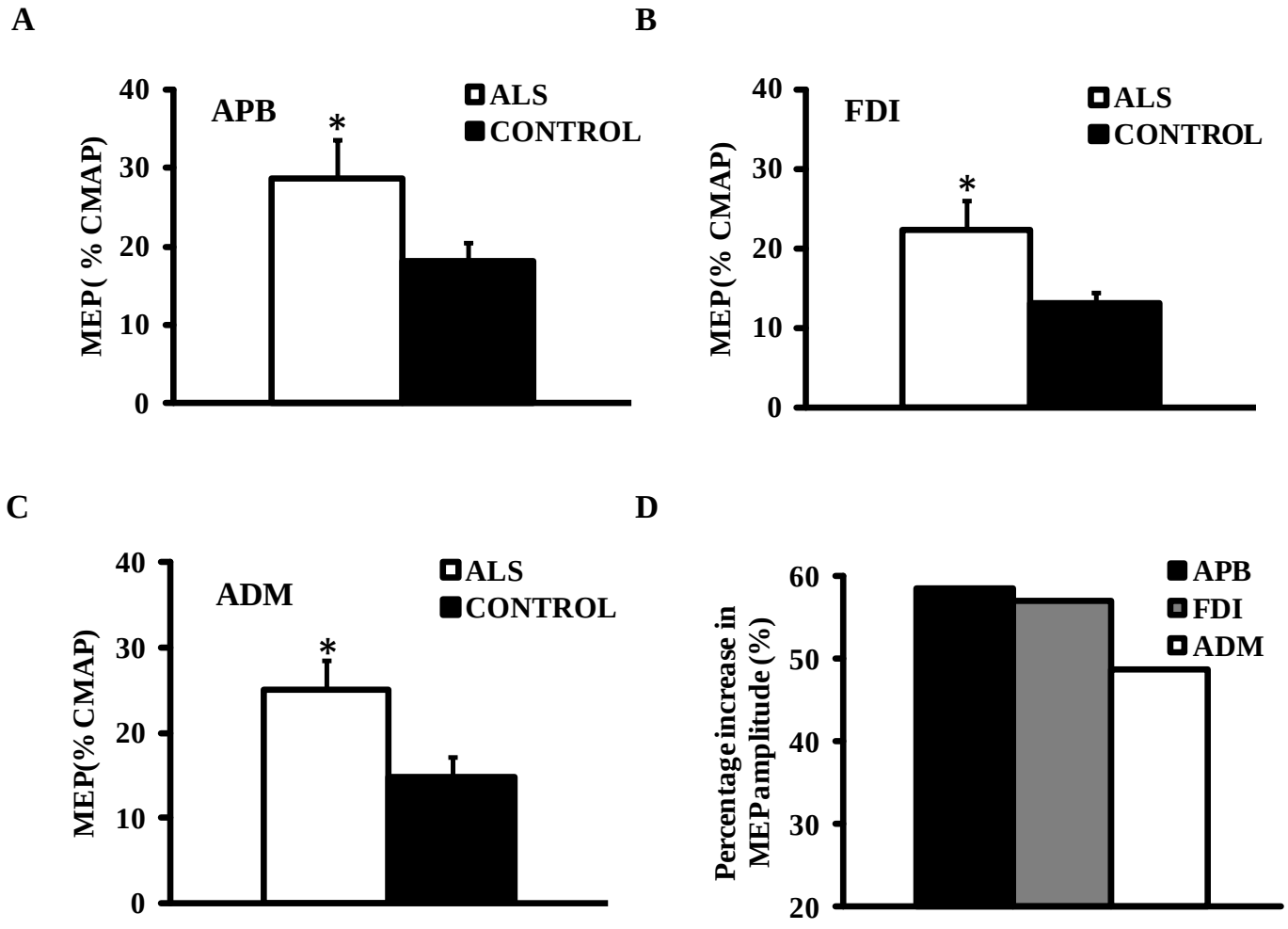

Figure 4.4: Motor evoked potential (MEP) amplitude, expressed as a percentage of the compound muscle action potential (CMAP) response, was significantly increased when recording over the **(A)** abductor pollicis brevis (APB), **(B)** first dorsal interosseous (FDI) and **(C)** abductor digit minimi (ADM) muscles. **(D)** The increase in MEP amplitude was most prominent when recording from the APB. *****$P < 0.05$; *******$P < 0.001$.

Single-pulse TMS technique disclosed that the MEP amplitude was significantly increased in ALS patients across the range of intrinsic hand muscles (ALS_{APB} 28.4±5.1%, controls $_{APB}$ 18.1±2.4%, P<0.05; ALS_{FDI} 24.2±3.6%, controls $_{FDI}$ 13.2±2.3%, P<0.05; ALS $_{ADM}$ 22.9±2.9, controls $_{ADM}$ 14.8±2.4%, P<0.05, Fig 4.4A-C). Of further relevance, there was a trend for the MEP amplitude increase to be greater when recording over the thenar muscles (APB $_{MEP\ INCREASE}$ 59%; FDI $_{MEP\ INCREASE}$ 57%; ADM $_{MEP\ INREASE}$ 48.6%, Fig. 4.4D). Of further relevance, the CSP duration was significantly reduced when recorded over the APB (ALS 170.1 ± 8.5ms, controls 200.4 ± 8.1ms, P < 0.05) and FDI (ALS 173.1 ± 9.2ms, controls 202.4 ± 6.8ms, P < 0.05) but not ADM (ALS 176.8 ± 9.2ms, controls 187.2 ± 6.0ms, P=0.17, Fig. 4.5). In contrast, there were no significant differences in RMT (ALS $_{APB}$ 56.1 ± 1.9%, controls $_{APB}$ 56.2 ± 1.8%, P = 0.48; ALS $_{FDI}$ 55.5 ± 1.9%, controls $_{FDI}$ 58.0 ± 2.1, P = 0.20; ALS $_{ADM}$ 54.5 ± 1.8, controls $_{ADM}$ 56.3 ± 2.0, P = 0.25) and central motor conduction time (F = 0.01, P = 0.99) between groups.

Axonal excitability

The strength-duration time constant, a biomarker of nodal persistent Na^+ conductance (85, 86, 333, 337, 541), was significantly increased when recorded over APB (ALS 0.51 ± 0.02 ms, controls 0.46 ± 0.02ms, P < 0.05, Fig. 4.6A) and ADM (ALS 0.49 ± 0.02ms, controls 0.44 ± 0.02ms, P < 0.05, Fig. 4.6B) muscles but not FDI (ALS 0.47 ± 0.02ms, controls 0.42 ± 0.02ms, P=0.06, Fig 4.6C). In contrast, there were no significant differences in rheobase between ALS patients and controls across the range of intrinsic hand muscles (APB, P = 0.19; FDI, P = 0.49; ADM, P = 0.33).

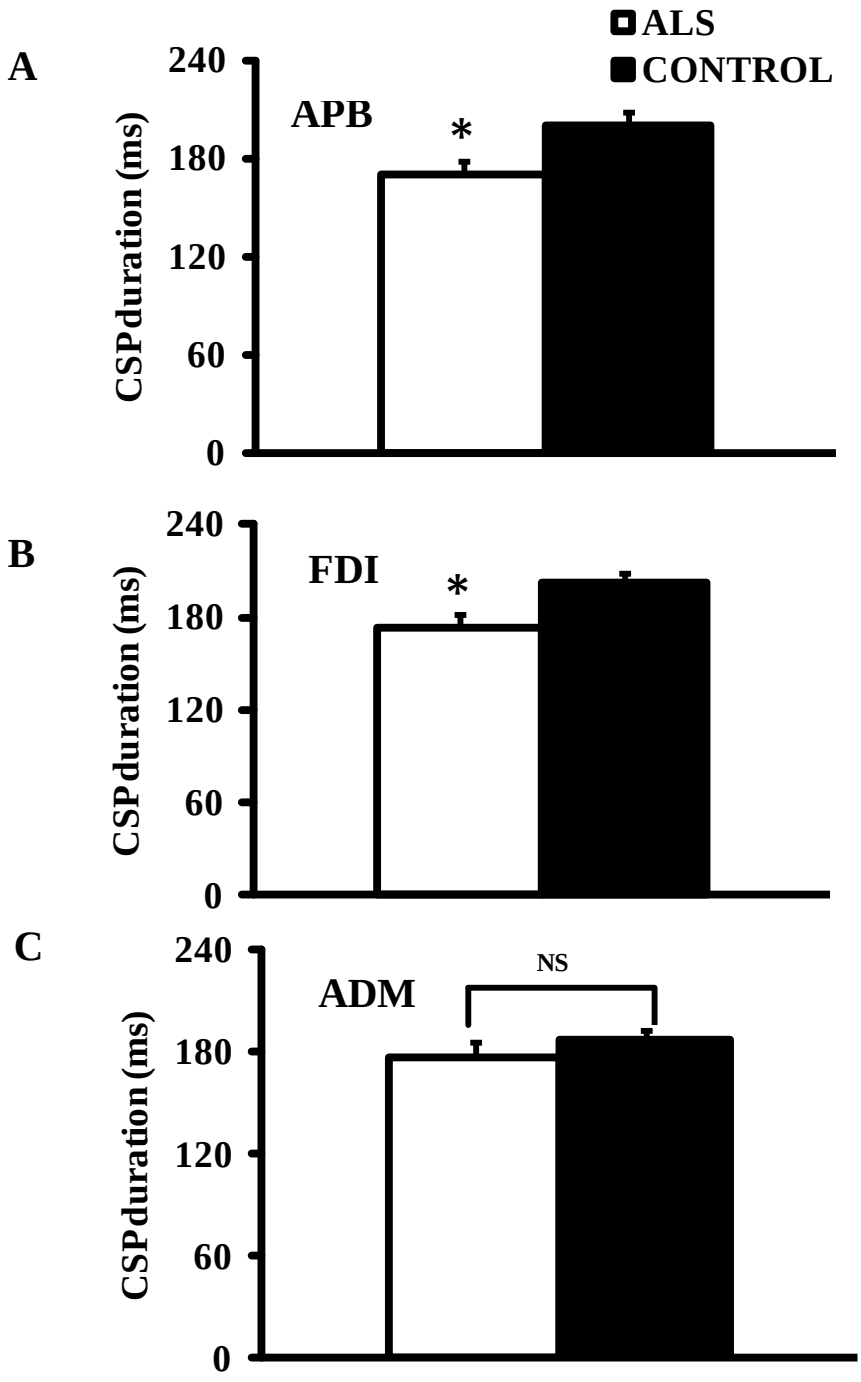

Figure 4.5: (A) The cortical silent period (CSP) duration was significantly reduced when recording when recording over the **(A)** abductor pollicis brevis (APB) and **(B)** first dorsal interosseous (FDI) muscles. **(C)** There was no significant (NS) reduction in CSP duration when recording over the abductor digit minimi (ADM) muscle. The reduction in CSP duration was most prominent when recording from the APB. *****$P < 0.05$.

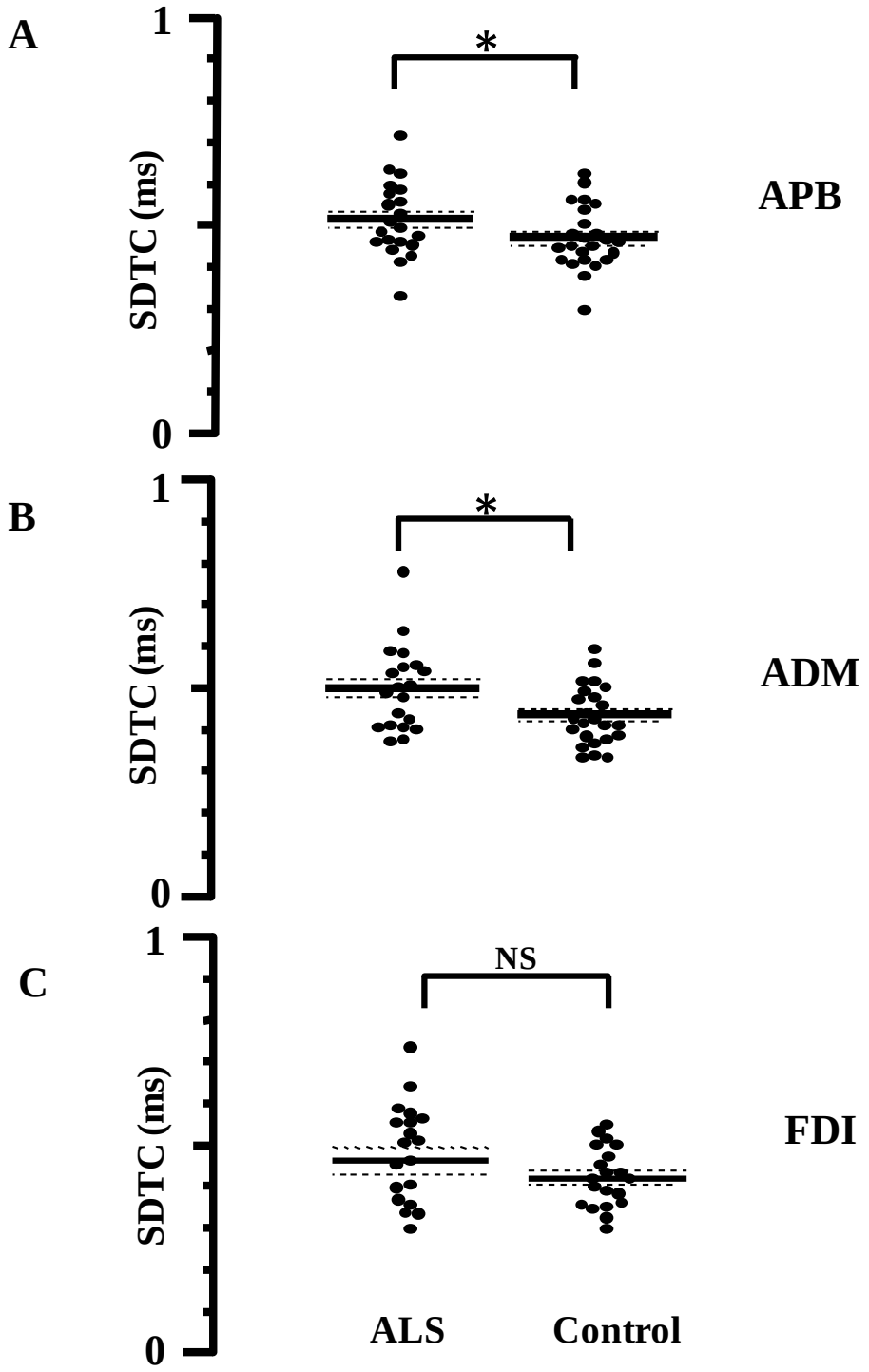

Figure 4.6: Strength duration time constant (SDTC), a biomarker of persistent Na^+ conductances, was significantly increased when recording from the **(A)** abductor pollicis brevis (APB) and **(B)** abductor digit minim (ADM) muscles, but not **(C)** first dorsal interosseous (FDI).

Threshold Electrotonus, a biomarker of internodal and paranodal K^+ conductance (85), again disclosed the presence of the type I abnormality of TE, whereby sub-threshold depolarizing currents induced greater changes in threshold (570) when recording from all three muscles. Specifically, depolarizing TE at 90-100 ms was significantly greater in ALS patients when recorded from the APB (ALS 50.3 ± 1.5%; controls 44.7 ± 0.8%, $P < 0.001$), ADM (ALS 48.5 ± 1.0%; controls 45.5 ± 0.7%, $P < 0.05$) and FDI (ALS 45.1 ± 1.5%; controls 40.0 ± 2.2%, $P < 0.05$) muscles. These changes in depolarising TE were accompanied by a significant increase in TEd at 40-60 ms when recording over APB (ALS 56.1 ± 1.7%; controls 52.6 ± 1.0%, $P < 0.05$) and ADM (ALS 53.6 ± 1.3%; controls 50.8 ± 0.9%, $P < 0.05$), but not FDI motor axons ($P=0.11$)

Of further relevance, superexcitability was significantly increased when recording from the APB (ALS -25.9 ± 1.4%; controls -21.6 ± 1.5%, $P < 0.05$) and FDI (ALS -27.3 ± 1.4%; controls -23.1 ± 1.2%, $P < 0.05$), but not ADM (ALS -25.1 ± 1.2%; controls -23.5 ± 1.3%, $P = 0.19$). In contrast, there were no significant changes in the relative refractory period (APB, $P = 0.18$; FDI, $P = 0.14$; ADM, $P = 0.37$) and late subexcitability (APB, $P = 0.12$; FDI, $P = 0.15$; ADM, $P = 0.10$) between ALS patients and controls across the range of intrinsic hand muscles. In addition, hyperpolarising I/V gradient was significantly increased in ALS patients when recording from the APB muscle (ALS 0.41±0.02, controls 0.36±0.01, $P <0.05$), but not the FDI ($P = 0.08$) and ADM ($P = 0.12$). Taken together, these findings reveal that while the abnormalities of axonal excitability were evident in ALS, they did not appear to follow a split-hand pattern.

Correlation studies

Combining clinical parameters with measures of cortical and axonal excitability, it was evident that the MEP amplitude ($R = -0.40$, $P<0.01$) and CSP duration ($R=0.34$, $P<0.01$) were significantly correlated with the split-hand index. Of relevance, there was a significant correlation between SICI and MRC upper limb score ($R = -0.3$, $P<0.05$). In contrast, there was no significant correlation between any of the axonal excitability parameters and split-hand index, CMAP amplitude, measures of cortical excitability and clinical parameters. Taken together, these findings suggest that cortical hyperexcitability may be linked to the development of the split-hand phenomenon in ALS.

Discussion

In the present study, cortical and peripheral axonal techniques were utilised to dissect the relative contribution of central and peripheral processes in development of the ALS split-hand. Cortical hyperexcitability, as indicated by a significant reduction in short interval intracortical inhibition and cortical silent period duration along with increases in motor evoked potential amplitude, was evident across the range of intrinsic hand muscles, although the degree of cortical hyperexcitability was most prominent when recorded from the APB and FDI muscles. Of further relevance, there was a significant correlation between measures of cortical excitability and the split-hand index, suggesting that cortical hyperexcitability was associated with development of the split-hand phenomenon in ALS. At a peripheral level, upregulation of persistent Na^+ conductances along with reduction in K^+ currents was evident, but did not appear to follow a split-hand distribution and was not correlated with the split-hand index, thereby arguing against a significant peripheral contribution in driving the development of the split-hand phenomenon in

ALS. The mechanisms underlying these central and peripheral excitability changes and their relevance for development of the split-hand phenomenon, with implications for ALS pathophysiology, will be discussed.

Origins of the split-hand phenomenon in ALS

While the pathophysiological mechanisms underlying the development of the split-hand phenomenon in ALS have not been established, central and peripheral processes have been implicated (44). A cortical basis was inferred from clinical observations that thenar muscles (APB/FDI) were critical in execution of complex hand tasks (44), and thereby would exhibit a greater cortical representation, a notion supported by TMS studies in healthy controls (54, 540, 571). Importantly preferential dysfunction of corticomotoneuronal pathways was previously established in ALS (54).

The novel findings from the present study provide critical support for a cortical basis in development of the ALS split-hand. Specifically, cortical dysfunction was heralded by marked reduction of SICI, a biomarker of strong inhibitory intracortical GABAergic function and weaker cortical glutamatergic facilitatory effects (426). Importantly, abnormalities of SICI in ALS appear to be mediated by a combination of glutamate excitotoxicity and degeneration of inhibitory cortical neurons(129, 480). The findings of more prominent SICI reduction when recorded over APB and FDI, would imply a greater level of cortical hyperexcitability to the APB and FDI motor neurons. Of further relevance, intracortical facilitation, a biomarker of glutamatergic function (87, 426), was significantly increased when recorded from the APB and

FDI but not hypothenar muscles. Taken together, these findings suggest that cortical processes, namely cortical hyperexcitability, may underlie the development of the split-hand sign in ALS. There was also a marked increase in MEP amplitude in the ALS cohort and was correlated with the split-hand index. Given that the MEP amplitude reflects the density of corticomotoneuronal projections onto motor neurons (401) as well as the level of glutamatergic neurotransmission in the central nervous system (87), the present findings lend further credence to the notion that cortical processes contribute to the development of the split-hand sign in ALS. Alternatively, it could also be argued that the increase in MEP amplitude may represent less phase cancellation due to fewer motor units or possibly repetitive firing of corticomotoneurons (572). In addition to changes in MEP amplitudes, a significant reduction of CSP duration was evident in the ALS cohort, but only when recorded over the thenar muscles (APB/FDI). Importantly, the CSP duration reflects the degree of cortical inhibition and appears to be mediated by inhibitory neurons acting via $GABA_B$ receptors (452, 453, 457, 458, 548, 549). Consequently, findings that identified a significant reduction in CSP duration when recording over APB/FDI muscles, suggest a greater level of cortical disinhibition and cortical hyperexcitability to the APB/FDI muscles, providing further support for a cortical mechanism as the basis of the split-hand phenomenon in ALS.

Alternatively, it could be argued that the differences in cortical excitability between the intrinsic muscles could be related to an interaction between stimulated cortical areas. Given that electromyography techniques were not utilised to ensure electrical silence of the "non-stimulated' intrinsic hand muscles, especially the APB and FDI, such a notion could not be absolutely discounted. It has also been argued that peripheral mechanisms may contribute to

development of the split-hand sign in ALS (44). More prominent membrane excitability abnormalities in the APB motor neurons, as indicated by longer τ_{SD}, was recently reported in ALS (352). Given that τ_{SD} is a biomarker of persistent Na^+ conductances (85), and linked to axonal degeneration (57, 126, 351), these findings implied that upregulation of persistent Na^+ conductances contributed to development of the split-hand phenomenon, although the properties of FDI motor axons were not assessed. In contrast, the present study established a comparable increase of τ_{SD} in APB and ADM axons, without significant increases of τ_{SD} in FDI axons, thereby arguing against a significant contribution of axonal dysfunction in development of the split-hand phenomenon in ALS.

In addition, a significant reduction in depolarising TE was also evident across the range of recorded motor axons. Given that depolarising TE is a biomarker of slow K^+ currents (85), the findings in the present study suggest that reduced slow K^+ currents is a feature of ALS and in keeping with previous studies (56, 57, 567). Importantly, the changes in depolarising TE did not appear to follow a split-hand distribution, thereby further arguing against a significant contribution of peripheral processes in development of the split-hand phenomenon in ALS.

Split-hand phenomenon and ALS pathophysiology

Emerging evidence suggests that genetic factors and molecular processes underlie the development of ALS (2). Cortical hyperexcitability was proposed as an important pathophysiological mechanism, whereby motor neuron degeneration was mediated via glutamate excitotoxicity process (25). Support for such a framework has been provided by TMS studies (49, 50) as well as transgenic SOD-1 mouse models studies (128). Additional support for

glutamate-mediated excitotoxity is provided by transgenic SOD-1 mouse model and human studies identifying abnormalities of the astrocytic glutamate transporter, excitatory amino acid transporter-2 (137, 573). Importantly, ALS motor neurons exhibit increased expression of Ca^{2+}-permeable AMPA receptors, thereby rendering these more susceptible to excitotoxicity (142).

The findings from the present study of more prominent cortical hyperexcitability to the APB and FDI muscles, together with an absence of a split-hand distribution of axonal excitability abnormalities, provide support for a cortical basis to ALS pathogenesis. The significant correlation between cortical hyperexcitability and the split-hand index, further suggests that glutamate-mediated cortical hyperexcitability may underlie the preferential degeneration of motor neurons in ALS.

Chapter 5

Cortical Hyperexcitability Precedes Lower Motor Neuron Dysfunction in ALS

Summary

After establishing that cortical dysfunction contributed to development of the split-hand in ALS, The present study was undertaken to determine whether cortical hyperexcitability preceded the development of lower motor neuron (LMN) dysfunction in sporadic amyotrophic lateral sclerosis (ALS). Cortical excitability studies were undertaken in 24 ALS patients utilising the threshold tracking transcranial magnetic stimulation (TMS) technique, with motor evoked potential (MEP) recorded over the abductor pollicis brevis (APB) muscle. In the same sitting, LMN function of the target APB muscle was assessed utilising a complex array of peripheral neurophysiological techniques, including conventional nerve conduction studies determining the compound muscle action potential (CMAP) amplitude and neurophysiological index, qualitative and quantitative electromyography (EMG) along with axonal excitability studies. At the time of assessment, the anatomical and functional integrity of the lower motor neuronal circuits innervating the target APB muscle was preserved in all ALS patients, confirmed by a normal CMAP amplitude ($P=0.37$), absence of fasciculations, or features of neurogenic change. In addition, the neurophysiological index and markers of peripheral axonal excitability were well within established normal ranges. Despite this apparent 'normality' cortical dysfunction was evident in ALS patients, with significant reduction of short interval intracortical inhibition (ALS 1.7±1.4%; controls 10.3±1.0%; $P<0.01$), resting motor threshold ($P<0.05$) and cortical silent period duration ($P<0.001$). In addition, the MEP amplitude ($P<0.05$) and intracortical facilitation ($P<0.05$) were significantly increased, providing additional support for the presence of cortical hyperexcitability upstream to a seemingly intact lower motor neuronal system. This study concluded that cortical hyperexcitability precedes the development of LMN dysfunction in ALS, suggesting a cortical origin for ALS.

Introduction

The primacy of corticomotoneuronal dysfunction in ALS pathogenesis was first postulated by Charcot (1), although contrasting views have suggested that corticomotoneuronal dysfunction occurred either as an independent process to lower motor neuron (LMN) dysfunction or was secondary to LMN degeneration via a dying back process (188, 189, 574). Resolution of this critical issue could potentially advance the understanding of ALS pathophysiology and would be of immense diagnostic and therapeutic significance.

Although ongoing debate regarding the processes underlying motor neuron degeneration in ALS continues, corticomotoneuronal hyperexcitability via an anterograde transsynaptic glutamatergic process(25), has been proposed as an underlying mechanism. Support for such mechanism has been provided by transcranial magnetic stimulation (TMS) studies establishing that cortical hyperexcitability was an early feature of ALS, linked to neurodegeneration and preceding the development of clinical features of LMN dysfunction(49, 50, 124, 174). The recent identification of the c9orf72 hexanucleotide repeat expansion as the causative genetic mutation in both ALS and frontotemporal dementia (FTD) (172, 173) has provided further support for a cortical origin of ALS.

As an alternative suggestion, corticomotoneuronal and spinal motor neuron degeneration may occur as independent processes in ALS. The lack of correlation between corticomotoneuronal and spinal motor neuron densities on neuropathological studies was previously reported in ALS as evidence arguing against the primacy of corticomotoneurons in ALS pathogenesis (189), (188). Such morphological techniques may potentially be confounded by the complexity of the human

motor system, particularly the synaptic relationship between corticomotoneurons and the spinal motor neurons (45). Specifically, there appears to be considerable variability in the corticomotoneuron to spinal motor neuron synaptic ratios, and attempts to correlate upper and lower motor neurons on autopsy studies may not be meaningful (186). Separately, evidence of hyperexcitable corticomotoneurons which may form the basis of ALS pathogenesis, will clearly not be detected by anatomical techniques.

The functional integrity of corticomotoneurons may be non-invasively assessed by utilising TMS techniques (87), while lower motor neuron function may be interrogated by utilising neurophysiological techniques such as nerve conduction studies for determining CMAP amplitude, electromyography with the addition of more novel research-based techniques such as neurophysiological index and axonal excitability techniques (65, 85). Consequently, the present study combined cortical assessment and clinical phenotype with a complex series of peripheral neurophysiological approaches, including qualitative and quantitative electromyography, to determine whether corticomotoneuronal hyperexcitability preceded lower motor neuron dysfunction in ALS.

Materials and Methods

Studies were undertaken on 24 patients with suspected ALS referred to our specialised multidisciplinary ALS clinic between January 2011 and March 2013. The abductor pollicis brevis (APB) strength was clinically normal in these 24 ALS patients, and there was subsequently determined to be no neurophysiological evidence (*see* below) of lower motor neuron dysfunction within the APB muscle at the time of assessment. All patients progressed to

develop probable or definite ALS , as defined by the Awaji criteria (82), during the follow-up period. Patients were clinically staged using the ALS functional rating scale-revised (ALSFRS-R) scale(511), while muscle strength was determined using the medical research council (MRC) rating scale (575). Muscle strength was scored using the following muscle groups: shoulder abduction, elbow flexion and extension, wrist dorsiflexion, finger abduction and thumb abduction, hip flexion, knee extension and ankle dorsiflexion bilaterally, generating a maximal MRC score of 90. All patients provided written informed consent to the procedures which were approved by the Western Sydney Local Health District Human Research Ethics Committee.

Cortical excitability

Paired-pulse threshold tracking TMS, using a 90 mm circular coil, was undertaken according to a previously reported technique (417). Briefly, the motor evoked potential (MEP) amplitude was fixed and changes in the test stimulus intensity required to generate a target response of 0.2 mV (± 20%), when preceded by a sub-threshold conditioning stimulus, was measured (417). The motor evoked potential (MEP) response was recorded over the abductor pollicis brevis muscle. Resting motor threshold (RMT) was defined as the stimulus intensity required to maintain this target MEP response.

Initially, **single pulse TMS** was utilized to determine the MEP amplitude (mV), MEP onset latency (ms) and cortical silent period (CSP) duration (ms). The MEP amplitude was recorded with magnetic stimulus intensity set to 150% of RMT. Three stimuli were delivered at this level of stimulus intensity. Subsequently, the CSP duration was assessed by instructing the subject to contract the target APB muscle at ~30% of maximal voluntary contraction with three stimuli

delivered at 150% of RMT. The CSP duration was measured from onset of MEP to return of EMG activity.

Paired-pulse threshold tracking was undertaken to determine short interval intracortical inhibition and intracortical facilitation according to a previously established technique (417). Short-interval intracortical inhibition (SICI) was determined over the following interstimulus intervals (ISIs): 1, 1.5, 2, 2.5, 3, 3.5, 4, 5, and 7 ms. Intracortical facilitation (ICF) was measured at ISIs of 10, 15, 20, 25 and 30 ms. TMS stimuli were delivered at a frequency of 0.1 Hz (stimulus delivery was limited by the charging capability of the BiStim system) and the computer advanced to the next ISI only when tracking was stable. SICI was measured as the increase in the test stimulus intensity required to evoke the target MEP. Inhibition was calculated off-line as follows (417):

Inhibition = (Conditioned test stimulus intensity – RMT)/RMT * 100

Facilitation was measured as the decrease in the conditioned test stimulus intensity required to evoke a target MEP.

Peripheral studies

Compound muscle action potential (CMAP) responses were recorded from the APB muscle with the active (G1) electrode positioned over the motor point and reference (G2) electrode placed over the base of the proximal thumb. The resultant baseline-peak CMAP amplitude (mV) and onset latency (ms) were measured.

Axonal excitability studies were undertaken on the median motor nerve according to a previously described protocol (354). Briefly, the median nerve was stimulated at the wrist using 5 mm non-polarizable Ag-AgCl electrodes (3M Healthcare, MN, USA) with the anode positioned ~ 10 centimeters proximal to the cathode over the lateral forearm. Test current pulses were applied at 0.5s intervals and combined with either sub-threshold polarizing currents or suprathreshold conditioning stimuli according to previously described protocols. Stimulation was computer controlled and converted to current using an isolated linear bipolar constant current simulator (maximal output ± 50 mA; DS5, Digitimer, Welwyn Garden City, UK). A tracking target was set to 40% of maximum CMAP response and proportional tracking was utilized to determine the changes in threshold current required to produced and maintain a target response (354). The temperature at recording site was maintained >32°C.

The following axonal excitability parameters were measured: (i) strength-duration time constant (τ_{SD}) and rheobase; (ii) depolarising and hyperpolarising threshold electrotonus (TE); (iii) current-threshold relationship (I/V); (iv) relative refractory period (RRP, ms), superexcitability (%) and late subexcitability (%). In addition, the neurophysiological index (NI) was derived according to a previously reported formula (65).

Qualitative needle electromyography (EMG) was undertaken on all patients, studying at least 3 regions and the APB muscle, utilising a 26G concentric needle. Quantitative EMG assessment, using Multi-MUP software (Synergy EMG machine, Neurocare Group, Madison, USA) was undertaken according to a previously reported technique (73). In total, 20 motor unit action potentials (MUAP) were collected from four different sites within the APB muscle using a 26G

concentric needle electrode. The MUAP peak-to-peak amplitude (mV) and duration (ms) were recorded.

Recordings of the CMAP and MEP responses were amplified and filtered (3 Hz-3 kHz) using a Nikolet-Biomedical EA-2 amplifier (Cardinal Health Viking Select version 11.1.0, Viasys Healthcare Neurocare Group, Madison, USA) and sampled at 10 kHz using a 16-bit data acquisition card (National Instruments PCI-MIO-16E-4). Data acquisition and stimulation delivery were controlled by QTRACS software (version 16/02/2009, © Professor Hugh Bostock, Institute of Neurology, Queen Square, London, UK).

Statistical Analysis

Cortical excitability studies in ALS patients were compared to control data obtained from 33 healthy controls (16 men, 17 women; mean age 55.7±1.7 years), while axonal excitability studies were compared to 24 healthy controls (12 men, 12 women; mean age 50.8±2.1 years). Quantitative EMG studies in ALS patients were compared to 20 age-matched healthy controls (6 men, 14 women, mean age 52.8±2.9 years). All data was tested for normality using the Shapiro-Wilk test. Student t-test was used for assessing differences between two groups, while analysis of variance (ANOVA) with post-hoc testing (Bonferroni correction) was used for multiple comparisons. Wilcoxon signed rank test for used to compare differences between clinical variables that exhibited a non-parametric distribution. Pearson's correlation coefficients were used to examine the relationship between parameters. A probability (P) value of <0.05 was considered statistically significant. Results were expressed as mean ± standard error of the mean or median (interquartile range).

Results

Clinical Characteristics

At time of testing the 24 ALS patients (14 male, 10 female; mean age 60.9±2.2 years) reported a median disease duration from symptom onset of 14.5 months (6-24 months), indicating that their assessment was undertaken towards the earlier stages of the disease. Limb-onset disease was evident in 37.5 %, while 62.5% of ALS patients exhibited bulbar-onset disease.

The median ALSFRS-R score was 43.5 (40-46) while the median ALSFRS-R fine motor sub score was 12 (10-12). Of further relevance, the median total MRC sum score was 89 (84-90, maximum score when normal 90), while the upper limb score was 60 (58-60, maximum score 60) and lower limb score was 30 (30-30, maximum score 30)(Table 5.1). Importantly, the muscle strength of the target APB muscle was normal in all patients at time of TMS testing.

All ALS patients progressed to clinically definite ALS, as per the Awaji criteria (82), over a median follow-up period of 22 months. In total, 33% of patients died during the follow-up period, with the median disease survival being 19 months. There was a significant reduction in the ALSFRS-R (33.5 [29.8-41.3], $P<0.001$) and total MRC (80.5 [72-88], $P<0.001$) scores during the follow-up period. In addition, there was a significant reduction in the APB muscle MRC score (MRC score 4 [3.75-5], $P<0.01$), signifying the development of clinical weakness in the target muscle.

Neurophysiological studies

Conventional neurophysiological investigations were undertaken to assess for the presence of lower motor neuron dysfunction in the target APB muscle. The CMAP amplitude (ALS 9.9±0.9 mV; controls 9.5±0.5 mV; P=0.37), and neurophysiological index (ALS 2.1±0.2; controls 2.3±0.1 mV, P=0.22) were comparable between ALS patients and controls.

Qualitative needle EMG examination of the APB muscle was normal at time of TMS testing. Importantly, quantitative EMG testing was also within normal limits. Specifically, the mean MUAP amplitude (ALS 1327.96 ±112.5 μV; controls 1203.3±165.4 μV; P=0.39) and duration (ALS 10.6±0.4 ms; controls 11.2±0.5 ms; P=0.11) were similar between ALS patients and controls confirming the absence of lower motor neuron dysfunction in the target APB muscle at time of assessment. Importantly, all patients developed weakness and atrophy of the tested APB muscle over the follow-up period (mean 22 months), indicating the evolution of LMN dysfunction.

Patient	Age (Years)	Sex	Onset	Disease duration (Months)	ALSFRS-R	MRC SUM
1	64	M	BULBAR	53	42	82
2	57	M	BULBAR	2	44	90
3	40	M	BULBAR	9	40	86
4	78	F	BULBAR	12	40	90
5	68	F	BULBAR	19	40	83
6	58	M	BULBAR	17	38	79
7	71	M	BULBAR	8	46	89
8	62	M	BULBAR	12	44	89
9	50	F	BULBAR	22	42	90
10	58	M	BULBAR	11	43	90
11	62	M	BULBAR	24	44	90
12¶	81	F	BULBAR	108	38	88
13	52	F	BULBAR	24	46	90
14	79	F	BULBAR	6	44	90
15	60	M	BULBAR	23	46	89
16	73	F	LIMB	6	42	83
17	45	M	LIMB	6	48	90
18	42	M	LIMB	4	46	90
19	71	F	LIMB	24	40	86
20	66	F	LIMB	38	38	83
21	68	M	LIMB	6	48	88
22#	47	M	LIMB	84	46	79
23*	53	F	LIMB	60	37	84
24	57	M	LIMB	6	48	90
Mean (SEM), Median(IQR)	**60.9 (±2.2)**			**14.5 (6-24)**	**43.5 (40-46)**	**89 (84-90)**

Table 5.1: Clinical characteristics of 24 amyotrophic lateral sclerosis (ALS) patients at the time of initial assessment. All patients were assessed using the ALS functional rating scale-revised (ALSFRS-R), and the Medical Research Council (MRC) score. The data is expressed as mean (standard error of the mean, SEM) and median (interquartile range, IQR). ¶ Patient 12 exhibited a predominantly upper motor neuron form of ALS, while patient #22 exhibited a flail-arm variant ALS and patient *23 a predominant bulbar palsy form of ALS. All patients, however, developed clinical evidence of LMN dysfunction in the target abductor pollicis brevis muscle with follow-up (median 22 months).

Cortical excitability

Paired-pulse threshold tracking TMS studies disclosed a marked reduction of short interval intracortical inhibition in ALS (Fig. 5.1). Specifically, averaged SICI between ISIs 1-7 ms, was significantly reduced in ALS patients when compared to controls (ALS 1.7±1.4%; controls 10.3±1.0%; P<0.01). Peak SICI at ISI 1 ms (ALS 0.7±0.8%; controls 6.1±1.2%; P<0.001, Fig. 5.2A) and 3 ms (ALS 3.2±1.8%; controls 15±1.5%; P<0.001, Fig. 5.2B) was also significantly reduced in ALS patients. Of further relevance, while the reduction of SICI was a uniform feature in ALS, the reduction was more prominent in patients with limb-onset disease (ALS_{LIMB} 0.16±1.54; ALS_{BULBAR} 3.98±1.54, F = 13.2, P<0.001, Fig. 5.2C).

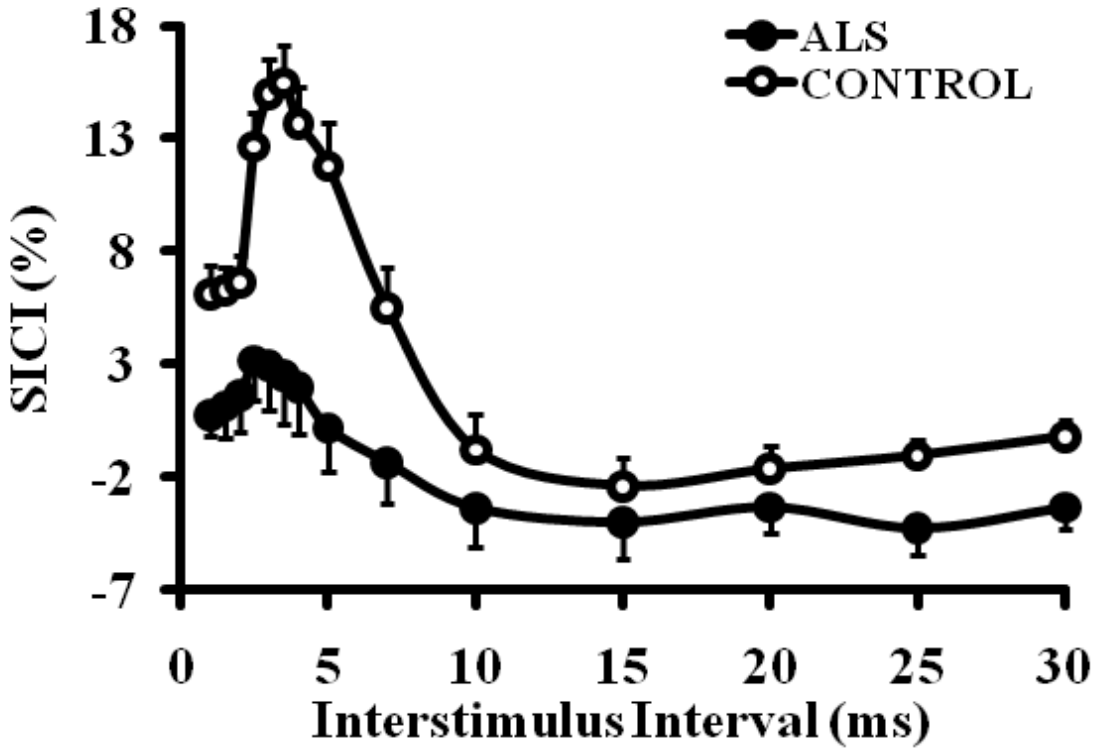

Figure 5.1: Short interval intracortical inhibition (SICI) was significantly reduced in amyotrophic lateral sclerosis (ALS) patients when compared controls.

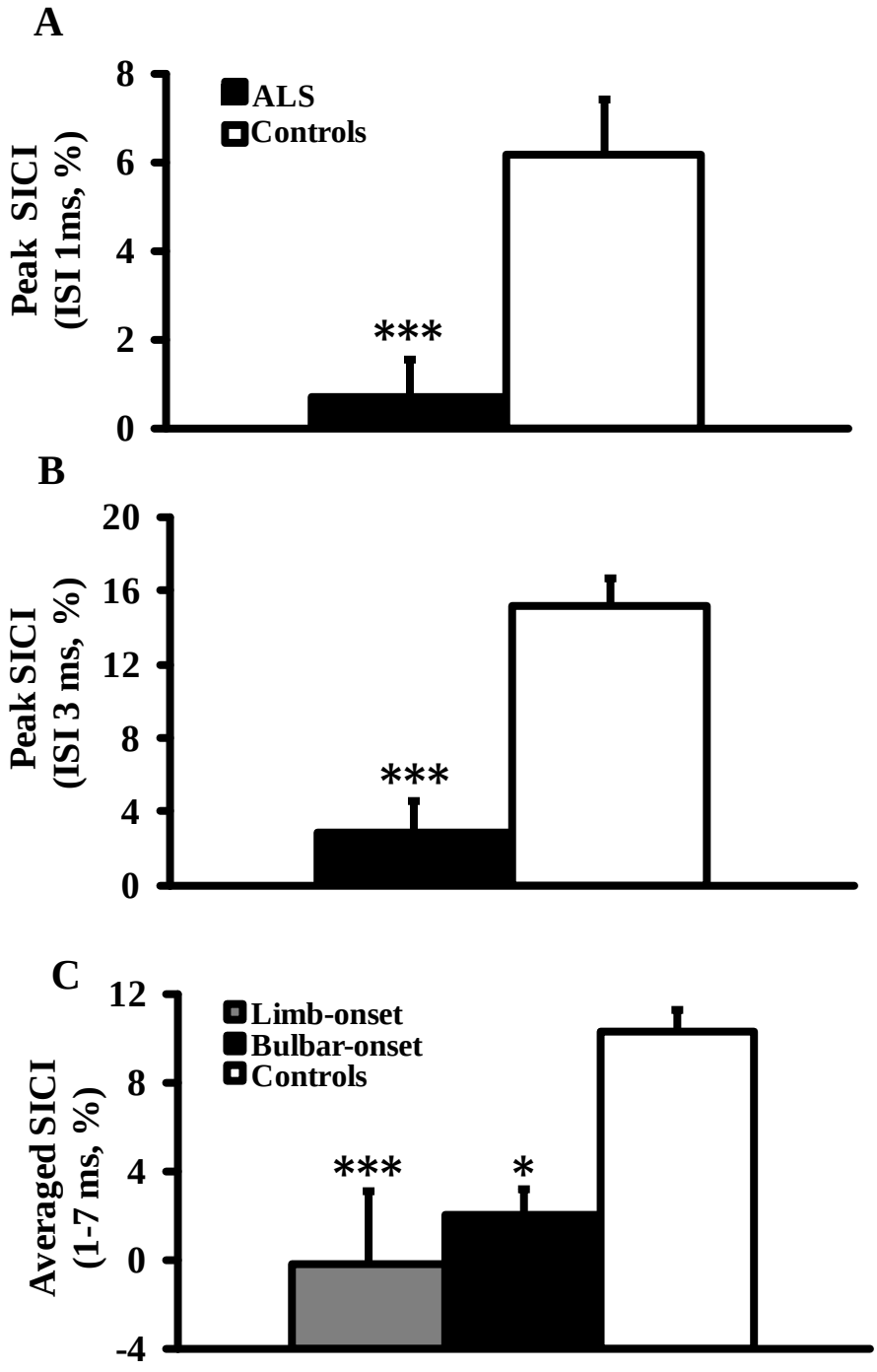

Figure 5.2: Peak short interval intracortical inhibition (SICI) at interstimulus interval (ISI) of **(A)** 1 ms and **(B)** 3 ms was significantly reduced in amyotrophic lateral sclerosis (ALS) patients when compared to controls. **(C)** The reduction in SICI was most prominent in ALS patients with limb-onset disease. *****P < 0.05; *******P< 0.001.

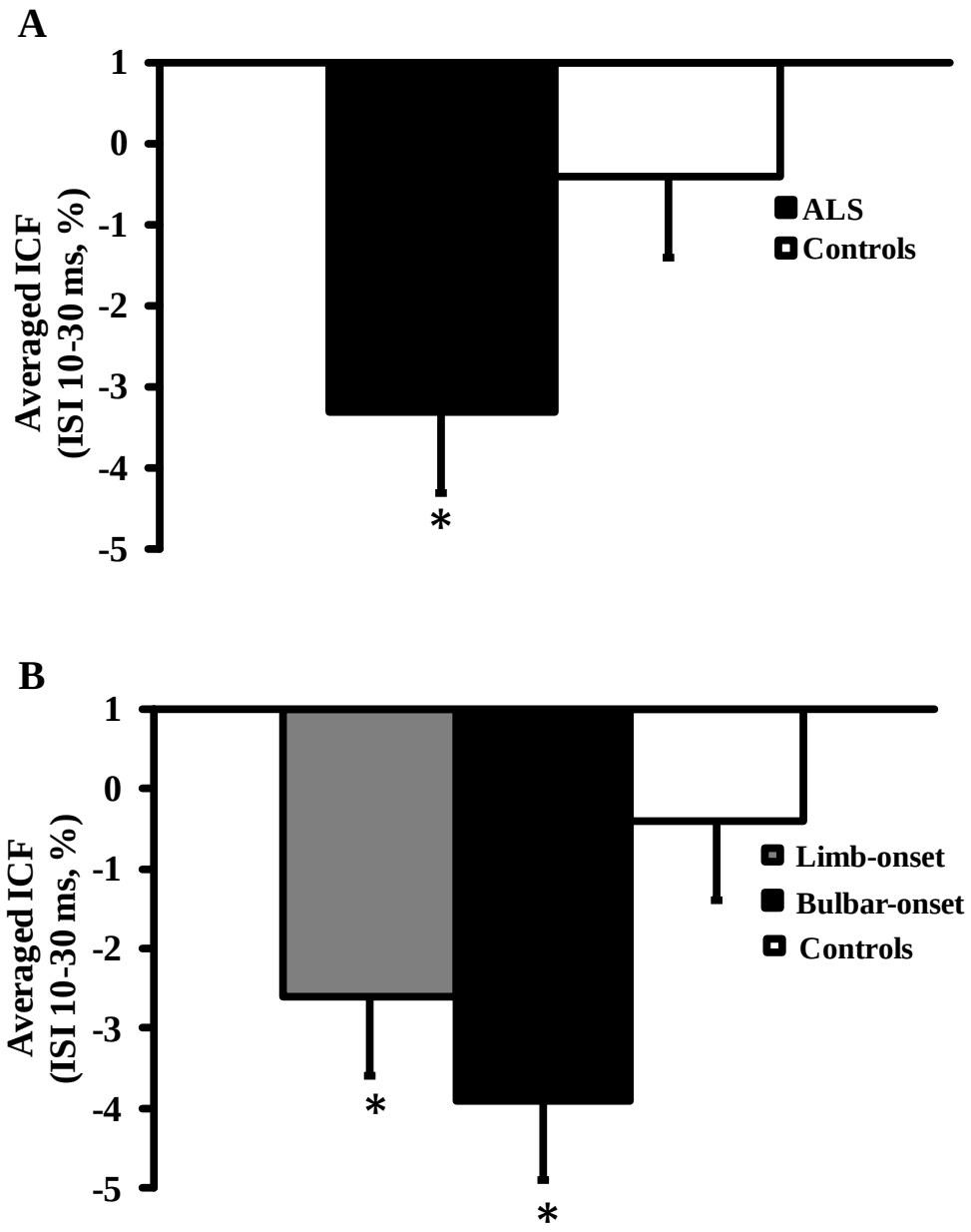

Figure 5.3: (A) Intracortical facilitation (ICF), averaged over interstimulus interval (ISI) of 10-30 ms, was significantly increased in amyotrophic lateral sclerosis (ALS) patients when compared to controls. **(B)** The increase in ICF was similar in ALS patients with limb and bulbar-onset disease. *****$P < 0.05$.

Intracortical facilitation was significantly increased in ALS patients when compared to controls (ALS -3.3±1.0%; controls -0.4±1.0%; P<0.05, Fig. 1, Fig. 3A). This increase in ICF was a ubiquitous finding, evident in bulbar and limb-onset ALS patients (bulbar-onset -3.9±1.7%; limb-onset -2.6±1.3%; P=0.27, Fig 5.3B).

Single pulse TMS studies disclosed a significant reduction of the RMT in ALS patients (ALS 54.9±2.2%; controls 60.5±1.4%; P<0.05, Fig. 5.4A). This reduction in RMT was a uniform finding, evident in both bulbar and limb onset ALS patients (bulbar-onset 55.9±3.6%; limb-onset 53.4±2.1%). The CSP duration was also significantly reduced in ALS when compared to controls (ALS 180.0±9.1 ms; controls 216.7±3.8 ms; P<0.001, Fig. 5.4B), and again was a ubiquitous finding in ALS (bulbar-onset 177.6±11.2 ms; limb-onset 188.4±10.7, P=0.33). In addition, the MEP amplitude was significantly increased in ALS patients (ALS 32.1±3.8%; controls 24.1±2.5%; P<0.05, Fig.5.4C), and was comparably increased in both bulbar and limb onset patients.

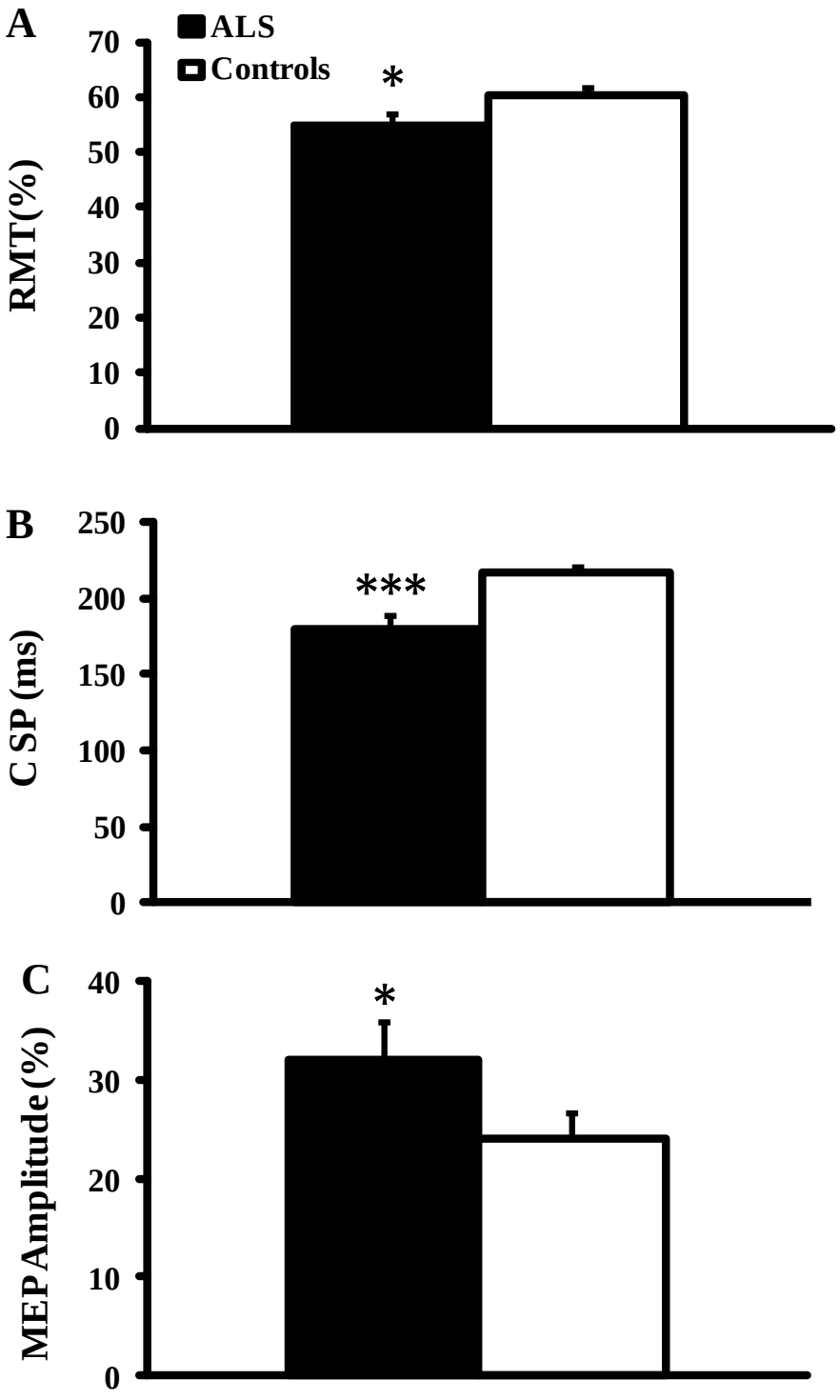

Figure 5.4: (A) The resting motor threshold (RMT) was significantly reduced in amyotrophic lateral sclerosis (ALS) patients. **(B)** The cortical silent period duration was significantly reduced in ALS patients when compared to controls. (C) The motor evoked potential (MEP) amplitude, expressed as a percentage of the compound muscle action potential amplitude, was significantly increased in ALS patients. *****$P < 0.05$; *******$P < 0.001$.

Axonal Excitability

In the same sitting, axonal excitability studies were undertaken on the median nerve at the wrist. The strength-duration time constant was comparable between groups (ALS 0.48 ± 0.02 ms; controls 0.48±0.02ms, P=0.45), as was the rheobase (P=0.21). In addition, depolarizing TE at 90-100 ms (ALS 46.8±1.1%; controls 44.9±0.7%, P = 0.09), and 40-60 ms (ALS 54.5 ± 1.6%; controls 52.8±0.9%, P=0.18), as well as hyperpolarising TE at 90-100 ms (P=0.42) was not significantly different in ALS patients when compared to controls.

The recovery cycle of excitability was also within normal limits in the ALS patients, with RRP (P=0.09), superexcitability (P=0.45) and late subexcitability (P=0.17) being similar between ALS patients and controls. In addition, there was no significant difference in the hyperpolarising I/V (P=0.29), resting I/V (P=0.19) and minimum I/V (P=0.06) gradients in ALS patients when compared to controls.

Discussion

In the present study, cortical and peripheral neurophysiological techniques were utilised to determine whether cortical hyperexcitability preceded the development of lower motor neuron dysfunction in ALS. Cortical hyperexcitability, as indicated by a significant reduction in short interval intracortical inhibition, resting motor threshold, and cortical silent period duration along with an increase in intracortical facilitation and motor evoked potential amplitude, was evident in the present ALS patient cohort when recorded from the APB muscle. Importantly, these central changes were evident when there was no clinical or neurophysiological evidence of lower motor neuron dysfunction within the target APB muscle. Taken together, these findings suggest that

cortical dysfunction may be identified and indeed precedes the development of LMN dysfunction, thereby favouring a cortical origin to the subsequent neurodegeneration that develops in ALS.

Corticomotoneuronal integrity and ALS

Although the pathophysiological mechanisms underlying ALS appear to be multifactorial, with evidence of a complex interaction between molecular and genetic factors (2); a cortically-based mechanism has been suggested whereby motor neuron degeneration in ALS may be mediated by corticomotoneuronal hyperexcitability via an anterograde glutamate-mediated excitotoxic process, the so-called "*dying forward*" hypothesis (25). Indirect support for a cortical origin of ALS has been provided by TMS studies identifying cortical hyperexcitability as an early feature in ALS, and linked to the process of anterior horn cell degeneration (49, 50, 122-124). Further, longitudinal studies in familial ALS cohorts have established that cortical hyperexcitability precedes the clinical development of ALS (50), although subclinical LMN dysfunction was not conclusively excluded.

Cortical hyperexcitability was evident in the present ALS cohort prior to development of lower motor neuron dysfunction. Evidence of cortical hyperexcitability was indicated by a marked reduction in SICI. It has been previously established that SICI reflects a balance between strong inhibitory tone, largely mediated by intracortical GABAergic circuits, along with weaker glutamatergic facilitatory effects on cortical output neurons (426, 488). In ALS, reduction of SICI appears to be mediated by degeneration of inhibitory cortical circuits along with glutamate-

mediated excitotoxicity (480, 497). Consequently, the finding of marked reduction in SICI, when recorded from a clinically and neurophysiologically normal target muscle, along with a significant increase in intracortical facilitation, a biomarker of glutamatergic function (87, 426), support the possibility that cortical hyperexcitability precedes the lower motor neuron dysfunction in ALS.

Further, a marked increase in MEP amplitude was also evident in the present ALS cohort. The MEP amplitude appears to be modulated by a variety of neurotransmitter systems, and importantly is enhanced by glutamatergic transmission (441). Increases in MEP amplitude are well established in ALS, correlate with motor neuron degeneration and appear to be excitotoxic in nature (49, 51). Consequently, the finding of increased MEP amplitude, in the setting of a normal target APB muscle, provides further support for a role of cortical hyperexcitability in ALS pathogenesis. Additional support for a cortical origin for ALS is provided by findings of a significant reduction in CSP duration, a biomarker of long-latency cortical inhibition(457, 458, 548), and RMT, a biomarker of cortical neuronal membrane excitability (426), in the setting of normal LMN function. Importantly, these neurophysiological findings are in keeping with recent neuropathological studies suggesting that pathogenic proteins involved in ALS disseminate from cortical neurons, via axonal projections and synaptic contacts to the spinal and bulbar motor neurons cord (576, 577).

At a peripheral level, the integrity of the lower motor neurons innervating the target APB muscle was established from a combination of electromyography and axonal excitability techniques. Given that qualitative EMG assessment may be insensitive at detecting LMN dysfunction in a

clinically normal muscle (73), the more sensitive quantitative EMG analysis was undertaken, and confirmed the absence of LMN dysfunction within the target APB muscle. Of relevance, upregulation of persistent Na^+ conductances along with reduction in internodal slow and paranodal fast K^+ currents has been established in ALS (57, 58, 561), and linked to development of neurodegeneration and fasciculations. The findings of normal axonal excitability in the present ALS cohort further confirm the functional integrity of axons innervating the APB muscle in the presence of cortical hyperexcitability.

Therapeutic implications in ALS

The finding that cortical dysfunction may be identified prior to lower motor neuron dysfunction implies a cortical origin of ALS. In terms of the process of neurodegeneration, there remains no unifying pathway. Support for a glutamate-mediated process has been provided by molecular studies identifying dysfunction of the astrocytic glutamate transporter, excitatory amino acid transporter 2 (EAAT-2), in human and animal studies (133, 578, 579). Importantly, down regulation of EAAT-2 function has been reported as a pre-symptomatic feature in ALS (578), with evidence emerging of spinal motor neurone degeneration occurring as a secondary to dysfunction of corticomotoneuronal pathways (128). While anti-glutamatergic agents, such as riluzole appear to exert modest clinical effectiveness in ALS (148, 528), in part related to partial normalisation of excitability(480), strategies aimed at restoring astrocytic function may yet prove to be of therapeutic benefit.

Chapter 6

The Split-Hand Plus Sign in ALS: Differential Involvement of the Flexor Pollicis Longus and Intrinsic Hand Muscles

Summary:

The selective vulnerability of muscles in ALS was further explored by measuring the strength of the flexor pollicis longus (FPL), a key muscle involved in fractionated thumb movements which appears relatively spared in amyotrophic lateral sclerosis (ALS) when compared to the thenar group of muscles. This clinical sign termed the ***split hand plus sign*** was prospectively assessed for diagnostic utility in ALS. In total, 103 patients (37 ALS and 66 non-ALS) with neuromuscular symptoms underwent assessment of FPL and APB strength using the Medical Research Council (MRC) score. A ***median nerve strength index*** (MSI) was developed to quantify differential involvement by expressing the APB strength scores as a fraction of the FPL strength score. The APB muscle strength was significantly reduced when compared to FPL strength in ALS patients ($P<0.0001$), but was comparable in the non-ALS disorders ($P=0.91$). In addition, there was a significant reduction of MSI scores in ALS patients (MSI_{ALS} 0.8; $MSI_{non\text{-}ALS}$ 1.0, $P<0.01$). Analysis of receiver operating characteristic (ROC) curves disclosed that MSI < 0.9 exhibited an area under the curve of 0.86 ($P<0.001$) with a sensitivity of 85% and specificity of 86% for limb-onset ALS. In conclusion, the ***split hand plus sign*** distinguished ALS from non-ALS neuromuscular disorders, thereby reinforcing the phenomenon of selective involvement of muscles and establishing a diagnostic utility of this novel clinical sign in ALS.

Introduction

Preferential atrophy of the abductor pollicis brevis (APB) and first dorsal interosseous (FDI) muscles, termed "***the split hand sign***", appears to be a specific clinical feature for amyotrophic lateral sclerosis (ALS)(20, 21, 44, 54, 519). Consequently, the finding of a split hand sign may aid in the diagnosis of ALS, complementing other clinical and neurophysiological techniques (519). In addition to its diagnostic utility, the split hand sign may provide insights into ALS pathophysiology.

Of further relevance, relative preservation of other key muscles involved in complex thumb movements, namely the flexor pollicis longus (FPL), appears to be a clinical feature of ALS. Although the APB and FPL muscles are innervated by the same spinal motor neurons (C8,T1) and nerve (median nerve), the function of FPL is relatively preserved in ALS (*personal observation*). This novel clinical phenomenon, that we termed the ***split-hand plus sign***, may be of further diagnostic utility in a clinical setting. To date, the sensitivity and specificity of this novel sign has not been prospectively assessed. The importance of prospectively assessing the diagnostic utility of the ***split-hand plus sign*** is underscored by previous reports questioning the specificity of the related split hand sign in ALS (559, 560). If established to be specific for ALS, the ***split-hand plus sign*** could potentially complement other clinical and neurophysiological findings in the diagnosis of ALS.

In order to assess its diagnostic utility, the ***split-hand plus sign*** was quantified by expressing the Medical Research Council (MRC) strength scores of the APB and FPL muscles in a novel index termed Median Nerve Strength Index (MSI). Consequently, the present study assessed the

diagnostic utility, and thereby specificity, of the novel ***split-hand plus sign*** in contributing to the diagnosis of ALS.

Materials and Methods

In total, 103 patients were recruited from our multidisciplinary neuromuscular clinics at Westmead and Prince of Wales Hospitals, between April 2011 and Mar 2012. All patients underwent clinical assessment, with the muscle strength graded using the Medical Research Council (MRC) strength score (575). Following extensive clinical assessment, investigations and follow-up 37 patients were diagnosed as "definite" or "probable" amyotrophic lateral sclerosis (22 male, 15 female; mean age 61.5 years, Fig. 1) according to the Awaji criteria (82). All ALS patients were classified according to the region of symptom onset (limb or bulbar onset), and were staged using the Amyotrophic Lateral Sclerosis Functional Rating Scale-Revised (ALSFRS-R)(511). Results were compared to 66 non-ALS patients (NALS : 37 Male; 29 Female; mean age 48.3 years; Fig 1). All patients provided informed consent for testing which was approved by the Sydney South West Area Ethics committee.

Muscle strength was assessed in the following muscle groups generating a maximum Medical Research Council (MRC) score of 90: ***Upper limbs***; shoulder abduction, elbow flexion and extension, wrist dorsiflexion, finger abduction and thumb abduction bilaterally; ***Lower limbs***; hip flexion, knee extension and ankle dorsiflexion bilaterally. Specifically, FPL muscle strength was assessed by instructing the patients to flex the distal phalanx of the thumb against resistance. The APB and FPL muscle strength was recorded to generate the MSI as represented by the following formula:

$$\mathbf{MSI} = \frac{\mathbf{APB\ MRC\ score}}{\mathbf{FPL\ MRC\ score}}$$

Statistical Analysis

Differences in muscle strength scores between and within groups were assessed using the Wilcoxon signed rank test, while the Mann Whitney U test was utilized to assess differences in MSI between ALS and non-ALS patients. Receiver Operating Characteristic Curves (ROC) were undertaken to determine the diagnostic utility of MSI. Results are expressed as mean ± standard error of mean and median (interquartile range). $P<0.05$ was considered statistically significant.

Results

Clinical characteristics

The clinical features for ALS patients are summarised in Figure 6.1. At the time of initial assessment, 76 % of patients were classified as "definite" or "probable" ALS according to Awaji-Shima criteria, while 24% were classified as "possible" ALS. 54% of ALS patients exhibited limb-onset disease while 46% presented with bulbar-onset disease. Median disease duration from symptom onset was 12(9-24) months, while the median ALSFRS-R score was 41 (30.5-44) and MRC sum score was 79 (67-88), signifying a mild to moderate degree of impairment. The diagnosis in the non-ALS cohort is outlined in Figure 1. None of the patient in this cohort developed ALS. The median MRC sum score for the non-ALS cohort was 84 (78-90) and was comparable to ALS patients.

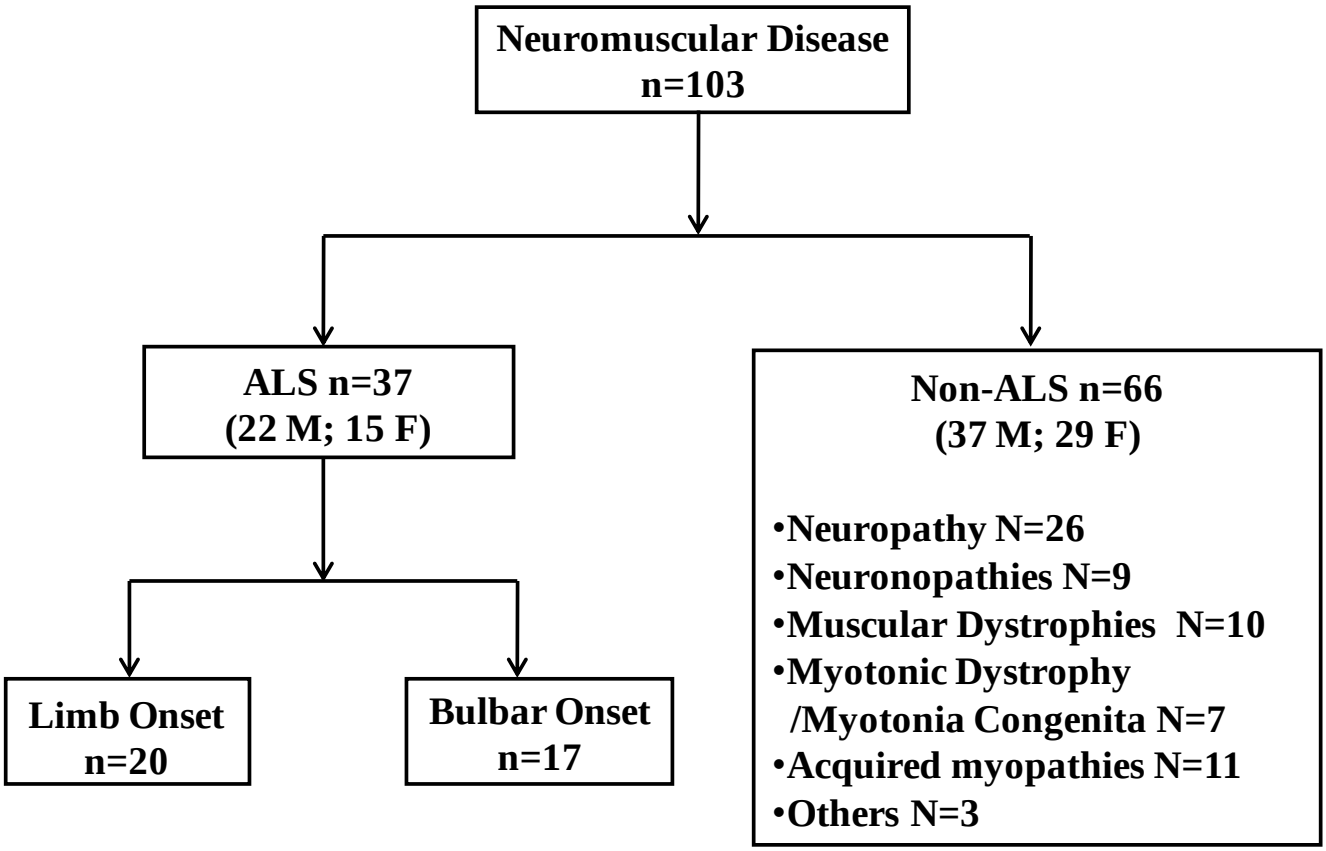

Figure 6.1: Flow diagram of prospective patient recruitment for assessment of the split hand plus sign with subsequent differentiation into Amyotrophic Lateral Sclerosis (ALS) and non-ALS groups based on the reference standard (Awaji Criteria). The ALS group was subdivided into limb and bulbar-onset disease. Non-ALS NALS group comprised a heterogeneous group of inherited and acquired neuromuscular disorders and included the following: (i) ***neuropathy*** [chronic inflammatory demyelinating polyradiculoneuropathy; Guillain-Barre syndrome; isolated peripheral nerve vasculitis; Kennedys disease]: ***neuronopathy*** [Sjorgen's syndrome ganglionopathy; spinal muscular atrophy; Hirayama's disease]: ***muscular dystrophy*** [Duchene's muscular dystrophy; Becker's muscular dystrophy; fascioscapulohumeral muscular dystrophy; limb girdle muscular dystrophy; central core myopathy; congenital myopathy; adult-onset Pompes disease]: ***myotonic dystrophy*** [myotonic dystrophy; myotonia congenital]: ***acquired myopathies*** [inclusion body myositis; inflammatory myopathy; myopathy of undetermined cause]: ***others*** [Ehlers-Danlos syndrome; complicated hereditary spastic paraplegia].

Differences in the FPL and APB muscle strength scores

In the ALS cohort, the APB muscle was significantly weaker when compared to FPL ($P < 0.01$, Fig. 6.2).

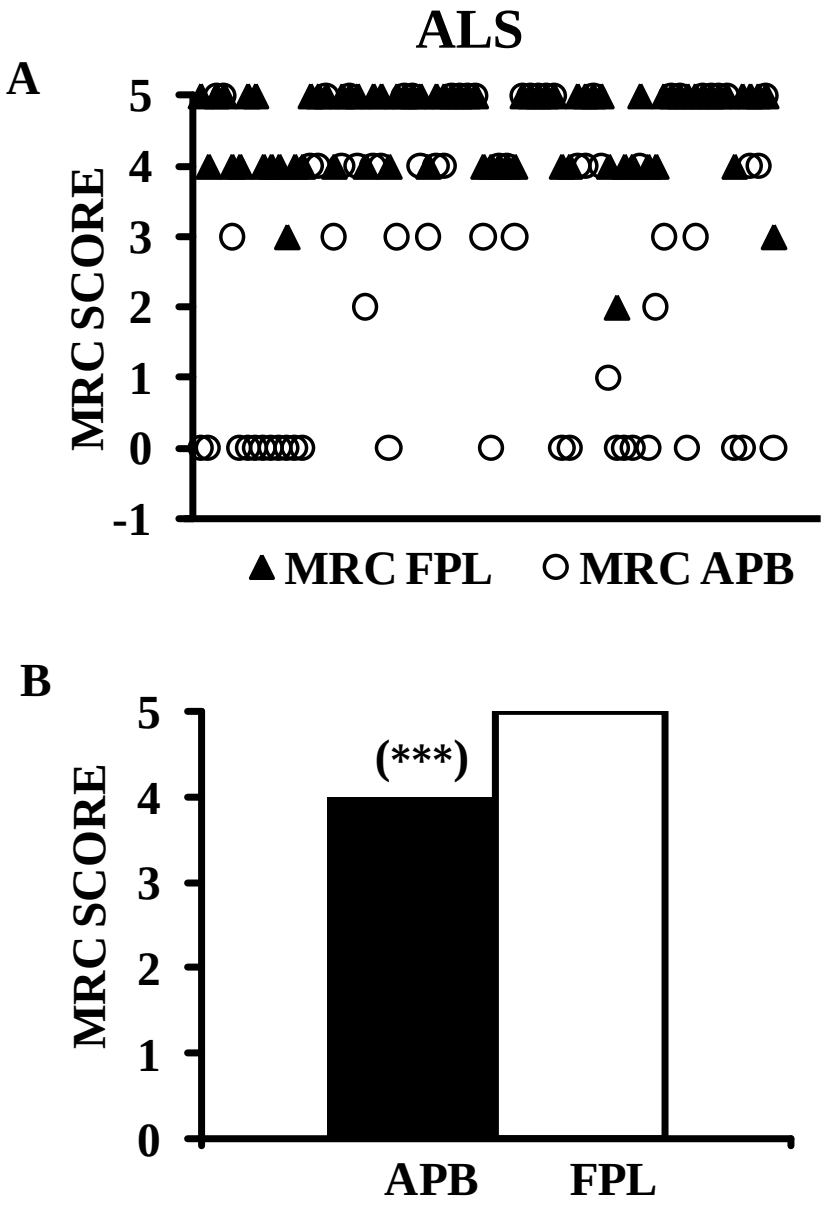

Figure 6.2: (A) In amyotrophic lateral sclerosis (ALS) patients, the abductor pollicis brevis (APB) was significantly weaker when compared to flexor pollicis longus (FPL), as measured by the Medical Research Council (MRC) strength score scatter plots. **(B)** The median MRC score was significantly reduced for the APB muscle compared to the FPL.

In contrast, there was a comparable degree of APB and FPL weakness in the non-ALS cohort (Fig. 6.3).

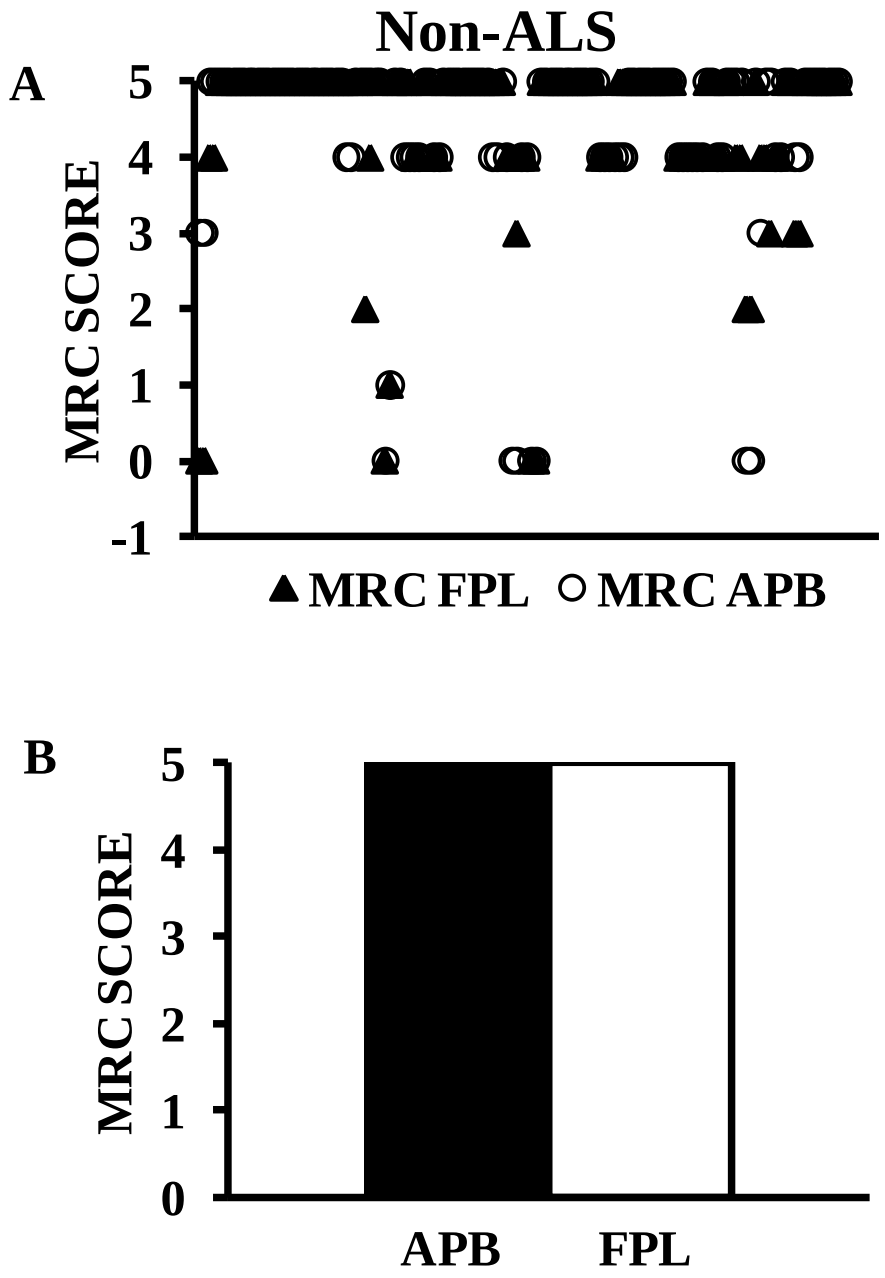

Figure 6.3: (A) The Medical Research Council (MRC) score for the abductor pollicis brevis (APB) and flexor pollicis longus (FPL) were similar in non-amyotrophic lateral sclerosis (non-ALS) patients. **(B)** Median MRC scores were comparable between the APB and FPL.

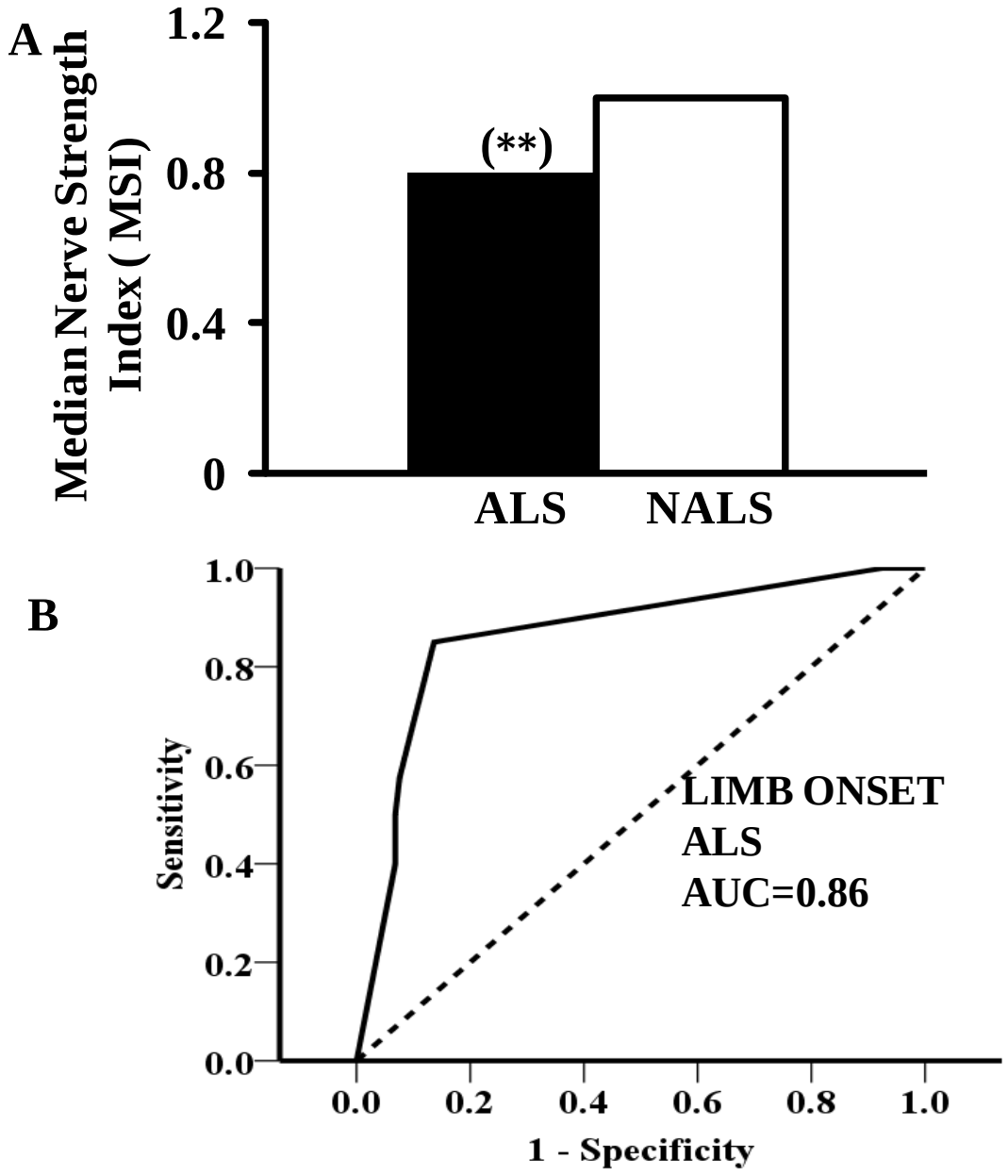

Figure 6.4: (A) The median nerve strength index (MSI, *see* Methods) was significantly reduced in amyotrophic lateral sclerosis (ALS) patients compared to non-amyotrophic lateral sclerosis (non-ALS). **(B)** Receiver operating characteristic (ROC) curve revealed that a cut-off value of 0.9 exhibited a sensitivity of 84% and specificity of 86% in differentiating ALS from non-ALS disorders. The area under the curve (AUC) was 0.86 ($P<0.001$) indicating a "good" diagnostic potential for the MSI in differentiating ALS from non-ALS.

The MSI score was significantly reduced in ALS patients when compared to non-ALS (MSI_{ALS} 0.8[0-1.0]; $MSI_{non\text{-}ALS}$ 1.0 [1.0-1.0], P<0.01, Fig. 6.4A). Subgroup analysis disclosed that the MSI was significantly reduced in limb-onset ALS patients when compared to bulbar-onset ALS ($MSI_{LIMB\text{-}ONSET}$ 0.75[0-0.8]; $MSI_{BULBAR\text{-}ONSET}$ 1.0 [0.6-1.0], P<0.01, Fig. 6.4B). Although the MSI was higher in the bulbar-onset ALS patients, it continued to be significantly reduced when compared to non-ALS (P<0.001).

Diagnostic utility of MSI

Assessment of the entire ALS cohort, disclosed and area under the curve of 0.8 (P<0.001), suggesting a good diagnostic accuracy of the MSI. Of relevance, an MSI value of 0.9 differentiated ALS from non-ALS cohort with a sensitivity of 66% and specificity of 86%. Subgroup analysis disclosed that in limb-onset ALS patients, an MSI value of 0.9 differentiated ALS from non-ALS with a sensitivity of 84% and specificity of 86%, with the area under the curve being 0.86 (P<0.001).

Discussion

The present study suggests that the ***split hand plus sign*** is a specific feature of ALS, clearly distinguishing ALS from non-ALS disorders. The ***split hand plus sign*** was characterised by a greater weakness and atrophy of the APB muscle when compared to the FPL, and was reflected by a significantly reduced median nerve strength index. Although the reduction in MSI was evident across the clinical spectrum of ALS, it was most pronounced in ALS patients with limb-onset disease. Importantly, a diagnostic MSI cut-off value of 0.9 reliably distinguished ALS

from non-ALS mimic disorders, thereby suggesting that the ***split hand plus sign*** may complement the diagnosis of ALS especially in limb-onset disease.

In the absence of a pathognomonic test, the diagnosis of ALS is based on clinical criteria, relying on the identification of a combination of upper and lower motor neuron signs (14, 82, 580). Upper motor neuron signs may be evident in ALS mimic disorders such as multifocal motor neuropathy with conduction block (581), potentially resulting in an erroneous diagnosis of ALS. The finding in the present study that the ***split-hand plus sign*** was a specific feature of ALS, clearly distinguishing ALS from non-ALS disorders, underscores the clinical utility of this novel clinical sign.

Although the specificity of the ***split-hand plus sign*** was high (84%), it was not 100%. Analysis of non-ALS patients with an MSI < 0.9 revealed that in 30% of cases assessment of FPL strength revealed a comparable or greater weakness than APB, a pattern that was distinct to that evident in ALS. In the remaining in 70% of non-ALS patients with MSI < 0.9, other clinical features, such as the presence of myotonia, distinguished non-ALS from ALS patients. Taken together, the findings in the present study suggest that the ***split-hand plus sign*** may be of utility as a complementary clinical finding in the diagnosis of ALS.

Although the reduction in MSI was also evident in bulbar-onset ALS patients, this reduction was not as pronounced as in limb-onset disease, thereby potentially limiting the diagnostic utility of the ***split-hand plus sign*** in bulbar-onset ALS. A likely explanation may relate to relative preservation of upper limb function in the current cohort of bulbar-onset ALS patients at the time

of assessment. Assessment of FPL, with either Magnetic Resonance Imaging (MRI) techniques for detecting muscle wasting, or needle EMG techniques for detecting lower motor neuron (LMN) dysfunction, may prove diagnostically useful. Further, correlation of FPL strength scores with more objective biomarkers of LMN dysfunction, such as abnormalities on needle EMG assessment, may be of further diagnostic utility.

The split-hand plus sign and the pathophysiology of ALS

In addition to being of diagnostic utility, ***split-hand plus sign*** may provide unique insights into ALS pathophysiology. Specifically, the "dying forward" hypothesis proposed that ALS was primarily a disorder of corticomotoneurons, with corticomotoneuronal hyperexcitability mediating anterior horn cell degeneration (25). The 'dying forward hypothesis' has been suggested as the basis of the split-hand sign in ALS, with the affected thenar group of muscles having a greater corticomotorneuronal input compared to other intrinsic hand muscles (54). Given the varied function of the APB and FPL (582), with the suggestion that the FPL exhibits less cortical representation (547, 583), the finding in the present study that the ***split-hand plus sign*** was specific to ALS, would lend support to a cortical mechanism in ALS. Future studies should combine central and peripheral nerve excitability techniques to the FPL muscle in order to dissect out the relative contributions of central and peripheral mechanisms to the development of the ***split-hand plus sign*** in ALS.

Chapter 7

Cortical Excitability differences between Flexor Pollicis Longus and Abductor Pollicis Brevis

Summary

After establishing that the ***split-hand plus sign*** was specific to ALS, the present study was undertaken to assess the relative contributions of central and peripheral mechanisms to the development of the split-hand plus sign. Although abductor pollicis brevis (APB) and flexor pollicis longus (FPL) share a common peripheral nerve supply, these muscles subserve different functions and may be differently affected in neurodegenerative disease such as amyotrophic lateral sclerosis (ALS). As a consequence, differences in cortical excitability may potentially develop in relation to these functional differences. Cortical excitability was assessed using the threshold tracking transcranial magnetic stimulation (TMS) technique in 15 healthy controls with motor responses recorded over the APB and FPL using surface electrode recordings. Short-interval intracortical inhibition (SICI) was significantly reduced from the FPL compared to APB ($SICI_{FPL}$ 6.9±1.8%; $SICI_{APB}$ 10.7±1.4%, $P<0.01$). In addition, the FPL motor evoked potential amplitude (MEP_{FPL} 14.7± 2.3%; MEP_{APB} 21.7±3.9%; $P<0.01$) and cortical silent period duration (CSP_{FPL} 174.7 ± 6.7ms; CSP_{APB} 205.4±3.9ms, $P<0.01$) were significantly smaller. The findings in the present study indicate that cortical inhibition and corticomotoneuronal output is reduced when recording over the FPL. The differences in cortical excitability may develop as a consequence of varied function and could potentially explain the dissociated muscle atrophy evident in ALS.

Introduction

Preferential wasting of the thenar complex, including the abductor pollicis brevis (APB) and first dorsal interosseous (FDI), appears to be a specific clinical feature in amyotrophic lateral sclerosis (ALS) (20, 21, 519, 584). This pattern of dissociated atrophy of the intrinsic hand muscles has been termed the split hand (21). Recently, this dissociated pattern of muscle wasting has been extended to include the flexor pollicis longus (FPL) with relative preservation of FPL strength in ALS, a phenomena termed the "***split-hand plus sign***" (585).

The pathophysiological mechanisms underlying this dissociated pattern of muscle wasting in ALS remains unclear. Dysfunction of local spinal segments is unlikely to account for such a pattern of muscle wasting given that all involved muscles are innervated by the same myotomes (C8, T1). Rather, a cortical mechanism has been proposed, whereby corticomotoneurons mediate anterior horn cell degeneration via an anterograde transsynaptic excitotoxic mechanism (25). Given that the thenar muscles are critically important for execution of fine fractionated finger movements, thereby potentially exhibiting a greater cortical representation, it was hypothesized that a cortical mechanisms underlies the development of dissociated muscle atrophy (the *split-hand*) in ALS (25, 44). Given the recent observation that the novel split-hand plus sign is a specific feature of ALS (585), it could also be hypothesized that a cortical mechanisms was responsible for the split-hand sign.

Cortical function and corticomotoneuronal output may be assessed by using paired pulse TMS techniques (401, 417, 468). Paired-pulse TMS has provided unique insights into the excitability of motor cortical inhibitory and facilitatory circuits, termed short interval intracortical inhibition

(SICI) and intracortical facilitation (ICF), thereby enabling an understanding into the cortical representation and the functional organization of motor outputs (401, 417, 468-470). Perhaps of relevance, the amplitude and time course of SICI is greater to the thenar complex when compared to the more proximal upper limb muscles (420, 540), a finding attributed to differences in cortical excitability (540, 586).

In contrast to thenar and proximal upper limb muscles, little is known about the cortical function, corticomotoneuronal representation and input to the FPL. Consequently, utilizing threshold tracking TMS techniques, the present study assessed cortical excitability from the FPL compared to thenar muscles in healthy controls, to determine whether differences in cortical excitability could form an underlying substrate and the pathophysiological basis for the development of the split hand-plus phenomena in ALS.

Materials and Methods:

Subjects

A total 15 healthy subjects (10 men and 5 women) were assessed, with median age of 34 years (age range 25 to 55 years). At the time of assessment, none of the subjects were medicated with psychotropic medications that could potentially influence cortical excitability. All subjects provided informed consent to the experimental procedures, which was approved by the South East Sydney and Sydney West Area Health Service Human Research Ethics Committees.

Peripheral nerve studies

Prior to undertaking cortical excitability studies, the median nerve was stimulated electrically at the wrist, for APB recordings, and at the elbow for FPL recordings, using 5-mm Ag-AgCl surface electrodes (ConMed, Utica, USA). The resultant compound muscle action potential [CMAP] was recorded from the APB and FPL muscles using surface electrodes according to previously reported methods (417, 587). For APB recordings, the G1 electrode was positioned over the belly of the APB while the G2 electrode was positioned over the base of the thumb. The positions of the recording electrodes were altered for the FPL muscle, such that the G1 electrode was positioned over the FPL belly 6-8 cm proximal to the radial styloid while the G2 electrode was placed on the radial styloid. The resultant CMAP onset latency and peak-peak amplitude were recorded from the APB and FPL muscles.

Cortical excitability

Cortical excitability studies were undertaken by applying a 90 mm circular coil to the motor cortex with currents generated by two high-power magnetic stimulators connected via a BiStim (Magstim Co., Whitland, South West Wales, UK). The coil position was adjusted for each muscle such that a maximal motor evoked potential (MEP) was elicited prior to proceeding with cortical excitability studies. The stimulating coil was adjusted such that the direction of current flow within the motor cortex was in a posterior-anterior direction when recording MEPs from both muscles.

TMS threshold tracking

In the conventional paired-pulse technique, the conditioning and test stimuli are kept at constant intensity, and changes in the motor evoked potential [MEP] amplitude are measured. In the present study the target MEP was of predetermined, fixed amplitude and changes in the test stimulus intensity required to generate this target response, when preceded by a subthreshold conditioning stimulus, was measured (416, 417). The threshold-tracking strategy used a target response of 0.2 mV [± 20%], located in the middle of the established linear relationship between the logarithm of the MEP amplitude and the stimulus intensity (416, 417). Resting motor threshold [RMT] was defined as the stimulus intensity required to produce and maintain this target MEP response.

Initially, the MEP amplitude was recorded with magnetic stimulus intensity set to 150% of RMT, and three stimuli were delivered at this level of stimulus intensity. Subsequent to recording the MEP responses, the cortical silent period (CSP) duration was assessed by instructing the subject to contract each muscle at ~30% of maximal voluntary contraction with stimulus intensity again set to 150% of RMT. Three stimuli were delivered at this level of stimulus intensity and the CSP was recorded contralateral to the side of stimulation. The CSP duration was measured from onset of MEP to return of EMG activity (455). The resumption of EMG activity was assessed visually.

Paired-pulse stimuli

Subsequently, a paired-pulse TMS technique was applied to determine the short-interval intracortical inhibition (SICI) and intracortical facilitation (ICF). Briefly, the changes in test

stimulus intensity required to generate the target MEP response of 0.2 mV, when preceded by a sub-threshold conditioning stimulus (set to 70% of RMT) reflected SICI and ICF. Short-interval intracortical inhibition (SICI) was determined over the following interstimulus intervals (ISIs): 1, 1.5, 2, 2.5, 3, 3.5, 4, 5, and 7 ms, while ICF was measured at ISIs of 10, 15, 20, 25 and 30 ms. Stimuli were delivered sequentially as a series of three channels: *channel 1*: stimulus intensity, or threshold (% maximal stimulator output) required to produce the unconditioned test response (i.e., RMT); *channel 2*: sub-threshold conditioning stimulus (70% RMT); and *channel 3* tracks the stimulus or threshold (% maximal stimulator output) required to produce the target MEP when conditioned by a sub-threshold stimulus equal in intensity set to 70% of RMT. Stimuli were delivered every 5–10 s (stimulus delivery was limited by the charging capability of the BiStim system) and the computer advanced to the next ISI only when tracking was stable.

All CMAP and MEP recordings were amplified and filtered (3 Hz-3 kHz) using a Grass ICP511 AC amplifier [Grass-Telefactor, Astro-Med Inc., West Warwick, RI, USA] and sampled at 10 kHz using a 12-bit data acquisition card (National Instruments PCI-MIO-16E-4). Data acquisition and stimulus delivery (both electrical and magnetic) were controlled by QTRACS software, Institute of Neurology, Queen Square, London, UK).

Data Analysis

SICI was measured as the increase in the test stimulus intensity required to evoke the target MEP. Inhibition was calculated off-line as follows (417):

Inhibition = (Conditioned test stimulus intensity – RMT)/RMT * 100

Facilitation was measured as the decrease in the conditioned test stimulus intensity required to evoke a target MEP.

Each data point was weighted [by the QTRACS software] such that any measures recorded outside the threshold target window, defined as values within 20% of the tracking target of 0.2mV [peak-to-peak], contributed least to the data analysis. All results were expressed as mean ± standard error of the mean. The neurophysiological variables were normally distributed as assessed by the Shapiro-Wilk test for normality. Paired samples t-test was used for assessing differences between two groups, while repeated measure analysis of variance (ANOVA), with ISI as the within subject factor and "muscle type" as the between subject factor. Pearson's correlation coefficient was used to examine the relationship of the TMS parameters between each muscle and with CMAP amplitude. A probability (P) value of <0.05 was considered statistically significant.

Results

A complete sequence of recordings was obtained from all subjects. Peak-to-peak CMAP amplitude was greater when recorded from the abductor pollicis brevis compared to the flexor pollicis longus muscle ($CMAP_{APB}$ 18.1 ± 1.4 mV; $CMAP_{FPL}$ 11.6 ± 1.2 mV, $P < 0.01$). In contrast, the median nerve distal motor latency was comparable between the two muscles ($CMAP_{APB}$ 3.9 ± 0.1 ms; $CMAP_{FPL}$ 3.5 ± 0.6 ms), consistent with previously reported normative data (417, 587).

Differences in intracortical inhibition and facilitation between APB and FPL

Paired-pulse threshold tracking TMS techniques were utilized to assess the cortical function of the APB and FPL muscles. The resting motor threshold (RMT), defined as the stimulus intensity required to produce and maintain the target MEP response of 0.2 mV, was comparable between the two muscles (RMT_{FPL} 53.8 ±3.2 %; RMT_{APB} 55.0 ±2.7%, P=0.37).

Subsequent to establishing a similar level of RMT, ***short interval intracortical inhibition*** was assessed as a biomarker of cortical inhibitory interneuronal network function (426). Repeated measure ANOVA demonstrated a significant effects of group or "muscle type" ($F = 9.3$, $P < 0.001$,) and interstimulus interval ($F = 8.2$, $P < 0.05$). In contrast the group (muscle type) x ISI interaction was not significant.

There was a significant reduction of SICI magnitude and time course when recording over the FPL muscle. In addition, while the presence of the previously established peaks of SICI at ISI of 1 and 2.5-3 ms (416, 417, 491) were re-affirmed when recording from the APB (Fig. 7.1, black arrows), only one smaller peak, at ISI 2.5 ms, was evident when recording over the FPL muscle (Fig. 7.1). Short interval intracortical inhibition at ISI 2.5-3 ms (FPL 11.6 ± 2.9%; APB 15.5 ± 2.3%, $P < 0.05$, Fig. 7.2A) and ISI 1 ms (FPL 6.8 ± 2.0%; APB 12.6 ± 1.8%, $P < 0.05$, Fig. 7.2B) were significantly smaller when recording over the FPL.

Following SICI, a period of intracortical facilitation develops between ISIs 10-30ms. This phenomenon was evident when recordings were undertaken from both muscles. Further, the mean ICF, recorded between ISIs 10-30 ms, was not significantly different between the two

muscles (ICF_{FPL} -0.6 ±1.2%; ICF_{APB} -0.9 ±1.6%, F= 0.5, P=0.4, Fig. 7.1).

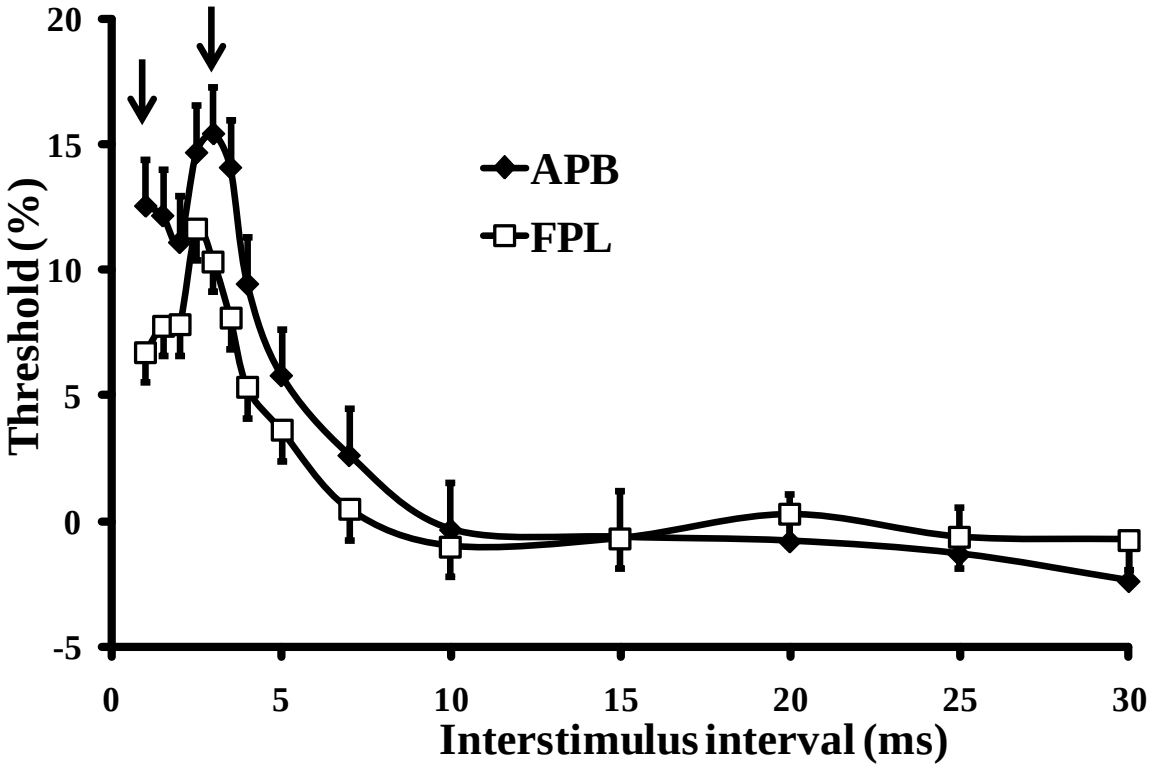

Figure 7.1: Short interval intracortical inhibition, defined as the stimulus intensity required to maintain a target response of 0.2 mV (*see* Methods), was recorded from both the abductor pollicis brevis (APB) and flexor pollicis longus (FPL) muscles. Two previously reported SICI peaks, at an interstimulus interval (ISI) of 1 and 3 ms, were again evident when recording over the APB. The SICI was significantly smaller when recording over the FPL compared to APB, and the previously established peaks at an ISI of 1 and 3 ms (as indicated by arrows) were not evident when recording over FPL.

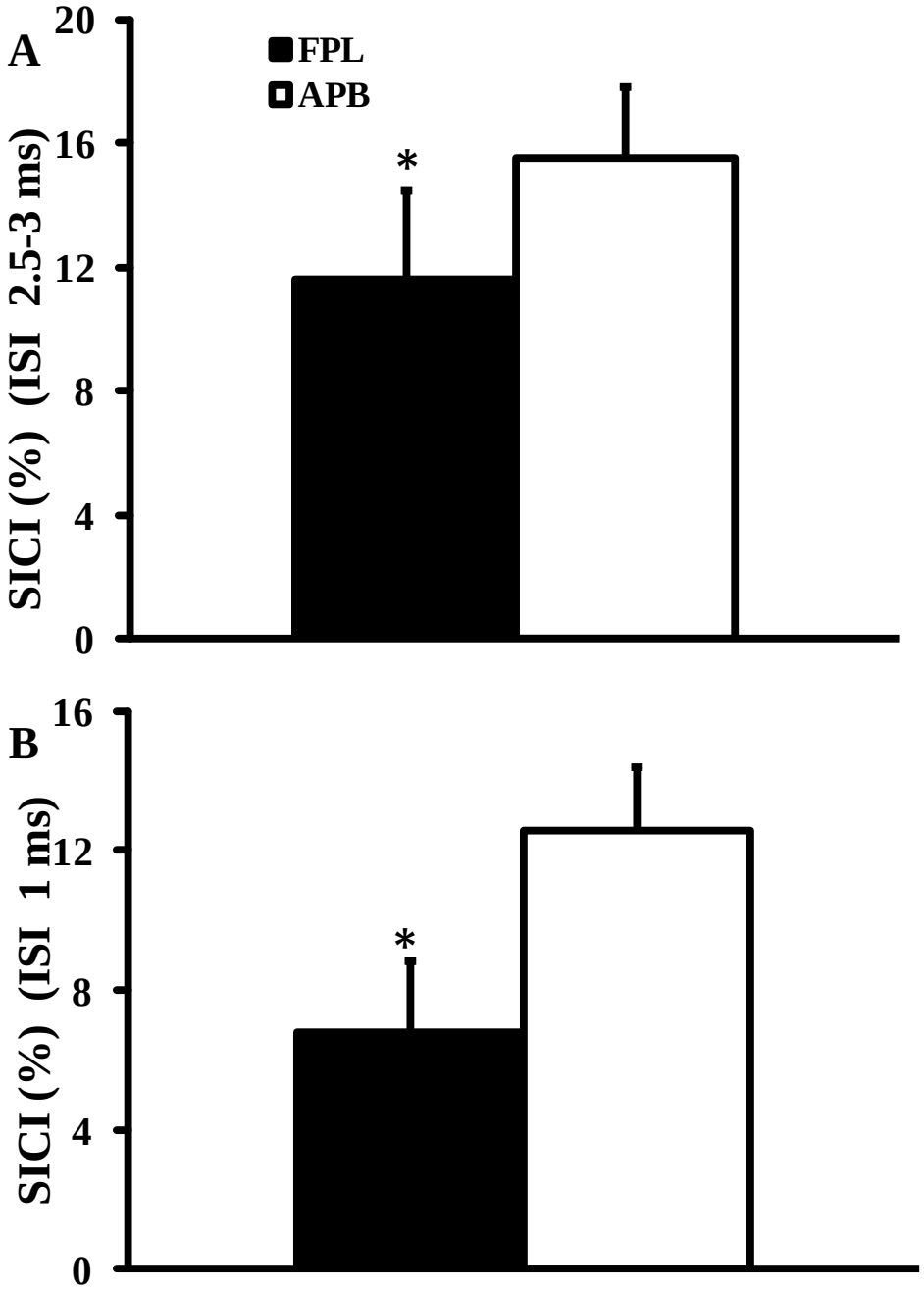

Figure 7.2: Peak short interval intracortical inhibition (SICI), defined as the difference between the conditioned test stimulus intensity recorded on channel 3 and unconditioned stimulus intensity recorded on channel 1 (*see* methods), at interstimulus intervals (ISI) of **(A)** 2.5-3 ms AND **(B)** at ISI 1 ms, was significantly reduced when recording over the flexor pollicis longus (FPL) compared to abductor pollicis brevis (APB). * $P < 0.05$.

Single pulse TMS techniques disclosed that the MEP amplitude, expressed as percentage of the CMAP response, was significantly smaller when recording over the FPL muscle (MEP_{FPL} 14.7 ± 2.3%; MEP_{APB} 21.7 ± 3.9%; $P < 0.01$, Fig. 7.3A). The MEP latency was significantly shorter to the FPL muscle ($MEP_{\text{latency FPL}}$ 18.8 ± 2.2 ms; $MEP_{\text{latency APB}}$ 20.0 ± 2.1 ms; $P < 0.01$), perhaps reflecting the shorter conducting distance to the FPL. In addition, mean CSP duration was significantly shorter when recording over the FPL muscle (CSP_{FPL} 174.7 ± 6.7ms; CSP_{APB} 205.4 ± 3.9ms, $P < 0.01$, Fig. 7.3B).

Correlation studies

In order to determine whether the differences in CMAP amplitudes between the APB and FPL could potentially account for the cortical excitability findings, correlation studies were undertaken. There was no significant correlation between CMAP amplitudes and any of the TMS parameters, thereby suggesting that differences in CMAP amplitudes did not account for the cortical excitability findings.

Of further relevance, it could also be argued that the observed differences in SICI were in part accounted for by differences in the MEP amplitude. As such, SICI was correlated with the absolute MEP amplitude and MEP amplitude expressed as percentage of CMAP response. There was no significant correlation between the absolute MEP amplitude ($R = 0.17$) or expressed MEP amplitude ($R = 0.2$) and SICI. This finding suggests that the reduction in cortical inhibitory effects in the FPL is independent of MEP size.

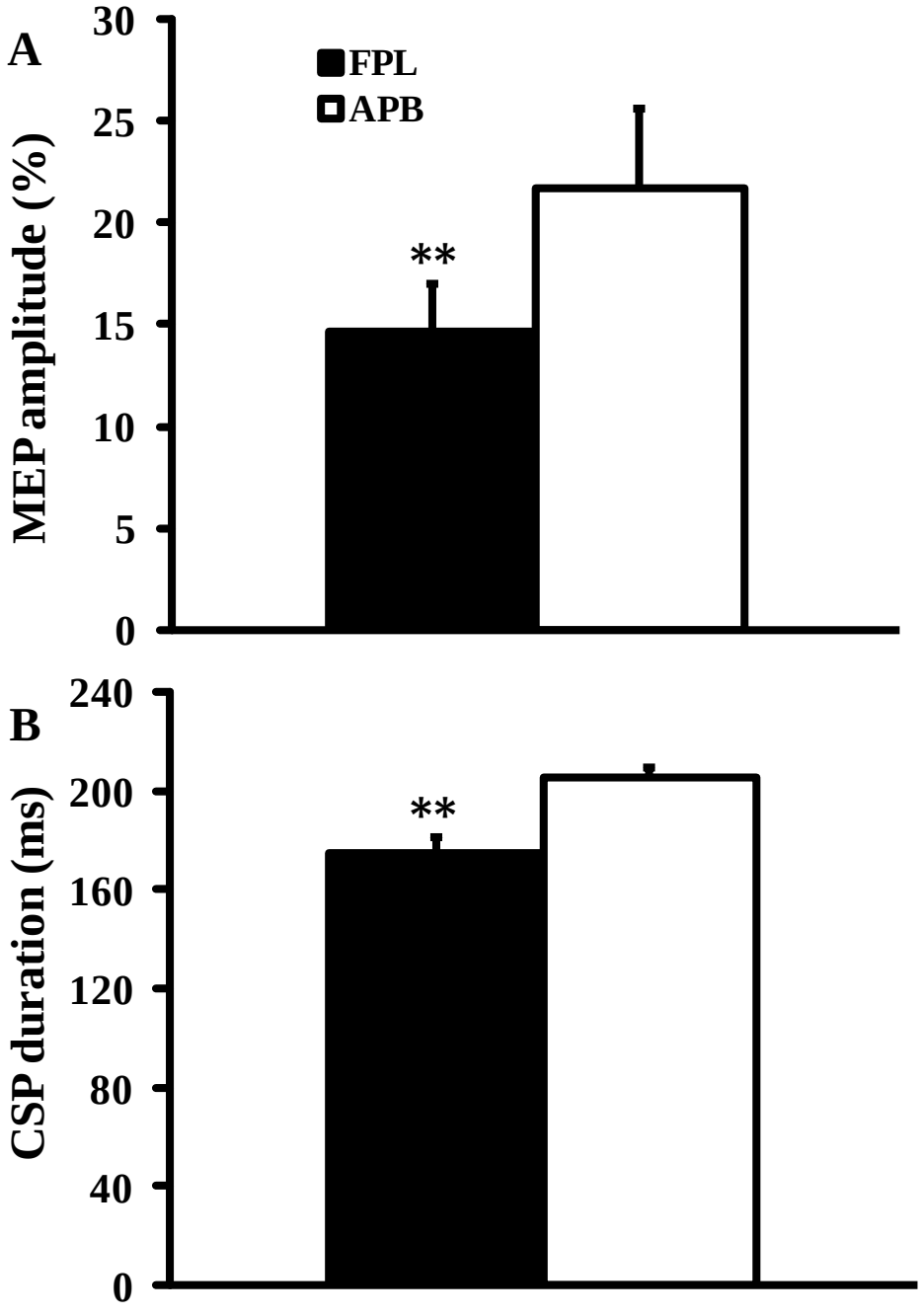

Figure 7.3: (A) The motor evoked potential amplitude (MEP), expressed as a percentage of the compound muscle action potential response, was significantly smaller when recording from the flexor pollicis longus (FPL) compared to abductor pollicis brevis. **(B)** The cortical silent period (CSP) duration was significantly shorter when recording from the FPL compared to APB.
**P < 0.01.

Discussion

Using threshold-tracking TMS experimental paradigms the present study has established significant differences in cortical excitability between the abductor pollicis brevis and flexor pollicis longus. Specifically, short interval intracortical inhibition was significantly reduced when recorded from the flexor pollicis longus muscles. Further, the time course of SICI was different, with two peaks evident from the APB and one peak when recording over the FPL. In addition, the motor evoked potential amplitude and cortical silent period duration were significantly reduced when recorded from the flexor pollicis longus. Taken together, these findings suggest differences in cortical excitability between the FPL and APB, with potentially less cortical output onto the spinal motor neurons innervating the FPL muscle.

Cortical processes appear to underlie differences in TMS parameters between APB and FPL

Short interval intracortical inhibition appears to be cortical in origin, mediated by GABAergic inhibitory interneurons acting via $GABA_A$ receptors (401, 441, 468, 544). Evidence supporting a cortical origin of SICI was provided by epidural recordings, in which the descending corticomotoneuronal volleys were inhibited during SICI (469, 470, 490, 542, 543). Further support for a cortical origin of SICI is provided by positron emission tomography (PET) studies revealing significant changes in cerebral blood flow in the motor cortex with paired-pulse TMS studies (588).

In the present study, there were significant differences in both the duration and degree of SICI when recording over the APB and FPL muscles, with SICI being significantly greater from the APB. Given that SICI is mediated by inhibitory interneuronal motor cortical networks (401,

441), the findings would seem to suggest that inhibitory circuits sub-serving the corticomotoneurons directed to the APB were of greater potency. Such findings would also be in keeping with previous TMS studies that demonstrated regional differences in cortical excitability, with cortical inhibition being greater in intrinsic hand muscles (420, 540).

Of further relevance, the two phases of SICI, at ISI 1- and 3 ms, appear to be mediated by distinct cortical synaptic circuits(589, 590). In the present study, the earlier phase of SICI, at ISI 1 ms, was not evident when recording over the FPL, while the second larger peak was significantly smaller when compared to recordings obtained from the APB. Such a finding would suggest that distinct cortical inhibitory circuits may underlie the generation of SICI in the two muscles, with the inhibitory effect being smaller when recorded from the FPL.

Providing further support for the notion that cortical output was less to the FPL, was the finding that the MEP amplitude, a measure of the density of corticomotoneuronal projections onto anterior horn cells (401), was significantly smaller when recorded from the FPL. Further, the CSP duration was also significantly shorter from FPL. Given that the CSP duration may be influenced by the density of corticomotoneuronal projections onto the anterior horn cells, with CSP duration being longest for intrinsic hand muscles (401), this finding further supports the suggestion that cortical output to the FPL was less when compared to APB.

It may also be suggested that the differences in the present TMS findings may be accounted for by use of a circular coil, which exerts effects over a wider cortical area, thereby resulting in non-specific activation of the motor cortex (591). This seems an unlikely explanation given that the

coil position was altered between each study such that an optimal MEP response was elicited prior to assessment of each muscle. Importantly, previous TMS studies failed to establish any qualitative differences in the pattern of inhibition when using either a circular or focal figure of eight coil (540).

It has also been suggested that differences in resting motor thresholds and MEP amplitude could in part explain the SICI findings (540). Specifically, higher subthreshold conditioning stimuli may result in activation of facilitatory circuits, thereby resulting in reduced SICI (590, 592). Given that motor thresholds were comparable between the two muscles and that sub-threshold conditioning stimuli were set to 70% of the RMT, a value at which SICI appears to be maximal (590), it seems unlikely that inadvertent activation of facilitatory circuits is a likely explanation for the observed findings. In addition, the absence of correlation between MEP amplitude and SICI would suggest that the differences in intracortical inhibition represent a true reduction in cortical inhibition onto anterior horn cells innervating the FPL muscle rather than MEP related effects.

The difference in cortical excitability between the APB and FPL muscles remains to be fully elucidated. Previously, differences in cortical excitability were established between the proximal upper limb muscles and APB. This finding was attributed to smaller corticomotoneuronal output onto the anterior horn cells innervating the proximal muscles (45, 593). By analogy, the differences in cortical excitability between the thenar muscles (APB) and FPL could also be accounted for by smaller corticomotoneuronal output onto the anterior horn cells innervating the FPL.

Clinical implications

The split-hand plus sign, whereby the function of FPL is relatively preserved compared to APB, was recently reported to be a specific feature of ALS, distinguishing ALS from mimic disorders (585). Given that FPL and APB are innervated by the same spinal segment (C8/T1) and nerve (median), cortical mechanisms may potentially underlie the development of the split hand plus sign in ALS. Of relevance, a cortical basis has been suggested as a possible mechanism for other forms of dissociated intrinsic hand muscle atrophy described in ALS, namely the split hand sign (54, 584), with that stronger corticomotoneuronal output mediating neurodegeneration via a transsynaptic anterograde excitotoxic process. The findings in the present study, revealing differences in cortical excitability between the APB and FPL, may lend further credence to the notion that cortical mechanism underlie the development of the split hand plus sign. If confirmed in ALS cohorts, this finding would have pathophysiological significance, in particular suggesting that ALS has a central basis.

Chapter 8

Cortical Hyperexcitability and the Split-Hand Plus Phenomenon: Pathophysiological insights in ALS

Summary

Differences in cortical excitability between the APB and FPL elicited in the previous experiment, suggested that cortical mechanisms may underlie the development of the split hand plus sign in ALS. In an attempt to understand the pathophysiological mechanisms underlying this clinical phenomenon, threshold tracking transcranial magnetic stimulation technique was utilized to assess whether cortical mechanisms may be a significant contributing influence. Cortical excitability studies were undertaken on 17 ALS patients, with motor evoked potentials (MEP) recorded from thenar muscles and FPL. Split-hand plus index (SHPI) was derived by dividing motor amplitudes recorded over APB with those recorded over FPL. The SHPI was significantly reduced in ALS ($SHPI_{ALS}$ 0.87±0.12; $SHPI_{CONTROLS}$ 1.7±0.2, $P<0.001$). Cortical studies disclosed significant increases in MEP amplitudes recorded over thenar muscles ($P<0.05$), but not FPL ($P=0.11$), and were significantly correlated with the SHPI ($R= -0.83$, $P<0.01$). The cortical silent period duration was reduced from thenar muscles ($P<0.01$). Although there was a ubiquitous reduction in short-interval intracortical inhibition (APB, $P<0.01$; FPL<0.05), this reduction was more prominent over the thenar muscles. Findings from the present study suggest that cortical dysfunction in the form of hyperexcitability contributes to the pathophysiological basis of the split-hand plus sign in ALS.

Introduction

The ***split-hand plus sign*** refers to preferential involvement of motor pathways that innervate thenar muscles, with apparent preservation of the flexor pollicis longus (FPL) (594). Recently, the split-hand plus sign was identified as a clinical feature of amyotrophic lateral sclerosis (ALS), distinguishing ALS from mimic disorder (594).

The pathophysiological mechanisms underlying the split-hand plus phenomenon remains to be elucidated, although a cortical basis has been proposed (571). While the thenar muscles and FPL are innervated by the same myotomes (C8,T1) and nerve (median), their function is different. Thenar muscles are critical for execution of fine fractionated finger movements (45), and may be expected to possess greater cortical representation and corticomotoneuronal input. Given that corticomotoneuronal hyperexcitability has been postulated to trigger anterior horn cell degeneration in ALS by means of an anterograde transsynaptic excitotoxic process (2, 25, 87), and also associated with development of the split-hand phenomenon (54), the development of the split-hand plus sign may potentially be explained by excessive glutamate excitotoxity.

Differences in cortical excitability have been previously established in healthy controls across a range of upper limb muscles (420, 540, 571, 595). Importantly, significant differences in cortical excitability were recently reported between thenar muscles and FPL (571). Specifically, short-interval intracortical inhibition, motor evoked potential amplitude and cortical silent period duration were significantly larger when recorded over the thenar muscles. This suggests a greater cortical representation/corticomotoneuronal input and simultaneously greater inhibition of the thenar muscles. Consequently, studies were undertaken with the aim of determining whether

differences in cortical excitability could form the pathophysiological basis for the split hand-plus phenomena in ALS.

Materials and Methods

Studies were undertaken on 17 patients with clinically probable or definite ALS (11 male, 6 female: mean age: 62 years, 40-83) as defined by the Awaji criteria (82). All patients provided written informed consent to the procedures which were approved by the South-Eastern Sydney and Illawarra Area Health Service Human Research Ethics Committee.

Phenotyping

ALS patients were clinically staged using the Amyotrophic Lateral Sclerosis Functional Rating Scale-Revised (ALSFRS-R)(511) and Medical Research Council (MRC) rating scale for strength (512). The total MRC sum score was derived by assessing the following muscle groups bilaterally: shoulder abduction, elbow flexion and extension, wrist dorsiflexion, finger extension, finger abduction, thumb abduction, distal thumb flexion, hip flexion, knee extension, and ankle dorsiflexion, yielding a maximal score of 120. Hand function was separately assessed using the Trigg's hand function score (434), while upper motor neuron (UMN) dysfunction was assessed by a specific UMN score (514). ALS patients were classified according to the site of disease onset as either limb or bulbar-onset.

Neurophysiological studies

Prior to undertaking cortical excitability studies, the degree of lower motor neuron dysfunction was determined by recording the compound muscle action potential (CMAP) responses from the APB and FPL muscles. The median nerves were stimulated at the wrist (APB) and elbow (FPL)

using 5 mm non-polarizable Ag-AgCl electrodes (3M Healthcare, MN, USA). Stimulation was computer controlled and converted to current using an isolated linear bipolar constant current simulator (DS5, Digitimer, Welwyn Garden City, UK). CMAP responses were recorded from the APB and FPL muscles with the active electrode positioned over the motor point and reference electrode placed over the proximal thumb (APB) and radial styloid (FPL) according to previously reported techniques (571, 596). A novel split-hand plus index was derived according to the following formula:

$$\textbf{Split-hand plus index} = \textbf{APB}_{\textbf{CMAP amplitude}}/\textbf{FPL}_{\textbf{CMAP amplitude}}$$

Cortical Excitability

Cortical excitability was undertaken by applying TMS to the motor cortex by means of a 90 mm circular coil oriented to induce current flow in a posterior-anterior direction. The coil was adjusted until the optimal position for the motor evoked potential (MEP) was obtained from the APB and FPL muscles as described previously (587, 596). Currents were generated by 2 high-power magnetic stimulators that were connected via a BiStim module (Magstim Co.), such that conditioning and test stimuli could be independently set and delivered through one coil.

Paired-pulse threshold tracking TMS was undertaken according to previously reported technique (416, 596). Specifically, the MEP amplitude was fixed and changes in the test stimulus intensity required to generate a target response of 0.2 mV (±20%), when preceded by sub-threshold conditioning stimuli, were measured. Resting motor threshold (RMT) was defined as the stimulus intensity required to maintain the target MEP response of 0.2 mV (±20%) (416, 596).

Short-interval intracortical inhibition (SICI) was determined by using subthreshold conditioning stimuli (70% RMT) at increasing interstimulus intervals (ISIs) as follows: 1, 1.5, 2, 2.5, 3, 3.5, 4, 5, and 7 ms. Subsequently, intracortical facilitation (ICF) was measured at ISIs of 10, 15, 20, 25 and 30 ms. Stimuli were delivered sequentially as a series of three channels according to a previously reported (596). SICI was measured as the increase in the test stimulus intensity required to evoke the target MEP. Inhibition was calculated off-line as follows (596).

Inhibition = (Conditioned test stimulus intensity–RMT)/RMT*100

Facilitation was measured as the decrease in the conditioned stimulus intensity required to evoke a target MEP. The SICI recorded from each muscle group was normalized so as to assess the degree of SICI reduction between the muscles.

Single pulse TMS technique determined the MEP amplitude (mV), MEP onset latency (ms) and cortical silent period duration (ms). The MEP amplitude was recorded with magnetic stimulus intensity set to 150% RMT and was expressed as a percentage of the CMAP response. Cortical silent period (CSP) duration was assessed by instructing the subject to contract the target muscle at ~30% of maximal voluntary contraction with TMS intensity set to 150% RMT. The CSP duration was measured from onset of MEP to return of EMG activity (455).

Recordings of CMAP and MEP responses were amplified and filtered (3 Hz-3 kHz) using a GRASS ICP511 AC amplifier (Grass-Telefactor, Astro-Med Inc., USA) and sampled at 10 kHz using a 16-bit data acquisition card (National Instruments PCI-MIO-16E-4). Data acquisition and stimulation delivery were controlled by QTRACS software (TROND-F, version

16/02/2009). Temperature was monitored with a purpose built thermometer at the stimulation site.

Statistical Analysis

Cortical excitability in ALS patients was compared to previously reported healthy controls (10 men and 5 women, mean age 34 years) (571). Unpaired sample t-test was used for assessing differences between two groups. All data was normally distributed as assessed using the Shapiro-Wilk test. Correlation between neurophysiological and clinical parameters was analyzed by either a Pearson's or Spearman's rank test. All results are expressed as mean ± standard error of the mean or median (interquartile range).

Results

Clinical features: From the clinical cohort of 17 ALS patients, limb-onset disease accounted for 65% of patients, while bulbar-onset disease was present in 35% (Table 1). At the time of assessment, the mean disease duration from symptom onset was 22.7±3.7 months. In addition, the median ALSFRS-R score was 42 (39-45) while the median Trigg's hand functions core 1 (0-1), and the total MRC score was 96 (84-97), suggesting a mild-moderate degree of disability. Of relevance, the UMN score was 12 (6-14), indicating a significant degree of UMN dysfunction. The split-hand plus sign, whereby preferential weakness of the thenar muscles was evident compared to the FPL (594), was evident in 62% of patients, while the split-hand sign, which refers to preferential dysfunction of the thenar muscles and first dorsal interosseous (20, 21, 558), was evident in 50% of patients.

Neurophysiological studies: Prior to undertaking cortical studies, the degree of the lower motor neuron dysfunction was determined for each muscle. The CMAP amplitude was reduced when recorded over the APB (ALS 8.1±1.2 mV, controls 18.1±1.5mV, P<0.0001) and FPL (ALS 9.1±1.8 mV, controls 11.6±1.2 mV, P=0.08). The split-hand plus index was significantly reduced in ALS patients ($SHPI_{ALS}$ 0.87±0.12; $SHPI_{CONTROLS}$ 1.7±0.2, P<0.001), suggesting preferential dysfunction of the motor neurons innervating the APB muscles. The reduction in split-hand plus index was a ubiquitous finding, evident in both limb and bulbar-onset patients ($SHPI_{LIMB\text{-}ONSET}$ 0.95±0.2; $SHPI_{BULBAR\text{-}ONSET}$ 0.88±0.17).

Cortical function: Transcranial magnetic stimulation studies identified an inexcitable motor cortex in three ALS patients. As such, cortical excitability was undertaken on 14 ALS patients.

Patients	Age (years) /sex	Disease onset	Disease duration (months)	MRC Sum score	Triggs hand score	UMN score	ALSFRS-R
1	79/M	LIMB	51	84	1	12	39
2	83/F	LIMB	8	80	1	8	38
3	71/F	LIMB	24	75	3	14	32
4	54/M	LIMB	16	85	0	14	41
5	67/M	LIMB	9	96	1	2	30
6	71/M	LIMB	19	85	1	8	42
7	40/M	LIMB	15	98	0	14	40
8	65/M	LIMB	49	72	3	14	36
9	69/M	LIMB	28	74	1	14	46
10	58/F	LIMB	10	86	1	5	45
11	62/M	LIMB	22	97	0	2	45
12	57/M	LIMB	18	97	0	14	44
13	49/F	BULBAR	37	96	0	12	42
14	62/F	BULBAR	45	96	0	15	40
15	50/M	BULBAR	7	100	0	6	46
16	47/M	BULBAR	8	100	0	1	46
17	62/F	BULBAR	35	96	1	10	42
Mean (SD)	**61.5 (11.5)**		**23.5 (14.8)**				
Median (IQR)				**96 (84-97)**	**1 (0-1)**	**12 (6-14)**	**42 (39-45)**

Table 8.1: Clinical details for 17 amyotrophic lateral sclerosis (ALS) patients. Muscle strength was clinically assessed using the Medical Research Council (MRC) yielding a maximal MRC score of 120 (see Methods). In addition, hand function was assessed by using the Trigg's hand score (*see* Methods). Upper motor neuron (UMN) score was used to assess the degree of UMN dysfunction ranging from 0= no UMN dysfunction to 16 maximal dysfunction. The amyotrophic lateral sclerosis functional rating scale- revised (ALSFRS-R) was used to assess for the degree of functional impairment. All data are expressed as mean (standard deviation, SD) or median (interquartile range, IQR)

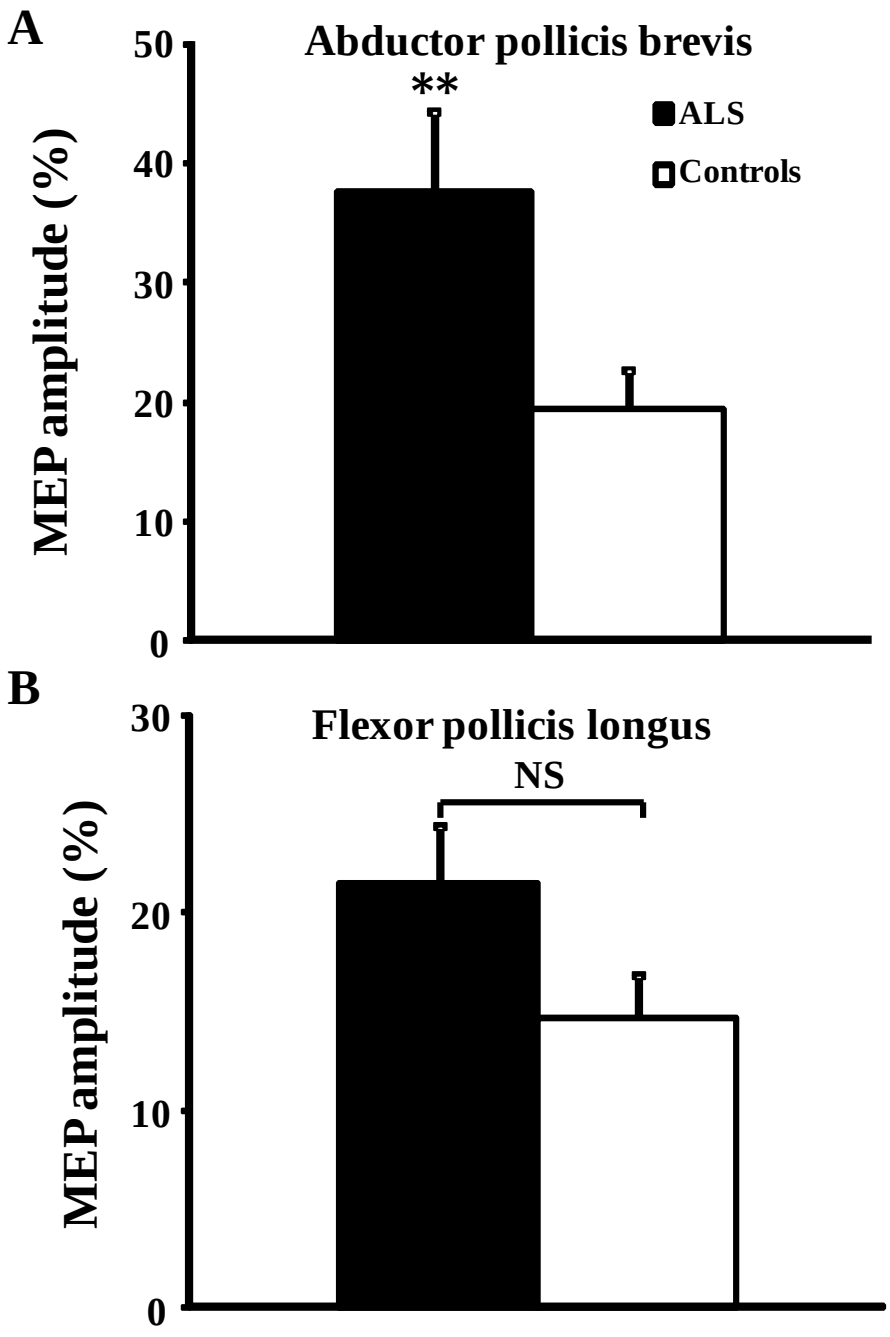

Figure 8.1: The motor evoked potential (MEP) amplitude, expressed as a percentage of the compound muscle action potential response, was significantly increased when recording from the **(A)** abductor pollicis brevis, but not the **(B)** flexor pollicis longus muscles in amyotrophic lateral sclerosis (ALS) patients compared to controls. *P < 0.05

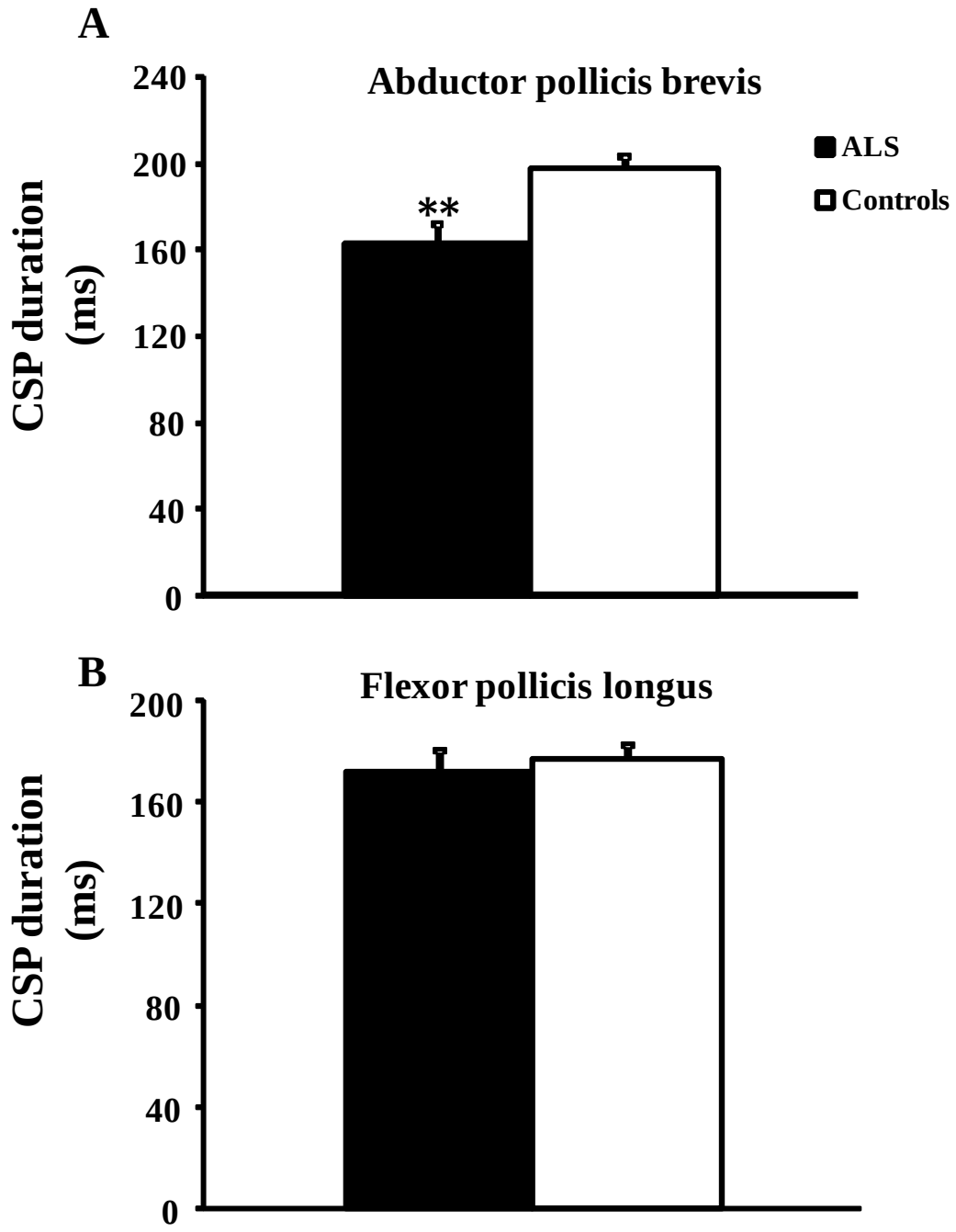

Figure 8.2: The cortical silent period duration was significantly reduced when recording from the **(A)** abductor pollicis brevis, but not the **(B)** flexor pollicis longus muscles in amyotrophic lateral sclerosis (ALS) patients compared to controls. **P < 0.01

Single pulse TMS technique determined that the MEP amplitude, expressed as a percentage of the CMAP response, was increased in ALS when recorded from the APB (ALS 37.6±6.8%; controls 19.3±3.3%, P<0.05, Fig.8.1A). The MEP amplitude was not significantly increased when recording from the FPL (ALS 21.4±3.0%; controls 14.7±2.2%, P=0.11, Fig. 8.1B). In addition, the CSP duration was significantly reduced when recorded over the APB (ALS 163.5±8.8 ms; controls 198.0±5.2 ms, P<0.01, Fig.8.2A), but not FPL (ALS 171.6±8.4ms; controls 176.3±6.3 ms, P=0.45, Fig.8.2B). There were no significant differences in the RMT between groups when recorded over APB (P=0.33) and FPL (P=0.37) muscles.

Paired-pulse TMS studies disclosed that SICI was significantly reduced in ALS (Fig. 8.3). Specifically, averaged SICI over ISIs 1-7 ms was significantly reduced when recording over APB (mean $SICI_{APB}$ 4.3±2.2%; controls 11.6±1.3%, P<0.01, Fig 8.3A, 8.4A). In addition, peak SICI at ISI 1 ms (ALS 0.9±1.0%; controls 10.8±1.8%; P<0.001, Fig. 8.3A) and 3 ms (ALS 8.0±3.6%; controls 16.5±1.2%; P<0.05, Fig.8.3A) was also significantly reduced when recorded over the APB. Averaged SICI (ALS 2.2±1.8%; controls 6.5±1.7%, P<0.05, Fig 8.3B, Fig.8.4B), peak SICI 1 ms (ALS 4.1±2.4%; controls 11.3±2.2%, P<0.05, Fig.8.3B) and ISI 3 ms (ALS 0.68±1.1%; controls 6.3±1.9%, P<0.05, Fig. 8.3B) were also reduced in ALS when recorded over FPL. The extent of SICI reduction was greater when recorded over thenar muscles ($SICI_{APB\ REDUCTION}$ 0.62; $SICI_{FPL\ REDUCTION}$ 0.70, P< 0.01, Fig. 8.4C).

Following SICI, a period of ICF develops (596). There were no significant differences in ICF between groups when recording over APB (P=0.18, Fig. 8.3A) and FPL (P=0.42, Fig. 8.3B),

although these findings should be interpreted cautiously as the study could have been potentially underpowered to detect differences in ICF.

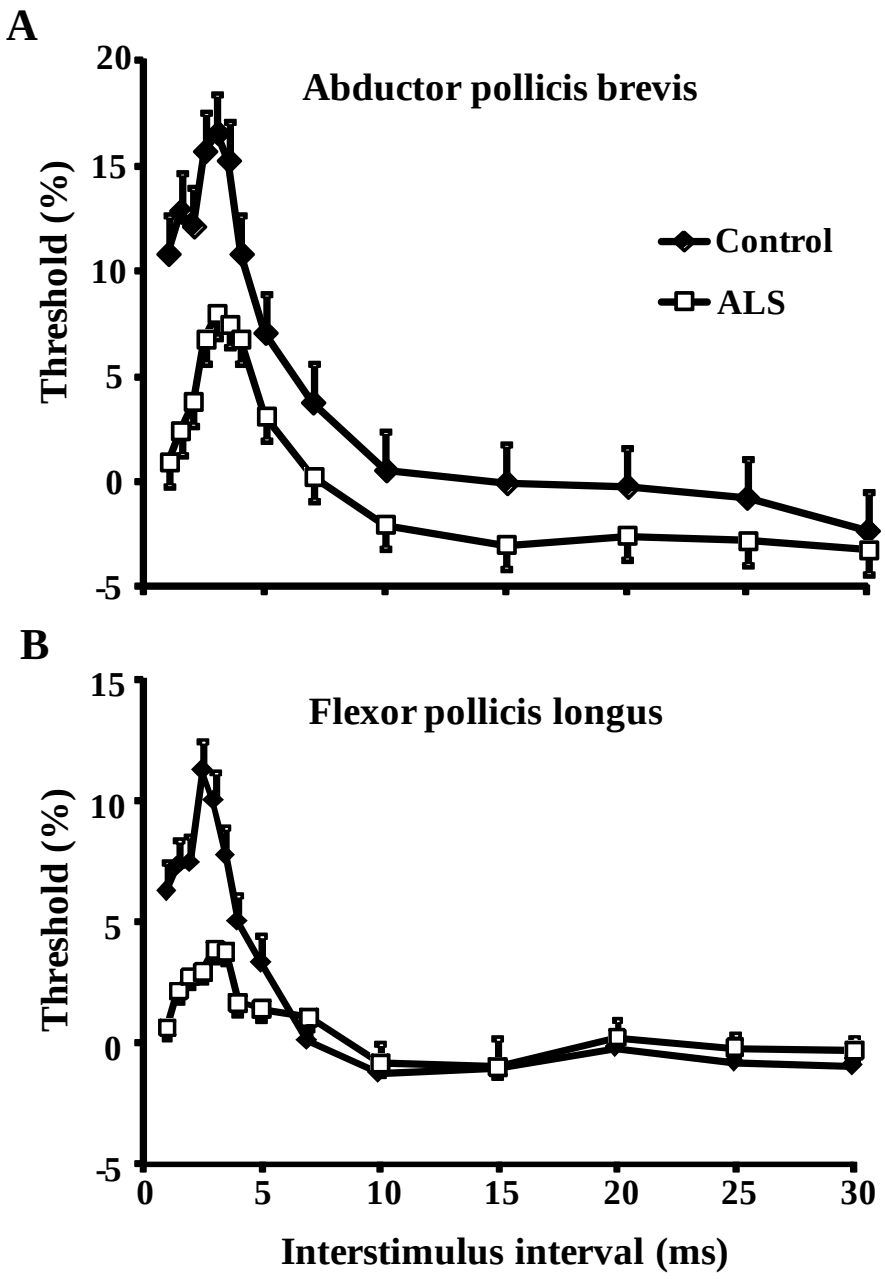

Figure 8.3: Short -interval intracortical inhibition (SICI), defined as the stimulus intensity required to maintain a target output of 0.2 mV (*see* methods) was significantly reduced in amyotrophic lateral sclerosis (ALS) patients compared to controls when recording from both the (**A)** abductor pollicis brevis, but not the **(B)** flexor pollicis longus muscles.

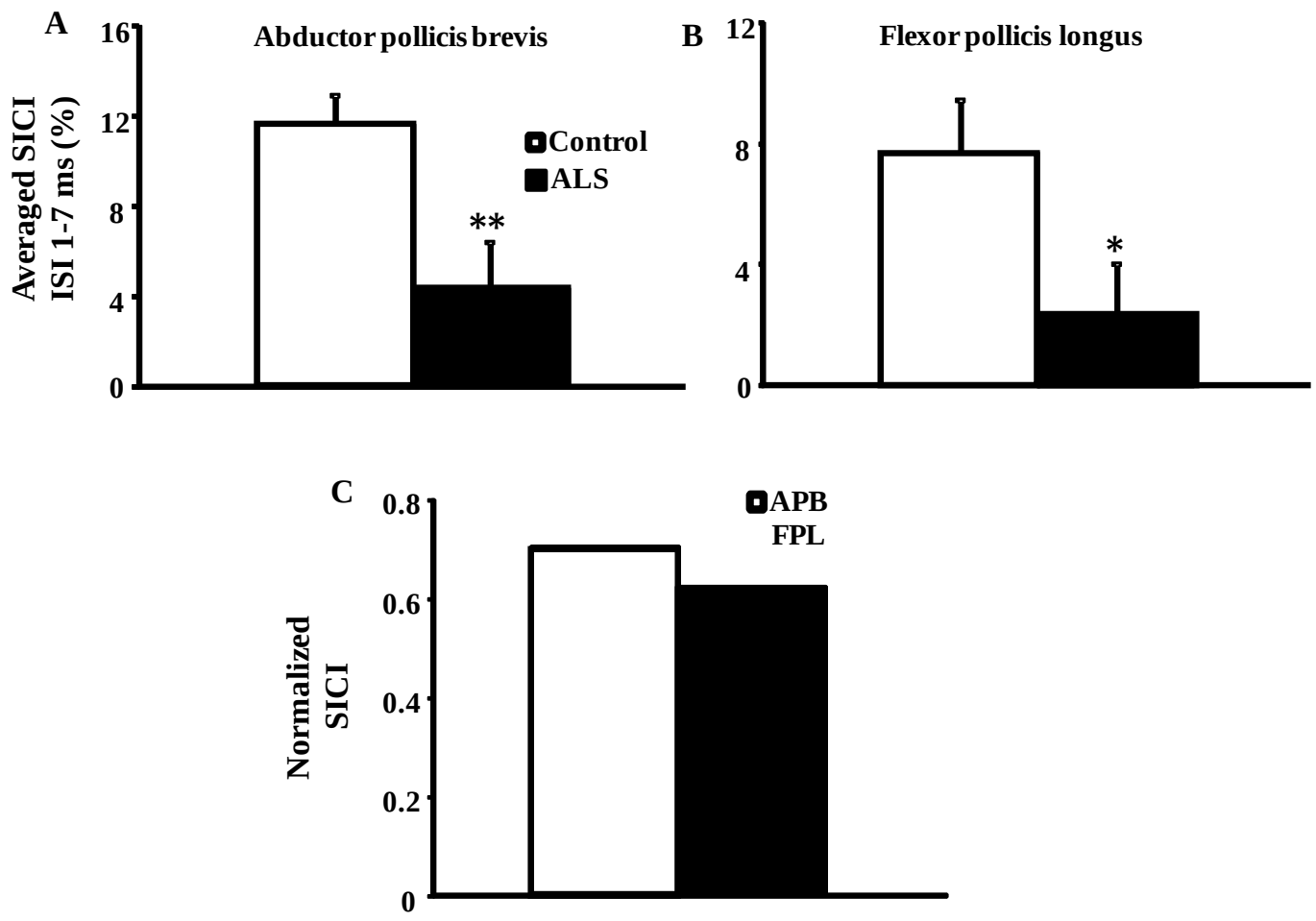

Figure 8.4: Average short -interval intracortical inhibition (SICI), between interstimulus intervals (ISI) of 1-7 ms, was significantly reduced in amyotrophic lateral sclerosis (ALS) patients compared to controls when recording from both the (**A)** abductor pollicis brevis (APB) and **(B)** flexor pollicis longus (FPL) muscles. **(C)** The degree of SICI reduction was greater when recording over the APB. *P< 0.05; **P< 0.01.

Combination of clinical and neurophysiological parameters determined that the MEP amplitude recorded over the APB were inversely correlated with the CMAP amplitude ($R = -0.82$, $P<0.01$) and split-hand plus index ($R = -0.83$, $P<0.01$). In addition, the CSP duration, recorded from the APB was significantly correlated with the ALSFRS-R ($R = -0.53$, $P<0.05$).

Discussion

In the present study, threshold tracking TMS techniques were utilized to investigate the pathophysiological processes that may contribute to development of the split-hand plus phenomenon in ALS (594). Cortical dysfunction was evident when recording over both the APB and FPL, although the apparent degree of excitatory/inhibitory imbalance was more prominent to the thenar eminence. Specifically, the MEP amplitude was significantly increased while the CSP duration reduced when recorded from thenar muscles. In addition, SICI was more prominently reduced when recorded over the APB. There was a significant correlation between cortical hyperexcitability and the split-hand plus index, a biomarker of the split-hand plus sign. These findings suggest that cortical mechanisms may in-part contribute to the development of the split-hand plus sign in ALS.

Prior to undertaking a discussion on the pathophysiological mechanisms underlying the split-hand plus sign, the diagnostic utility of this novel sign was reassessed. A previous study established the diagnostic utility of the split-hand plus sign, which reliably distinguished ALS from mimic disorders (594). Importantly, the sensitivity and specificity appeared comparable to the more conventional split hand sign (20, 21, 529, 558). The present study established a comparable sensitivity of the split-hand plus and split-hand sign in ALS patients. Of further relevance, the significant correlation between the MEP amplitude and split-hand plus index suggests that cortical hyperexcitability may contribute to development of the split-hand plus phenomenon.

Origin of the split-hand plus sign

The MEP amplitude is a biomarker of the density of corticomotoneuronal projections onto anterior horn cells (87, 441) and may be enhanced by glutamate excitotoxity (444). Increases in MEP amplitude have been extensively documented in ALS (31, 49, 50) and linked to motor neuron degeneration (49, 126), a finding re-affirmed in the present study. The MEP amplitude, expressed as a percentage of CMAP response, was significantly increased when recorded over the thenar muscles, a finding that could be explained by a combination of thenar muscle wasting and cortical hyperexcitability.

Of further relevance, a significant reduction in CSP duration was evident when recording from thenar muscles but not FPL. Given that CSP duration is mediated by cortical inhibitory processes acting via $GABA_B$ receptors (87, 453, 455, 457, 458, 548), the present findings would seem to suggest more prominent cortical disinhibition, and thereby excitatory/inhibitory imbalance, of the thenar muscles, thereby underscoring the notion of a cortical basis for the split-hand plus phenomenon. In addition, abnormalities of SICI were also evident in the present ALS cohort and appeared to be more prominent when recorded from thenar muscles. Importantly, SICI appears to be a biomarker of cortical inhibitory interneuronal function acting through $GABA_A$ receptors(401, 441, 468, 544), as well as glutamate-mediated cortical excitability (478, 597). Given that there was a more prominent reduction of SICI when recorded over the thenar muscle, these findings may suggest a more prominent imbalance of cortical excitatory-inhibitory tone, with GABA receptors leading to glutamate-mediated excitotoxicity and loss of inhibition, thereby implying a cortical basis for the split-hand plus phenomenon in ALS.

A potential explanation for the vulnerability of thenar motor neurons to glutamate-mediated excitotoxicity may relate to greater cortical representation and more prominent corticomotoneuronal input to thenar muscles. Differences in cortical representation were postulated to reflect varied functions of the muscles in execution of complex hand tasks (45). Specifically, the FPL appears to have evolved a well developed sensory function in human dexterity, with a high capacity in sensing thumb forces during voluntary movement as well as exhibiting a greater role in proprioceptive acuity of the thumb (598, 599). Recent TMS studies have established more prominent corticomotoneuronal projections to thenar motor neurons when compared to the FPL motor neurons (571). Consequently, thenar motor neurons could be more prone to glutamate-mediated excitotoxic degeneration in ALS by virtue of a more prominent corticomotoneuronal supply.

A potential limitation of the present study relates to the possibility that recordings over the FPL muscle were confounded by volume conduction. While such a possibility could not be discounted, it seems an unlikely explanation for cortical excitability differences given that responses recorded over the thenar muscles could also be confounded by volume conduction. In addition, given that the control population was significantly younger than the ALS cohort, the possibility of the aging process confounding the results could not be discounted.

Alternatively, it could be argued that peripheral mechanisms contributed to development of the split-hand plus phenomenon in ALS. Hyperexcitability of axons innervating the thenar muscles was postulated to contribute to development of dissociated muscle atrophy in ALS (563). Recent studies have failed to establish that abnormalities of axonal excitability followed a split-hand

pattern distribution (600), but rather argued that these changes in axonal excitability reflected downstream effects of primary pathophysiological processes. While a peripheral contribution to the split-hand plus phenomenon could not be absolutely discounted, the findings of more prominent cortical hyperexcitability, when recording over the thenar muscles, suggests a predominance of cortical processes in development of the split-hand plus phenomenon in ALS.

SUMMARY AND CONCLUSIONS

The studies comprising this thesis were undertaken in order to gain further insights into the pathophysiological mechanism underlying the development of ALS, particularly the role of corticomotoneurons. In ***chapter 1***, the specificity of the ***split-hand sign***, which refers to preferential dysfunction of the thenar complex group of muscles (APB and FDI) compared to the hypothenar group, was established in ALS by developing a novel split-hand index. The split-hand index was determined to be a robust diagnostic marker of ALS, reliably differentiating ALS from neuromuscular mimic disorders with a diagnostic cut off value of 5.2. Given that the thenar and hypothenar muscles are innervated by the C8/T1 myotomes, it was inferred that cortical mechanisms form the basis of the split-hand sign in ALS.

Consequently, in ***chapter 2***, threshold tracking transcranial magnetic stimulation and axonal excitability techniques were utilised to dissect out differences in corticomotoneuronal input and biophysical properties of the motor axons innervating the thenar and hypothenar muscle groups in healthy controls. Importantly, this series of studies established a greater corticomotoneuronal input and greater cortical representation of the thenar group of muscles. In contrast, the peripheral axonal properties of the motor axons innervating the thenar and hypothenar muscles did not follow a split-hand pattern. As such, the findings in the present study confirmed, for the first time, the existence of differences primarily in corticomotoneuronal input between the thenar and hypothenar muscles underlying the preferential thenar intrinsic hand muscle (split-hand) wasting noted in ALS thereby suggesting a cortical basis for selective muscle vulnerability in ALS.

Recent studies in ALS patients, however, suggested that peripheral processes, namely differences in motor axonal excitability, formed the basis of the split-hand in ALS. This notion was investigated in ***chapter 3***, whereby axonal excitability studies were undertaken on motor axons innervating the thenar (APB and FDI) and hypothenar muscles. The studies in chapter 3 confirmed that changes in axonal excitability did not follow a split-hand pattern, thereby arguing against a significant contribution of peripheral processes to the development of the split-hand phenomenon in ALS.

In ***chapter 4***, simultaneous cortical and axonal excitability studies were undertaken on ALS patients in order to assess whether corticomotoneuronal hyperexcitability formed the basis of the split-hand sign and thereby the pathophysiological basis in ALS. While cortical hyperexcitability was established as a global phenomenon in ALS irrespective of the recording muscle, the degree of cortical hyperexcitability was greater over the thenar group of muscle (APB and FDI). Corresponding changes in axonal excitability did not follow a split-hand pattern. Taken together, these findings imply a cortical basis for the split-hand sign and re-enforced the importance of cortical hyperexcitability in ALS pathogenesis.

Complementing the results of chapters 1-4, the findings in ***chapter 5*** provided additional support for a cortical basis of ALS pathophysiology. Utilising a combination of threshold tracking TMS, axonal excitability and needle electromyography techniques, the findings in chapter 5 established the development of corticomotoneuronal hyperexcitability prior to onset of lower motor neuron dysfunction in ALS. Importantly, all ALS patients progressed to develop LMN dysfunction in

the target APB muscle during follow-up. As such, the findings in chapter 5 provided strong support for an important role of the corticomotoneuronal system in ALS pathogenesis.

The theme of selective motor neuronal degeneration was further examined in ***chapter 6***. Specifically, a novel ***split hand plus sign*** was described to be a specific feature of ALS, and refers to preferential dysfunction of APB muscle with relative preservation of the flexor pollicis longus (FPL) muscle, despite a common myotomal innervation (C8/T1). These findings reinforced the phenomenon of selective vulnerability of motor neurons in ALS, with implications for a cortical basis of ALS pathogenesis.

In order to explore the possibility of a cortical basis of the split hand plus sign, threshold tracking TMS studies were undertaken in healthy controls, with responses recorded over the APB and FPL muscles. In concordance with studies in chapter 2, the findings in ***chapter 7*** established greater corticomotoneuronal input and cortical representation of the APB muscle. The differences in critical excitability between the APB and FPL muscles was attributed to functional differences, but more importantly suggested that cortical processes could mediate the development of the split hand plus sign in ALS.

In an attempt to further explore this possibility, threshold tracking TMS studies were undertaken in a cohort of ALS patients with responses recorded over the APB and FPL muscles. The study detailed in ***Chapter 8***, significantly confirms a greater degree of cortical hyperexcitability over the APB, implying the importance of cortical processes in development of the split-hand plus phenomenon, and thereby inferring a cortical basis for ALS pathogenesis.

In summary, the findings of the present thesis suggest that corticomotoneuronal dysfunction, namely hyperexcitability, forms the basis of ALS pathogenesis, resulting in development of specific clinical features and progressive neurodegeneration. This finding is supported by previous studies on the occurrence of cortical hyperexcitability preceding the onset of clinical disease in genetic mutation carriers in ALS and by the association of frontotemporal lobe dementia (FTLD), a pure cortical dysfunction, as a disease spectrum of ALS. Future therapeutic strategies aimed at modulating cortical hyperexcitability, either via pharmacological or cell based approaches, may prove therapeutically useful.

Future Directions

Cortical hyperexcitability appears to precede the development of LMN dysfunction in ALS when assessing one body region (the upper limb). Future studies will utilise threshold tracking TMS techniques in order to explore whether the development of cortical hyperexcitability occurs prior to onset of disease in other body regions, such as cranial and lumbosacral. These studies will assist in establishing the pattern of disease spread, namely whether the corticomotoneurons are a conduit for ALS progression in a non-contiguous manner. In addition, longitudinal studies will be undertaken on the recently described c9orf72 hexanucleotide expansion carriers combining threshold tracking TMS techniques with measures of peripheral disease burden including motor unit number estimation (using Bayesian statistical method), conventional nerve conduction studies and needle electromyography techniques. Longitudinal studies in this cohort will help confirm the finding reported in SOD-1 mutation carriers that cortical hyperexcitability is an acquired phenomenon even in genetic ALS and appears to precede the onset of clinical disease.

Of further relevance, the role of corticomotoneurons in ALS pathogenesis will be further investigated by combing threshold tracking TMS techniques with sophisticated neuroimaging. Specifically, cross-sectional and longitudinal studies will be undertaken on apparently "sporadic" ALS patients and c9orf72 mutation carriers. The corticomotoneuronal function will be assessed by utilising cortical thickness analysis, resting state networks and sodium coil imaging in concert with TMS studies, in order to establish the timing and site of disease onset, along with patterns of disease spread. Ultimately, such an approach will shed further light on ALS pathogenesis, with the hope of uncovering novel therapeutic targets.

Separately, prognostic biomarkers for ALS will be developed focussing on the split-hand index. Although cross-sectional study suggested a prognostic utility of the split-hand index in ALS, longitudinal studies, over 24 months, will be undertaken to assess and compare the prognostic utility of the split-hand index with established prognostic biomarkers in ALS, including the ASLFRS-R, CMAP amplitude, neurophysiological index, motor unit number estimation (using Bayesian statistical method), dynamometry and electrode impedance myography. If established to be of prognostic utility, the split hand index, will provide a simple neurophysiological prognostic biomarker in future therapeutic trials.

GLOSSARY OF ABBREVIATIONS

ADM	abductor digiti minimi
AHC	anterior horn cell
ALS	amyotrophic lateral sclerosis
ALSFRS-R	amyotrophic lateral sclerosis functional rating scale-revised
AMPA	α amino 3 hydroxy 5 methyl 4 isoxazole proprionic acid
ANOVA	analysis of variance
APB	abductor pollicis brevis
AR	androgen receptor
ATP	adenosine tri phosphate
CMAP	compound muscle action potential
CMCT	central motor conduction time
CSP	cortical silent period
DAP	depolarizing after depolarization
DNA	deoxyribonucleic acid
EMG	electromyography
FDI	first dorsal interosseous
FPL	flexor pollicis longus
FTD	frontotemporal dementia
FUS	fused in sarcoma
GABA	gamma amino butyric acid
ICF	intracortical facilitation
ITPR	inositol 1,4,5-triphosphate receptor

I/V	current threshold relationship
KD	Kennedy's Disease
LA	latent addition
LICI	long interval intracortical inhibition
LMN	lower motor neuron
MEP	motor evoked potential
MMNCB	multifocal motor neuropathy with conduction block
MND	motor neuron disease
MRC	Medical Research Council
MT	motor threshold
MUNE	motor unit number estimation
MUP	motor unit potential
NCS	nerve conduction study
NI	neurophysiological index
NMDA	N-methyl, D-aspartate receptor
PBP	progressive bulbar palsy
PLS	primary lateral sclerosis
PMA	progressive muscular atrophy
PSW	positive sharp waves
PTN	pyramidal tract neuron
RMT	resting motor threshold
RNA	ribonucleic acid
ROC	receiver operating characteristic

RRP	relative refractory period
SBMA	spinobulbar muscular atrophy
SDTC	strength duration time constant
SI	split-hand index
SICI	short-interval intracortical inhibition
SMA	spinal muscular atrophy
SOD	superoxide dismutase
SR	stimulus response curve
STARD	standards for reporting of diagnostic accuracy
TARDBP	transactive region deoxyribonucleic acid binding protein
TEd	threshold electrotonus depolarising
TEh	threshold electrotonus hyperpolarising
TMS	transcranial magnetic stimulation
UMN	upper motor neuron

References

1. Charcot J, Joffroy A. Deux cas d'atrophie musculaire progressive avec lesion de la substance grise et des faisceaux antero-lateraux de la moelle epiniere. Arch Physiol Neurol Pathol. 1869;2:744-54.
2. Kiernan MC, Vucic S, Cheah BC, Turner MR, Eisen A, Hardiman O, et al. Amyotrophic lateral sclerosis. Lancet. 2011;377(9769):942-55.
3. Renton AE, Majounie E, Waite A, Simón-Sánchez J, Rollinson S, Gibbs JR, et al. A Hexanucleotide Repeat Expansion in< i> C9ORF72</i> Is the Cause of Chromosome 9p21-Linked ALS-FTD. Neuron. 2011;72(2):257-68.
4. DeJesus-Hernandez M, Mackenzie IR, Boeve BF, Boxer AL, Baker M, Rutherford NJ, et al. Expanded GGGGCC Hexanucleotide Repeat in Noncoding Region of< i> C9ORF72</i> Causes Chromosome 9p-Linked FTD and ALS. Neuron. 2011;72(2):245-56.
5. Lomen-Hoerth C, Anderson T, Miller B. The overlap of amyotrophic lateral sclerosis and frontotemporal dementia. Neurology. 2002;59(7):1077-9.
6. Hardiman O, van den Berg LH, Kiernan MC. Clinical diagnosis and management of amyotrophic lateral sclerosis. Nat Rev Neurol. 2011;7(11):639-49.
7. Ferraiuolo L, Kirby J, Grierson AJ, Sendtner M, Shaw PJ. Molecular pathways of motor neuron injury in amyotrophic lateral sclerosis. Nat Rev Neurol. 2011;7(11):616-30.
8. Lomen-Hoerth C, Anderson T, Miller B. The overlap of amyotrophic lateral sclerosis and frontotemporal dementia. Neurology. 2002;59(7):1077-9. Epub 2002/10/09.
9. Ripps ME, Huntley GW, Hof PR, Morrison JH, Gordon JW. Transgenic mice expressing an altered murine superoxide dismutase gene provide an animal model of amyotrophic lateral sclerosis. Proc Natl Acad Sci USA. 1995;92(3):689-93.
10. Arai T, Hasegawa M, Akiyama H, Ikeda K, Nonaka T, Mori H, et al. TDP-43 is a component of ubiquitin-positive tau-negative inclusions in frontotemporal lobar degeneration and amyotrophic lateral sclerosis. Biochem Biophys Res Commun. 2006;351:602 - 11.
11. Hudson AJ, Kiernan JN. PRESERVATION OF CERTAIN VOLUNTARY MUSCLES IN MOTONEURONE DISEASE. The Lancet. 1988;331(8586):652-3.
12. Turner MR, Hardiman O, Benatar M, Brooks BR, Chio A, de Carvalho M, et al. Controversies and priorities in amyotrophic lateral sclerosis. The Lancet Neurology. 2013;12(3):310-22.
13. Brooks BR. El Escorial World Federation of Neurology criteria for the diagnosis of amyotrophic lateral sclerosis. Subcommittee on Motor Neuron Diseases/Amyotrophic Lateral Sclerosis of the World Federation of Neurology Research Group on Neuromuscular Diseases and the El Escorial "Clinical limits of amyotrophic lateral sclerosis" workshop contributors. J Neurol Sci. 1994;124 Suppl:96-107.
14. Brooks BR, Miller RG, Swash M, Munsat TL. El Escorial revisited: revised criteria for the diagnosis of amyotrophic lateral sclerosis. Amyotroph Lateral Scler. 2000;1:293-9.
15. Talbot K. Motor neurone disease. Postgrad Med J. 2002;78(923):513-9.
16. Logroscino G, Traynor BJ, Hardiman O, ChiÃ² A, Mitchell D, Swingler RJ, et al. Incidence of amyotrophic lateral sclerosis in Europe. J Neurol, Neurosurg, Psychiatry. 2010;81(4):385-90.
17. Traynor BJ, Codd MB, Corr B, Forde C, Frost E, Hardiman OM. Clinical features of amyotrophic lateral sclerosis according to the El Escorial and Airlie House diagnostic criteria: A population-based study. Arch Neurol. 2000;57(8):1171-6.

18. Ravits J, Paul P, Jorg C. Focality of upper and lower motor neuron degeneration at the clinical onset of ALS. Neurology. 2007;68(19):1571-5.
19. Ravits JM, La Spada AR. ALS motor phenotype heterogeneity, focality, and spread Deconstructing motor neuron degeneration. Neurology. 2009;73(10):805-11.
20. Kuwabara S, Sonoo M, Komori T, Shimizu T, Hirashima F, Inaba A, et al. Dissociated small hand muscle atrophy in amyotrophic lateral sclerosis: frequency, extent, and specificity. Muscle Nerve. 2008;37(4):426-30. Epub 2008/02/01.
21. Wilbourn AJ. The "split hand syndrome". Muscle Nerve. 2000;23(1):138.
22. Gubbay SS, Kahana E, Zilber N, Cooper G, Pintov S, Leibowitz Y. Amyotrophic lateral sclerosis. A study of its presentation and prognosis. J Neurol. 1985;232(5):295-300.
23. Li TM, Alberman E, Swash M. Clinical features and associations of 560 cases of motor neuron disease. J Neurol Neurosurg Psychiatry. 1990;53(12):1043-5.
24. de Carvalho M, Swash M. Cramps, muscle pain, and fasciculations: not always benign? Neurology. 2004;63(4):721-3.
25. Eisen A, Kim S, Pant B. Amyotrophic lateral sclerosis (ALS): a phylogenetic disease of the corticomotoneuron? Muscle Nerve. 1992;15:219-24.
26. Traynor BJ, Alexander M, Corr B, Frost E, Hardiman O. Effect of a multidisciplinary amyotrophic lateral sclerosis (ALS) clinic on ALS survival: a population based study, 1996-2000. J Neurol Neurosurg Psychiatry. 2003;74:1258-61. Epub 2003/08/23.
27. Kurian KM, Forbes RB, Colville S, Swingler RJ. Cause of death and clinical grading criteria in a cohort of amyotrophic lateral sclerosis cases undergoing autopsy from the Scottish Motor Neurone Disease Register. J Neurol Neurosurg Psychiatry. 2009;80(1):84-7.
28. Scelsa SN, Yakubov B, Salzman SH. Dyspnea-fasciculation syndrome: early respiratory failure in ALS with minimal motor signs. Amyotroph Lateral Scler Other Motor Neuron Disord. 2002;3(4):239-43.
29. de Carvalho M, Matias T, Coelho F, Evangelista T, Pinto A, Luis ML. Motor neuron disease presenting with respiratory failure. Journal of the Neurological Sciences. 1996;139 Suppl:117-22.
30. Czaplinski A, Strobel W, Gobbi C, Steck AJ, Fuhr P, Leppert D. Respiratory failure due to bilateral diaphragm palsy as an early manifestation of ALS. Medical Science Monitor. 2003;9(5):CS34-6.
31. Vucic S, Kiernan MC. Abnormalities in cortical and peripheral excitability in flail arm variant amyotrophic lateral sclerosis. J Neurol Neurosurg Psychiatry. 2007;78:849-52.
32. Vulpian A. Maladies du système nerveux (moelle épinière). Paris: Octave Doin; 1886. p. 436.
33. Hu M, Ellis C, Al-Chalabi A, Leigh P, Shaw C. Flail arm syndrome: a distinctive variant of amyotrophic lateral sclerosis. Journal of Neurology, Neurosurgery & Psychiatry. 1998;65(6):950-1.
34. Katz JS, Wolfe GI, Andersson PB, Saperstein DS, Elliott JL, Nations SP, et al. Brachial amyotrophic diplegia: a slowly progressive motor neuron disorder. Neurology. 1999;53(5):1071-6.
35. Gamez J, Cervera C, Codina A. Flail arm syndrome of Vulpian-Bernhart's form of amyotrophic lateral sclerosis. J Neurol Neurosurg Psychiatry. 1999;67(2):258.
36. Wijesekera L, Mathers S, Talman P, Galtrey C, Parkinson M, Ganesalingam J, et al. Natural history and clinical features of the flail arm and flail leg ALS variants. Neurology. 2009;72(12):1087-94.

37. Visser J, van den Berg-Vos RM, Franssen H, van den Berg LH, Wokke JH, de Jong JM, et al. Disease course and prognostic factors of progressive muscular atrophy. Archives of neurology. 2007;64(4):522-8. Epub 2007/04/11.
38. Ince PG, Evans J, Knopp M, Forster G, Hamdalla HH, Wharton SB, et al. Corticospinal tract degeneration in the progressive muscular atrophy variant of ALS. Neurology. 2003;60(8):1252-8.
39. Gordon PH, Cheng B, Katz IB, Pinto M, Hays AP, Mitsumoto H, et al. The natural history of primary lateral sclerosis. Neurology. 2006;66(5):647-53. Epub 2006/03/15.
40. Burrell JR, Vucic S, Kiernan MC. Isolated bulbar phenotype of amyotrophic lateral sclerosis. Amyotrophic Lateral Sclerosis. 2011;12(4):283-9.
41. Phukan J, Elamin M, Bede P, Jordan N, Gallagher L, Byrne S, et al. The syndrome of cognitive impairment in amyotrophic lateral sclerosis: a population-based study. J Neurol Neurosurg Psychiatry. 2012;83(1):102-8.
42. Lomen-Hoerth C, Murphy J, Langmore S, Kramer JH, Olney RK, Miller B. Are amyotrophic lateral sclerosis patients cognitively normal? Neurology. 2003;60(7):1094-7. Epub 2003/04/12.
43. Snowden JS, Harris J, Richardson A, Rollinson S, Thompson JC, Neary D, et al. Frontotemporal dementia with amyotrophic lateral sclerosis: a clinical comparison of patients with and without repeat expansions in C9orf72. Amyotrophic lateral sclerosis & frontotemporal degeneration. 2013;14(3):172-6. Epub 2013/02/21.
44. Eisen A, Kuwabara S. The split hand syndrome in amyotrophic lateral sclerosis. J Neurol Neurosurg Psychiatry. 2012;83:399-403.
45. Lemon RN, Griffiths J. Comparing the function of the corticospinal system in different species: organizational differences for motor specialization? Muscle Nerve. 2005;32(3):261-79.
46. Eisen AA, Shtybel W. AAEM minimonograph #35: Clinical experience with transcranial magnetic stimulation. Muscle Nerve. 1990;13(11):995-1011.
47. Porter R. The corticomotoneuronal component of the pyramidal tract: corticomotoneuronal connections and functions in primates. Brain Res. 1985;357(1):1-26.
48. Porter R. The Florey lecture, 1987. Corticomotoneuronal projections: synaptic events related to skilled movement. Proc R Soc Lond B Biol Sci. 1987;231(1263):147-68.
49. Vucic S, Kiernan MC. Novel threshold tracking techniques suggest that cortical hyperexcitability is an early feature of motor neuron disease. Brain : a journal of neurology. 2006;129:2436-46.
50. Vucic S, Nicholson GA, Kiernan MC. Cortical hyperexcitability may precede the onset of familial amyotrophic lateral sclerosis. Brain : a journal of neurology. 2008;131:1540-50.
51. Vucic S, Kiernan MC. Cortical excitability testing distinguishes Kennedy's disease from amyotrophic lateral sclerosis. Clin Neurophysiol. 2008;119:1088-96.
52. Vucic S, Cheah BC, Yiannikas C, Kiernan MC. Cortical excitability distinguishes ALS from mimic disorders. Clin Neurophysiol. 2011;122:1860-6.
53. Vucic S, Cheah BC, Yiannikas C, Vincent A, Kiernan MC. Corticomotoneuronal function and hyperexcitability in acquired neuromyotonia. 2010;Brain 133(Brain 9):2727-33. Epub 2010/08/26.
54. Weber M, Eisen A, Stewart H, Hirota N. The split hand in ALS has a cortical basis. J Neurol Sci. 2000;180(1-2):66-70.
55. Bae JS, Sawai S, Misawa S, Kanai K, Isose S, Kuwabara S. Differences in excitability properties of FDI and ADM motor axons. Muscle Nerve. 2009;39(3):350-4.

56. Vucic S, Kiernan MC. Axonal excitability properties in amyotrophic lateral sclerosis. Clin Neurophysiol. 2006;117:1458-66.
57. Kanai K, Kuwabara S, Misawa S, Tamura N, Ogawara K, Nakata M, et al. Altered axonal excitability properties in amyotrophic lateral sclerosis: impaired potassium channel function related to disease stage. Brain : a journal of neurology. 2006;129:953-62.
58. Mogyoros I, Kiernan M, Burke D, Bostock H. Strength-duration properties of sensory and motor axons in amyotrophic lateral sclerosis. Brain : a journal of neurology. 1998;121:851-9.
59. Kanai K, Kuwabara S, Arai K, Sung JY, Ogawara K, Hattori T. Muscle cramp in Machado-Joseph disease: altered motor axonal excitability properties and mexiletine treatment. Brain : a journal of neurology. 2003;126:965-73.
60. Vucic S, Kiernan MC. Pathophysiological insights into motor axonal function in Kennedy's disease. Neurology. 2007;69:1828-35.
61. van Schaik IN, Leger JM, Nobile-Orazio E, Cornblath DR, Hadden RD, Koski CL, et al. European Federation of Neurological Societies/Peripheral Nerve Society Guideline on management of multifocal motor neuropathy. Report of a Joint Task Force of the European Federation of Neurological Societies and the Peripheral Nerve Society – first revision. J Periph Nerv System. 2010;15(4):295-301.
62. Eisen A. Clinical electrophysiology of the upper and lower motor neuron in amyotrophic lateral sclerosis. Sem Neurol. 2001;21:141-54.
63. Chang J, Lomen-Hoerth C, Murphy J, Henry R, Kramer J, Miller B, et al. A voxel-based morphometry study of patterns of brain atrophy in ALS and ALS/FTLD. Neurology. 2005;65(1):75-80.
64. Magistris M, Rösler K, Truffert A, Landis T, Hess C. A clinical study of motor evoked potentials using a triple stimulation technique. Brain : a journal of neurology. 1999;122(2):265-79.
65. de Carvalho M, Swash M. Nerve conduction studies in amyotrophic lateral sclerosis. Muscle Nerve. 2000;23:344-52.
66. Daube JR. Electrodiagnostic studies in amyotrophic lateral sclerosis and other motor neuron disorders. Muscle Nerve. 2000;23(10):1488-502.
67. de Carvalho M, Scotto M, Lopes A, Swash M. Clinical and neurophysiological evaluation of progression in amyotrophic lateral sclerosis. Muscle & Nerve. 2003;28(5):630-3.
68. de Carvalho M, Scotto M, Lopes A, Swash M. Quantitating progression in ALS. Neurology. 2005;64(10):1783-5.
69. Mills KR. Characteristics of fasciculations in amyotrophic lateral sclerosis and the benign fasciculation syndrome. Brain 2010;133(11):3458-69.
70. Roth G. The origin of fasciculations. Ann Neurol. 1982;12(6):542-7.
71. Roth G. Fasciculations and their F-response. Localisation of their axonal origin. J Neurol Sci. 1984;63(3):299-306.
72. Miller TM, Layzer RB. Muscle cramps. Muscle Nerve. 2005;32:431-42.
73. Krarup C. Lower motor neuron involvement examined by quantitative electromyography in amyotrophic lateral sclerosis. Clin Neurophysiol. 2011;122(2):414-22. Epub 2010/07/28.
74. Douglass CP, Kandler RH, Shaw PJ, McDermott CJ. An evaluation of neurophysiological criteria used in the diagnosis of motor neuron disease. J Neurol Neurosurg Psychiatry. 2010;81(6):646-9. Epub 2010/06/05.
75. de Carvalho M, Swash M. Awaji diagnostic algorithm increases sensitivity of El Escorial criteria for ALS diagnosis. Amyotroph Lateral Scler. 2009;10(1):53-7. Epub 2008/11/06.

76. Boekestein WA, Kleine BU, Hageman G, Schelhaas HJ, Zwarts MJ. Sensitivity and specificity of the 'Awaji' electrodiagnostic criteria for amyotrophic lateral sclerosis: Retrospective comparison of the Awaji and revised El Escorial criteria for ALS. Amyotroph Lateral Scler. 2010;11:497-501. Epub 2010/06/12.
77. Schrooten M, Smetcoren C, Robberecht W, Van Damme P. Benefit of the Awaji diagnostic algorithm for amyotrophic lateral sclerosis: A prospective study. Ann Neurol. 2011;70(1):79-83. Epub 2011/03/26.
78. Costa J, Swash M, de Carvalho M. Awaji criteria for the diagnosis of amyotrophic lateral sclerosis:a systematic review. Archives of neurology. 2012;69(11):1410-6. Epub 2012/08/16.
79. de Carvalho M, Dengler R, Eisen A, England JD, Kaji R, Kimura J, et al. The Awaji criteria for diagnosis of ALS. Muscle Nerve. 2011;44(3):456-7; author reply 7. Epub 2011/10/15.
80. Okita T, Nodera H, Shibuta Y, Nodera A, Asanuma K, Shimatani Y, et al. Can Awaji ALS criteria provide earlier diagnosis than the revised El Escorial criteria? J Neurol Sci. 2011;302(1–2):29-32.
81. Chen A, Weimer L, Brannagan T, 3rd, Colin M, Andrews J, Mitsumoto H, et al. Experience with the Awaji Island modifications to the ALS diagnostic criteria. Muscle Nerve. 2010;42(5):831-2. Epub 2010/10/12.
82. de Carvalho M, Dengler R, Eisen A, England JD, Kaji R, Kimura J, et al. Electrodiagnostic criteria for diagnosis of ALS. Clin Neurophysiol. 2008;119(3):497-503.
83. Bowser R, Turner MR, Shefner J. Biomarkers in amyotrophic lateral sclerosis: opportunities and limitations. Nat Rev Neurol. 2011;7(11):631-8.
84. Rutkove SB, Zhang H, Schoenfeld DA, Raynor EM, Shefner JM, Cudkowicz ME, et al. Electrical impedance myography to assess outcome in amyotrophic lateral sclerosis clinical trials. Clin Neurophysiol. 2007;118(11):2413-8.
85. Burke D, Kiernan MC, Bostock H. Excitability of human axons. Clin Neurophysiol. 2001;112:1575-85.
86. Bostock H, Cikurel K, Burke D. Threshold tracking techniques in the study of human peripheral nerve. Muscle Nerve. 1998;21(2):137-58.
87. Vucic S, Ziemann U, Eisen A, Hallett M, Kiernan MC. Transcranial magnetic stimulation and amyotrophic lateral sclerosis: pathophysiological insights. J Neurol, Neurosurg & Psychiatry. 2013:in press. Epub December 21, 2012.
88. Fisher KM, Zaaimi B, Williams TL, Baker SN, Baker MR. Beta-band intermuscular coherence: a novel biomarker of upper motor neuron dysfunction in motor neuron disease. Brain 2012;135(9):2849-64.
89. Gros-Louis F, Gaspar C, Rouleau GA. Genetics of familial and sporadic amyotrophic lateral sclerosis. Biochim Biophys Acta. 2006;1762:956-72.
90. Pasinelli P, Brown RH. Molecular biology of amyotrophic lateral sclerosis: insights from genetics. Nat Rev Neurosci. 2006;7(9):710-23.
91. Patel SA, Maragakis NJ. Amyotrophic lateral sclerosis: pathogenesis, differential diagnoses, and potential interventions. J Spinal Cord Med. 2002;25(4):262-73.
92. Neusch C, Bahr M, Schneider-Gold C. Glia cells in amyotrophic lateral sclerosis: new clues to understanding an old disease? Muscle Nerve. 2007;35(6):712-24.
93. Gonzalez de Aguilar JL, Echaniz-Laguna A, Fergani A, Rene F, Meininger V, Loeffler JP, et al. Amyotrophic lateral sclerosis: all roads lead to Rome. J Neurochem. 2007;101(5):1153-60.

94. Vucic S, Kiernan M. Pathophysiology of degeneration in familial amyotrophic lateral sclerosis. Curr Mol Med. 2009;9:255-72.
95. Boillee S, Vande Velde C, Cleveland DW. ALS: a disease of motor neurons and their nonneuronal neighbors. Neuron. 2006;52:39-59.
96. Watkins JC, Evans RH. Excitatory amino acid transmitters. Annu Rev Pharmacol Toxicol. 1981;21:165-204.
97. Heath PR, Shaw PJ. Update on the glutamatergic neurotransmitter system and the role of excitotoxicity in amyotrophic lateral sclerosis. Muscle Nerve. 2002;26(4):438-58.
98. Dong H, Zhang P, Song I, Petralia RS, Liao D, Huganir RL. Characterization of the glutamate receptor-interacting proteins GRIP1 and GRIP2. J Neurosci. 1999;19(16):6930-41.
99. Vandenberg RJ. Molecular pharmacology and physiology of glutamate transporters in the central nervous system. Clin Exp Pharmacol Physiol. 1998;25(6):393-400.
100. Laake JH, Slyngstad TA, Haug FM, Ottersen OP. Glutamine from glial cells is essential for the maintenance of the nerve terminal pool of glutamate: immunogold evidence from hippocampal slice cultures. J Neurochem. 1995;65(2):871-81.
101. Simeone TA, Sanchez RM, Rho JM. Molecular biology and ontogeny of glutamate receptors in the mammalian central nervous system. J Child Neurol. 2004;19(5):343-60.
102. MacDermott AB, Mayer ML, Westbrook GL, Smith SJ, Barker JL. NMDA-receptor activation increases cytoplasmic calcium concentration in cultured spinal cord neurones. Nature. 1986;321(6069):519-22.
103. Traven HG, Brodin L, Lansner A, Ekeberg O, Wallen P, Grillner S. Computer simulations of NMDA and non-NMDA receptor-mediated synaptic drive: sensory and supraspinal modulation of neurons and small networks. J Neurophysiol. 1993;70(2):695-709.
104. Komuro H, Rakic P. Modulation of neuronal migration by NMDA receptors. Science. 1993;260(5104):95-7.
105. Bliss TV, Collingridge GL. A synaptic model of memory: long-term potentiation in the hippocampus. Nature. 1993;361(6407):31-9.
106. Kutsuwada T, Kashiwabuchi N, Mori H, Sakimura K, Kushiya E, Araki K, et al. Molecular diversity of the NMDA receptor channel. Nature. 1992;358(6381):36-41.
107. Meguro H, Mori H, Araki K, Kushiya E, Kutsuwada T, Yamazaki M, et al. Functional characterization of a heteromeric NMDA receptor channel expressed from cloned cDNAs. Nature. 1992;357(6373):70-4.
108. Michaelis EK. Molecular biology of glutamate receptors in the central nervous system and their role in excitotoxicity, oxidative stress and aging. Prog Neurobiol. 1998;54(4):369-415.
109. Monyer H, Sprengel R, Schoepfer R, Herb A, Higuchi M, Lomeli H, et al. Heteromeric NMDA receptors: molecular and functional distinction of subtypes. Science. 1992;256(5060):1217-21.
110. Ishii T, Moriyoshi K, Sugihara H, Sakurada K, Kadotani H, Yokoi M, et al. Molecular characterization of the family of the N-methyl-D-aspartate receptor subunits. J Biol Chem. 1993;268(4):2836-43.
111. Watanabe M, Inoue Y, Sakimura K, Mishina M. Distinct spatio-temporal distributions of the NMDA receptor channel subunit mRNAs in the brain. Ann N Y Acad Sci. 1993;707:463-6.
112. Watanabe M, Inoue Y, Sakimura K, Mishina M. Distinct distributions of five N-methyl-D-aspartate receptor channel subunit mRNAs in the forebrain. J Comp Neurol. 1993;338(3):377-90.

113. Watanabe M, Mishina M, Inoue Y. Distinct distributions of five NMDA receptor channel subunit mRNAs in the brainstem. J Comp Neurol. 1994;343(4):520-31.
114. Watanabe M, Mishina M, Inoue Y. Distinct spatiotemporal expressions of five NMDA receptor channel subunit mRNAs in the cerebellum. J Comp Neurol. 1994;343(4):513-9.
115. Ciabarra AM, Sevarino KA. An anti-chi-1 antibody recognizes a heavily glycosylated protein in rat brain. Brain Res Mol Brain Res. 1997;46(1-2):85-90.
116. Nishi M, Hinds H, Lu HP, Kawata M, Hayashi Y. Motoneuron-specific expression of NR3B, a novel NMDA-type glutamate receptor subunit that works in a dominant-negative manner. J Neurosci. 2001;21(23):RC185.
117. Chatterton JE, Awobuluyi M, Premkumar LS, Takahashi H, Talantova M, Shin Y, et al. Excitatory glycine receptors containing the NR3 family of NMDA receptor subunits. Nature. 2002;415(6873):793-8.
118. Dingledine R, Borges K, Bowie D, Traynelis SF. The glutamate receptor ion channels. Pharmacol Rev. 1999;51(1):7-61.
119. Heath P, Shaw P. Update on the glutamatergic neurotransmitter system and the role of excitotoxicity in amyotrophic lateral sclerosis. Muscle Nerve. 2002;26:438 - 58.
120. Chittajallu R, Braithwaite SP, Clarke VR, Henley JM. Kainate receptors: subunits, synaptic localization and function. Trends in pharmacological sciences. 1999;20(1):26-35.
121. Lerma J. Roles and rules of kainate receptors in synaptic transmission. Nature Reviews Neuroscience. 2003;4(6):481-95.
122. Caramia MD, Cicinelli P, Paradiso C, Mariorenzi R, Zarola F, Bernardi G, et al. 'Excitability changes of muscular responses to magnetic brain stimulation in patients with central motor disorders. Electroencephalogr Clin Neurophysiol. 1991;81:243-50.
123. Desiato M, Bernardi, G, Hagi, AH, Boffa L, Caramia, MD. Transcranial magnetic stimulation of motor pathways directed to muscles supplied by cranial nerves in ALS. Clin Neurophysiol. 2002;113:132-40.
124. Eisen A, Pant B, Stewart H. Cortical excitability in amyotrophic lateral sclerosis: a clue to pathogenesis. Can J Neurol Sci. 1993;20:11-6.
125. Prout AJ, Eisen A. The cortical silent period and ALS. Muscle Nerve. 1994;17:217-23.
126. Vucic S, Kiernan MC. Upregulation of persistent sodium conductances in familial ALS. J Neurol Neurosurg Psychiatry. 2010;81(2):222-7.
127. Blair IP, Williams KL, Warraich ST, Durnall JC, Thoeng AD, Manavis J, et al. FUS mutations in amyotrophic lateral sclerosis: clinical, pathological, neurophysiological and genetic analysis. J Neurol Neurosurg Psychiatry. 2009. Epub 2009/12/08.
128. Browne SE, Yang L, DiMauro JP, Fuller SW, Licata SC, Beal MF. Bioenergetic abnormalities in discrete cerebral motor pathways presage spinal cord pathology in the G93A SOD1 mouse model of ALS. Neurobiol Dis. 2006;22:599-610.
129. Nihei K, McKee AC, Kowall NW. Patterns of neuronal degeneration in the motor cortex of amyotrophic lateral sclerosis patients. Acta Neuropathologica. 1993;86:55-64.
130. Foerster BR, Callaghan BC, Petrou M, Edden RA, Chenevert TL, Feldman EL. Decreased motor cortex gamma-aminobutyric acid in amyotrophic lateral sclerosis. Neurology. 2012;78(20):1596-600. Epub 2012/04/21.
131. Ionov ID. Survey of ALS-associated factors potentially promoting Ca(2+) overload of motor neurons. Amyotroph Lateral Scler. 2007;8(5):260-5.
132. Rothstein JD, Jin L, Dykes-Hoberg M, Kuncl RW. Chronic inhibition of glutamate uptake produces a model of slow neurotoxicity. Proc Natl Acad Sci U S A. 1993;90(14):6591-5.

133. Rothstein JD, Van Kammen M, Levey AI, Martin LJ, Kuncl RW. Selective loss of glial glutamate transporter GLT-1 in amyotrophic lateral sclerosis. Ann Neurol. 1995;38(1):73-84.
134. Trotti D, Rolfs A, Danbolt NC, Brown RH, Jr., Hediger MA. SOD1 mutants linked to amyotrophic lateral sclerosis selectively inactivate a glial glutamate transporter. Nat Neurosci. 1999;2(9):848.
135. Boston-Howes W, Gibb SL, Williams EO, Pasinelli P, Brown RH, Jr., Trotti D. Caspase-3 cleaves and inactivates the glutamate transporter EAAT2. J Biol Chem. 2006;281(20):14076-84.
136. Gibb SL, Boston-Howes W, Lavina ZS, Gustincich S, Brown RH, Jr., Pasinelli P, et al. A Caspase-3-cleaved Fragment of the Glial Glutamate Transporter EAAT2 Is Sumoylated and Targeted to Promyelocytic Leukemia Nuclear Bodies in Mutant SOD1-linked Amyotrophic Lateral Sclerosis. J Biol Chem. 2007;282(44):32480-90.
137. Rothstein JD, Patel S, Regan MR, Haenggeli C, Huang YH, Bergles DE, et al. Beta-lactam antibiotics offer neuroprotection by increasing glutamate transporter expression. Nature. 2005;433(7021):73-7. Epub 2005/01/07.
138. Guo H, Lai L, Butchbach ME, Stockinger MP, Shan X, Bishop GA, et al. Increased expression of the glial glutamate transporter EAAT2 modulates excitotoxicity and delays the onset but not the outcome of ALS in mice. Hum Mol Genet. 2003;12(19):2519-32.
139. Kawahara Y, Ito K, Sun H, Aizawa H, Kanazawa I, Kwak S. Glutamate receptors: RNA editing and death of motor neurons. Nature. 2004;427(6977):801.
140. Kwak S, Kawahara Y. Deficient RNA editing of GluR2 and neuronal death in amyotropic lateral sclerosis. J Mol Med. 2005;83(2):110-20.
141. Takuma H, Kwak S, Yoshizawa T, Kanazawa I. Reduction of GluR2 RNA editing, a molecular change that increases calcium influx through AMPA receptors, selective in the spinal ventral gray of patients with amyotrophic lateral sclerosis. Ann Neurol. 1999;46(6):806-15.
142. Van Damme P, Braeken D, Callewaert G, Robberecht W, Van Den Bosch L. GluR2 deficiency accelerates motor neuron degeneration in a mouse model of amyotrophic lateral sclerosis. J Neuropathol Exp Neurol. 2005;64(7):605-12.
143. Van Damme P, Van Den Bosch L, Van Houtte E, Callewaert G, Robberecht W. GluR2-dependent properties of AMPA receptors determine the selective vulnerability of motor neurons to excitotoxicity. J Neurophysiol. 2002;88(3):1279-87.
144. Cox L, Kirby J, Shaw P. Pathogenesis of motor neurone disease. In: Kiernan M, editor. The Motor Neurone Disease Handbook. Sydney: Australasian Medical Publishing Company Limited
2007. p. 26-55.
145. Bensimon G, Lacomblez L, Meininger V. A controlled trial of riluzole in amyotrophic lateral sclerosis. ALS/Riluzole Study Group. N Engl J Med. 1994;330:585-91.
146. Gurney ME, Cutting FB, Zhai P, Doble A, Taylor CP, Andrus PK, et al. Benefit of vitamin E, riluzole, and gabapentin in a transgenic model of familial amyotrophic lateral sclerosis. Ann Neurol. 1996;39(2):147-57.
147. Gurney ME, Fleck TJ, Himes CS, Hall ED. Riluzole preserves motor function in a transgenic model of familial amyotrophic lateral sclerosis. Neurology. 1998;50(1):62-6.
148. Lacomblez L, Bensimon G, Leigh PN, Guillet P, Meininger V. Dose-ranging study of riluzole in amyotrophic lateral sclerosis. Amyotrophic Lateral Sclerosis/Riluzole Study Group II. Lancet. 1996;347:1425-31.

149. Cheah B, Vucic S, Krishnan A, Kiernan M. Riluzole, neuroprotection and amyotrophic lateral sclerosis. Current medicinal chemistry. 2010;17(18):1942-59.
150. Quinlan KA. Links between Electrophysiological and Molecular Pathology of Amyotrophic Lateral Sclerosis. Integ Comp Biol. 2011;51(6):913-25.
151. Wang SJ, Wang KY, Wang WC. Mechanisms underlying the riluzole inhibition of glutamate release from rat cerebral cortex nerve terminals (synaptosomes). Neuroscience. 2004;125(1):191-201.
152. Azbill RD, Mu X, Springer JE. Riluzole increases high-affinity glutamate uptake in rat spinal cord synaptosomes. Brain Research. 2000;871(2):175-80.
153. Cheah BC, Vucic S, Krishnan AV, Kiernan MC. Riluzole, neuroprotection and amyotrophic lateral sclerosis. Curr Med Chem. 2010;17(18):1942-199. Epub 2010/04/10.
154. Ince P, Stout N, Shaw P, Slade J, Hunziker W, Heizmann CW, et al. Parvalbumin and calbindin D-28k in the human motor system and in motor neuron disease. Neuropathol Appl Neurobiol. 1993;19(4):291-9.
155. van Es MA, Van Vught PW, Blauw HM, Franke L, Saris CG, Andersen PM, et al. ITPR2 as a susceptibility gene in sporadic amyotrophic lateral sclerosis: a genome-wide association study. Lancet Neurol. 2007.
156. Choe CU, Ehrlich BE. The inositol 1,4,5-trisphosphate receptor (IP3R) and its regulators: sometimes good and sometimes bad teamwork. Sci STKE. 2006;2006(363):re15.
157. Gutstein DE, Marks AR. Role of inositol 1,4,5-trisphosphate receptors in regulating apoptotic signaling and heart failure. Heart Vessels. 1997;Suppl 12:53-7.
158. Amendola J, Durand J. Morphological differences between wild-type and transgenic superoxide dismutase 1 lumbar motoneurons in postnatal mice. J Comp Neurol. 2008;511(3):329-41.
159. Choi DW. Ionic dependence of glutamate neurotoxicity. J Neurosci. 1987;7(2):369-79.
160. Shaw P, Kuncl R. Current concepts in the pathogenesis of ALS. In: WR K, editor. Motor Neuron Disease. Lodon: WB Saunders; 2002. p. 37-73.
161. Stys PK. Anoxic and ischemic injury of myelinated axons in CNS white matter: from mechanistic concepts to therapeutics. J Cereb Blood Flow Metab. 1998;18(1):2-25.
162. Miller RJ, Murphy SN, Glaum SR. Neuronal Ca2+ channels and their regulation by excitatory amino acids. Ann N Y Acad Sci. 1989;568:149-58.
163. Meldrum B, Garthwaite J. Excitatory amino acid neurotoxicity and neurodegenerative disease. Trends Pharmacol Sci. 1990;11(9):379-87.
164. Regan RF, Panter SS, Witz A, Tilly JL, Giffard RG. Ultrastructure of excitotoxic neuronal death in murine cortical culture. Brain Res. 1995;705(1-2):188-98.
165. Bondy SC, Lee DK. Oxidative stress induced by glutamate receptor agonists. Brain Res. 1993;610(2):229-33.
166. Lees GJ. Contributory mechanisms in the causation of neurodegenerative disorders. Neuroscience. 1993;54(2):287-322.
167. Maher P, Davis JB. The role of monoamine metabolism in oxidative glutamate toxicity. J Neurosci. 1996;16(20):6394-401.
168. Goetz CG. Amyotrophic lateral sclerosis: early contributions of Jean-Martin Charcot. Muscle & Nerve. 2000;23(3):336-43.
169. Armand J. The origin, course and terminations of corticospinal fibers in various mammals. Prog Brain Res. 1982;57:329-60.

170. Lillo P, Hodges JR. Frontotemporal dementia and motor neurone disease: overlapping clinic-pathological disorders. J Clin Neurosci. 2009;16(9):1131-5.
171. Neumann M, Sampathu DM, Kwong LK, Truax AC, Micsenyi MC, Chou TT, et al. Ubiquitinated TDP-43 in Frontotemporal Lobar Degeneration and Amyotrophic Lateral Sclerosis. Science. 2006;314(5796):130-3.
172. Renton Alan E, Majounie E, Waite A, Simón-Sánchez J, Rollinson S, Gibbs JR, et al. A Hexanucleotide Repeat Expansion in C9ORF72 Is the Cause of Chromosome 9p21-Linked ALS-FTD. Neuron. 2011;72:257-68.
173. DeJesus-Hernandez M, Mackenzie Ian R, Boeve Bradley F, Boxer Adam L, Baker M, Rutherford Nicola J, et al. Expanded GGGGCC Hexanucleotide Repeat in Noncoding Region of C9ORF72 Causes Chromosome 9p-Linked FTD and ALS. Neuron. 2011;72:245-56.
174. Zanette G, Tamburin S, Manganotti P, Refatti N, Forgione A, Rizzuto N. Different mechanisms contribute to motor cortex hyperexcitability in amyotrophic lateral sclerosis. Clin Neurophysiol. 2002;113(11):1688-97.
175. Kennedy WR, Alter M, Sung JH. Progressive proximal spinal and bulbar muscular atrophy of late onset. A sex-linked recessive trait. Neurology. 1968;18:671-80.
176. La Spada AR, Wilson EM, Lubahn DB, Harding AE, Fischbeck KH. Androgen receptor gene mutations in X-linked spinal and bulbar muscular atrophy. Nature. 1991;352:77-9.
177. Hu MT, Ellis CM, Al-Chalabi A, Leigh PN, Shaw CE. Flail arm syndrome: a distinctive variant of amyotrophic lateral sclerosis. J Neurol Neurosurg Psychiatry. 1998;65(6):950-1.
178. Vucic S, Kiernan MC. Flail-limb variant of motor neuron disease has evidence of central and peripheral nerve dysfunction. Amyotroph Lateral Scler Other Motor Neuron Disord. 2005;6(Suppl1):125.
179. Chou SM, Norris FH. Amyotrophic lateral sclerosis: lower motor neuron disease spreading to upper motor neurons. Muscle Nerve. 1993;16(8):864-9.
180. Gould TW, Buss RR, Vinsant S, Prevette D, Sun W, Knudson CM, et al. Complete dissociation of motor neuron death from motor dysfunction by Bax deletion in a mouse model of ALS. J Neurosci. 2006;26(34):8774-86.
181. Pagani MR, Reisin RC, Uchitel OD. Calcium signaling pathways mediating synaptic potentiation triggered by amyotrophic lateral sclerosis IgG in motor nerve terminals. J Neurosci. 2006;26(10):2661-72.
182. Pun S, Santos AF, Saxena S, Xu L, Caroni P. Selective vulnerability and pruning of phasic motoneuron axons in motoneuron disease alleviated by CNTF. Nat Neurosci. 2006;9(3):408-19.
183. Miller RG, Jackson CE, Kasarskis EJ, England JD, Forshew D, Johnston W, et al. Practice parameter update: The care of the patient with amyotrophic lateral sclerosis: multidisciplinary care, symptom management, and cognitive/behavioral impairment (an evidence-based review): report of the Quality Standards Subcommittee of the American Academy of Neurology. Neurology. 2009;73(15):1227-33. Epub 2009/10/14.
184. Turner MR, Kiernan MC, Leigh PN, Talbot K. Biomarkers in amyotrophic lateral sclerosis. Lancet Neurol. 2009;8:94-109.
185. Vucic S, Burke D, Kiernan MC. Diagnosis of motor neuron disease. In: Kiernan MC, editor. The Motor Neuron Disease Handbook. Sydney: Australasian Medical Publishing Company Limited; 2007. p. 89-115.
186. Eisen A, Weber M. The motor cortex and amyotrophic lateral sclerosis. Muscle Nerve. 2001;24(4):564-73.

187. Gowers WR. Manual of Diseases of the Nervous System. London: Churchill; 1886-88.
188. Kiernan J, Hudson A. Changes in sizes of cortical and lower motor neurons in amyotrophic lateral sclerosis. Brain. 1991(114):843-53.
189. Pamphlett R, Kril J, Hng T. Motor neuron disease: a primary disorder of corticomotoneurons? . Muscle Nerve 1995(18):314-8.
190. Flament D, Goldsmith P, Buckley CJ, Lemon RN. Task dependence of responses in first dorsal interosseous muscle to magnetic brain stimulation in man. J Physiol. 1993;464:361-78.
191. Siddique T, Figlewicz DA, Pericak-Vance MA, Haines JL, Rouleau G, Jeffers AJ, et al. Linkage of a gene causing familial amyotrophic lateral sclerosis to chromosome 21 and evidence of genetic-locus heterogeneity. N Engl J Med. 1991;324(20):1381-4.
192. Andersen P. Amyotrophic lateral sclerosis genetics with Mendelian inheritance. In: Brown Jr R, Swash M, Pasinelli P, editors. Amyotrophic Lateral Sclerosis. 2nd ed. London: Informa Healthcare; 2006. p. 187-207.
193. Dewil M, Andersen P, Van Den Bosch L, Robberecht W. Genetics of amyotrophic lateral sclerosis. In: Eisen A, Mauguiere F, editors. Clinical Neurophysiology of Motor Neuron Diseases. Amsterdam: Elsevier; 2004. p. 169-86.
194. Robberecht W. Genetics of familial amyotrophic lateral sclerosis and ethical aspects. In: Kuncl R, editor. Motor Neuron Disease. London: W.B. Saunders; 2002. p. 75-95.
195. Levanon D, Lieman-Hurwitz J, Dafni N, Wigderson M, Sherman L, Bernstein Y, et al. Architecture and anatomy of the chromosomal locus in human chromosome 21 encoding the Cu/Zn superoxide dismutase. Embo J. 1985;4(1):77-84.
196. Fridovich I. Superoxide dismutases. Adv Enzymol Relat Areas Mol Biol. 1986;58:61-97.
197. Bowling AC, Barkowski EE, McKenna-Yasek D, Sapp P, Horvitz HR, Beal MF, et al. Superoxide dismutase concentration and activity in familial amyotrophic lateral sclerosis. J Neurochem. 1995;64(5):2366-9.
198. Pardo CA, Xu Z, Borchelt DR, Price DL, Sisodia SS, Cleveland DW. Superoxide dismutase is an abundant component in cell bodies, dendrites, and axons of motor neurons and in a subset of other neurons. Proc Natl Acad Sci U S A. 1995;92(4):954-8.
199. Cudkowicz ME, McKenna-Yasek D, Sapp PE, Chin W, Geller B, Hayden DL, et al. Epidemiology of mutations in superoxide dismutase in amyotrophic lateral sclerosis. Ann Neurol. 1997;41(2):210-21.
200. Orrell RW, Habgood JJ, Gardiner I, King AW, Bowe FA, Hallewell RA, et al. Clinical and functional investigation of 10 missense mutations and a novel frameshift insertion mutation of the gene for copper-zinc superoxide dismutase in UK families with amyotrophic lateral sclerosis. Neurology. 1997;48(3):746-51.
201. Shaw CE, Enayat ZE, Chioza BA, Al-Chalabi A, Radunovic A, Powell JF, et al. Mutations in all five exons of SOD-1 may cause ALS. Ann Neurol. 1998;43(3):390-4.
202. Andersen PM, Al-Chalabi A. Clinical genetics of amyotrophic lateral sclerosis: what do we really know? Nat Rev Neurol. 2011;7(11):603-15.
203. Gros-Louis F, Gaspar C, Rouleau GA. Genetics of familial and sporadic amyotrophic lateral sclerosis. Biochim Biophys Acta. 2006.
204. Juneja T, Pericak-Vance MA, Laing NG, Dave S, Siddique T. Prognosis in familial amyotrophic lateral sclerosis: progression and survival in patients with glu100gly and ala4val mutations in Cu,Zn superoxide dismutase. Neurology. 1997;48(1):55-7.
205. Aoki M, Ogasawara M, Matsubara Y, Narisawa K, Nakamura S, Itoyama Y, et al. Mild ALS in Japan associated with novel SOD mutation. Nat Genet. 1993;5(4):323-4.

206. Al-Chalabi A, Andersen PM, Chioza B, Shaw C, Sham PC, Robberecht W, et al. Recessive amyotrophic lateral sclerosis families with the D90A SOD1 mutation share a common founder: evidence for a linked protective factor. Hum Mol Genet. 1998;7(13):2045-50.
207. Suthers G, Laing N, Wilton S, Dorosz S, Waddy H. "Sporadic" motoneuron disease due to familial SOD1 mutation with low penetrance. Lancet. 1994;344(8939-8940):1773.
208. Jones CT, Swingler RJ, Simpson SA, Brock DJ. Superoxide dismutase mutations in an unselected cohort of Scottish amyotrophic lateral sclerosis patients. J Med Genet. 1995;32(4):290-2.
209. Bruijn LI, Beal MF, Becher MW, Schulz JB, Wong PC, Price DL, et al. Elevated free nitrotyrosine levels, but not protein-bound nitrotyrosine or hydroxyl radicals, throughout amyotrophic lateral sclerosis (ALS)-like disease implicate tyrosine nitration as an aberrant in vivo property of one familial ALS-linked superoxide dismutase 1 mutant. Proc Natl Acad Sci U S A. 1997;94(14):7606-11.
210. Bruijn LI, Houseweart MK, Kato S, Anderson KL, Anderson SD, Ohama E, et al. Aggregation and motor neuron toxicity of an ALS-linked SOD1 mutant independent from wild-type SOD1. Science. 1998;281(5384):1851-4.
211. Bruijn LI, Miller TM, Cleveland DW. Unraveling the mechanisms involved in motor neuron degeneration in ALS. Annu Rev Neurosci. 2004;27:723-49.
212. Beckman JS, Carson M, Smith CD, Koppenol WH. ALS, SOD and peroxynitrite. Nature. 1993;364(6438):584.
213. Andrus PK, Fleck TJ, Gurney ME, Hall ED. Protein oxidative damage in a transgenic mouse model of familial amyotrophic lateral sclerosis. J Neurochem. 1998;71(5):2041-8.
214. Bogdanov MB, Ramos LE, Xu Z, Beal MF. Elevated "hydroxyl radical" generation in vivo in an animal model of amyotrophic lateral sclerosis. J Neurochem. 1998;71(3):1321-4.
215. Liu R, Althaus JS, Ellerbrock BR, Becker DA, Gurney ME. Enhanced oxygen radical production in a transgenic mouse model of familial amyotrophic lateral sclerosis. Ann Neurol. 1998;44(5):763-70.
216. Beckman JS, Koppenol WH. Nitric oxide, superoxide, and peroxynitrite: the good, the bad, and ugly. Am J Physiol. 1996;271(5 Pt 1):1424-37.
217. Crow JP, Sampson JB, Zhuang Y, Thompson JA, Beckman JS. Decreased zinc affinity of amyotrophic lateral sclerosis-associated superoxide dismutase mutants leads to enhanced catalysis of tyrosine nitration by peroxynitrite. J Neurochem. 1997;69(5):1936-44.
218. Smith RG, Henry YK, Mattson MP, Appel SH. Presence of 4-hydroxynonenal in cerebrospinal fluid of patients with sporadic amyotrophic lateral sclerosis. Ann Neurol. 1998;44(4):696-9. Epub 1998/10/20.
219. Simpson EP, Henry YK, Henkel JS, Smith RG, Appel SH. Increased lipid peroxidation in sera of ALS patients: a potential biomarker of disease burden. Neurology. 2004;62(10):1758-65.
220. Mitsumoto H, Santella RM, Liu X, Bogdanov M, Zipprich J, Wu HC, et al. Oxidative stress biomarkers in sporadic ALS. Amyotroph Lateral Scler. 2008;9(3):177-83. Epub 2008/06/25.
221. Shaw PJ, Ince PG, Falkous G, Mantle D. Oxidative damage to protein in sporadic motor neuron disease spinal cord. Ann Neurol. 1995;38(4):691-5. Epub 1995/10/01.
222. Fitzmaurice PS, Shaw IC, Kleiner HE, Miller RT, Monks TJ, Lau SS, et al. Evidence for DNA damage in amyotrophic lateral sclerosis. Muscle Nerve. 1996;19(6):797-8. Epub 1996/06/01.

223. Chang Y, Kong Q, Shan X, Tian G, Ilieva H, Cleveland DW, et al. Messenger RNA oxidation occurs early in disease pathogenesis and promotes motor neuron degeneration in ALS. PloS one. 2008;3(8):e2849. Epub 2008/08/07.
224. Gurney ME, Pu H, Chiu AY, Dal Canto MC, Polchow CY, Alexander DD, et al. Motor neuron degeneration in mice that express a human Cu,Zn superoxide dismutase mutation. Science. 1994;264(5166):1772-5.
225. Prudencio M, Hart PJ, Borchelt DR, Andersen PM. Variation in aggregation propensities among ALS-associated variants of SOD1: Correlation to human disease. Hum Mol Genet. 2009;18(17):3217-26.
226. Orrell RW, Lane RJ, Ross M. A systematic review of antioxidant treatment for amyotrophic lateral sclerosis/motor neuron disease. Amyotroph Lateral Scler. 2008;9(4):195-211. Epub 2008/07/09.
227. Jonsson PA, Graffmo KS, Brannstrom T, Nilsson P, Andersen PM, Marklund SL. Motor neuron disease in mice expressing the wild type-like D90A mutant superoxide dismutase-1. J Neuropathol Exp Neurol. 2006;65(12):1126-36.
228. Zetterstrom P, Stewart HG, Bergemalm D, Jonsson PA, Graffmo KS, Andersen PM, et al. Soluble misfolded subfractions of mutant superoxide dismutase-1s are enriched in spinal cords throughout life in murine ALS models. Proc Natl Acad Sci U S A. 2007;104(35):14157-62.
229. Williamson TL, Cleveland DW. Slowing of axonal transport is a very early event in the toxicity of ALS-linked SOD1 mutants to motor neurons. Nat Neurosci. 1999;2(1):50-6.
230. Boillee S, Vande Velde C, Cleveland DW. ALS: a disease of motor neurons and their nonneuronal neighbors. Neuron. 2006;52(1):39-59.
231. Chung MJ, Suh YL. Ultrastructural changes of mitochondria in the skeletal muscle of patients with amyotrophic lateral sclerosis. Ultrastruct Pathol. 2002;26(1):3-7.
232. Higgins CM, Jung C, Xu Z. ALS-associated mutant SOD1G93A causes mitochondrial vacuolation by expansion of the intermembrane space and by involvement of SOD1 aggregation and peroxisomes. BMC Neurosci. 2003;4:16.
233. Kirkinezos IG, Bacman SR, Hernandez D, Oca-Cossio J, Arias LJ, Perez-Pinzon MA, et al. Cytochrome c association with the inner mitochondrial membrane is impaired in the CNS of G93A-SOD1 mice. J Neurosci. 2005;25(1):164-72.
234. Lederer CW, Torrisi A, Pantelidou M, Santama N, Cavallaro S. Pathways and genes differentially expressed in the motor cortex of patients with sporadic amyotrophic lateral sclerosis. BMC Genomics. 2007;8:26.
235. Xu Z, Jung C, Higgins C, Levine J, Kong J. Mitochondrial degeneration in amyotrophic lateral sclerosis. J Bioenerg Biomembr. 2004;36(4):395-9.
236. Dugan LL, Choi DW. Excitotoxicity, free radicals, and cell membrane changes. Ann Neurol. 1994;35:S17-21.
237. Bowling AC, Beal MF. Bioenergetic and oxidative stress in neurodegenerative diseases. Life Sci. 1995;56(14):1151-71.
238. Kong J, Xu Z. Massive mitochondrial degeneration in motor neurons triggers the onset of amyotrophic lateral sclerosis in mice expressing a mutant SOD1. J Neurosci. 1998;18(9):3241-50.
239. Comi GP, Bordoni A, Salani S, Franceschina L, Sciacco M, Prelle A, et al. Cytochrome c oxidase subunit I microdeletion in a patient with motor neuron disease. Ann Neurol. 1998;43(1):110-6.

240. Fujita K, Yamauchi M, Shibayama K, Ando M, Honda M, Nagata Y. Decreased cytochrome c oxidase activity but unchanged superoxide dismutase and glutathione peroxidase activities in the spinal cords of patients with amyotrophic lateral sclerosis. J Neurosci Res. 1996;45(3):276-81.
241. Jung C, Higgins CM, Xu Z. Mitochondrial electron transport chain complex dysfunction in a transgenic mouse model for amyotrophic lateral sclerosis. J Neurochem. 2002;83(3):535-45.
242. Bilsland LG, Nirmalananthan N, Yip J, Greensmith L, Duchen MR. Expression of mutant SOD1G93A in astrocytes induces functional deficits in motoneuron mitochondria. J Neurochem. 2008;107(5):1271-83.
243. Damiano M, Starkov AA, Petri S, Kipiani K, Kiaei M, Mattiazzi M, et al. Neural mitochondrial Ca2+ capacity impairment precedes the onset of motor symptoms in G93A Cu/Zn-superoxide dismutase mutant mice. J Neurochem. 2006;96(5):1349-61.
244. Jaiswal M, Zech W-D, Goos M, Leutbecher C, Ferri A, Zippelius A, et al. Impairment of mitochondrial calcium handling in a mtSOD1 cell culture model of motoneuron disease. BMC Neuroscience. 2009;10(1):64.
245. Nguyen KT, GarcÃa-ChacÃ³n LE, Barrett JN, Barrett EF, David G. The Î¨m depolarization that accompanies mitochondrial Ca2+ uptake is greater in mutant SOD1 than in wild-type mouse motor terminals. Proc Nat Acad Sci USA. 2009;106(6):2007-11.
246. Li Q, Vande Velde C, Israelson A, Xie J, Bailey AO, Dong M-Q, et al. ALS-linked mutant superoxide dismutase 1 (SOD1) alters mitochondrial protein composition and decreases protein import. Proc Nat Acad Sci USA. 2010;107(49):21146-51.
247. MacAskill AF, Atkin TA, Kittler JT. Mitochondrial trafficking and the provision of energy and calcium buffering at excitatory synapses. Eur J Neurosci. 2010;32(2):231-40.
248. MacAskill AF, Rinholm JE, Twelvetrees AE, Arancibia-Carcamo IL, Muir J, Fransson A, et al. Miro1 Is a Calcium Sensor for Glutamate Receptor-Dependent Localization of Mitochondria at Synapses. Neuron. 2009;61(4):541-55.
249. Bilsland LG, Sahai E, Kelly G, Golding M, Greensmith L, Schiavo G. Deficits in axonal transport precede ALS symptoms in vivo. Proc Natl Acad Sci U S A. 2010;107(47):20523-8. Epub 2010/11/10.
250. De Vos KJ, Chapman AL, Tennant ME, Manser C, Tudor EL, Lau K-F, et al. Familial amyotrophic lateral sclerosis-linked SOD1 mutants perturb fast axonal transport to reduce axonal mitochondria content. Human Molecular Genetics. 2007;16(22):2720-8.
251. Cheah BC, Kiernan MC. Dexpramipexole, the R(+) enantiomer of pramipexole, for the potential treatment of amyotrophic lateral sclerosis. IDrugs. 2010;13(12):911-20.
252. Cudkowicz M, Bozik ME, Ingersoll EW, Miller R, Mitsumoto H, Shefner J, et al. The effects of dexpramipexole (KNS-760704) in individuals with amyotrophic lateral sclerosis. Nat Med. 2011;17:1652-56.
253. Cudkowicz ME, van den Berg LH, Shefner JM, Mitsumoto H, Mora JS, Ludolph A, et al. Dexpramipexole versus placebo for patients with amyotrophic lateral sclerosis (EMPOWER): a randomised, double-blind, phase 3 trial. The Lancet Neurology. 2013;12(11):1059-67.
254. Sasaki S, Iwata M. Impairment of fast axonal transport in the proximal axons of anterior horn neurons in amyotrophic lateral sclerosis. Neurology. 1996;47(2):535-40.
255. Borchelt DR, Wong PC, Becher MW, Pardo CA, Lee MK, Xu ZS, et al. Axonal transport of mutant superoxide dismutase 1 and focal axonal abnormalities in the proximal axons of transgenic mice. Neurobiol Dis. 1998;5(1):27-35.

256. Chow CY, Landers JE, Bergren SK, Sapp PC, Grant AE, Jones JM, et al. Deleterious Variants of FIG4, a Phosphoinositide Phosphatase, in Patients with ALS. Am J Hum Gen. 2009;84(1):85-8.
257. Cox LE, Ferraiuolo L, Goodall EF, Heath PR, Higginbottom A, Mortiboys H, et al. Mutations in CHMP2B in lower motor neuron predominant amyotrophic lateral sclerosis (ALS). PloS one. 2010;5(3):e9872. Epub 2010/03/31.
258. Kieran D, Hafezparast M, Bohnert S, Dick JR, Martin J, Schiavo G, et al. A mutation in dynein rescues axonal transport defects and extends the life span of ALS mice. J Cell Biol. 2005;169(4):561-7.
259. Beers DR, Henkel JS, Xiao Q, Zhao W, Wang J, Yen AA, et al. Wild-type microglia extend survival in PU.1 knockout mice with familial amyotrophic lateral sclerosis. Proc Natl Acad Sci U S A. 2006;103(43):16021-6.
260. Henkel JS, Beers DR, Wen S, Rivera AL, Toennis KM, Appel JE, et al. Regulatory T-lymphocytes mediate amyotrophic lateral sclerosis progression and survival. EMBO Mol Med. 2013;5(1):64-79.
261. Zhao W, Beers D, Appel S. Immune-mediated Mechanisms in the Pathoprogression of Amyotrophic Lateral Sclerosis. J Neuroimmune Pharmacol. 2013;8(4):888-99.
262. Atkin JD, Farg MA, Turner BJ, Tomas D, Lysaght JA, Nunan J, et al. Induction of the unfolded protein response in familial amyotrophic lateral sclerosis and association of protein-disulfide isomerase with superoxide dismutase 1. The Journal of biological chemistry. 2006;281(40):30152-65. Epub 2006/07/19.
263. Atkin JD, Farg MA, Walker AK, McLean C, Tomas D, Horne MK. Endoplasmic reticulum stress and induction of the unfolded protein response in human sporadic amyotrophic lateral sclerosis. Neurobiology of disease. 2008;30(3):400-7. Epub 2008/04/29.
264. Boillee S, Yamanaka K, Lobsiger CS, Copeland NG, Jenkins NA, Kassiotis G, et al. Onset and progression in inherited ALS determined by motor neurons and microglia. Science. 2006;312:1389-92.
265. Nagai M. Rats expressing human cytosolic copper-zinc superoxide dismutase transgenes with amyotrophic lateral sclerosis: associated mutations develop motor neuron disease. J Neurosci. 2001;21:9246-54.
266. Haidet-Phillips AM, Hester ME, Miranda CJ, Meyer K, Braun L, Frakes A, et al. Astrocytes from familial and sporadic ALS patients are toxic to motor neurons. Nat Biotech. 2011;29(9):824-8.
267. Yamanaka K, Chun SJ, Boillee S, Fujimori-Tonou N, Yamashita H, Gutmann DH, et al. Astrocytes as determinants of disease progression in inherited amyotrophic lateral sclerosis. Nat Neurosci. 2008;11(3):251-3.
268. Lino MM, Schneider C, Caroni P. Accumulation of SOD1 mutants in postnatal motoneurons does not cause motoneuron pathology or motoneuron disease. J Neurosci. 2002;22(12):4825-32.
269. Pramatarova A, Laganiere J, Roussel J, Brisebois K, Rouleau GA. Neuron-specific expression of mutant superoxide dismutase 1 in transgenic mice does not lead to motor impairment. J Neurosci. 2001;21(10):3369-74.
270. Gong YH, Parsadanian AS, Andreeva A, Snider WD, Elliott JL. Restricted expression of G86R Cu/Zn superoxide dismutase in astrocytes results in astrocytosis but does not cause motoneuron degeneration. J Neurosci. 2000;20(2):660-5.

271. Vucic S, Kiernan MC. Pathophysiology of neurodegeneration in familial amyotrophic lateral sclerosis. Curr Mol Med. 2009;9(3):255-72. Epub 2009/04/10.
272. Majounie E, Renton AE, Mok K, Dopper EGP, Waite A, Rollinson S, et al. Frequency of the C9orf72 hexanucleotide repeat expansion in patients with amyotrophic lateral sclerosis and frontotemporal dementia: a cross-sectional study. The Lancet Neurology. 2012;11(4):323-30.
273. Al-Sarraj S, King A, Troakes C, Smith B, Maekawa S, Bodi I, et al. P62 positive, TDP-43 negative, neuronal cytoplasmic and intranuclear inclusions in the cerebellum and hippocampus define the pathology of C9orf72-linked FTLD and MND/ALS. Acta neuropathologica. 2011;122(6):691-702.
274. Ling S-C, Polymenidou M, Cleveland DonÂ W. Converging Mechanisms in ALS and FTD: Disrupted RNA and Protein Homeostasis. Neuron. 2013;79(3):416-38.
275. Gijselinck I, Van Langenhove T, van der Zee J, Sleegers K, Philtjens S, Kleinberger G, et al. A C9orf72 promoter repeat expansion in a Flanders-Belgian cohort with disorders of the frontotemporal lobar degeneration-amyotrophic lateral sclerosis spectrum: a gene identification study. Lancet Neurol. 2012;11(1):54-65.
276. Ciura S, Lattante S, Le Ber I, Latouche M, Tostivint H, Brice A, et al. Loss of function of C9orf72 causes motor deficits in a zebrafish model of Amyotrophic Lateral Sclerosis. Ann Neurol. 2013:doi: 10.1002/ana.23946.
277. Mori K, Lammich S, Mackenzie IR, Forne I, Zilow S, Kretzschmar H, et al. hnRNP A3 binds to GGGGCC repeats and is a constituent of p62-positive/TDP43-negative inclusions in the hippocampus of patients with C9orf72 mutations. Acta neuropathologica. 2013;125(3):413-23. Epub 2013/02/06.
278. Donnelly Christopher J, Zhang P-W, Pham Jacqueline T, Heusler Aaron R, Mistry Nipun A, Vidensky S, et al. RNA Toxicity from the ALS/FTD C9ORF72 Expansion Is Mitigated by Antisense Intervention. Neuron. 2013;80(2):415-28.
279. Zu T, Gibbens B, Doty NS, Gomes-Pereira M, Huguet A, Stone MD, et al. Non-ATG–initiated translation directed by microsatellite expansions. Proc Natl Acad Sci USA. 2011;108(1):260-5.
280. Mori K, Weng S-M, Arzberger T, May S, Rentzsch K, Kremmer E, et al. The C9orf72 GGGGCC Repeat Is Translated into Aggregating Dipeptide-Repeat Proteins in FTLD/ALS. Science. 2013;339(6125):1335-8.
281. Ash Peter EA, Bieniek Kevin F, Gendron Tania F, Caulfield T, Lin W-L, DeJesus-Hernandez M, et al. Unconventional Translation of C9ORF72 GGGGCC Expansion Generates Insoluble Polypeptides Specific to c9FTD/ALS. Neuron. 2013;77(4):639-46.
282. Sreedharan J, Blair IP, Tripathi VB, Hu X, Vance C, Rogelj B, et al. TDP-43 mutations in familial and sporadic amyotrophic lateral sclerosis. Science. 2008;319(5870):1668-72.
283. Vance C, Rogelj B, Hortobagyi T, De Vos KJ, Nishimura AL, Sreedharan J, et al. Mutations in FUS, an RNA processing protein, cause familial amyotrophic lateral sclerosis type 6. Science. 2009;323(5918):1208-11. Epub 2009/03/03.
284. Daoud H, Valdmanis PN, Kabashi E, Dion P, Dupré N, Camu W, et al. Contribution of TARDBP mutations to sporadic amyotrophic lateral sclerosis. Journal of medical genetics. 2009;46(2):112-4.
285. Dewey CM, Cenik B, Sephton CF, Dries DR, Mayer P, Good SK, et al. TDP-43 Is Directed to Stress Granules by Sorbitol, a Novel Physiological Osmotic and Oxidative Stressor. Mol Cell Biol. 2011;31(5):1098-108.

286. Sama RRK, Ward CL, Kaushansky LJ, Lemay N, Ishigaki S, Urano F, et al. FUS/TLS assembles into stress granules and is a prosurvival factor during hyperosmolar stress. J Cell Physiol. 2013;228(11):2222-31.
287. Sephton CF, Cenik C, Kucukural A, Dammer EB, Cenik B, Han Y, et al. Identification of neuronal RNA targets of TDP-43-containing ribonucleoprotein complexes. The Journal of biological chemistry. 2011;286(2):1204-15. Epub 2010/11/06.
288. Lagier-Tourenne C, Polymenidou M, Cleveland DW. TDP-43 and FUS/TLS: emerging roles in RNA processing and neurodegeneration. Hum Mol Genet. 2010;19(R1):R46-R64.
289. Kwiatkowski TJ, Jr., Bosco DA, Leclerc AL, Tamrazian E, Vanderburg CR, Russ C, et al. Mutations in the FUS/TLS gene on chromosome 16 cause familial amyotrophic lateral sclerosis. Science. 2009;323(5918):1205-8. Epub 2009/03/03.
290. Blair IP, Williams KL, Warraich ST, Durnall JC, Thoeng AD, Manavis J, et al. FUS mutations in amyotrophic lateral sclerosis: clinical, pathological, neurophysiological and genetic analysis. J Neurol Neurosurg Psychiatry. 2010;81:1286-8. Epub 2009/12/08.
291. Ticozzi N, Silani V, LeClerc AL, Keagle P, Gellera C, Ratti A, et al. Analysis of FUS gene mutation in familial amyotrophic lateral sclerosis within an Italian cohort. Neurology. 2009;73(15):1180-5. Epub 2009/09/11.
292. Yan J, Deng HX, Siddique N, Fecto F, Chen W, Yang Y, et al. Frameshift and novel mutations in FUS in familial amyotrophic lateral sclerosis and ALS/dementia. Neurology. 2010;75(9):807-14. Epub 2010/07/30.
293. Van Langenhove T, van der Zee J, Sleegers K, Engelborghs S, Vandenberghe R, Gijselinck I, et al. Genetic contribution of FUS to frontotemporal lobar degeneration. Neurology. 2010;74(5):366-71. Epub 2010/02/04.
294. Chio A, Borghero G, Pugliatti M, Ticca A, Calvo A, Moglia C, et al. Large proportion of amyotrophic lateral sclerosis cases in Sardinia due to a single founder mutation of the TARDBP gene. Archives of neurology. 2011;68(5):594-8. Epub 2011/01/12.
295. Millecamps S, Salachas F, Cazeneuve C, Gordon P, Bricka B, Camuzat A, et al. SOD1, ANG, VAPB, TARDBP, and FUS mutations in familial amyotrophic lateral sclerosis: genotype–phenotype correlations. Journal of medical genetics. 2010;47(8):554-60.
296. Benajiba L, Le Ber I, Camuzat A, Lacoste M, Thomas-Anterion C, Couratier P, et al. TARDBP mutations in motoneuron disease with frontotemporal lobar degeneration. Ann Neurol. 2009;65(4):470-3.
297. Quadri M, Cossu G, Saddi V, Simons E, Murgia D, Melis M, et al. Broadening the phenotype of TARDBP mutations: the TARDBP Ala382Thr mutation and Parkinson's disease in Sardinia. Neurogenetics. 2011;12(3):203-9.
298. Xu Y-F, Zhang Y-J, Lin W-L, Cao X, Stetler C, Dickson D, et al. Expression of mutant TDP-43 induces neuronal dysfunction in transgenic mice. Molecular Neurodegeneration. 2011;6(1):73.
299. Wils H, Kleinberger G, Janssens J, Pereson S, Joris G, Cuijt I, et al. TDP-43 transgenic mice develop spastic paralysis and neuronal inclusions characteristic of ALS and frontotemporal lobar degeneration. Proc Natl Acad Sci USA. 2010;107:3858 - 63.
300. Xu Y, Gendron T, Zhang Y, Lin W, D'Alton S, Sheng H, et al. Wild-type human TDP-43 expression causes TDP-43 phosphorylation, mitochondrial aggregation, motor deficits, and early mortality in transgenic mice. The Journal of neuroscience : the official journal of the Society for Neuroscience. 2010;30:10851 - 9.

301. Igaz L, Kwong L, Lee E, Chen-Plotkin A, Swanson E, Unger T, et al. Dysregulation of the ALS-associated gene TDP-43 leads to neuronal death and degeneration in mice. The Journal of clinical investigation. 2011;121:726 - 38.
302. Shan X, Chiang P, Price D, Wong P. Altered distributions of Gemini of coiled bodies and mitochondria in motor neurons of TDP-43 transgenic mice. Proc Natl Acad Sci USA. 2010;107:16325 - 30.
303. Swarup V, Phaneuf D, Bareil C, Robertson J, Rouleau G, Kriz J, et al. Pathological hallmarks of amyotrophic lateral sclerosis/frontotemporal lobar degeneration in transgenic mice produced with TDP-43 genomic fragments. Brain. 2011;134:2610 - 26.
304. Tsai K, Yang C, Fang Y, Cho K, Chien W, Wang W, et al. Elevated expression of TDP-43 in the forebrain of mice is sufficient to cause neurological and pathological phenotypes mimicking FTLD-U. J Exp Med. 2010;207:1661 - 73.
305. Wegorzewska I, Bell S, Cairns N, Miller T, Baloh R. TDP-43 mutant transgenic mice develop features of ALS and frontotemporal lobar degeneration. Proc Natl Acad Sci USA. 2009;106:18809 - 14.
306. Van Deerlin VM, Leverenz JB, Bekris LM, Bird TD, Yuan W, Elman LB, et al. TARDBP mutations in amyotrophic lateral sclerosis with TDP-43 neuropathology: a genetic and histopathological analysis. Lancet Neurol. 2008;7(5):409-16.
307. Wu LS, Cheng WC, Shen CK. Targeted depletion of TDP-43 expression in the spinal cord motor neurons leads to the development of amyotrophic lateral sclerosis-like phenotypes in mice. The Journal of biological chemistry. 2012;287(33):27335-44. Epub 2012/06/22.
308. Iguchi Y, Katsuno M, Niwa J-i, Takagi S, Ishigaki S, Ikenaka K, et al. Loss of TDP-43 causes age-dependent progressive motor neuron degeneration. Brain. 2013;136(5):1371-82.
309. Shelkovnikova TA, Peters OM, Deykin AV, Connor-Robson N, Robinson H, Ustyugov AA, et al. Fused in Sarcoma (FUS) Protein Lacking Nuclear Localization Signal (NLS) and Major RNA Binding Motifs Triggers Proteinopathy and Severe Motor Phenotype in Transgenic Mice. The Journal of biological chemistry. 2013;288(35):25266-74. Epub 2013/07/23.
310. Murakami T, Yang SP, Xie L, Kawano T, Fu D, Mukai A, et al. ALS mutations in FUS cause neuronal dysfunction and death in Caenorhabditis elegans by a dominant gain-of-function mechanism. Hum Mol Genet. 2012;21(1):1-9. Epub 2011/09/29.
311. Colombrita C, Zennaro E, Fallini C, Weber M, Sommacal A, Buratti E, et al. TDP-43 is recruited to stress granules in conditions of oxidative insult. J Neurochem. 2009;111(4):1051-61.
312. Andersson M, Stahlberg A, Arvidsson Y, Olofsson A, Semb H, Stenman G, et al. The multifunctional FUS, EWS and TAF15 proto-oncoproteins show cell type-specific expression patterns and involvement in cell spreading and stress response. BMC Cell Biology. 2008;9(1):37.
313. Liu-Yesucevitz L, Bilgutay A, Zhang YJ, Vanderweyde T, Citro A, Mehta T, et al. Tar DNA binding protein-43 (TDP-43) associates with stress granules: analysis of cultured cells and pathological brain tissue. PloS one. 2010;5(10):e13250. Epub 2010/10/16.
314. Ito D, Seki M, Tsunoda Y, Uchiyama H, Suzuki N. Nuclear transport impairment of amyotrophic lateral sclerosis-linked mutations in FUS/TLS. Ann Neurology. 2011;69(1):152-62.
315. Bosco DA, Lemay N, Ko HK, Zhou H, Burke C, Kwiatkowski TJ, et al. Mutant FUS proteins that cause amyotrophic lateral sclerosis incorporate into stress granules. Hum Mol Genet. 2010;19(21):4160-75.
316. Bentmann E, Haass C, Dormann D. Stress granules in neurodegeneration – lessons learnt from TAR DNA binding protein of 43 kDa and fused in sarcoma. FEBS J. 2013;280(18):4348-70.

317. Dormann D, Rodde R, Edbauer D, Bentmann E, Fischer I, Hruscha A, et al. ALS-associated fused in sarcoma (FUS) mutations disrupt Transportin-mediated nuclear import. EMBO J. 2010;29(16):2841-57.
318. Dewey CM, Cenik B, Sephton CF, Johnson BA, Herz J, Yu G. TDP-43 aggregation in neurodegeneration: are stress granules the key? Brain Res. 2012;1462:16-25. Epub 2012/03/13.
319. Deng H-X, Chen W, Hong S-T, Boycott KM, Gorrie GH, Siddique N, et al. Mutations in UBQLN2 cause dominant X-linked juvenile and adult-onset ALS and ALS/dementia. Nature. 2011;477(7363):211-5.
320. van Es MA, Veldink JH, Saris CGJ, Blauw HM, van Vught PWJ, Birve A, et al. Genome-wide association study identifies 19p13.3 (UNC13A) and 9p21.2 as susceptibility loci for sporadic amyotrophic lateral sclerosis. Nature genetics. 2009;41(10):1083-7.
321. Chen HJ, Anagnostou G, Chai A, Withers J, Morris A, Adhikaree J, et al. Characterization of the properties of a novel mutation in VAPB in familial amyotrophic lateral sclerosis. J Bio Chem. 2010;285(51):40266-81.
322. Johnson JO, Mandrioli J, Benatar M, Abramzon Y, Van Deerlin VM, Trojanowski JQ, et al. Exome Sequencing Reveals VCP Mutations as a Cause of Familial ALS. Neuron. 2010;68(5):857-64.
323. Fecto F, Yan J, Vemula SP, Liu E, Yang Y, Chen W, et al. SQSTM1 mutations in familial and sporadic amyotrophic lateral sclerosis. Archives of neurology. 2011;68(11):1440-6.
324. Del Bo R, Tiloca C, Pensato V, Corrado L, Ratti A, Ticozzi N, et al. Novel optineurin mutations in patients with familial and sporadic amyotrophic lateral sclerosis. Journal of Neurology, Neurosurgery and Psychiatry. 2011;82(11):1239-43.
325. Bostock H, Sharief MK, Reid G, Murray NM. Axonal ion channel dysfunction in amyotrophic lateral sclerosis. Brain 1995;118:217-25.
326. Kiernan M, Burke D. Threshold electrotonus in the assessment of Motor Neuron Disease. In: Daube J, Mauguiere F, editors. Handbook of Clinical Neurophysiology. Amsterdam: Elsevier; 2004. p. 359-66.
327. Mogyoros I, Kiernan MC, Burke D, Bostock H. Ischemic resistance of cutaneous afferents and motor axons in patients with amyotrophic lateral sclerosis. Muscle Nerve. 1998;21(12):1692-700.
328. Baker M, Bostock H. Depolarization changes the mechanism of accommodation in rat and human motor axons. J Physiol (Lond). 1989;411:545-61.
329. Bostock H, Burke D, Hales JP. Differences in behaviour of sensory and motor axons following release of ischaemia. Brain : a journal of neurology. 1994;117(Pt 2):225-34.
330. Mogyoros I, Kiernan MC, Burke D, Bostock H. Excitability changes in human sensory and motor axons during hyperventilation and ischaemia. Brain : a journal of neurology. 1997;120(Pt 2):317-25.
331. Grosskreutz J, Lin C, Mogyoros I, Burke D. Changes in excitability indices of cutaneous afferents produced by ischaemia in human subjects. J Physiol (Lond). 1999;518(Pt 1):301-14.
332. Grosskreutz J, Lin CS, Mogyoros I, Burke D. Ischaemic changes in refractoriness of human cutaneous afferents under threshold-clamp conditions. J Physiol (Lond). 2000;523:807-15.
333. Bostock H. The strength-duration relationship for excitation of myelinated nerve: computed dependence on membrane parameters. J Physiol (Lond). 1983;341:59-74.
334. Mogyoros I, Kiernan MC, Burke D. Strength-duration properties of human peripheral nerve. Brain. 1996;119(2):439-47.

335. Mogyoros I, Lin C, Dowla S, Grosskreutz J, Burke D. Strength-duration properties and their voltage dependence at different sites along the median nerve. Clin Neurophysiol. 1999;110(9):1618-24.
336. Weiss G. Sur la possibilité de rendre comparables entre eux les appareils servant l'excitation électrique. Arch Ital Biol. 1901;35:413-46.
337. Bostock H, Rothwell JC. Latent addition in motor and sensory fibres of human peripheral nerve. J Physiol (Lond). 1997;498(Pt 1):277-94.
338. French CR, Sah P, Buckett KJ, Gage PW. A voltage-dependent persistent sodium current in mammalian hippocampal neurons. J Gen Physiol. 1990;95:1139-57.
339. Crill WE. Persistent sodium current in mammalian central neurons. Annu Rev Physiol. 1996;58:349-62.
340. Catterall WA. From ionic currents to molecular mechanisms: the structure and function of voltage-gated sodium channels. Neuron. 2000;26(1):13-25.
341. Catterall WA, Goldin AL, Waxman SG. International Union of Pharmacology. XLVII. Nomenclature and structure-function relationships of voltage-gated sodium channels. Pharmacol Rev. 2005;57:397-409.
342. Baker MD, Bostock H. Inactivation of macroscopic late Na+ current and characteristics of unitary late Na+ currents in sensory neurons. J Neurophysiol. 1998;80:2538-49.
343. Catterall WA. Voltage-gated sodium channels at 60: structure, function and pathophysiology. J Physiol. 2012;590(11):2577-89.
344. Goldin AL. Resurgence of sodium channel research. Annu Rev Physiol. 2001;63:871-94.
345. Brown AM, Schwindt PC, Crill WE. Different voltage dependence of transient and persistent Na+ currents is compatible with modal-gating hypothesis for sodium channels. J Neurophysiol. 1994;71:2562-5.
346. Chen Y, Yu FH, Surmeier DJ, Scheuer T, Catterall WA. Neuromodulation of Na+ channel slow inactivation via cAMP-dependent protein kinase and protein kinase C. Neuron. 2006;49(3):409-20.
347. Carr DB, Day M, Cantrell AR, Held J, Scheuer T, Catterall WA, et al. Transmitter modulation of slow, activity-dependent alterations in sodium channel availability endows neurons with a novel form of cellular plasticity. Neuron. 2003;39(5):793-806.
348. Brismar T. Electrical properties of isolated demyelinated rat nerve fibres. Acta Physiol Scand. 1981;113(2):161-6.
349. Mogyoros I, Kiernan MC, Gracies JM, Burke D. The effect of stimulus duration on the latency of submaximal nerve volleys. Muscle Nerve. 1996;19(10):1354-6.
350. Kiernan MC, Krishnan AV, Lin CS, Burke D, Berkovic SF. Mutation in the Na+ channel subunit SCN1B produces paradoxical changes in peripheral nerve excitability. Brain : a journal of neurology. 2005;128(Pt 8):1841-6.
351. Kuo JJ, Siddique T, Fu R, Heckman CJ. Increased persistent Na(+) current and its effect on excitability in motoneurones cultured from mutant SOD1 mice. J Physiol (Lond). 2005;563(Pt 3):843-54.
352. Shibuya K, Misawa S, Nasu S, Sekiguchi Y, Mitsuma S, Beppu M, et al. Split hand syndrome in amyotrophic lateral sclerosis: different excitability changes in the thenar and hypothenar motor axons. J Neurol Neurosurg Psychiatry. 2013;84(9):969-72.
353. Kiernan MC, Burke, D. Threshold electronus and the assessment of nerve excitability in amyotrophic lateral sclerosis. In: Eisen A, editor. Clinical Neurophysiology of Motor Neuron Diseases. Amsterdam: Elsevier; 2004. p. 359-66.

354. Kiernan MC, Burke D, Andersen KV, Bostock H. Multiple measures of axonal excitability: a new approach in clinical testing. Muscle Nerve. 2000;23(3):399-409.
355. Kiernan MC, Lin CS, Andersen KV, Murray NM, Bostock H. Clinical evaluation of excitability measures in sensory nerve. Muscle Nerve. 2001;24(7):883-92.
356. Bostock H, Baker M. Evidence for two types of potassium channel in human motor axons in vivo. Brain Research. 1988;462(2):354-8.
357. Krishnan AV, Lin CS, Park SB, Kiernan MC. Axonal ion channels from bench to bedside: a translational neuroscience perspective. Prog Neurobiol. 2009;89(3):288-313. Epub 2009/08/25.
358. Pape HC. Queer current and pacemaker: the hyperpolarization-activated cation current in neurons. Annu Rev Physiol. 1996;58:299-327.
359. Yu FH, Yarov-Yarovoy V, Gutman GA, Catterall WA. Overview of molecular relationships in the voltage-gated ion channel superfamily. Pharmacol Rev. 2005;57:387-95.
360. Judge SI, Bever CT, Jr. Potassium channel blockers in multiple sclerosis: neuronal Kv channels and effects of symptomatic treatment. Pharmacol Ther. 2006;111:224-59.
361. Baker M, Bostock H, Grafe P, Martius P. Function and distribution of three types of rectifying channel in rat spinal root myelinated axons. J Physiol (Lond). 1987;383:45-67.
362. Gordon TR, Kocsis JD, Waxman SG. Evidence for the presence of two types of potassium channels in the rat optic nerve. Brain Res. 1988;447(1):1-9.
363. Safronov BV, Bischoff U, Vogel W. Single voltage-gated K+ channels and their functions in small dorsal root ganglion neurones of rat. J Physiol (Lond). 1996;493:393-408.
364. Safronov BV, Kampe K, Vogel W. Single voltage-dependent potassium channels in rat peripheral nerve membrane. J Physiol (Lond). 1993;460:675-91.
365. Roper J, Schwarz JR. Heterogeneous distribution of fast and slow potassium channels in myelinated rat nerve fibres. J Physiol (Lond). 1989;416:93-110.
366. Chiu SY, Ritchie JM. On the physiological role of internodal potassium channels and the security of conduction in myelinated nerve fibres. Proc R Soc Lond B Biol Sci. 1984;220(1221):415-22.
367. Kiernan MC, Bostock H. Effects of membrane polarization and ischaemia on the excitability properties of human motor axons. Brain : a journal of neurology. 2000;123:2542-51.
368. Bostock H, Sharief MK, Reid G, Murray NMF. Axonal ion channel dysfunction in amyotrophic lateral sclerosis. Brain. 1995;118(1):217-25.
369. Kiernan MC, Guglielmi JM, Kaji R, Murray NM, Bostock H. Evidence for axonal membrane hyperpolarization in multifocal motor neuropathy with conduction block. Brain : a journal of neurology. 2002;125(Pt 3):664-75.
370. Kiernan MC, Walters RJ, Andersen KV, Taube D, Murray NM, Bostock H. Nerve excitability changes in chronic renal failure indicate membrane depolarization due to hyperkalaemia. Brain : a journal of neurology. 2002;125(Pt 6):1366-78.
371. Horn S, Quasthoff S, Grafe P, Bostock H, Renner R, Schrank B. Abnormal axonal inward rectification in diabetic neuropathy. Muscle Nerve. 1996;19(10):1268-75.
372. Krishnan AV, Kiernan MC. Altered nerve excitability properties in established diabetic neuropathy. Brain : a journal of neurology. 2005;128(Pt 5):1178-87.
373. Krishnan AV, Phoon RK, Pussell BA, Charlesworth JA, Bostock H, Kiernan MC. Altered motor nerve excitability in end-stage kidney disease. Brain : a journal of neurology. 2005;128(Pt 9):2164-74.

374. Krishnan AV, Phoon RK, Pussell BA, Charlesworth JA, Bostock H, Kiernan MC. Neuropathy, axonal Na(+)/K(+) pump function and activity-dependent excitability changes in end-stage kidney disease. Clin Neurophysiol. 2006.
375. Krishnan AV, Phoon RK, Pussell BA, Charlesworth JA, Kiernan MC. Sensory nerve excitability and neuropathy in end stage kidney disease. J Neurol Neurosurg Psychiatry. 2006;77(4):548-51.
376. Park SB, Lin CS-Y, Krishnan AV, Goldstein D, Friedlander ML, Kiernan MC. Oxaliplatin-induced neurotoxicity: changes in axonal excitability precede development of neuropathy. Brain : a journal of neurology. 2009;132(10):2712-23.
377. Mayer M, Westbrook G. A voltage-clamp analysis of inward (anomalous) rectification in mouse spinal sensory ganglion neurones. The Journal of physiology. 1983;340(1):19-45.
378. Pape H-C. Queer current and pacemaker: the hyperpolarization-activated cation current in neurons. Annual Review of Physiology. 1996;58(1):299-327.
379. Jan LY, Jan YN. Voltage-gated and inwardly rectifying potassium channels. The Journal of physiology. 1997;505(2):267-82.
380. Baker M, Bostock H, Grafe P, Martius P. Function and distribution of three types of rectifying channel in rat spinal root myelinated axons. The Journal of physiology. 1987;383(1):45-67.
381. Bader C, Bertrand D. Effect of changes in intra-and extracellular sodium on the inward (anomalous) rectification in salamander photoreceptors. The Journal of physiology. 1984;347(1):611-31.
382. Bayliss DA, Viana F, Bellingham MC, Berger AJ. Characteristics and postnatal development of a hyperpolarization-activated inward current in rat hypoglossal motoneurons in vitro. Journal of Neurophysiology. 1994;71(1):119-28.
383. Vagg R, Mogyoros I, Kiernan MC, Burke D. Activity-dependent hyperpolarization of human motor axons produced by natural activity. The Journal of physiology. 1998;507(3):919-25.
384. Kaji R, Bostock H, Kohara N, Murase N, Kimura J, Shibasaki H. Activity-dependent conduction block in multifocal motor neuropathy. Brain. 2000;123(8):1602-11.
385. Cappelen-Smith C, Kuwabara S, Lin CSY, Mogyoros I, Burke D. Activity-dependent hyperpolarization and conduction block in chronic inflammatory demyelinating polyneuropathy. Annals of neurology. 2000;48(6):826-32.
386. Kiernan MC, Lin CSY, Burke D. Differences in activity-dependent hyperpolarization in human sensory and motor axons. The Journal of physiology. 2004;558(1):341-9.
387. Lin CS, Kuwabara S, Cappelen-Smith C, Burke D. Responses of human sensory and motor axons to the release of ischaemia and to hyperpolarizing currents. The Journal of physiology. 2002;541(3):1025-39.
388. Hodgkin A, Huxley A. A quantitative descirption of membrane current and its application to conduction and excitation in nerve. J Physiol (Lond). 1952(117):500-44.
389. Scholz A, Reid G, Vogel W, Bostock H. Ion channels in human axons. J Neurophysiol. 1993;70:1274-9.
390. Burke D, Kiernan M, Mogyoros I, Bostock H. Susceptibility to conduction block: differences in the biophysical properties of cutaneous afferents and motor axons. Physiology of ALS and Related Diseases. 1997:43-53.
391. Kiernan MC, Cikurel K, Bostock H. Effects of temperature on the excitability properties of human motor axons. Brain. 2001;124(4):816-25.

392. Barrett EF, Barrett JN. Intracellular recording from vertebrate myelinated axons: mechanism of the depolarizing afterpotential. J Physiol (Lond). 1982;323:117-44.
393. McIntyre CC, Richardson AG, Grill WM. Modeling the excitability of mammalian nerve fibers: influence of afterpotentials on the recovery cycle. J Neurophysiol. 2002;87(2):995-1006.
394. Jonas P, Brau ME, Hermsteiner M, Vogel W. Single-channel recording in myelinated nerve fibers reveals one type of Na channel but different K channels. Proc Natl Acad Sci U S A. 1989;86:7238-42.
395. Vabnick I, Shrager P. Ion channel redistribution and function during development of the myelinated axon. J Neurobiol. 1998;37(1):80-96.
396. Reid G, Scholz A, Bostock H, Vogel W. Human axons contain at least five types of voltage-dependent potassium channel. J Physiol (Lond). 1999;518:681-96.
397. Barrett EF, Barrett JN. Intracellular recording from vertebrate myelinated axons: mechanism of the depolarizing afterpotential. The Journal of physiology. 1982;323(1):117-44.
398. Krishnan AV, Phoon RK, Pussell BA, Charlesworth JA, Bostock H, Kiernan MC. Altered motor nerve excitability in end-stage kidney disease. Brain. 2005;128(9):2164-74.
399. Barker AT, Jalinous R, Freeston IL. Non-invasive magnetic stimulation of human motor cortex. Lancet. 1985;1(8437):1106-7.
400. Rossini PM, Barker AT, Berardelli A, Caramia MD, Caruso G, Cracco RQ, et al. Non-invasive electrical and magnetic stimulation of the brain, spinal cord and roots: basic principles and procedures for routine clinical application. Report of an IFCN committee. Electroencephalogr Clin Neurophysiol. 1994;91(2):79-92.
401. Chen R, Cros D, Curra A, Di Lazzaro V, Lefaucheur JP, Magistris MR, et al. The clinical diagnostic utility of transcranial magnetic stimulation: report of an IFCN committee. Clin Neurophysiol. 2008;119:504-32.
402. Abdeen MA, Stuchly MA. Modeling of magnetic field stimulation of bent neurons. IEEE Trans Biomed Eng. 1994;41(11):1092-5.
403. Mills K. Magnetic stimulation and central conduction time. Eisen A, editor. Amsterdam: Elsevier B.V.; 2004. 283-93 p.
404. Patton HD, Amassian VE. Single and multiple-unit analysis of cortical stage of pyramidal tract activation. J Neurophysiol. 1954;17(4):345-63.
405. Rudiak D, Marg E. Finding the depth of magnetic brain stimulation: a re-evaluation. Electroencephalogr Clin Neurophysiol. 1994;93(5):358-71.
406. Kaneko K, Fuchigami Y, Morita H, Ofuji A, Kawai S. Effect of coil position and stimulus intensity in transcranial magnetic stimulation on human brain. J Neurol Sci. 1997;147(2):155-9.
407. Di Lazzaro V, Oliviero A, Profice P, Saturno E, Pilato F, Insola A, et al. Comparison of descending volleys evoked by transcranial magnetic and electric stimulation in conscious humans. Electroencephalography and Clinical Neurophysiology/Electromyography and Motor Control. 1998;109(5):397-401.
408. Werhahn KJ, Fong JK, Meyer BU, Priori A, Rothwell JC, Day BL, et al. The effect of magnetic coil orientation on the latency of surface EMG and single motor unit responses in the first dorsal interosseous muscle. Electroencephalogr Clin Neurophysiol. 1994;93(2):138-46.
409. Kaneko K, Kawai S, Fuchigami Y, Morita H, Ofuji A. The effect of current direction induced by transcranial magnetic stimulation on the corticospinal excitability in human brain. Electroencephalogr Clin Neurophysiol. 1996;101(6):478-82.

410. Sakai K, Ugawa Y, Terao Y, Hanajima R, Furubayashi T, Kanazawa I. Preferential activation of different I waves by transcranial magnetic stimulation with a figure-of-eight-shaped coil. Exp Brain Res. 1997;113(1):24-32.
411. Di Lazzaro V, Oliviero A, Mazzone P, Pilato F, Saturno E, Dileone M, et al. Generation of I waves in the human: spinal recordings. Supplements to Clinical Neurophysiology. 2003;56:143-52.
412. Di Lazzaro V, Oliviero A, Pilato F, Mazzone P, Insola A, Ranieri F, et al. Corticospinal volleys evoked by transcranial stimulation of the brain in conscious humans. Neurological Research. 2003;25(2):143-50.
413. Day BL, Dressler D, Maertens de Noordhout A, Marsden CD, Nakashima K, Rothwell JC, et al. Electric and magnetic stimulation of human motor cortex: surface EMG and single motor unit responses. J Physiol (Lond). 1989;412:449-73.
414. Ziemann U, Rothwell JC. I-waves in motor cortex. J Clin Neurophysiol. 2000;17(4):397-405.
415. Rossini PM, Berardelli A, Deuschl G, Hallett M, Maertens de Noordhout AM, Paulus W, et al. Applications of magnetic cortical stimulation. The International Federation of Clinical Neurophysiology. Electroencephalogr Clin Neurophysiol Suppl. 1999;52:171-85.
416. Fisher RJ, Nakamura Y, Bestmann S, Rothwell JC, Bostock H. Two phases of intracortical inhibition revealed by transcranial magnetic threshold tracking. Exp Brain Res. 2002;143:240-8.
417. Vucic S, Howells J, Trevillion L, Kiernan MC. Assessment of cortical excitability using threshold tracking techniques. Muscle Nerve. 2006;33:477-86.
418. Groppa S, Oliviero A, Eisen A, Quartarone A, Cohen LG, Mall V, et al. A practical guide to diagnostic transcranial magnetic stimulation: report of an IFCN committee. Clin Neurophysiol. 2012;123(5):858-82. Epub 2012/02/22.
419. Brouwer B, Ashby P. Corticospinal projections to upper and lower limb spinal motoneurons in man. Electroencephalogr Clin Neurophysiol. 1990;76(6):509-19.
420. Chen R, Tam A, Butefisch C, Corwell B, Ziemann U, Rothwell JC, et al. Intracortical inhibition and facilitation in different representations of the human motor cortex. J Neurophysiol. 1998;80(6):2870-81.
421. Macdonell RA, Shapiro BE, Chiappa KH, Helmers SL, Cros D, Day BJ, et al. Hemispheric threshold differences for motor evoked potentials produced by magnetic coil stimulation. Neurology. 1991;41(9):1441-4.
422. Triggs WJ, Calvanio R, Levine M. Transcranial magnetic stimulation reveals a hemispheric asymmetry correlate of intermanual differences in motor performance. Neuropsychologia. 1997;35(10):1355-63.
423. Amassian VE, Stewart M, Quirk GJ, Rosenthal JL. Physiological basis of motor effects of a transient stimulus to cerebral cortex. Neurosurgery. 1987;20(1):74-93.
424. Epstein CM, Schwartzberg DG, Davey KR, Sudderth DB. Localizing the site of magnetic brain stimulation in humans. Neurology. 1990;40(4):666-70.
425. Di Lazzaro V, Oliviero A, Profice P, Pennisi MA, Pilato F, Zito G, et al. Ketamine increases human motor cortex excitability to transcranial magnetic stimulation. Journal of Physiology. 2003;547(Pt 2):485-96.
426. Ziemann U. TMS and drugs. Clin Neurophysiol. 2004;115:1717-29.

427. Rossini PM, Desiato M, Lavaroni F, Caramia M. Brain excitability and electroencephalographic activation: non-invasive evaluation in healthy humans via transcranial magnetic stimulation. Brain Research. 1991;567(1):111-9.
428. Attarian S, Azulay JP, Lardillier D, Verschueren A, Pouget J. Transcranial magnetic stimulation in lower motor neuron diseases. Clin Neurophysiol. 2005;116:35-42.
429. Berardelli A, Inghilleri M, Cruccu G, Mercuri B, Manfredi M. Electrical and magnetic transcranial stimulation in patients with corticospinal damage due to stroke or motor neurone disease. Electroencephalogr Clin Neurophysiol. 1991;81(5):389-96.
430. Eisen A, Shytbel W, Murphy K, Hoirch M. Cortical magnetic stimulation in amyotrophic lateral sclerosis. Muscle Nerve. 1990;13(2):146-51.
431. de Carvalho M, Turkman A, Swash M. Motor responses evoked by transcranial magnetic stimulation and peripheral nerve stimulation in the ulnar innervation in amyotrophic lateral sclerosis: the effect of upper and lower motor neuron lesion. J Neurol Sci. 2003;210(1-2):83-90.
432. Miscio G, Pisano F, Mora G, Mazzini L. Motor neuron disease: usefulness of transcranial magnetic stimulation in improving the diagnosis. Clin Neurophysiol. 1999;110(5):975-81.
433. Triggs WJ, Macdonell RA, Cros D, Chiappa KH, Shahani BT, Day BJ. Motor inhibition and excitation are independent effects of magnetic cortical stimulation. Annals of Neurol. 1992;32(3):345-51.
434. Triggs WJ, Menkes D, Onorato J, Yan RS, Young MS, Newell K, et al. Transcranial magnetic stimulation identifies upper motor neuron involvement in motor neuron disease. Neurology. 1999;53:605-11.
435. Urban P, Wicht S, Hopf H. Sensitivity of transcranial magnetic stimulation of cortico-bulbar vs. cortico-spinal tract involvement in ALS. J Neurol. 2001;248(248):850-5.
436. Kohara N, Kaji R, Kojima Y, Mills KR, Fujii H, Hamano T, et al. Abnormal excitability of the corticospinal pathway in patients with amyotrophic lateral sclerosis: a single motor unit study using transcranial magnetic stimulation. Electroencephalogr Clin Neurophysiol. 1996;101(1):32-41.
437. Mills KR, Nithi KA. Corticomotor threshold is reduced in early sporadic amyotrophic lateral sclerosis. Muscle Nerve. 1997;20:1137-41.
438. Hirota N, Eisen A, Weber M. Complex fasciculations and their origin in amyotrophic lateral sclerosis and Kennedy's disease. Muscle Nerve. 2000;23:1872-5.
439. Di Lazzaro V, Restuccia D, Oliviero A, Profice P, Ferrara L, Insola A, et al. Magnetic transcranial stimulation at intensities below active motor threshold activates intracortical inhibitory circuits. Exp Brain Res. 1998;119:265-8.
440. Devanne H, Lavoie BA, Capaday C. Input-output properties and gain changes in the human corticospinal pathway. Exp Brain Res. 1997;114(2):329-38.
441. Ziemann U. Cortical threshold and excitability measurements. In: Eisen A, editor. Clinical Neurophysiology of Motor Neuron Diseases Handbook of Clinical Neurophysiology. Amsterdam: Elsevier; 2004. p. 317-35.
442. Hess CW, Mills KR, Murray NM, Schriefer TN. Magnetic brain stimulation: central motor conduction studies in multiple sclerosis. Ann Neurol. 1987;22(6):744-52.
443. Paulus W, Classen J, Cohen LG, Large CH, Di Lazzaro V, Nitsche M, et al. State of the art: Pharmacologic effects on cortical excitability measures tested by transcranial magnetic stimulation. Brain Stimul. 2008;1(3):151-63. Epub 2008/07/01.
444. Boroojerdi B, Battaglia F, Muellbacher W, Cohen LG. Mechanisms influencing stimulus-response properties of the human corticospinal system. Clin Neurophysiol. 2001;112(5):931-7.

445. Vucic S, Nicholson GA, Kiernan MC. Cortical excitability in hereditary motor neuronopathy with pyramidal signs: comparison with ALS. J Neurol Neurosurg Psychiatry. 2010;81(1):97-100.
446. Mills K. Magnetic stimulation and central conduction time. In: A E, editor. Clinical Neurophysiology of Motor Neuron Diseases Handbook of Clinical Neurophysiology. Amsterdam: Elsevier; 2004. p. 283-93.
447. Claus D. Central motor conduction: method and normal results. Muscle Nerve. 1990;13(12):1125-32.
448. Mills KR, Murray NM. Electrical stimulation over the human vertebral column: which neural elements are excited? Electroencephalogr Clin Neurophysiol. 1986;63(6):582-9.
449. Mills KR. The natural history of central motor abnormalities in amyotrophic lateral sclerosis. Brain 2003;126:2558-66.
450. Eisen A, Entezari-Taher M, Stewart H. Cortical projections to spinal motoneurons: changes with aging and amyotrophic lateral sclerosis. Neurology. 1996;46(5):1396-404.
451. Komissarow L, Rollnik JD, Bogdanova D, Krampfl K, Khabirov FA, Kossev A, et al. Triple stimulation technique (TST) in amyotrophic lateral sclerosis. Clin Neurophysiol. 2004;115(2):356-60.
452. Cantello R, Gianelli M, Civardi C, Mutani R. Magnetic brain stimulation: the silent period after the motor evoked potential. Neurology. 1992;42(10):1951-9.
453. Inghilleri M, Berardelli A, Cruccu G, Manfredi M. Silent period evoked by transcranial stimulation of the human cortex and cervicomedullary junction. J Physiol (Lond). 1993;466:521-34.
454. Triggs WJ, Kiers L, Cros D, Fang J, Chiappa KH. Facilitation of magnetic motor evoked potentials during the cortical stimulation silent period. Neurology. 1993;43(12):2615-20.
455. Cantello R, Gianelli M, Civardi C, Mutani R. Magnetic brain stimulation: the silent period after the motor evoked potential. Neurology. 1992;42:1951-9.
456. Connors BW, Malenka RC, Silva LR. Two inhibitory postsynaptic potentials, and GABAA and GABAB receptor-mediated responses in neocortex of rat and cat. J Physiol (Lond). 1988;406:443-68.
457. Siebner HR, Dressnandt J, Auer C, Conrad B. Continuous intrathecal baclofen infusions induced a marked increase of the transcranially evoked silent period in a patient with generalized dystonia. Muscle Nerve. 1998;21(9):1209-12.
458. Werhahn KJ, Kunesch E, Noachtar S, Benecke R, Classen J. Differential effects on motorcortical inhibition induced by blockade of GABA uptake in humans. J Physiol (Lond). 1999;517:591-7.
459. Kornau H-C. GABAB receptors and synaptic modulation. Cell and tissue research. 2006;326(2):517-33.
460. Wu LG, Saggau P. Presynaptic inhibition of elicited neurotransmitter release. Trends Neurosci. 1997;20(5):204-12.
461. Takahashi T, Kajikawa Y, Tsujimoto T. G-Protein-coupled modulation of presynaptic calcium currents and transmitter release by a GABAB receptor. J Neurosci. 1998;18(9):3138-46.
462. Filippov AK, Couve A, Pangalos MN, Walsh FS, Brown DA, Moss SJ. Heteromeric assembly of GABA(B)R1 and GABA(B)R2 receptor subunits inhibits Ca(2+) current in sympathetic neurons. J Neurosci. 2000;20(8):2867-74.
463. Priori A, Berardelli A, Inghilleri M, Accornero N, Manfredi M. Motor cortical inhibition and the dopaminergic system. Pharmacological changes in the silent period after transcranial

brain stimulation in normal subjects, patients with Parkinson's disease and drug-induced parkinsonism. Brain : a journal of neurology. 1994;117:317-23.
464. Ziemann U, Bruns D, Paulus W. Enhancement of human motor cortex inhibition by the dopamine receptor agonist pergolide: evidence from transcranial magnetic stimulation. Neurosci Lett. 1996;208(3):187-90.
465. Desiato MT, Caramia MD. Towards a neurophysiological marker of amyotrophic lateral sclerosis as revealed by changes in cortical excitability. Electroencephalogr Clin Neurophysiol. 1997;105(1):1-7.
466. Siciliano G, Manca ML, Sagliocco L, Pastorini E, Pellegrinetti A, Sartucci F, et al. Cortical silent period in patients with amyotrophic lateral sclerosis. J Neurol Sci. 1999;169(1-2):93-7.
467. Wittstock M, Wolters A, Benecke R. Transcallosal inhibition in amyotrophic lateral sclerosis. Clin Neurophysiol. 2007;118(2):301-7.
468. Kujirai T, Caramia MD, Rothwell JC, Day BL, Thompson PD, Ferbert A, et al. Corticocortical inhibition in human motor cortex. J Physiol (Lond). 1993;471:501-19.
469. Hanajima R, Ugawa Y, Terao Y, Sakai K, Furubayashi T, Machii K, et al. Paired-pulse magnetic stimulation of the human motor cortex: differences among I waves. J Physiol (Lond). 1998;509:607-18.
470. Nakamura H, Kitagawa H, Kawaguchi Y, Tsuji H. Intracortical facilitation and inhibition after transcranial magnetic stimulation in conscious humans. J Physiol (Lond). 1997;498:817-23.
471. Di Lazzaro V, Oliviero A, Meglio M, Cioni B, Tamburrini G, Tonali P, et al. Direct demonstration of the effect of lorazepam on the excitability of the human motor cortex. Clin Neurophysiol. 2000;111(5):794-9.
472. Bormann J. Electrophysiology of GABAA and GABAB receptor subtypes. Trends Neurosci. 1988;11(3):112-6.
473. Macdonald RL, Olsen RW. GABAA receptor channels. Annu Rev Neurosci. 1994;17:569-602.
474. Mohler H. GABA(A) receptor diversity and pharmacology. Cell Tissue Res. 2006;326(2):505-16.
475. Barnard EA, Skolnick P, Olsen RW, Mohler H, Sieghart W, Biggio G, et al. International Union of Pharmacology. XV. Subtypes of gamma-aminobutyric acidA receptors: classification on the basis of subunit structure and receptor function. Pharmacol Rev. 1998;50(2):291-313.
476. Rudolph U, Mohler H. GABA-based therapeutic approaches: GABAA receptor subtype functions. Curr Opin Pharmacol. 2006;6(1):18-23.
477. Di Lazzaro V, Pilato F, Dileone M, Profice P, Ranieri F, Ricci V, et al. Segregating two inhibitory circuits in human motor cortex at the level of GABAA receptor subtypes: A TMS study. Clin Neurophysiol. 2007;118(10):2207-14.
478. Stefan K, Kunesch E, Benecke R, Classen J. Effects of riluzole on cortical excitability in patients with amyotrophic lateral sclerosis. Ann Neurol. 2001;49:536-9.
479. Schwenkreis P, Liepert J, Witscher K, Fischer W, Weiller C, Malin JP, et al. Riluzole suppresses motor cortex facilitation in correlation to its plasma level. A study using transcranial magnetic stimulation. Exp Brain Res. 2000;135(3):293-9.
480. Vucic S, Lin CS-Y, Cheah BC, Murray J, Menon P, Krishnan AV, et al. Riluzole exerts central and peripheral modulating effects in amyotrophic lateral sclerosis. Brain. 2013;136(5):1361-70.

481. Ziemann U, Tergau F, Bruns D, Baudewig J, Paulus W. Changes in human motor cortex excitability induced by dopaminergic and anti-dopaminergic drugs. Electroencephalogr Clin Neurophysiol. 1997;105(6):430-7.
482. Ilic TV, Korchounov A, Ziemann U. Complex modulation of human motor cortex excitability by the specific serotonin re-uptake inhibitor sertraline. Neurosci Lett. 2002;319:116-20.
483. Ziemann U, Rothwell JC, Ridding MC. Interaction between intracortical inhibition and facilitation in human motor cortex. J Physiol (Lond). 1996;496:873-81.
484. Kiers L, Cros D, Chiappa KH, Fang J. Variability of motor potentials evoked by transcranial magnetic stimulation. Electroencephalogr Clin Neurophysiol. 1993;89:415-23.
485. Vucic S, Cheah BC, Krishnan AV, Burke D, Kiernan MC. The effects of alterations in conditioning stimulus intensity on short interval intracortical inhibition. Brain Res. 2009:1273 39-47.
486. Vucic S, Cheah BC, Kiernan MC. Dissecting the Mechanisms Underlying Short-Interval Intracortical Inhibition Using Exercise. Cereb Cortex. 2011(21):1639-44.
487. Ziemann U, Lonnecker S, Steinhoff BJ, Paulus W. The effect of lorazepam on the motor cortical excitability in man. Exp Brain Res. 1996;109:127-35.
488. Ilic TV, Meintzschel F, Cleff U, Ruge D, Kessler KR, Ziemann U. Short-interval paired-pulse inhibition and facilitation of human motor cortex: the dimension of stimulus intensity. J Physiol (Lond). 2002;545(Pt 1):153-67.
489. Di Lazzaro V, Pilato F, Dileone M, Ranieri F, Ricci V, Profice P, et al. GABAA receptor subtype specific enhancement of inhibition in human motor cortex. J Physiol. 2006;575(Pt 3):721-6. Epub 2006/07/01.
490. Hanajima R, Furubayashi T, Iwata NK, Shiio Y, Okabe S, Kanazawa I, et al. Further evidence to support different mechanisms underlying intracortical inhibition of the motor cortex. Exp Brain Res. 2003;151(4):427-34.
491. Roshan L, Paradiso GO, Chen R. Two phases of short-interval intracortical inhibition. Exp Brain Res. 2003;151(3):330-7.
492. Hanajima R, Ugawa Y, Terao Y, Ogata K, Kanazawa I. Ipsilateral cortico-cortical inhibition of the motor cortex in various neurological disorders J Neurol Sci 1996(140):109-16.
493. Yokota T, Yoshino A, Inaba A, Saito Y. Double cortical stimulation in amyotrophic lateral sclerosis. J Neurol Neurosurg Psychiatry. 1996;61:596-600.
494. Ziemann U, Winter M, Reimers CD, Reimers K, Tergau F, Paulus W. Impaired motor cortex inhibition in patients with amyotrophic lateral sclerosis. Evidence from paired transcranial magnetic stimulation. Neurology. 1997;49(5):1292-8.
495. Sommer M, Tergau F, Wischer S, Reimers CD, Beuche W, Paulus W. Riluzole does not have an acute effect on motor thresholds and the intracortical excitability in amyotrophic lateral sclerosis. J Neurol. 1999;246 Suppl 3:III22-6.
496. Nihei K, McKee AC, Kowall NW. Patterns of neuronal degeneration in the motor cortex of amyotrophic lateral sclerosis patients. Acta Neuropathologica. 1993;86(1):55-64.
497. Vucic S, Cheah BC, Kiernan MC. Defining the mechanisms that underlie cortical hyperexcitability in amyotrophic lateral sclerosis. Exp Neurol. 2009;220:177-82.
498. Ziemann U, Lönnecker S, Steinhoff B, Paulus W. Effects of antiepileptic drugs on motor cortex excitability in humans: a transcranial magnetic stimulation study. Annals of neurology. 1996;40(3):367-78.

499. Ziemann U, Tergau F, Bruns D, Baudewig J, Paulus W. Changes in human motor cortex excitability induced by dopaminergic and anti-dopaminergic drugs. Electroencephalography and Clinical Neurophysiology/Electromyography and Motor Control. 1997;105(6):430-7.
500. Ziemann U. Pharmacology of TMS. Clin Neurophysiol. 2003;56:226-31.
501. Bostock H, Baker M. Evidence for two types of potassium channel in human motor axons in vivo. Brain Research. 1988;462(2):354-8.
502. Bostock H, Rothwell J. Latent addition in motor and sensory fibres of human peripheral nerve. The Journal of physiology. 1997;498(Pt 1):277-94.
503. Menon P, Kiernan MC, Vucic S. ALS pathophysiology: Insights from the split-hand phenomenon. Clinical Neurophysiology. 2014;125(1):186-93.
504. Fisher R, Nakamura Y, Bestmann S, Rothwell J, Bostock H. Two phases of intracortical inhibition revealed by transcranial magnetic threshold tracking. Experimental Brain Research. 2002;143(2):240-8.
505. Di Lazzaro V, Oliviero A, Profice P, Ferrara L, Saturno E, Pilato F, et al. The diagnostic value of motor evoked potentials. Clinical Neurophysiology. 1999;110(7):1297-307.
506. Mills K, Murray N, Hess C. Magnetic and electrical transcranial brain stimulation: physiological mechanisms and clinical applications. Neurosurgery. 1987;20(1):164-8.
507. Cantello R, Gianelli M, Civardi C, Mutani R. Magnetic brain stimulation The silent period after the motor evoked potential. Neurology. 1992;42(10):1951-.
508. Bischoff C, Stålberg E, Falck B, Eeg-Olofsson KE. Reference values of motor unit action potentials obtained with multi-MUAP analysis. Muscle & Nerve. 1994;17(8):842-51.
509. Stålberg E, Falck B, Sonoo M, Stålberg S, Åström M. Multi-MUP EMG analysis—a two year experience in daily clinical work. Electroencephalography and Clinical Neurophysiology/Electromyography and Motor Control. 1995;97(3):145-54.
510. Nandedkar SD, Barkhaus PE, Charles A. Multi-motor unit action potential analysis (MMA). Muscle & Nerve. 1995;18(10):1155-66.
511. Cedarbaum JM, Stambler N, Malta E, Fuller C, Hilt D, Thurmond B, et al. The ALSFRS-R: a revised ALS functional rating scale that incorporates assessments of respiratory function. BDNF ALS Study Group (Phase III). J Neurol Sci. 1999;169:13-21.
512. O'Brien MD. Aid to the examination of the peripheral nervous system. 4 ed. London: W.B.Saunders; 2004. p. 1-3.
513. Triggs W, Menkes D, Onorato J, Yan R-H, Young M, Newell K, et al. Transcranial magnetic stimulation identifies upper motor neuron involvement in motor neuron disease. Neurology. 1999;53(3):605-.
514. Turner MR, Cagnin A, Turkheimer FE, Miller CC, Shaw CE, Brooks DJ, et al. Evidence of widespread cerebral microglial activation in amyotrophic lateral sclerosis: an [11C](R)-PK11195 positron emission tomography study. Neurobiol Dis. 2004;15(3):601-9.
515. Chio A. ISIS Survey: an international study on the diagnostic process and its implications in amyotrophic lateral sclerosis. J Neurol. 1999;246 Suppl 3:1-5.
516. Aggarwal S, Cudkowicz M. ALS drug development: reflections from the past and a way forward. Neurotherapeutics. 2008;5(4):516-27. Epub 2008/11/21.
517. Swash M. Early diagnosis of ALS/MND. Journal of the Neurological Sciences. 1998;160 Suppl 1:S33-6.
518. Noto YI, Misawa S, Kanai K, Shibuya K, Isose S, Nasu S, et al. Awaji ALS criteria increase the diagnostic sensitivity in patients with bulbar onset. Clin Neurophysiol. 2012;123:382-5. Epub 2011/07/19.

519. Menon P, Kiernan MC, Vucic S. Appearance, phenomenology and diagnostic utility of the split hand in amyotrophic lateral sclerosis. Neurodeg Dis Management. 2011;1(6):457-62.
520. Kimura F, Fujimura C, Ishida S, Nakajima H, Furutama D, Uehara H, et al. Progression rate of ALSFRS-R at time of diagnosis predicts survival time in ALS. Neurology. 2006;66(2):265-7. Epub 2006/01/26.
521. O'Brien MD. Aid to the examination of the peripheral nervous system. 5th ed. Edinburgh: Saunders Elsevier; 2010. 2 p.
522. De Carvalho M, Swash M. Nerve conduction studies in amyotrophic lateral sclerosis. Muscle Nerve. 2000;23:344-52.
523. Lehky TJ, Chen CJ, di Prospero NA, Rhodes LE, Fischbeck K, Floeter MK. Standard and modified statistical MUNE evaluations in spinal-bulbar muscular atrophy. Muscle Nerve. 2009;40:809-14. Epub 2009/08/12.
524. Rutkove SB, Shefner JM, Gregas M, Butler H, Caracciolo J, Lin C, et al. Characterizing spinal muscular atrophy with electrical impedance myography. Muscle Nerve. 2010;42(6):915-21.
525. Jokic N, Gonzalez de Aguilar JL, Pradat PF, Dupuis L, Echaniz-Laguna A, Muller A, et al. Nogo expression in muscle correlates with amyotrophic lateral sclerosis severity. Ann Neurol. 2005;57:553-6. Epub 2005/03/24.
526. Askanas V, Wojcik S, Engel WK. Expression of Nogo-A in human muscle fibers is not specific for amyotrophic lateral sclerosis. Ann Neurol. 2007;62:676-7. Epub 2007/09/27.
527. Moore DH, Katz JS, Miller RG. A review of clinical trial designs in amyotrophic lateral sclerosis. Neurodegenerative Disease Management. 2011;1(6):481-90.
528. Bensimon G, Lacomblez L, Delumeau JC, Bejuit R, Truffinet P, Meininger V. A study of riluzole in the treatment of advanced stage or elderly patients with amyotrophic lateral sclerosis. J Neurol. 2002;249(5):609-15. Epub 2002/05/22.
529. Menon P, Kiernan MC, Yiannikas C, Stroud J, Vucic S. Split-hand index for the diagnosis of amyotrophic lateral sclerosis. Clin Neurophysiol. 2013;124(2):410-6.
530. Menzies F, Ince P, Shaw P. Mitochondrial involvement in amyotrophic lateral sclerosis. Neurochem Inter. 2002;40:543 - 51.
531. Brochier T, Spinks RL, Umilta MA, Lemon RN. Patterns of Muscle Activity Underlying Object-Specific Grasp by the Macaque Monkey. J Neurophysiol. 2004;92(3):1770-82.
532. Forssberg H, Eliasson AC, Kinoshita H, Johansson RS, Westling G. Development of human precision grip. I: Basic coordination of force. Exp Brain Res. 1991;85(2):451-7. Epub 1991/01/01.
533. Johanson ME, Valero-Cuevas FJ, Hentz VR. Activation patterns of the thumb muscles during stable and unstable pinch tasks. J Hand Surg Am. 2001;26(4):698-705.
534. Jeannerod M. The formation of finger grip during prehension. A cortically mediated visuomotor pattern. Behav Brain Res. 1986;19(2):99-116. Epub 1986/02/01.
535. Maier MA, Hepp-Reymond MC. EMG activation patterns during force production in precision grip. II. Muscular synergies in the spatial and temporal domain. Exp Brain Res. 1995;103(1):123-36. Epub 1995/01/01.
536. Marzke MW. Precision grips, hand morphology, and tools. Am J Phys Anthropol. 1997;102(1):91-110.
537. Marzke MW, Toth N, Schick K, Reece S, Steinberg B, Hunt K, et al. EMG study of hand muscle recruitment during hard hammer percussion manufacture of Oldowan tools. Am J Phys Anthrop. 1998;105(3):315-32.

538. Napier JR. The prehensile movements of the human hand. J Bone Joint Surg Br. 1956;38-B(4):902-13.
539. Long C, 2nd, Conrad PW, Hall EA, Furler SL. Intrinsic-extrinsic muscle control of the hand in power grip and precision handling. An electromyographic study. J Bone Joint Surg Am. 1970;52(5):853-67. Epub 1970/07/01.
540. Abbruzzese G, Assini A, Buccolieri A, Schieppati M, Trompetto C. Comparison of intracortical inhibition and facilitation in distal and proximal arm muscles in humans. J Physiol (Lond). 1999;514:895-903. Epub 1999/01/12.
541. Mogyoros I, Kiernan MC, Burke D. Strength-duration properties of human peripheral nerve. Brain : a journal of neurology. 1996;119(Pt 2):439-47.
542. Di Lazzaro V, Oliviero A, Profice P, Saturno E, Pilato F, Insola A, et al. Comparison of descending volleys evoked by transcranial magnetic and electric stimulation in conscious humans. Electroencephalogr Clin Neurophysiol. 1998;109(5):397-401.
543. Di Lazzaro V, Oliviero A, Profice P, Insola A, Mazzone P, Tonali P, et al. Direct recordings of descending volleys after transcranial magnetic and electric motor cortex stimulation in conscious humans. Electroencephalography & Clinical Neurophysiology - Supp. 1999;51:120-6.
544. Chen R. Interactions between inhibitory and excitatory circuits in the human motor cortex. Exp Brain Res. 2004;154(1):1-10.
545. Jaarsma D, Rognoni F, Duijn W, Verspaget H, Haasdijk E, Holstege J. Cu-Zn superoxide dismutase (SOD1) accumulates in vacuolated mitochondria in transgenic mice expressing amyotrophic lateral sclerosis-linked SOD1 mutations. Acta Neuropath. 2001;102:293 - 305.
546. de Noordhout AM, Rapisarda G, Bogacz D, Gerard P, De Pasqua V, Pennisi G, et al. Corticomotoneuronal synaptic connections in normal man: An electrophysiological study. Brain. 1999;122(7):1327-40.
547. Lemon RN. Mechansim of cortical control of hand function. The Neuroscientist. 1997;3:389-98.
548. Chen R, Lozano AM, Ashby P. Mechanism of the silent period following transcranial magnetic stimulation. Evidence from epidural recordings. Exp Brain Res. 1999;128(4):539-42.
549. Stetkarova I, Kofler M. Differential effects of cortical and spinal inhibitory circuits. Clin Neurophysiol. 2012:In press.
550. Orth M, Rothwell JC. The cortical silent period: intrinsic variability and relation to the waveform of the transcranial magnetic stimulation pulse. Clin Neurophysiol. 2004;115(5):1076-82.
551. Kraskov A, Dancause N, Quallo MM, Shepherd S, Lemon RN. Corticospinal neurons in macaque ventral premotor cortex with mirror properties: a potential mechanism for action suppression? Neuron. 2009;64(6):922-30.
552. Rosenkranz K, Rothwell JC. Differential effect of muscle vibration on intracortical inhibitory circuits in humans. J Physiol. 2003;551(Pt 2):649-60.
553. Benwell NM, Sacco P, Hammond GR, Byrnes ML, Mastaglia FL, Thickbroom GW. Short-interval cortical inhibition and corticomotor excitability with fatiguing hand exercise: a central adaptation to fatigue? Exp Brain Res. 2006;170(2):191-8.
554. Ridding MC, Pearce SL, Flavel SC. Modulation of intracortical excitability in human hand motor areas. The effect of cutaneous stimulation and its topographical arrangement. Exp Brain Res. 2005;163(3):335-43.

555. Rogasch NC, Dartnall TJ, Cirillo J, Nordstrom MA, Semmler JG. Corticomotor plasticity and learning of a ballistic thumb training task are diminished in older adults. J App Physiol. 2009;107(6):1874-83.
556. Säisänen L, Julkunen P, Niskanen E, Hukkanen T, Mervaala E, Karhu J, et al. Short- and intermediate-interval cortical inhibition and facilitation assessed by navigated transcranial magnetic stimulation. J Neurosci Methods. 2011;195(2):241-8.
557. Stys PK. General mechanisms of axonal damage and its prevention. J Neurol Sci. 2005;233:3-13.
558. Kuwabara S, Mizobuchi K, Ogawara K, Hattori T. Dissociated small hand muscle involvement in amyotrophic lateral sclerosis detected by motor unit number estimates. Muscle Nerve. 1999;22(7):870-3.
559. Schelhaas HJ, van de Warrenburg BP, Kremer HP, Zwarts MJ. The "split hand" phenomenon: evidence of a spinal origin. Neurology. 2003;61(11):1619-20. Epub 2003/12/10.
560. Voermans NC, Schelhaas HJ, Munneke M, Zwarts MJ. Dissociated small hand muscle atrophy in aging: the 'senile hand' is a split hand. Eur J Neurol. 2006;13(12):1381-4.
561. Bostock H, Sharief MK, Reid G, Murray NM. Axonal ion channel dysfunction in amyotrophic lateral sclerosis. Brain 1995;118:217-25.
562. Kanai K, Shibuya K, Sato Y, Misawa S, Nasu S, Sekiguchi Y, et al. Motor axonal excitability properties are strong predictors for survival in amyotrophic lateral sclerosis. J Neurol Neurosurg Psychiatry. 2012;83(7):734-8.
563. Shibuya K, Misawa S, Nasu S, Sekiguchi Y, Mitsuma S, Beppu M, et al. Split hand syndrome in amyotrophic lateral sclerosis: different excitability changes in the thenar and hypothenar motor axons. J Neurol Neurosurg Psychiatry, doi:101136/jnnp-2012-304109 2013.
564. Jankelowitz SK, Howells J, Burke D. Plasticity of inwardly rectifying conductances following a corticospinal lesion in human subjects. J Physiol. 2007;581(Pt 3):927-40. Epub 2007/03/17.
565. Ng K, Howells J, Pollard JD, Burke D. Up-regulation of slow K+ channels in peripheral motor axons: a transcriptional channelopathy in multiple sclerosis. Brain : a journal of neurology. 2008;131(11):3062-71.
566. FRIEDMAN AP, FREEDMAN D. Amyotrophic lateral sclerosis. The Journal of nervous and mental disease. 1950;111(1):1-18.
567. Rowland LP, Shneider NA. Amyotrophic lateral sclerosis. New England Journal of Medicine. 2001;344(22):1688-700.
568. Menon P, Kiernan MC, Vucic S. Cortical excitability differences in hand muscles follow a split-hand pattern in healthy controls. Muscle Nerve. 2013:doi: 10.1002/mus.24072.
569. Mills KR, Murray NM. Electrical stimulation over the human vertebral column: which neural elements are excited? Electroencephalogr Clin Neurophysiol. 1986;63:582-9.
570. Bostock H. Mechanisms of accommodation and adaptation in myelinated axons. In: Waxman SG, Kocsis JD, Stys PK, editors. The Axon. New York: Oxford Univerisy Press; 1995. p. 311-27.
571. Bae JS, Menon P, Mioshi E, Kiernan MC, Vucic S. Cortical excitability differences between flexor pollicis longus and APB. Neurosci Lett. 2013;541:150-4.
572. Komissarow L, Rollnik JD, Bogdanova D, Krampfl K, Khabirov FA, Kossev A, et al. Triple stimulation technique (TST) in amyotrophic lateral sclerosis.[see comment]. Clinical Neurophysiology. 2004;115(2):356-60.

573. Trotti D, Rolfs A, Danbolt N, Brown R, Hediger M. SOD1 mutants linked to amyotrophic lateral sclerosis selectively inactivate a glial glutamate transporter. Nat Neurosci. 1999;2:427 - 33.
574. Gowers W. A Manual of Diseases of the Nervous System: spinal cord and nerves. London: Churchill; 1888. p. 356-81.
575. O'Brien M. Aids to the examination of the peripheral nervous system: Saunders Ltd; 2000.
576. Braak H, Brettschneider J, Ludolph AC, Lee VM, Trojanowski JQ, Tredici KD. Amyotrophic lateral sclerosis: a model of corticofugal axonal spread. Nat Rev Neurol. 2013;9(12):708-14.
577. Brettschneider J, Del Tredici K, Toledo JB, Robinson JL, Irwin DJ, Grossman M, et al. Stages of pTDP-43 pathology in amyotrophic lateral sclerosis. Ann Neurol. 2013;74(1):20-38.
578. Howland DS, Liu J, She Y, Goad B, Maragakis NJ, Kim B, et al. Focal loss of the glutamate transporter EAAT2 in a transgenic rat model of SOD1 mutant-mediated amyotrophic lateral sclerosis (ALS). Proc Natl Acad Sci U S A. 2002;99(3):1604-9. Epub 2002/01/31.
579. Pardo AC, Wong V, Benson LM, Dykes M, Tanaka K, Rothstein JD, et al. Loss of the astrocyte glutamate transporter GLT1 modifies disease in SOD1(G93A) mice. Exp Neurol. 2006;201(1):120-30. Epub 2006/06/07.
580. Kiernan MC, Vucic S, Cheah BC, Turner MR, Eisen A, Hardiman O, et al. Amyotrophic lateral sclerosis. The Lancet. 2011.
581. Cats EA, van der Pol WL, Piepers S, Franssen H, Jacobs BC, van den Berg-Vos RM, et al. Correlates of outcome and response to IVIg in 88 patients with multifocal motor neuropathy. Neurology. 2010;75(9):818-25. Epub 2010/09/02.
582. Hamrick MW, Churchill SE, Schmitt D, Hylander WL. EMG of the human flexor pollicis longus muscle: implications for the evolution of hominid tool use. J Hum Evol. 1998;34(2):123-36. Epub 1998/03/21.
583. Lemon RN, Johansson RS, Westling G. Modulation of corticospinal influence over hand muscles during gripping tasks in man and monkey. Can J Physiol Pharmacol. 1996;74(4):547-58. Epub 1996/04/01.
584. Eisen A, Kuwabara S. The split hand syndrome in amyotrophic lateral sclerosis. J Neurol, Neurosurg & Psychiatry. 2012;83(4):399-403.
585. Menon P, Bae JS, Mioshi E, Kiernan MC, Vucic S. Split-hand plus sign in ALS: Differential involvement of the flexor pollicis longus and intrinsic hand muscles. Amyotroph Lateral Scler. 2012. Epub in press.
586. Colebatch JG, Rothwell JC, Day BL, Thompson PD, Marsden CD. Cortical outflow to proximal arm muscles in man. Brain : a journal of neurology. 1990;113:1843-56. Epub 1990/12/01.
587. Vucic S, Yiannikas C. Anterior interosseous nerve conduction study: normative data. Muscle Nerve. 2007;35(1):119-21.
588. Strafella AP, Paus T. Cerebral blood-flow changes induced by paired-pulse transcranial magnetic stimulation of the primary motor cortex. J Neurophysiol. 2001;85(6):2624-9.
589. Vucic S, Cheah BC, Kiernan MC. Dissecting the Mechanisms Underlying Short-Interval Intracortical Inhibition Using Exercise. Cerebral Cortex. 2011;21(7):1639-44.
590. Vucic S, Cheah BC, Krishnan AV, Burke D, Kiernan MC. The effects of alterations in conditioning stimulus intensity on short interval intracortical inhibition. Brain Res. 2009;1273(0):39-47.

591. Merton PA, Morton HB. Stimulation of the cerebral cortex in the intact human subject. Nature. 1980;285(5762):227.
592. Peurala S, Muller-Dahlhaus JFM, Arai N, Ziemann U. Interference of short-interval intracortical inbition (SICI) and short-interval intracortical facilitation. Clin Neurophysiol. 2008;119(10):2291-7.
593. Palmer E, Ashby P. Corticospinal projections to upper limb motoneurones in humans. J Physiol. 1992;448:397-412. Epub 1992/03/01.
594. Menon P, Bae JS, Mioshi E, Kiernan MC, Vucic S. Split-hand plus sign in ALS: Differential involvement of the flexor pollicis longus and intrinsic hand muscles. Amyotroph Lateral Scler. 2013;14(4):315-8.
595. Zoghi M, Pearce SL, Nordstrom MA. Differential Modulation of Intracortical Inhibition in Human Motor Cortex during Selective Activation of an Intrinsic Hand Muscle. J Physiol (Lond). 2003;550(3):933-46.
596. Vucic S, Howells J, Trevillion L, Kiernan MC. Assessment of cortical excitability using threshold tracking techniques. Muscle Nerve. 2006;33(4):477-86. Epub 2005/11/30.
597. Vucic S, Cheah BC, Yiannikas C, Vincent A, Kiernan MC. Corticomotoneuronal function and hyperexcitability in acquired neuromyotonia. Brain 2010;133(9):2727-33. Epub 2010/08/26.
598. Kilbreath SL, Gandevia SC. Neural and biomechanical specializations of human thumb muscles revealed by matching weights and grasping objects. J Physiol. 1993;472:537-56. Epub 1993/12/01.
599. Refshauge KM, Kilbreath SL, Gandevia SC. Movement detection at the distal joint of the human thumb and fingers. Exp Brain Res. 1998;122(1):85-92.
600. Menon P, Kiernan MC, Vucic S. ALS pathophysiology: Insights form the split-hand phenomenon. Clin neurophysiol. 2013:doi:pii: S1388-2457(13)00994-2. 10.1016.